RECLAMATION

Managing Water in the West

Technical Report No. SRH-2009-27

Calibration of Numerical Models for the Simulation of Sediment Transport, River Migration, and Vegetation Growth on the Sacramento River, California

NODOS Investigation Report

U.S. Department of the Interior
Bureau of Reclamation

March 2011

Mission Statements

The mission of the Department of the Interior is to protect and provide access to our Nation's natural and cultural heritage and honor our trust responsibilities to Indian Tribes and our commitments to island communities.

The mission of the Bureau of Reclamation is to manage, develop, and protect water and related resources in an environmentally and economically sound manner.

Technical Report No. SRH-2009-27

Calibration of Numerical Models for the Simulation of Sediment Transport, River Migration, and Vegetation Growth on the Sacramento River, California

NODOS Investigation Report

Prepared by:

Bureau of Reclamation, Technical Service Center, Denver, Colorado
Blair Greimann, P.E., Ph.D., Hydraulic Engineer
Lisa Fotherby, P.E., Hydraulic Engineer
Yong Lai, P.E., Ph.D., Hydraulic Engineer
David Varyu, M.S., Hydraulic Engineer

Bureau of Reclamation, Mid-Pacific Region, Sacramento, California
Michael K. Tansey, Ph.D., Hydrologist, Soil Scientist

Stockholm Environment Institute
Chuck Young, Ph.D., Water Resource Engineer

Colorado State University, Fort Collins, Colorado
Jianchun Huang, Ph.D., Research Scientist

U.S. Department of the Interior
Bureau of Reclamation

March 2011

BUREAU OF RECLAMATION
Technical Service Center, Denver, Colorado
Sedimentation and River Hydraulics Group, 86-68240

Technical Report No. SRH-2009-27

Calibration of Numerical Models for the Simulation of Sediment Transport, River Migration, and Vegetation Growth on the Sacramento River, California

Prepared: Blair P. Greimann, P.E., Ph.D.
Hydraulic Engineer, Sedimentation and River Hydraulics Group, 86-68240

Prepared: Lisa Fotherby, P.E.
Hydraulic Engineer, Sedimentation and River Hydraulics Group, 86-68240

Prepared: Yong Lai, P.E., Ph.D.
Hydraulic Engineer, Sedimentation and River Hydraulics Group, 86-68240

Prepared: David Varyu, M.S.
Hydraulic Engineer, Sedimentation and River Hydraulics Group, 86-68240

Peer Reviewed: Elaina Holburn Gordon, M.S., P.E.
Hydraulic Engineer, Sedimentation and River Hydraulics Group, 86-68240

Acknowledgments

The California Department of Water Resources Northern District was responsible for the majority of the data collection listed in this report. Special thanks are due:

Clint Anderson, Senior Engineer
Stacey Cepello, Senior Environmental Scientist
David Forwalter, Associate Engineering Geologist
Glen Gordon, Engineering Geologist
Lester Grade, Water Resources Engineer
Adam Henderson, Environmental Scientist
Scott Kennedy, Water Resources Engineer
Dan McManus, Associate Engineering Geologist
Jon Mulder, Associate Engineering Geologist
Bruce Ross, Associate Engineering Geologist
Nancy Snodgrass, Water Resources Engineer
Jim West, Professional Surveyor

Executive Summary

This Executive Summary describes the five models used in this analysis and lists the next steps and recommendations.

This report describes the calibration and/or application of five numerical models that together simulate processes of flow hydraulics, sediment transport, river meandering, and the establishment and survival of riparian vegetation in the Sacramento River Corridor in California. The study area extends from Red Bluff Diversion Dam to Colusa. Results of this modeling effort will be used to analyze the effects of project operations on the Sacramento River for the Bureau of Reclamation's (Reclamation) Mid-Pacific Region.

Numerical models can be practical tools for testing alternatives, especially in physical river studies where aspects of the system are deterministic (i.e., the same input factors will result in the same values) and there is a good scientific basis for predictive descriptions of both physical and ecosystem representations. These predictive tools provide quantifiable responses for a range of imposed conditions or operating scenarios. Data and knowledge are used to develop a numerical model that can mathematically portray a "prototype" or the reality to be studied. In this case, the model predicts how river processes and river form are impacted by changes including adjustments in the flow regime. Developing a model begins with studying the prototype and ends with the interpretation of the model results to draw conclusions.

Despite the power of this analysis tool, there is no single model that can simulate all interacting river processes in complete detail. The strategy applied in this investigation was to use models that focus on different processes and different scales so that a more complete understanding of each process, and process interactions, could be understood. Five models are used to examine hydraulics, sediment transport, river meandering, and vegetation establishment and survival.

Sediment Transport for the Study Area: Sedimentation River Hydraulics Capacity Model

The Sedimentation River Hydraulics Capacity Model (SRH-Capacity) was used to estimate the contribution of tributary sediment to the main stem of the Sacramento River and to develop a sediment balance for the main stem river in the study area. A sediment balance is critical to estimating sustainability and future trends of river processes including riparian vegetation growth. Sensitivity analysis and calibration of the model were also conducted as part of this study.

See Chapter 2. As this effort has not been previously reported, Appendix A provides a detailed description of the model development.

Results from SRH-Capacity contributed to an understanding of the physical processes of the system and, in turn, aided development and calibration of the Sedimentation and River Hydraulics Meander Model (SRH-Meander), Sedimentation River Hydraulics Two-Dimensional Model (SRH-2D), and One-Dimensional Sediment Transport and Vegetation Dynamics Model (SRH-1DV) through input to these models.

River Meandering: Sedimentation River Hydraulics Meander Model

SRH-Meander, which predicts bend migration in meander river systems, was calibrated at three reaches of the Sacramento River. Bank erosion coefficients were the primary calibration parameters. SRH-Meander was also used to simulate future meander tendencies of the river in those reaches. Model capabilities for calculating area of erosion and changes to flood plain topography were also demonstrated.

Results of the calibration indicate that SRH-Meander will be useful in estimating and comparing relative meander rates and tendencies among alternatives. Model simulations can also help identify infrastructure that may be impacted by river meandering in the near future. See Chapter 3.

Sediment Transport for a Local Reach: Sedimentation River Hydraulics Two-Dimensional Model

SRH-2D was applied to a specific reach of the Sacramento River, and modeled flow was validated against velocity data obtained in the same reach. Modeling of two-dimensional sediment transport was demonstrated by simulating erosion and deposition in the same reach during a historical flood.

Based on these studies, SRH-2D will be useful in addressing flow and sediment issues at local scales. Simulations can also help identify likely locations of point bar scour and suitable hydraulic habitat for fish and other aquatic species. It can also be used to assess project impacts at specific structures or locations. See Chapter 4.

Vegetation Establishment: Riparian Habitat Establishment Model

The Riparian Habitat Establishment Model (RHEM) has been developed by Reclamation's Mid-Pacific Region and the Stockholm Environment Institute (SEI). The RHEM simulates individual cottonwood seedling growth while incorporating the effects of sediment texture and hydraulic properties, water table depth, and atmospheric conditions. It is a modified version of the variably saturated flow code HYDRUS 2-D.[1] RHEM is intended to improve our understanding of cottonwood seedling establishment. RHEM assisted in developing a less detailed model of vegetation establishment and growth that is incorporated into the SRH-1DV.

The RHEM model is intended to simulate the establishment of cottonwoods at a particular cross section or point bar. SRH-1DV is intended to simulate the establishment, growth, and mortality of cottonwoods throughout the entire project reach. See Chapter 5.

Vegetation Survival: One-Dimensional Sediment Transport and Vegetation Dynamics Model

SRH-1DV pulls together aspects and outcomes of modeling from SRH-Capacity, Sedimentation and River Hydraulics One-Dimensional Sediment Transport Dynamics Model (SRH-1D), and RHEM for a construction of flow, sediment transport, and vegetation growth and removal river processes. This tool provides a system-wide assessment over an extensive period for expanded comprehension of existing and predicted river response.

The SRH-1DV model, simulating vegetation growth in addition to flow and sediment transport, was initially developed and later expanded for the Sacramento River project area. Calibration of flow, sediment, and vegetation modules of the SRH-1DV model are described and also included is a validation of the cottonwood vegetation for this study of the Sacramento River. The flow portion of the model was calibrated to the stage measurements at two river bends in the study area where detailed measurements are available. The sediment transport module was calibrated to suspended load and bed load measurements at the Hamilton City U.S. Geological Survey stream gage. Ground water parameters and cottonwood parameters of the vegetation module were calibrated to cottonwood mortality and growth observations in 2005 and 2006 at the same two river bends where the water stage was measured.

[1] HYDRUS is a Microsoft Windows based modeling environment developed by the U.S. Salinity Laboratory, U.S. Department of Agriculture (USDA), Agricultural Research Service (ARS), Riverside, California.

In a second phase of model development, multiple vegetation types were added along with significant code advances—including capabilities to describe vegetation density, canopy growth for shading, competition mortality, shading mortality, and propagation by water-borne parts. Cottonwood growth was validated using GIS vegetation mapping from 1999 and 2007. Added vegetation types of mixed forest, Gooding's black willow, narrow-leaf willow, and riparian invasive plants were calibrated using the 1999 and 2007 vegetation mapping. In this Sacramento River application, SRH-1DV simulated 8 years of flow, sediment transport and vegetation growth throughout the project area from Red Bluff Diversion Dam to Colusa. SRH-1DV will help in quantifying the survivability of cottonwoods and other riparian vegetation including invasive plants, for various river and reservoir operational strategies. See Chapter 6.

Recommendations and Next Steps

Modeling tools can aid river managers through improved understanding of a complex and changing environment and predictions of future response. On challenging projects, it is often not sufficient to represent physical processes with a single model. There are also large benefits to integrating ecological systems into physical process models where systems and processes are linked. Thus, Reclamation's Technical Service Center (TSC) has developed, calibrated, and verified this suite of models to provide a system-wide assessment of various operational scenarios in the upper Sacramento River Basin. These models can also be used in the North-of-the-Delta Off Stream Storage (NODOS) to examine potential offstream surface water storage alternatives that could improve water supply and reliability, enhance anadromous fish survival, sustain or improve riparian habitat and provide high-quality water for agricultural, municipal and industrial, and environmental uses.

Use **SRH-Capacity** to estimate tributary supplies of gravel to the Sacramento River as well as general assessments of reach averaged erosion and deposition in the Sacramento River. This information is useful for determining input to SRH-1D and the U2Rans, to improve model results.

Use **SRH-Meander** to:

- Identify the reaches that will be relatively most active
- Identify locations where bank erosion bank impact infrastructure in the near future
- Assess the relative bank erosion rates among flow and land management alternatives

Use **SRH-2D** to help advance understanding and describe processes at river bends, flow splits and locations of flow convergence including bar growth and cottonwood establishment. Results can be applied in a new study of vegetation establishment as a function of soils, using SRH-1DV. Flow computations have been verified and validated. The next steps to improve model effectiveness for sediment transport computations are to:

- Collect more sediment data on existing bed gradations
- Carry out a validation study on the bed gradations on a system-wide basis.

Use **RHEM** for an in-depth assessment of seedling establishment, growth and mortality at specific locations and flow periods. The next steps are to refine some aspects of the algorithms for specific stresses, such as root elongation under conditions of severe water stress.

Use **SRH-1DV** to assess the relationships between management actions, physical river processes and riparian vegetation growth in the Sacramento River for both environmental and management benefits. Examples of questions that could be addressed include:

- How do we manage the flow regime to optimize new cottonwood/native riparian vegetation establishment and survival?

- Which locations support desirable native riparian vegetation?

- Could invasive riparian plants be a problem and what flow regimes would restrain them?

- How can we maximize our success with vegetation on Program restoration lands?

Contents

Page

1. Modeling Strategy 1-1
   - 1.1 Analysis Methods (Modeling Introduction) 1-1
   - 1.2 Using Models 1-3
     - 1.2.1 How Numerical Models Work 1-4
     - 1.2.2 How NODOS Models Work Together 1-5
   - 1.3 Model Descriptions 1-5
     - 1.3.1 Relationship to CALSIM-II 1-6
     - 1.3.2 SRH-Capacity 1-8
     - 1.3.3 SRH –Meander 1-8
     - 1.3.4 SRH-2D 1-9
     - 1.3.5 RHEM 1-10
     - 1.3.6 U^2RANS 1-11
     - 1.3.7 SRH-1D and SRH-1DV 1-11
   - 1.4 Report Organization 1-13
   - 1.5 Study Team 1-14
2. Sedimentation River and Hydraulics Capacity Model 2-1
   - 2.1 Range in Tributary Sediment Loads 2-2
   - 2.2 Range in Estimates of Main Stem Sediment Bed Loads 2-9
   - 2.3 Sediment Mass Balance in Main Stem 2-17
   - 2.4 Conclusions and Recommendations 2-21
     - 2.4.1 Erosion and Deposition Patterns 2-21
     - 2.4.2 Recommendations 2-23
     - 2.4.3 Model Use 2-23
3. Meander Modeling 3-1
   - 3.1 Model Description 3-1
   - 3.2 Model Calibration Using Laboratory Data 3-2
     - 3.2.1 Input Data 3-4

Contents (continued)

Page

3.2.2 Calibration Process 3-6
3.2.3 Model Calibration Not Incorporating Vertical Erosion 3-6
3.2.4 Model Calibration With Raster Elevation Update and Bank Height Resistance Coefficient 3-8
3.3 Calibration Using Field Data 3-12
3.3.1 Data Preprocessing 3-12
3.3.2 Model Calibration 3-14
3.5 Conclusions 3-21
4. Multidimensional Modeling 4-1
4.1 General Capability Description 4-1
4.1.1 U^2RANS 4-1
4.1.2 SRH-2D 4-2
4.2 Calibration Data for SRH-2D and U2RANS 4-2
4.3 Verification and Validation for SRH-2D and U2RANS 4-5
4.3.1 Velocity Data near RM 192.5 4-5
4.3.2 Mesh Development 4-5
4.3.3 Model Description 4-8
4.3.4 Results and Discussion for Verification and Validation 4-9
4.4 Mobile Bed Simulation for the 1986 Flood 4-18
4.4.1 Sediment Transport Data 4-18
4.4.2 Mesh Development 4-19
4.4.3 Sediment Classes 4-21
4.4.4 Initial and Boundary Conditions 4-21
4.4.5 Results and Discussion for Mobile Bed Simulation 4-25
4.5 Concluding Remarks 4-30
5. RHEM 5-1
5.1 Controlled Seedling Growth Experiments 5-1

Contents (continued)

Page

5.1.1 Experiment Design 5-1
5.1.2 Experiment Results and Discussion 5-3
5.2 Model Algorithms 5-5
5.2.1 Plant Growth 5-5
5.2.2 Root Growth 5-8
5.2.3 Plant Transpiration 5-11
5.3 Calibration 5-14
5.4 Validation 5-17
5.4.1 River Mile 192.5 – Sand 5-17
5.4.2 River Mile 192.5 – Gravel 5-19
5.4.3 Validation Results 5-19
5.5 Determining the Parameters for SRH-1DV 5-20
5.6 Concluding Remarks 5-24
6. One-Dimensional Modeling (SRH-1DV) 6-1
6.1 Groundwater Module 6-2
6.2 Vegetation Module 6-3
6.2.1 Establishment Module 6-4
6.2.2 Growth Module 6-7
6.2.3 Mortality Module 6-7
6.2.4 Vegetation Types 6-10
6.2.5 Use 6-12
6.3 Input Data 6-12
6.3.1 Flow Data 6-13
6.3.2 Geometry Data 6-13
6.3.3 Sediment Data 6-18
6.3.4 Ground Water Parameters 6-23
6.3.5 Vegetation Parameters 6-23

Contents (continued)

Page

6.4 Calibration of Flow and Ground Water Modules 6-36
6.5 Calibration of Sediment Module..... 6-39
6.6 Cottonwood Calibration with Field Data..... 6-40
6.6.1 2005 Data..... 6-41
6.6.2 2006 Data..... 6-43
6.7 Calibration of Multiple Vegetation Types with Vegetation Mapping..... 6-45
6.7.1 Methodology for Computing Mapping Values..... 6-47
6.7.2 Methodology for Computing Modeled Values..... 6-48
6.7.3 Results of Multiple Vegetation Calibration..... 6-49
6.8 Multiple Vegetation Application to Sacramento River 6-51
6.8.1 Vegetated Area From a Multiple Vegetation Simulation..... 6-52
6.8.2 Plant Germination..... 6-55
6.8.3 Hydrologic Regime and Desiccation 6-56
6.8.4 Inundation 6-58
6.8.5 Maximum Extent of Invasive Riparian Plants..... 6-60
6.9 Summary and Conclusions 6-61

Appendix A: Methods Used in SRH-Capacity for Computing Sediment Transport Capacity and the Sediment Budget

Appendix B: Description of Vegetation Input Files for SRH-1DV

Figures

Page

1-1 Map of study area..... 1-2
1-2 Computer modeling cycle from prototype to the modeling results..... 1-4
1-3 Information flow diagram for numerical model integration..... 1-7

Figures (continued)

Page

2-1 Annual tributary yield based on surface material (MPN shear, Scenario 784); very fine sand to small boulders 2-7

2-2 Annual tributary yield based on surface material (Parker defaults); very fine sand to small boulders 2-8

2-3 Annual tributary yield based on surface samples (MPN shear, Scenario 4); very fine gravel to small boulders 2-8

2-4 Annual tributary yield based on surface samples (Parker defaults); very fine gravel to small boulders..... 2-9

2-5 Annual main stem yield based on surface material (MPN shear, Scenario 4); very fine sand to small boulders 2-11

2-6 Annual main stem yield based on surface material (Parker defaults, Scenario 5); very fine sand to small boulders ... 2-11

2-7 Annual main stem yield based on surface material (MPN reference shear, Scenario 4); very fine gravel to small boulders..... 2-12

2-8 Annual main stem yield based on surface material (Parker defaults); very fine gravel to small boulders (Scenario 5)..... 2-12

2-9 Range of sediment yield for material greater than 2 mm..... 2-14

2-10 Range of sediment yield for material greater than 8 mm..... 2-14

2-11 Energy slope in Sacramento River at 90,000 cfs 2-15

2-12 Representative bed material diameter in Sacramento River..... 2-15

2-13 Schematic of mass balance calculations for reach (i) 2-17

2-14 Mass balance of surface material greater than 2 mm based on historical hydrology. 2-19

2-15 Mass balance of surface material greater than 8 mm based on historical hydrology. 2-20

2-16 Erosional and depositional reaches as predicted by SRH-Capacity. Flow is to the south..... 2-22

3-1 Post-test and pre-test photos of the study channel, from USACE (1945)..... 3-3

3-2 Thalweg traces at periodic time intervals, from USACE (1945).. 3-3

3-3 Centerlines for four time steps along with the valley axis of the channel 3-5

Figures (continued)

Page

3-4 Calibration resulting in the first bend being modeled..... 3-6

3-5 Calibration resulting in the second bend being modeled..... 3-7

3-6 Calibration resulting in the third bend being modeled..... 3-7

3-7 Calibration resulting in the fourth bend being modeled 3-8

3-8 Calibration results with raster elevation update and bank height resistance coefficient..... 3-11

3-9 Comparison of channel topography between laboratory model and computational model. The top picture is from USACE (1945). The bottom is simulated in SRH-Meander..... 3-11

3-10 SRH-Meander project reach 3-13

3-11 Flow discharge data at Vina Woodson Bridge at RM 219 (VIN)..... 3-15

3-12 Flow discharge data at Hamilton City gauge at RM 199.2 (HMC)..... 3-15

3-13 Flow discharge data at flow hydrograph from DWR gauge Ord Ferry at RM 184.2 (ORD) 3-16

3-14 Calibration result in reach 1..... 3-18

3-15 Calibration result in reach 2..... 3-19

3-16 Calibration result in reach 3..... 3-20

4-1 Survey points (in red) for the river topography at RM 192.5 4-3

4-2 Bed elevation contours based on the TIN formed from all survey points 4-4

4-3 Bed elevation contours when extra topographic data are added at the left downstream bar..... 4-4

4-4 Plan view of all velocity measurement points (in red) at RM 192.5 4-5

4-5 Solution domain and the 2D mesh for the SRH-2D simulation.... 4-6

4-6 A zoom-in view of the 2D mesh at the bar area 4-7

4-7 Bed elevation contours based on the 2D mesh 4-7

4-8 A 3D view of the bed for the bend at 192.5 RM; 1:10 vertical distortion 4-8

Figures (continued)

Page

4-9 Comparison of measured and computed water depth at all velocity measurement points 4-10

4-10 Comparison of velocity vectors at all measurement points between measured and SRH-2D data 4-11

4-11 Comparison of velocity vectors at measurement points between measured and U^2RANS data 4-11

4-12 Comparison of velocity vectors at cross section 1 between measured and SRH-2D data 4-12

4-13 Comparison of velocity vectors at cross section 2 between measured and SRH-2D data 4-12

4-14 Comparison of velocity vectors at cross section 3 between measured and SRH-2D data 4-13

4-15 Comparison of velocity vectors at cross section 4 between measured and SRH-2D data 4-13

4-16 Comparison of velocity vectors at cross section 1 between measured and U^2RANS data 4-14

4-17 Comparison of velocity vectors at cross section 2 between measured and U2RANS data 4-14

4-18 Comparison of velocity vectors at cross section 3 between measured and U^2RANS data 4-15

4-19 Comparison of velocity vectors at cross section 4 between measured and U^2RANS data 4-15

4-20 Comparison of relative velocity magnitude at cross section 1 4-16

4-21 Comparison of relative velocity magnitude at cross section 2 4-16

4-22 Comparison of relative velocity magnitude at cross section 3 4-17

4-23 Comparison of relative velocity magnitude at cross section 4 4-17

4-24 Solution domain and the mesh used for SRH-2D simulation 4-20

4-25 Bed elevation contours based on the elevations represented by the mesh in figure 4-24 4-20

4-26 Flow hydrograph representing the 1986 floodflow recorded below Glen-Colusa Irrigation District (GCID) 4-21

Figures (continued)

Page

4-27 The stage-discharge rating curve based on SRH±-1D simulation results 4-22

4-28 Partition of the solution domain into four gradation zones..... 4-23

4-29 The bed gradations used for each zone of the solution domain.... 4-24

4-30 Simulated velocity at the constant flow discharge of 4,431 cfs; results are used as the initial conditions..... 4-24

4-31 Net eroded (positive) and deposited (negative) depth in feet on January 18 and 31, relative to the bed elevation on January 1 4-25

4-32 Net eroded (positive) and deposited (negative) depth in feet on March 31 and April 30, relative to the bed elevation on January 1 4-26

4-33 Inundation and velocity contours at various times 4-27

4-34 Net eroded (positive) and deposited (negative) depth, relative to January 1, 1986, at various times..... 4-28

4-35 Sediment sorting with d50 distribution at various times 4-29

5-1 Left: Photograph looking north, showing the tops of 12 rhizopods located on the southern end of the rhizopod system. An additional 18 rhizopods are located on the north side of the entryway. Right: Seedlings in the T1 (top) and T5 (bottom) treatments after 62 days of growth..... 5-3

5-2 Seedling survival during controlled water table decline experiments 5-4

5-3 Daily average reduction in potential transpiration due to drought stress 5-17

5-4 Soil water characteristics for gravel and sand soils located on Sacramento River point bar at RM 192.5. Matric head is the negative of the soil water pressure head. 5-18

5-5 Comparison of ET reduction factor due to drought stress for seedlings grown on sand and gravel at RM 192.5 on the Sacramento River during 2006 5-20

5-6 ET reduction factor for various daily water table decline rates for the sand sediment type. 5-22

Figures (continued)

Page

5-7 Recovery of ET reduction factor for different rates of daily water table elevation increase 5-22

5-8 Desiccation and recovery rates for sand and gravel sediment as a function of water table decline rate..... 5-23

6-1 Flowchart for the Vegetation Module..... 6-4

6-2 Flow chart for the Establishment Module..... 6-6

6-3 Flow chart for the Growth Module 6-7

6-4 Flow chart for the Mortality Module 6-8

6-5 Comparison of CDWR (1991) and USACE (2002) river mile designations with overlap from RM 182 to RM 183)..... 6-15

6-6 Comparison of CDWR (1991) and USACE (2002) river mile designations with overlap from RM 190 to RM 194 6-16

6-7 Bed slope and energy grade line at a flow of 20,000 cfs 6-17

6-8 Stream profile from RM 80 to RM 215 (from HEC-RAS 3.1). The water surface elevations at flows of 20,000 and 90,000 cfs are shown..... 6-18

6-9 Sediment load at USGS gage on Sacramento River at Hamilton City..... 6-19

6-10 All available USGS bed load measurements along project reach..... 6-21

6-11 Gravel bed load data in project reach 6-22

6-12 Comparison between simulated and measured river stage at CDWR RM 183. The flow rate and simulated average bed elevation are also shown 6-38

6-13 Comparison between simulated and measured river stage at CDWR RM 192.5. The flow rate is also shown 6-38

6-14 Comparison between simulated and measured ground water elevation at CDWR RM 192.5..... 6-39

6-15 Comparison between measured and predicted gravel bed load transport near Hamilton City Bridge (RM 199)..... 6-40

6-16 Seed release characteristics at CDWR study sites RM 183 and 192.5. Catkins are a strand of tiny, inconspicuous and short lived flowers on cottonwoods 6-41

Figures (continued)

Page

6-17 Seedling dispersal patterns in 2005. Note gravel sized material at RM 183 6-42

6-18 Simulated area of cottonwood recruitment at RM 183 and RM 192.5 compared to measured seedling density 6-43

6-19 Simulated elevation above low water (6,000 cfs) of cottonwood recruitment, compared to measured elevations of recruitment in 2006. Site has gravel soil on a point bar at RM 192.5..... 6-44

6-20 Simulated elevations above low water (6,000 cfs) of cottonwood recruitment compared to measured elevations in 2006. Site has sandy soil on a point bar at RM 192.5..... 6-44

6-21 Illustration of trimming GIS coverage to match land area 6-48

6-22 Total vegetated area computed by SRH-1DV every 4 months (on 1 day in October, February, and June) for 8 years 6-52

6-23 Existing vegetation by cross section location in June 2007 (year 8)..... 6-53

6-24 2007 vegetation mapping at RM 186 to RM 190 6-54

6-25 New plants, 0 to 1 year, by river mile and vegetation type in October 2000, year 2..... 6-55

6-26 New plants, 0 to 1 year, by river mile and vegetation type in October 2007, year 8..... 6-56

6-27 Daily flows at 5 stations for an 8-year period as input to SRH-1DV..... 6-56

6-28 Total acres of desiccated plants for 8 years of simulation by river mile and vegetation type..... 6-57

6-29 Flow regime at Keswick and at RM 237.6 shown with total acres of desiccation for each vegetation type presented over time for 8 years of simulation. The upper chart shows the hydrologic regime (gage data) and the lower chart shows the acres of desiccation..... 6-58

Figures (continued)

Page

6-30 Total plant mortality from inundation with respect to time, shown with Figure 6-29 and 2 flow regimes (gage at Keswick and RM 237.5). 6-59

6-31 SRH-1DV simulation from October 2007 (8th year) with unlimited availability of seed and propagules where germination of invasive plants is not restricted to downstream locations. Peak not shown is over 700 acres. 6-60

Tables

Page

2-1 Tributaries Included in Analysis 2-3

2-2 Tributaries Excluded from Analysis 2-3

2-3 Scenarios Used to Compute Sediment Load Using Parker (1990) Equation 2-5

2-4 Phi Scale (log base 2) Grain Size Classification in mm 2-5

2-5 Range of Surface Material Sediment Yield (tons/year) 2-6

2-6 Range of Estimated Bed Load 2-13

3-1 Rating Curve 3-16

3-2 Summary of Parameters Used in Calibrating the SRH-Meander Model 3-17

4-1 Sediment Diameters of Each Size Class for the Simulation 4-21

4-2 The Surface Gradations at Selected Sample Locations Collected in 1981 4-23

4-3 The Bed Gradations Used for Each Zone of the Solution Domain 4-23

5-1 Grain Size Analysis for Sand Used in Controlled Experiments ... 5-2

5-2 Soil Physical Properties and Fitted van Genuchten Parameters for Sand Used in Controlled Experiments 5-2

Tables (continued)

		Page
5-3	Total Average Per-Plant Biomass (mg)	5-4
5-4	Total Average Maximum Root Depth (cm)	5-4
5-5	Model Parameters Set Using Field Observations	5-14
5-6	Observed and RHEM Simulated Per-Plant Biomass (mg) at H4 (Note: all T4 plants were dead by H4)	5-16
5-7	Observed and RHEM Simulated Maximum Root Depth (cm) at H4 (Note: all T4 plants were dead by H4)	5-16
5-8	van Genuchten (1980) Parameters Used to Characterize Gravel and Sand Gradation Soils from Sacramento River Point Bar at RM 192.5.	5-18
5-9	Observed and Modeled Plant Growth Values for a Seedling on Sand Sediment Located at RM 192.5 (June 1-August 16, 2006)..	5-19
6-1	Description of Groundwater Input Parameters for SRH-1DV	6-3
6-2	List of Active Stream Gages on Sacramento River	6-14
6-3	Manning's Roughness Coefficients Used in the SRH-1DV Model. (Roughness coefficient values are listed at locations where values change.)	6-17
6-4	Bed Material Distribution Averaged from USACE Samples between RM 140 to RM 226	6-18
6-5	Size Distribution for Incoming Sediment Load	6-20
6-6	Ground Water Parameters for Simulation	6-23
6-7	VIV Records Used in the 1999 to 2007 Simulation Matching Existing Mapped Vegetation to Initial Vegetation Conditions in the Model.	6-25
6-8	Vegetation Parameters for Model Simulation	6-28
6-9	Desiccation Rate of Cottonwoods for Sand and Gravel Soils	6-36
6-10	Model Sediment Parameters Used in the SRH-1DV Simulation..	6-40
6-11	Comparison of Vegetation Mapping Classification Systems Used for the Sacramento River in 1999 and 2007	6-46
6-12	Comparison of Changes in Area Simulated by Vegetation Modeling to Changes in Area Measured from Vegetation Mapping Between 1999 (Year 1) and 2007 (Year 8).	6-50

Tables (continued)

Page

6-13 Vegetation Divisions Based on Individual Vegetation Types with More than 50 Acres per Cross Section 6-54

6-14 A Comparison of Vegetation Coverage Under Two Scenarios of Invasive Plant Establishment..... 6-61

Chapter 1

Modeling Strategy

Contents

Page

1. Modeling Strategy 1-1
   - 1.1 Analysis Methods (Modeling Introduction) 1-1
   - 1.2 Using Models 1-3
     - 1.2.1 How Numerical Models Work 1-4
     - 1.2.2 How NODOS Models Work Together 1-5
   - 1.3 Model Descriptions 1-5
     - 1.3.1 Relationship to CALSIM-II 1-6
     - 1.3.2 SRH-Capacity 1-8
     - 1.3.3 SRH –Meander 1-8
     - 1.3.4 SRH-2D 1-9
     - 1.3.5 RHEM 1-10
     - 1.3.6 U^2RANS 1-11
     - 1.3.7 SRH-1D and SRH-1DV 1-11
   - 1.4 Report Organization 1-13
   - 1.5 Study Team 1-14

Figures

Page

1-1 Map of study area 1-2

1-2 Computer modeling cycle from prototype to the modeling results 1-4

1-3 Information flow diagram for numerical model integration 1-7

1. Modeling Strategy

Chapter 1 provides an overview of the models and how they work together.

The North of the Delta Offstream Storage (NODOS) Investigation evaluates the feasibility of offstream storage in the northern Sacramento Valley to improve water supply and water supply reliability, improve water quality, and enhance survival of anadromous fish and other aquatic species in the Sacramento River. The Bureau of Reclamation's (Reclamation) Mid-Pacific Region tasked the Sedimentation and River Hydraulics (SRH) Group at the Technical Service Center (TSC) to provide technical service to aid in evaluating potential NODOS alternatives.

This report documents the usefulness and accuracy of a suite of models in analyzing the effect of alternative flow operations on the riparian corridor of the Sacramento River from Colusa to Red Bluff (see the map of the study area in figure 1-1). Conceptual formulation of the modeling approach is documented in Reclamation (2006b). Additional model refinements (e.g., vegetation modeling) are discussed in this report**.** The models are intended to simulate aspects of:

- Flow hydraulics
- Sediment transport
- River meandering
- Establishment and survival of Freemont cottonwoods
- Interactions between these processes

1.1 Analysis Methods (Modeling Introduction)

Desired conditions and habitat can be associated with specific forms of the river as defined by the cross-sectional shape, longitudinal profile, and plan form (form as viewed from an airplane) of the river. River form is controlled through stream processes through several geomorphic factors: stream power (flow regime and bed slope); sediment (transport and grain size); and physical conditions of bank stability and valley topography. Desirable conditions for the Sacramento River can be directly related to river form and a specific combination of geomorphic factors. Regardless of the combination, river form will evolve and stabilize to match the geomorphic factors if the geomorphic factors persist over time.

The historical form of the Sacramento River and its associated geomorphic factors supported thriving fisheries and a diverse aquatic, riparian and terrestrial system. Today, the river also serves societal needs for water conveyance and crop cultivation, and these demands impose an altered set of geomorphic factors. With time, the river has adjusted to the new conditions, and river form today may differ

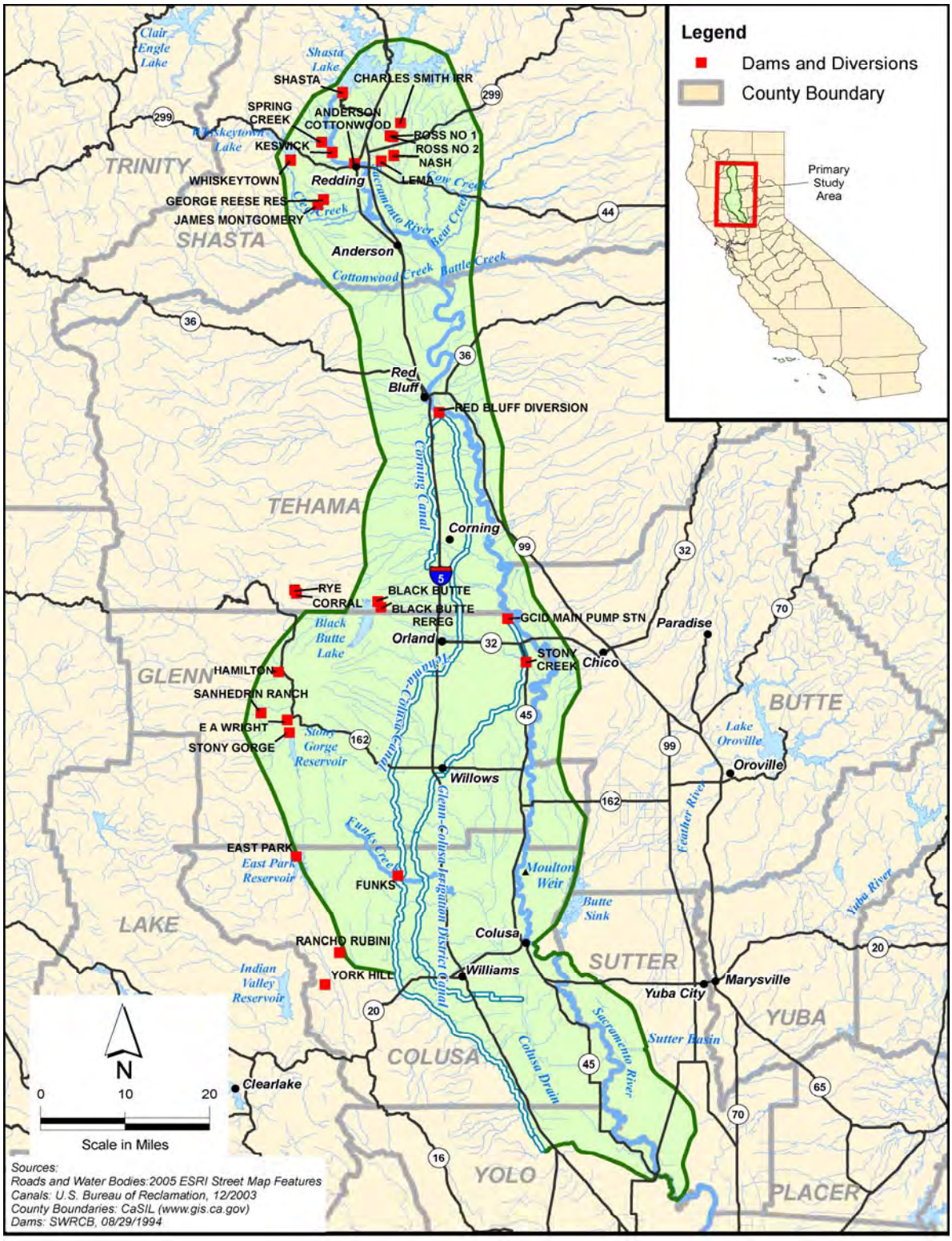

Figure 1-1. Map of study area.

in some ways from the historical form. Although alterations to flow regime and flood plain terrain can impose changes on sediment regime and ultimately river form, these actions, if accomplished in an informed manner, can both fulfill societal requirements and enhance desired ecological function such as restoration of a diverse riparian corridor.

The models will be an integral part of the overall approach to informed river management:

- Step 1: Analyze the existing river form and geomorphic factors
- Step 2: Identify management actions that may impact river geomorphic factors
- Step 3: Design, test, and refine management actions for impacts on river form
- Step 4: Implement refined management actions with desired river impacts
- Step 5: Monitor to ensure results match predicted outcome

These models will be invaluable in informing Step 3. Step 3 can be repeated multiple times in the search to determine beneficial management actions, so the test methods should be cost effective and timely, in addition to providing the level of analysis required. Models fulfill this analytical need within Step 3. Monitoring results in Step 5 can then inform the next repetition of Step 3.

1.2 Using Models

Two methods for testing river response are field implementation (implementing a solution on the ground and then using adaptive management for river responses) or modeling (using numerical data and algorithms to extrapolate river responses under various scenarios). Field implementation can be a useful approach for complex ecosystems with a high level of uncertainty; however, field implementation can be resource demanding and require long periods of study. Numerical models are a practical alternative, especially with physical river studies where aspects of the system are deterministic and there is a good scientific basis for predictive descriptions of both physical and ecosystem representations.

Numerical models are predictive tools that provide quantifiable responses for a range of imposed conditions or operating scenarios. Numerous parameters and operating constraints can be compared in a relatively short time, aiding the assessment of alternatives for informed decision making.

1.2.1 How Numerical Models Work

Models use data and knowledge to mathematically portray a "prototype" or the reality to be studied—how a river actually operates. The data represent boundary conditions, such as bathymetry, water discharges, sediment particle size distributions, vegetation types, etc. The knowledge is composed of the physical processes that are known to determine the system's behavior (i.e., the geomorphic factors that determine the rivers form, such as flow movement within the described terrain, flow friction and channel conveyance, sediment erosion and deposition, and vegetation growth and resistance).

Developing a model begins with studying the prototype and ends with the interpretation of the model results to draw conclusions. Figure 1-2 shows the cycle for developing models and interpreting them to provide results that can be used to compare operating scenarios.

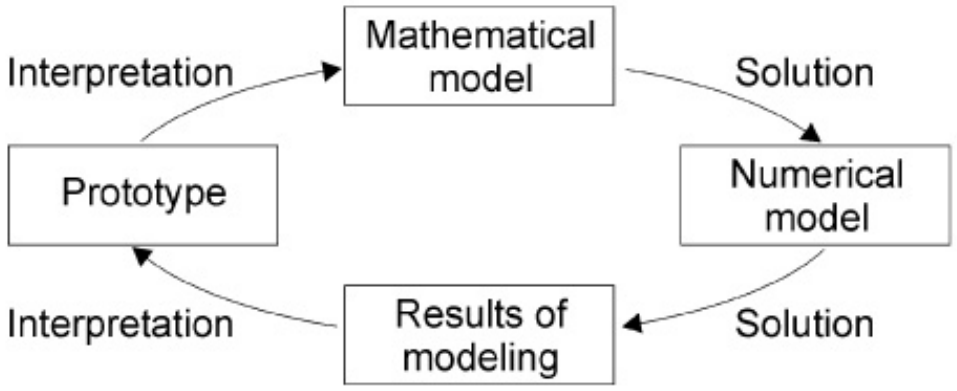

Figure 1-2. Computer modeling cycle from prototype to the modeling results.

The first process in a computer modeling cycle (figure 1-2) is to define the prototype and the data necessary to describe the system. In this first process of the cycle, all the relevant physical processes that were identified in the prototype are translated into governing equations that are compiled into the mathematical model. This mathematical model thus first approximates the problem.

Next, a solution process is required to solve the mathematical model.

The numerical model embodies the numerical techniques used to solve the set of governing equations that form the mathematical model. Then the data need to be interpreted and placed in the appropriate prototype context.

This last interpretation process closes the modeling cycle and ultimately provides the scenarios to be compared.

1.2.2 How NODOS Models Work Together

Despite the power of these analysis tools, there is no single model that can simulate all interacting river processes in complete detail. To incorporate all geomorphic factors for a prediction of the final river form; a series of models, informing each other, is often the best strategy. Each model can be used independently to address important management questions and can also be used to inform the other models. The output from several modeling tools describes the final river form and helps determine if management actions will have the beneficial or desired impacts on river form and the floodplain.

The strategy applied in this investigation was to use different process-based models that focus on different processes or simulate the process at a different scale so that a more complete understanding of each process, and the interactions of each process, could be understood. For example, the detailed RHEM model simulates the unsaturated flow field and bioenergetics of cottonwoods, but the model can only simulate laboratory or field conditions that occur at a single location such as a single point bar. Therefore, RHEM is used to develop computationally simplified relationships that capture most of the complexities between river and sediment processes and mortality of cottonwood seedlings, and these more efficiently parameterized relationships are then incorporated into the SRH-1DV model, which can be applied to the entire study area.

1.3 Model Descriptions

Each modeling activity is briefly described in this chapter. The process of applying the models could be iterative. For instance, an initial discharge hydrograph from CALSIM-II/USRDOM is used as input to the suite of models. Based on final results from the suite of models, operating conditions within CALSIM II can be modified to incorporate components for riparian vegetation survival that balance water storage and delivery needs with sustainable cottonwood forests. Alternative restoration strategies could also be evaluated involving removal of bank protection and planting native terrace forests in place of cleared exotic or agricultural vegetation.

Five models are used to examine the four processes of hydraulics, sediment transport, river meandering, and cottonwood establishment and survival:

1. **SRH-Capacity:** Simulates tributary supplies of sediment to the Sacramento River as well as reach-averaged erosion and deposition in the Sacramento River.

2. **SRH-Meander:** Simulates river meandering processes and bank erosion.

3. **Sedimentation and River Hydraulics Two Dimensional Model (SRH-2D) and Unsteady and Unstructured Reynolds Averaged Navier-Stokes Solver (U^2RANS) Three-Dimensional Model:** SRH-2D simulates lateral and longitudinal velocity, erosion, and deposition patterns within the Sacramento River. U^2RANS simulates lateral, longitudinal, and vertical velocity and flow patterns.

4. **RHEM:** Simulates unsaturated ground water flow and detailed bioenergetics of individual cottonwood plants.

5. **SRH-1DV:** Simulates flow hydraulics, sediment transport, and vegetation establishment and survival of the entire study area (Red Bluff to Colusa).

A flowchart of model inputs, linkages, and results is shown in Figure 1-3. Starting from the top, daily flow input was necessary for all the models in this strategy.

1.3.1 Relationship to CALSIM-II

Flow input was developed from an operational model, CALSIM-II,[1] which was constructed independent of this study. Information on the Sacramento River CALSIM-II model for NODOS is available in Reclamation (2006b). CALSIM-II provides monthly discharge volumes based on current or proposed water storage and delivery operations impacting the Sacramento River flow hydrograph. However, all five models listed above require daily flow values. Upper Sacramento River Daily Operations Model (USRDOM) was developed by CH_2MHILL for Reclamation to create daily flows from monthly values (Reclamation 2006b). Details of the CALSIM II and the USRDOM models are not contained within the present study.

[1] CALSIM-II is a generalized water resources simulation model for evaluating operational alternatives of large, complex river basins.

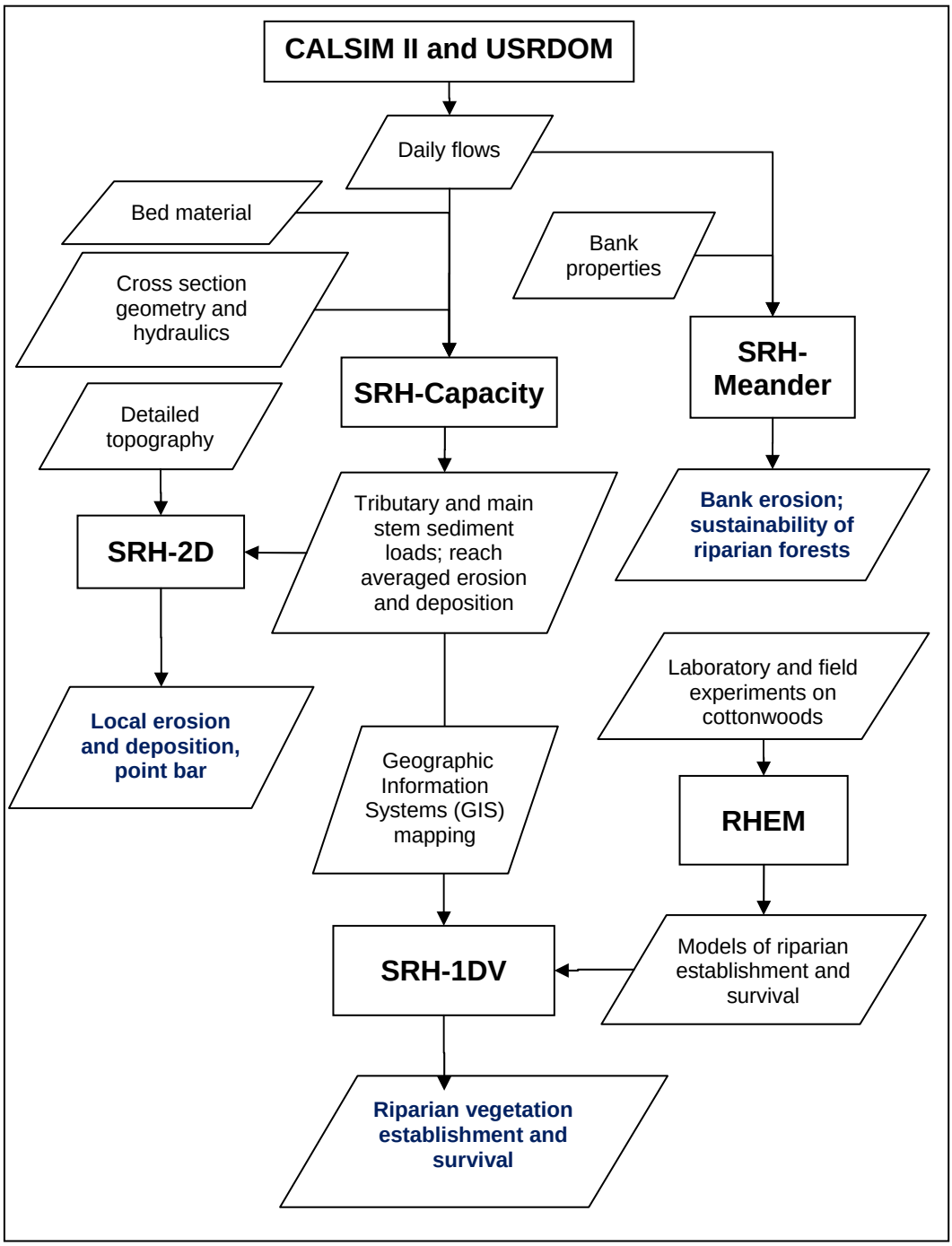

Figure 1-3. Information flow diagram for numerical model integration. Note that rectangles indicate models and parallelograms indicate data or knowledge transfer between models. Blue bolded text indicates end data results.

1.3.2 SRH-Capacity

1.3.2.1 Use

SRH-Capacity is used to evaluate current and future trends in transporting gravel in the Sacramento River. SRH-Capacity is used to compute the supply of gravel to the Sacramento River from tributaries and the transport capacity of the Sacramento River. The difference between the supply to the main stem and the capacity of the main stem can be used to compute the erosion and deposition that will occur in the Sacramento River.

1.3.2.2 Simulation

The input to the SRH-Capacity is a record of daily average flows at a particular site, cross section geometry, reach-averaged hydraulics, and sediment bed material. There must be a series of cross sections surveyed upstream and downstream of the location where a bed material sample was collected. The daily average flow record should be of sufficient length to determine a flow duration curve. The bed material sample should be of both surface and subsurface material. The sample should be large enough to represent the average gradation of the surface and subsurface material. The output from SRH-Capacity can provide sediment load boundary conditions for SRH-Meander and SRH-1DV.

1.3.2.3 Limitations

SRH-Capacity assumes that the hydraulic properties in the rivers remain constant and does not account for changes that may occur due to river meander processes or cutoff processes. It also does not account for the feedback between the erosion and deposition processes and the flow hydraulics.

SRH-Capacity is described in more detail in Chapter 2 and Appendix A.

1.3.3 SRH –Meander

1.3.3.1 Use

SRH-Meander is used to evaluate historical and future meander patterns in the Sacramento River. There are no currently available sediment transport models that can also model river meandering at the scale of the project reach (approximately 100 miles); therefore, SRH-Meander is intended to only simulate the meander processes and greatly simplifies some of the other detailed sediment transport processes. The other sediment models employed in this study assume that the channel position stays fixed in the horizontal plane.

1.3.3.2 Simulation

A recently reworked sediment bar is required for cottonwoods to establish. Therefore, downstream or lateral migration in areas targeted for cottonwood establishment is beneficial. Natural constraints on the channel or placed bank protection can prevent channel migration, causing continually reworking of point

bars and limiting opportunities for seedling establishment. SRH-Meander can be used to assess the ability of the river to continue to meander and regenerate the cottonwood forests.

Inputs to the model include daily flows, average cross section geometry, and bank erosion coefficients. Bank erosion coefficients are the primary calibration parameters, and historical migration data are necessary to calibrate these coefficients. Output from the migration model can be used to assess areas most likely to experience bank erosion, lateral channel migration, and avulsion. The model can be used to indicate which reaches will be the most active meandering reaches and, therefore, more likely to generate new areas for cottonwood recruitment. The model can also be used to indicate where bank protection is limiting channel migration. Model output can identify infrastructure or sensitive land that may be impacted by river meandering processes.

1.3.3.3 Limitations

SRH-Meander is limited because it does not directly simulate erosion or deposition. It also does not direct compute cottonwood establishment or survival. The bank resistance coefficients are calibrated based upon historical river meander rates. There are no generally accepted methods to predict bank resistance coefficients based upon physical properties. Therefore, historical information on the channel alignments and bank erosion are required to make predictions into the future.

1.3.4 SRH-2D

1.3.4.1 Use

SRH-2D is a two-dimensional hydraulic and sediment transport model. SRH-2D can predict flow patterns laterally and longitudinally and can simulate erosion and deposition throughout a channel for specific discharges. The model is capable of computing complex river hydraulics, including approximate secondary currents and lateral nonuniformity through meander bend and chute cutoff channels. SRH-2D can further model fluvial processes of point bar formation and development.

1.3.4.2 Simulation

Required model inputs include detailed topography of the stream channel and overbanks integrated into a two-dimensional mesh. The other inputs include the roughness of the channel and overbanks, downstream water surface elevations, and detailed information on bed material in the stream channel and flood plain. Water surface elevations can be obtained using one-dimensional hydraulics, and sediment load input can be obtained from SRH-Capacity.

SRH-2D has two main components: the hydraulic module and the sediment transport module. The hydraulic module solves for the flow depth and depth-averaged velocity at every point in the mesh. The flow depth and velocity

are then used in the sediment transport routines to compute sediment transport rates and erosion and deposition at every point in the mesh. The updated bed surface then is input into the hydraulic model and the simulation progresses for a specified time period.

1.3.4.3 Limitations

The main limitation to SRH-2D is the requirement of detailed geometry data to obtain a satisfactory resolution. The model output can only be as accurate as the topographic information input to the model. Resources are often limited in obtaining sufficient in-channel and overbank topography. Also, because of the heavy computational load of 2D sediment models, the simulation area is limited to a few miles for one high flow season to compute sediment transport and bed evolution. Larger reaches can be simulated if just flow information is desired.

1.3.5 RHEM

1.3.5.1 Use

RHEM couples biologic and hydrologic information to simulate growth of riparian vegetation during the initial recruitment period. RHEM dynamically simulates riparian shoot and root growth as a function of soil moisture content and plant transpiration requirements. The model simulates soil moisture content and water table beneath the point bar surface as a function of plant transpiration, river stage, aquifer properties, and local and regional scale ground water conditions. Ground water flux is estimated and tracked from lateral and vertical boundary conditions. Evapotranspiration and precipitation boundary conditions at the point bar surface are obtained from meteorological data. Physical and hydraulic properties of point bar sediments are also required model inputs for RHEM to simulate unsaturated flow in the root zone. Reclamation and Dr. Jim Richards of the University of California, Davis, conducted extensive field trials under controlled conditions to develop the parameters that RHEM requires for simulating cottonwood growth.

1.3.5.2 Simulation

RHEM is a cross section model which works effectively with the SRH suite of models; however, RHEM is a computationally intensive model and is not suitable for application over large river reaches. Consequently, RHEM is used to perform detailed simulations for particular types of point bar cross sections to determine the range of root zone thicknesses in which adequate soil moisture levels are present for vegetation survival during the initial growth period. Information from RHEM is used to determine the parameters for the larger scale, nonbiophysical model, SRH-1DV.

1.3.5.3 Limitations

Some aspects of the RHEM algorithms need further refinement. In particular, the root front velocity algorithm may need to be altered account for severe water stress and reduce the maximum root front velocity in this simulation.

1.3.6 U^{2}RANS

1.3.6.1 Use

U^{2}RANS is a comprehensive, general-purpose model routinely used to address many hydraulic engineering problems such as:

- Flow hydrodynamics in pools and river reaches upstream of hydropower dams
- Detailed flow characteristics around hydraulic structures
- Hydraulic impact of different project alternatives
- Fish passage facility design and evaluation
- Thermal mixing zone determination
- Design optimization, reservoir/lake stratification, selective cold water withdrawal, etc.

1.3.6.2 Simulation

U^{2}RANS is a three-dimensional hydraulics (3D) model applied to many research and engineering projects to understand flow and sediment dynamics. U^{2}RANS uses state-of-the-art, unstructured computational fluid dynamics technology to unify multi block structured mesh and unstructured mesh elements into a single platform, and combines two-dimensional (2D) and 3D solvers in a common framework. U^{2}RANS can compute the vertical and horizontal velocity field on a very detailed scale. The turbulence is simulated using two-equation turbulence models.

1.3.6.3 Limitations

The main limitation of U^{2}RANS models is that they are usually applied to a river reach less than 5 miles long due to their heavy requirement for computer power. Similar to the 2D model, U^{2}RANS requires substantial topographic information and can only provide results to the resolution of the topography.

1.3.7 SRH-1D and SRH-1DV

SRH-1D is a cross-section based model for assessing flow hydraulics and sediment transport in the general direction of flow (Huang and Greimann 2007). SRH-1DV uses SRH-1D as the base code with the addition of a module for the simulation of ground water, and a vegetation module for simulating the establishment, growth and survival of multiple vegetation types. Like SRH-1D, the water surface and hydraulics can be computed in one dimension, and a channel can adjust to changes in sediment and water balances by aggrading or eroding the bed. The model also tracks the growth of multiple types of

vegetation, including cottonwood, at every point in every cross section of the model. The simulation predicts vegetation growth and mortality on a daily basis for multiple vegetation types in the floodplain from Red Bluff Diversion Dam to Colusa across an eight-year simulation period.

1.3.7.1 Simulation

Input data required by the model include cross section geometry, sediment loading determined from SRH-Capacity, and daily flow values from CALSIM-II and USRDOM. The input to support the simulation of vegetation includes the initial vegetation types of the reach of interest as well as several vegetation parameters. The vegetation parameters control the response of vegetation to the hydraulic and sediment conditions. The model does not attempt to directly simulate the biologic processes that occur in a particular vegetation type. Instead, the user is responsible for inputting such information as the typical germination periods, root growth rates, and the rate at which desiccation occurs when roots are separated from the water table. This information is used in conjunction with the hydraulic information from SRH-1DV to compute the germination, growth, growth and mortality of each vegetation type.

SRH-1DV provides stage-discharge relationships for all cross sections and tracks how these stage-discharge relationships vary in time. Ground water is also estimated based on the river water surface and soil conductivity. The model tracks the water table for each cross section. The model assumes that ground water at one cross section is not significantly affected by ground water at another cross section. Vegetation establishment, growth, and mortality are computed in response to daily inputs of flow and computations of hydraulics, ground water surface and sediment transport. Five vegetation types are studied: cottonwood, mixed forest, Gooding's black willow, narrow leaf willow, and riparian invasive plants, with three additional types for land-use tracking. The establishment, growth, and death of each vegetation type are tracked at each point within each cross section. After establishment, the growth of roots, stems, and canopies are simulated, and the competition between plant types is predicted. Modes of plant mortality can include desiccation, inundation (drowning), burial, scour, competition, shading or senescence (age). The RHEM model is incorporated to govern the determination of young cottonwood dessication. With this approach, SRH-1DV is used to simulate vegetation survival, including cottonwoods, over longer river reaches and time scales than RHEM.

1.3.7.2 Limitations

Assessments of vegetation growth are limited to the framework of cross section points of a one-dimensional (1D) model. No vegetation growth is simulated between cross sections so each point represents a strip of land extending half the distance upstream or downstream to adjacent cross sections. Computations are large scale and focus on average response. Also the model is limited to a study of riparian vegetation depends on the river water surface—and not on rain fall and resulting soil moisture storage. Several vegetation parameters are required to

perform simulations and each parameter requires field or laboratory data to verify. For example, the desiccation rate of each plant as a function of water table drawdown rates is input. These desiccation rates need to be obtained from laboratory experiments and other detailed studies. In addition, the input parameters such as root growth rates may be dependent upon other factors not represented in the model, such as nutrients in the soil. Parameters are assigned based on the known range of real world values but predictive accuracy can be improved with calibrations that help account for 1D model structure in describing plant cycles.

1.4 Report Organization

The following chapters of the report correspond to each of the five models listed above.

- Chapter 2 contains details of the application of SRH-Capacity to the Sacramento Basin. An extensive data collection effort to obtain the necessary data input to the model is documented. However, little data exist with which to calibrate or verify the model results. Within Chapter 2, SRH-Capacity results are reported on estimated tributary bed material entering the Sacramento River and trends in movement through the main stem river. Methods for model development are reported in detail in Appendix A.

- Chapter 3 details the calibration of SRH-Meander. Historic river centerlines are used to calibrate bank erosion coefficients in three reaches of the Sacramento River.

- Chapter 4 describes the validation of SRH-2D using measured velocity and water surface elevation data from a specific reach of the Sacramento River. SRH-2D was also applied using an historical flow event to demonstrate simulation of sediment erosion and deposition within a meander bend

- Chapter 5 contains the testing of RHEM against controlled seedling growth experiments, calibrations and validations with laboratory and field experiments as well as observed conditions, and application of the model to determine parameters for the SRH-1DV model.

- Chapter 6 describes the development and calibration of SRH-1DV. In the first phase of development, three aspects the model are calibrated:

    - Channel roughness values are calibrated to match known water surface elevation data

- Sediment transport equations are calibrated to match sediment load data

- Vegetation growth parameters are calibrated to match known cottonwood survival data

In the second phase of SRH-1DV model development, vegetation module capabilities are expanded and five additional vegetation types are added. Cottonwood modeling is validated, and four vegetation types are calibrated using GIS vegetation mapping from 1999 and 2007. SRH-1DV simulates vegetation growth across the floodplain of the project area (Red Bluff Diversion to Colusa) for a period of 8 years.

Appendix B describes the computer field codes needed for the vegetation input files for SRH-1DV.

1.5 Study Team

The study team for this effort consisted of Reclamation engineers and scientists from the Mid-Pacific Regional (Sacramento, California), the TSC (Denver, Colorado), and the Stockholm Environment Institute (SEI) (Davis, California). Significant data collection support was afforded by the California Department of Water Resources. The Reclamation Mid-Pacific Office contracted SEI to provide a database of readily available data from past Sacramento River studies.

Chapter 2

Sedimentation River and Hydraulics Capacity Model

Contents

Page

2. Sedimentation River and Hydraulics Capacity Model..... 2-1
   - 2.1 Range in Tributary Sediment Loads 2-2
   - 2.2 Range in Estimates of Main Stem Sediment Bed Loads 2-9
   - 2.3 Sediment Mass Balance in Main Stem 2-17
   - 2.4 Conclusions and Recommendations 2-21
     - 2.4.1 Erosion and Deposition Patterns 2-21
     - 2.4.2 Recommendations 2-23
     - 2.4.3 Model Use 2-23

Figures

Page

2-1 Annual tributary yield based on surface material (MPN shear, Scenario 784); very fine sand to small boulders..... 2-7

2-2 Annual tributary yield based on surface material (Parker defaults); very fine sand to small boulders..... 2-8

2-3 Annual tributary yield based on surface samples (MPN shear, Scenario 4); very fine gravel to small boulders..... 2-8

2-4 Annual tributary yield based on surface samples (Parker defaults); very fine gravel to small boulders..... 2-9

2-5 Annual main stem yield based on surface material (MPN shear, Scenario 4); very fine sand to small boulders..... 2-11

2-6 Annual main stem yield based on surface material (Parker defaults, Scenario 5); very fine sand to small boulders..... 2-11

2-7 Annual main stem yield based on surface material (MPN reference shear, Scenario 4); very fine gravel to small boulders 2-12

2-8 Annual main stem yield based on surface material (Parker defaults); very fine gravel to small boulders (Scenario 5) 2-12

2-9 Range of sediment yield for material greater than 2 mm 2-14

2-10 Range of sediment yield for material greater than 8 mm 2-14

2-11 Energy slope in Sacramento River at 90,000 cfs..... 2-15

2-12 Representative bed material diameter in Sacramento River 2-15

Figures (continued)

		Page
2-13	Schematic of mass balance calculations for reach (i).....	2-17
2-14	Mass balance of surface material greater than 2 mm based on historical hydrology.....	2-19
2-15	Mass balance of surface material greater than 8 mm based on historical hydrology.....	2-20
2-16	Erosional and depositional reaches as predicted by SRH-Capacity. Flow is to the south.	2-22

Tables

		Page
2-1	Tributaries Included in Analysis	2-22
2-2	Tributaries Excluded from Analysis.....	2-3
2-3	Scenarios Used to Compute Sediment Load Using Parker (1990) Equation	2-5
2-4	Phi Scale (log base 2) Grain Size Classification in mm.....	2-5
2-5	Range of Surface Material Sediment Yield (tons/year)	2-6
2-6	Range of Estimated Bed Load.....	2-13

2. Sedimentation River and Hydraulics Capacity Model

The Sedimentation and River Hydraulics Capacity Model (SRH-Capacity) used to simulate tributary supplies of sediment to the Sacramento River as well as reach-averaged erosion and deposition in the Sacramento River. Chapter 2 describes how SRH-Capacity functions and how it was applied to the Sacramento River.

This model calculates transport capacity and was used to:

- Compute estimates of tributary sediment
- Detect trends of erosion or aggradation in the system
- Construct a sediment budget

These results are incorporated with the results of the other models to improve understanding of sediment transport processes, channel change in response to water management operations, and to support the establishment and survival of cottonwoods in the Sacramento River study area.

The SRH-Capacity model is a hydraulic and sediment transport numerical model developed to calculate sediment transport capacity, incipient motion, and annual sediment loads. The Bureau of Reclamation's (Reclamation) Technical Service Center (TSC) Sedimentation and River Hydraulics Group developed this program. Some of the model's capabilities are:

- Sediment transport capacity in a river reach, given reach hydraulics
- Incipient motion hydraulics for each sediment size class
- Computation of annual sediment load
- Multiple noncohesive sediment transport equations that are applicable to a wide range of hydraulic and sediment conditions

Both tributary and main stem computations focus on bed load and not total sediment load (bed load plus suspended load) computations. In the Sacramento River, bed load is assumed to be as the fraction of sediment load most important for determining bed elevation changes. Suspended load may also play a role in determining bank heights and flood plain elevations, but this load does not significantly interact with the bed. The suspended load is primarily composed of fine sands and silts. The bed material of the Sacramento River in the reach of interest is primarily comprised of gravel sizes (>2 millimeters [mm]), which will only move as bed load.

Sediment transport capacity depends on the bed material, hydraulics, shear stresses, and the selected sediment transport function. The surface sediment characteristics provide information related to the Sacramento River geomorphology. The analysis of surface, subsurface, and combined sediment data for the tributaries is discussed in Appendix A. Appendix A also presents the development of the hydrology, channel hydraulics, and bed material. Sediment transport capacity for the Sacramento River is calculated using the Parker (1990) transport function and utilizes the Mueller et al. (2005) approach to estimating the reference shear stress as a function of channel slope. This chapter focuses on surface sediment calculations:

- Section 2.1, Range in Tributary Sediment Loads, describes the calculations for determining the sediment load in relevant Sacramento River tributaries. This section provides a range of values for tributary sediment loads based on a sensitivity study of transport equations and parameters.

- Section 2.2, Range in Estimates of Main Stem Sediment Loads, describes the calculations for determining the sediment load in the main stem of the Sacramento River. This section provides a range of values for Sacramento River sediment loads based on a sensitivity study of transport equations and parameters.

- Section 2.3, Sediment Mass Balance in Main Stem, presents a sediment budget (comparing the contributing load from the upstream reaches and the tributaries to the transport capacity of each reach) that identifies erosional and depositional reaches.

- Section 2.4, Conclusions and Recommendations, presents conclusions from this study.

Incorporating tributary sediment estimates, the Sacramento main stem is modeled to examine sediment movement using SRH-Capacity. The methods used in modeling the main stem sediment loads are described in Appendix A, Section A.2, and a range of values for main stem sediment load by reach is presented in Section 2.4.

2.1 Range in Tributary Sediment Loads

The investigation of tributary sediment loads provides information on a natural source of material to the Sacramento River downstream of Shasta Reservoir. Results support development of a sediment budget and estimates of the present and future geomorphic impacts on the Sacramento River as a result of imbalances in sediment supply and transport. Data sources include cross section surveys, bed

material sampling, U.S. Geologic Survey (USGS) Digital Elevation Models (DEM), and USGS stream gages. Table 2-1 shows the tributaries included in the analysis, their delineated watershed areas in square miles, and reaches (described in Section 2.4.1).

Table 2-1. Tributaries Included in Analysis

Name	River Mile (RM)	Delineated Area (mi2)	Reach
Stony	190	780.7	11
Big Chico	192.8	78.2	12
Sandy	192.8	7.5	13
Deer	219.5	206	14
Thomes	225.3	292.9	15
Mill	229.9	134.3	15
Elder	230.4	138.9	15
Antelope	234.7	166.1	16
Red Bank	243.1	109.7	17
Reeds	244.8	64.8	17
Dibble	246.6	32.2	17
Blue Tent	247.7	17.7	17
Battle	271.4	362.4	18
Cottonwood	273.5	918.6	18
Bear	277.6	111.4	19
Dry	277.6	9.7	19
Cow	280.1	421.4	19
Stillwater	280.8	66.1	20
Clear	289.3	241	20

Note: mi^2 = square miles

Table 2-2 shows tributaries that were excluded from the analysis because they were assumed to exert minor influence. There may be a need to revise the analysis if some of these are found to contribute significant amounts of sediment.

Table 2-2. Tributaries Excluded from Analysis

Tributary	River Mile (RM)	Area (mi^2)
Mud Creek	193.00	150.7
Kusal Slough	194.64	64.3
Pine Creek	196.43	145.4
Burch Creek	209.40	146.2
Toomes Creek	223.0	73.8

Table 2-2. Tributaries Excluded from Analysis

Tributary	River Mile (RM)	Area (mi^2)
McClure Creek	226.50	41.4
Coyote Creek	233.14	25.4
Dye Creek	234.11	41.3
Salt Creek	240.15	46.1
Paynes Creek	253.00	95.1
Inks Creek	264.54	29.9
Ash Creek	277.22	29.9
Anderson Creek	278.31	19.9
Churn Creek	291.35	34.7

Basin cross section surveys and sediment sampling were performed within 74 percent of the drainage area. Identified but unmeasured tributary basins account for 17 percent of the drainage area. The remaining 9 percent of the Lower Sacramento Basin area drains directly into the main stem of the Sacramento River. The cross section surveys were performed at the sediment sample location as well as upstream and downstream of the sediment sampling location.

Sediment yields for each tributary were computed based on methods described in Appendix A, Section A.1.4, Sediment Transport. A sensitivity analysis of sediment load computation methods with varying sediment transport equations, reference shear stress values, and hiding factors is also presented in Appendix A, Section A.1.4.

Within the Parker (1990) equation for computing bed load, two parameters are included that require calibration through bedload samples: the reference shear stress and the hiding factor. Because bedload sampling with which to calibrate the two parameters is typically unavailable, Mueller, Pitlick, and Nelson (Mueller et al. 2005) developed a method of estimating the reference shear stress for a gravel bed river (abbreviated as MPN). The MPN can be used to compute the reference shear stress based on river slope in lieu of using the default reference shear stress value from Parker (1990), which may or may not be applicable to a given river system. Five different combinations of the reference shear stress and a hiding factor were evaluated. In addition to calculating the tributary loads using the Parker default reference shear stress and hiding factor (**Scenario 5**) , there were four iterations of the model for which sensitivity analyses were performed:

- **Scenario 1.** The MPN reference shear stress combined with the default hiding factor from Parker (1990).

- **Scenario 2**. Increasing the MPN reference shear stress by 25 percent, combined with the default hiding factor from Parker (1990).

- **Scenario 3.** Decreasing the MPN reference shear stress by 25 percent, combined with the default hiding factor from Parker (1990).

- **Scenario 4**. Combining the 100-percent MPN reference shear stress with a hiding factor of 0.67.

Table 2-3 shows these scenarios.

Table 2-3. Scenarios Used to Compute Sediment Load Using Parker (1990) Equation

Input Parameter	Scenario 1	Scenario 2	Scenario 3	Scenario 4	Scenario 5
Reference shear	100% MPN: 0.022	125% MPN: 0.027	75% MPN: 0.016	100% MPN: 0.022	Parker: 0.0386
Hiding factor	Default: 0.905	Default: 0.905	Default: 0.905	Low: 0.67	Default: 0.905

The results are presented for material greater than 2 mm and for material greater than 8 mm. Gravel is typically defined as material greater than 2 mm; however, very fine gravel and fine gravel (2-8 mm) material may not play a large role in bed morphology. As such, the sediment yield results are presented for two sediment ranges: (1) sediment larger than 2 mm and (2) sediment larger than 8mm. Table 2-4 shows the grain size classification in mm. Table 2-5 shows the potential range of surface material sediment yields resulting from the five scenarios.

Table 2-4. Phi Scale (log base 2) Grain Size Classification in mm

Description		Lower Limit	Upper Limit
Very fine sand	vfs	0.0625	0.125
Fine sand	fs	0.125	0.25
Medium sand	ms	0.25	0.5
Coarse sand	cs	0.5	1
Very coarse sand	vcs	1	2
Very fine gravel	vfg	2	4
Fine gravel	fg	4	8
Medium gravel	mg	8	16
Coarse gravel	cg	16	32
Very coarse gravel	vcg	32	64
Small cobble	sc	64	128
Large cobble	lc	128	256
Small boulder	sb	256	512

Table 2-5. Range of Surface Material Sediment Yield (tons/year)

Site	Maximum and Minimum Yields Resulting From Scenarios 1, 2, 3, 4				Scenario 5	
	Upper Yield (>2 mm)	Upper Yield (>8 mm)	Lower Yield (>2 mm)	Lower Yield (>8 mm)	Parker Default Yield (>2 mm)	Parker Default Yield (>8 mm)
Clear surface	23,395	23,356	5,497	5,484	3,561	3,551
Stillwater surface	1,984	1,800	58	42	10	6
Cow surface	85,201	85,201	11,303	11,303	5,201	5,201
Dry surface	520	427	7	4	1	0
Bear surface	1,806	1,604	121	94	5	3
Cottonwood surface	73,956	63,494	10,182	8,707	3,490	2,937
Battle surface	42,430	42,430	3,898	3,898	3,138	3,138
Blue Tent surface	79,585	47,676	29,140	16,952	33,176	19,230
Dibble surface	12,245	9,222	3,165	2,269	1,935	1,358
Reeds surface	61,671	46,043	29,453	21,584	24,270	17,663
Red Bank surface	132,063	93,558	55,743	38,296	38,851	26,750
Antelope surface	150,527	150,527	24,617	24,617	39,016	39,016
Elder surface	56,860	41,717	28,309	20,323	19,084	13,483
Mill surface	36,577	36,435	7,143	7,098	8,700	8,649
Thomes surface	154,009	102,110	33,992	22,292	15,772	10,017
Deer surface	155,420	153,758	43,383	42,891	35,110	34,709
Sandy surface	68,458	56,201	15,055	11,867	28,787	23,263
Big Chico surface	223,095	196,862	77,909	68,083	51,980	45,089
Stony surface	194,130	152,802	74,600	59,132	44,200	34,609
Grand total	1,553,932	1,305,223	453,574	364,937	356,286	288,672

As can be seen in table 2-4, the total annual sediment yield from the tributaries computed with the default Parker reference shear stress and hiding factor is lower than the sediment yield when using the MPN reference shear stress. The upper bound on yield results from either the 75-percent MPN coupled with the default hiding factor (Scenario 3) or the 100-percent MPN reference shear stress coupled with the 0.67 hiding factor (Scenario 4).

Figures 2-1 and 2-2 compare the annual tributary yield based on MPN reference shear (Scenario 4) and Parker default reference shear (Scenario 5), respectively, for material ranging from very fine sand to small boulders. Figures 2-3 and 2-4 compare the annual tributary yield based on Scenario 4 and 5, respectively, for material ranging from very fine gravel to small boulders.

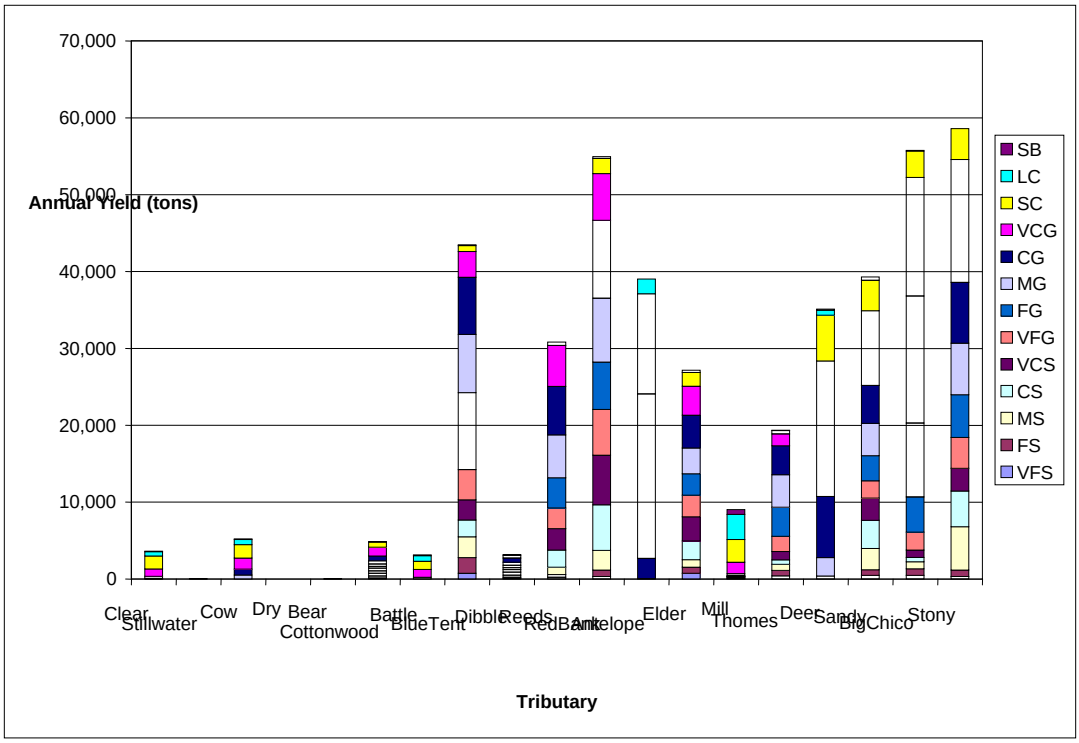

Figure 2-1. Annual tributary yield based on surface material (MPN shear, Scenario 784); very fine sand to small boulders.[1]

Based on table 2-4, Big Chico Creek has the highest calculated annual tributary yield of material greater than 2 mm; however, the sediment connectivity between Big Chico Creek and the Sacramento River is tenuous due to the number of diversions and other anthropogenic influences on Big Chico Creek. The connectivity of Sandy Creek to the Sacramento River has also been altered and the sediment load that reaches the Sacramento may be significantly less. Only Cow, Battle, and Mill Creeks contributed a significant mass of small boulders. Bear, Dry, and Stillwater Creeks contributed negligible sediment material.

[1] For figures 2-1 through 2-4, SB = Small Boulder, LC = Large Cobble, SC = Small Cobble, VCG = Very Course Gravel, CG = Course Gravel, MG = Medium Gravel, FG = Fine Gravel, VFG = Very Fine Gravel, VCS = Very Coarse Sand, CS = Course Sand, MS = Medium Sand, FS = Fine Sand, VFS = Very Fine Sand, and CM = Coarse Silt.

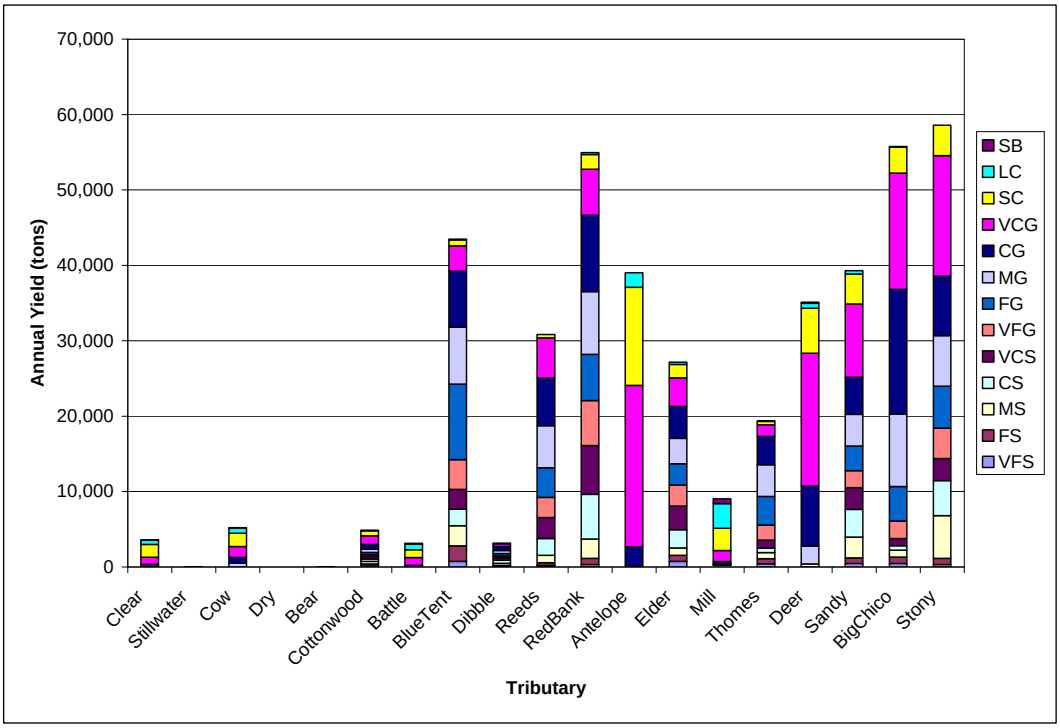

Figure 2-2. Annual tributary yield based on surface material (Parker defaults); very fine sand to small boulders.

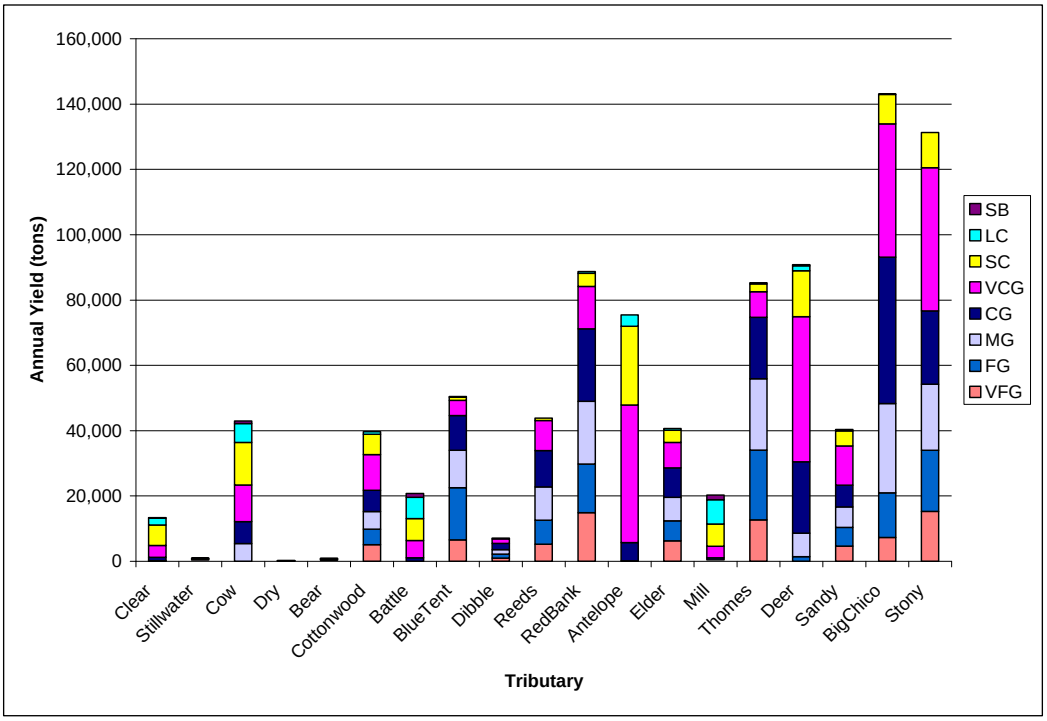

Figure 2-3. Annual tributary yield based on surface samples (MPN shear, Scenario 4); very fine gravel to small boulders.

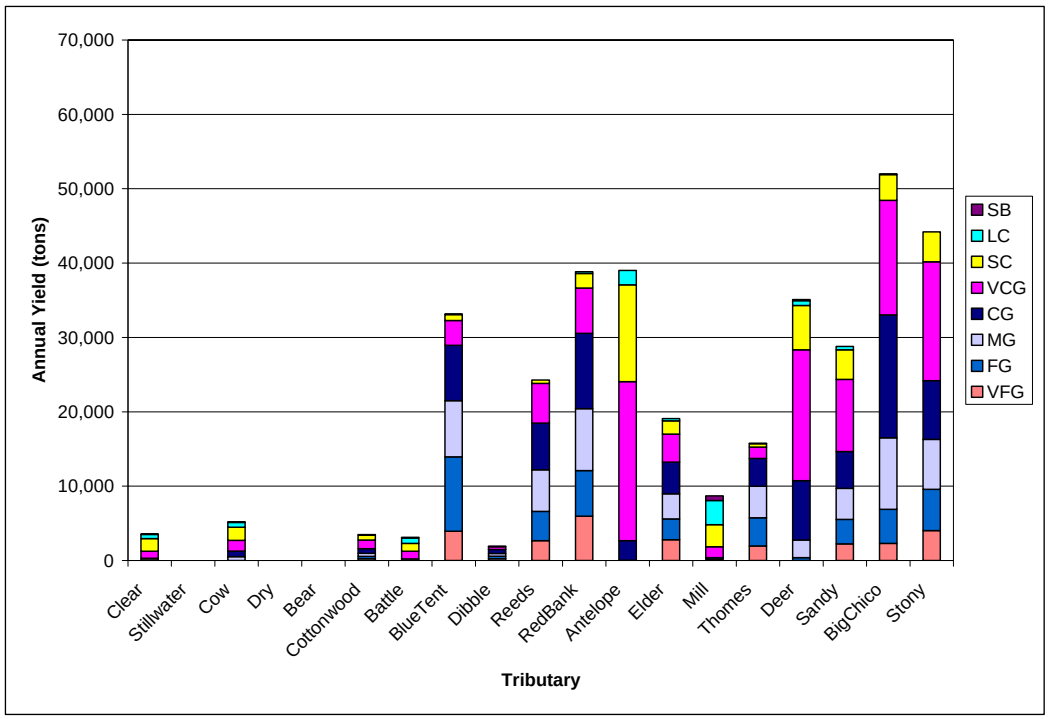

Figure 2-4. Annual tributary yield based on surface samples (Parker defaults); very fine gravel to small boulders.

2.2 Range in Estimates of Main Stem Sediment Bed Loads

The investigation of main channel sediment loads provides information on the Sacramento River's ability to transport tributary material downstream of Keswick Dam under historical flow conditions. Data sources include existing hydraulic models, existing bed material grain size distributions, and USGS stream gages. Methods for computing main stem sediment loads are described in more detail in Appendix A, Section 2.

Main channel sediment loads for historical flow conditions for 23 distinct reaches between RM 296 and RM 80 (Keswick Dam to Knights Landing) using SRH-Capacity. Reaches were identified using hydraulic parameters and are described in Appendix A, Section 2. Sediment yields were determined by multiplying the sediment transport capacity (tons per day) by the average number of days per year experiencing the flow rate to obtain an average annual sediment yield in tons per year. Only gravel-sized materials (greater than 2 mm) are considered in the computation of sediment yield due to the importance of gravel in determining river bed morphology.

USGS has collected many suspended load samples in the Sacramento River, but gravel moves only as bed load and there are significantly less bed load measurements in the river (USGS 2010). Chapter 6 contains a plot of the available data (figure 6-10). Note that there is only one measurement for flows above 25,000 cfs, which is still considered a relatively low flow in a river where flows over 100,000 cfs are common. Most bedload transport would occur at flows above 25,000 cfs. Therefore, it is difficult to determine transport rates throughout the river based upon this one flow measurement.

There is considerable uncertainty regarding the computation of sediment bed load in the absence of bed load measurements. To estimate the range of possibility of sediment loads in the Sacramento River, a range of potential sediment parameters is used. Table 2-5 presents the five scenarios (combinations of reference shear and hiding factors used for surface material grain size distributions). Table 2-6 shows the potential range of sediment yields for reaches 23 through 10, resulting from the sensitivity study.

Figure 2-5 shows the estimated average annual yield for each reach broken down by size class ranging from very fine sand to small boulders for Scenario 4. Figure 2-6 shows the average annual yield based on Parker default values (Scenario 5) for each reach broken down by size class ranging from very fine sand to small boulders. Figure 2-7 shows the Scenario 4 estimate of average annual yield for each reach broken down by size class ranging from very fine gravel to small boulders. Figure 2-8 shows the average annual yield for Scenario 5 for each reach broken down by size class (ranging from very fine gravel to small boulders).

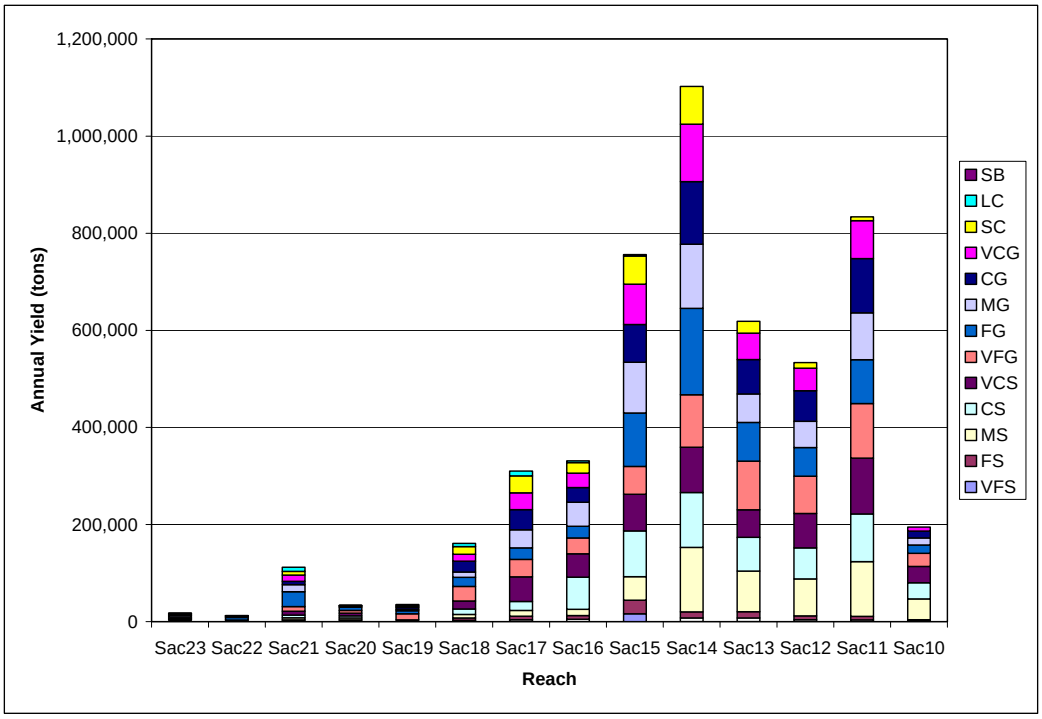

Figure 2-5. Annual main stem yield based on surface material (MPN shear, Scenario 4); very fine sand to small boulders.

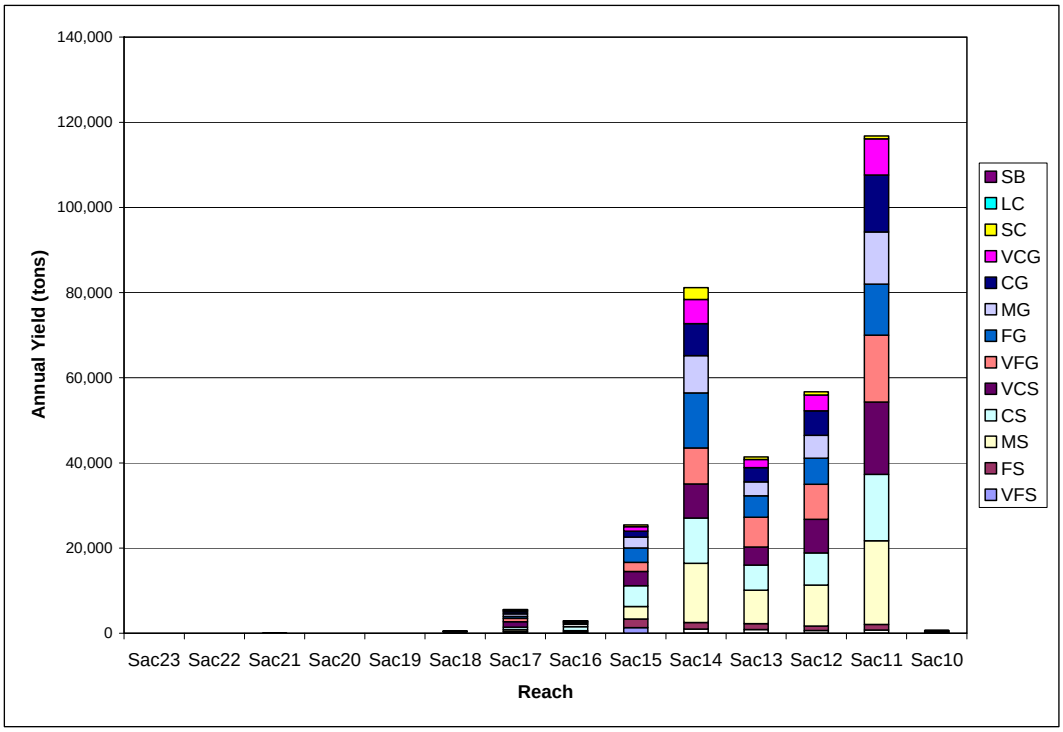

Figure 2-6. Annual main stem yield based on surface material (Parker defaults, Scenario 5); very fine sand to small boulders.

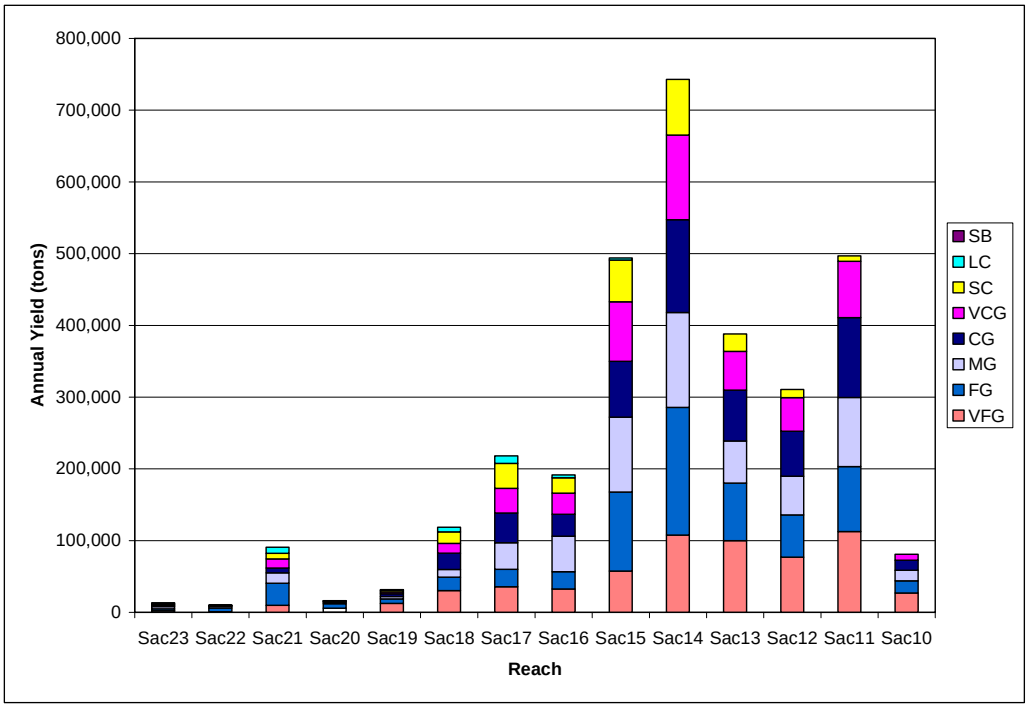

Figure 2-7. Annual main stem yield based on surface material (MPN reference shear, Scenario 4); very fine gravel to small boulders.

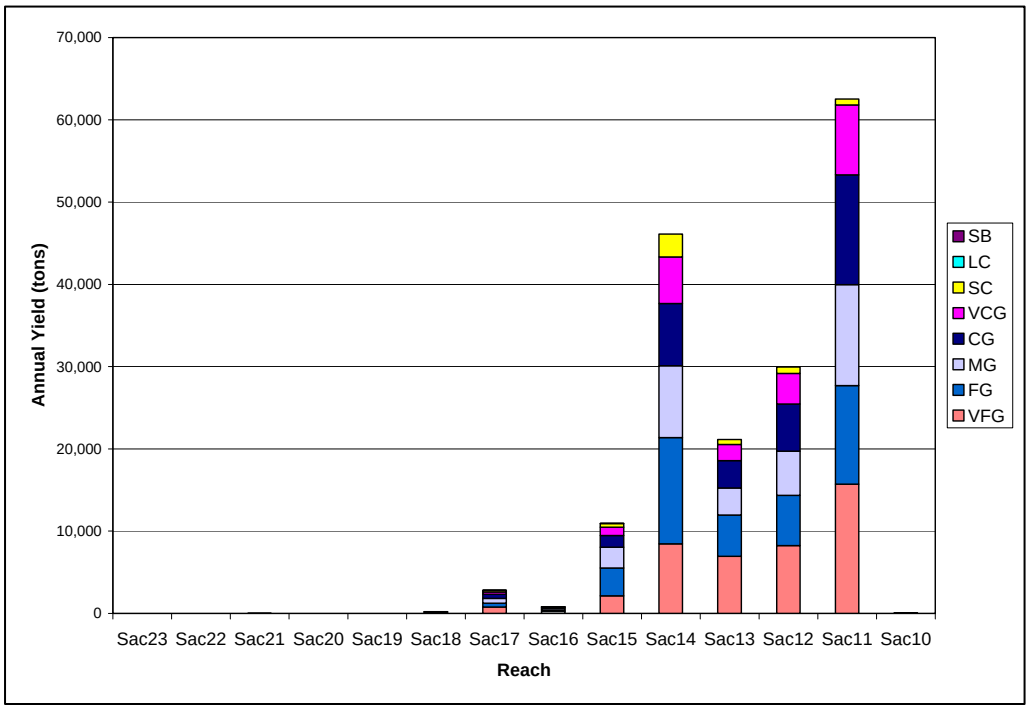

Figure 2-8. Annual main stem yield based on surface material (Parker defaults); very fine gravel to small boulders (Scenario 5).

Table 2-6. Range of Estimated Bed Load

	Maximum and Minimum Yields Resulting from Scenarios 1, 2, 3, 4				Scenario 5	
Reach/River Mile	Upper Yield (>2 mm)	Upper Yield (>8 mm)	Lower Yield (>2 mm)	Lower Yield (>8 mm)	Parker Default Yield (>2 mm)	Parker Default Yield (>8 mm)
23 / 296.0-292.5	31,794	15,979	170	90	2	1
22 / 292.5-290.0	31,641	9,973	18	8	0	0
21 / 290.0-283.5	206,356	111,256	2,217	1,174	28	11
20 / 283.5-275.0	52,494	9,046	24	9	0	0
19 / 275.0-268.0	77,091	31,084	544	180	6	1
18 / 268.0-252.3	214,129	164,101	8,364	4,662	215	70
17 / 252.3-243.0	397,816	334,879	42,146	31,478	2,836	1,597
16 / 243.0-225.3	377,111	311,196	24,964	17,439	834	404
15 / 225.3-215.0	938,071	712,122	123,096	83,096	10,939	5,417
14 / 215.0-203.6	1,345,016	947,676	258,454	164,736	46,108	24,743
13 / 203.6-190.0	705,377	449,750	130,503	72,537	21,140	9,162
12 / 190.0-175.6	556,699	358,990	127,784	75,226	29,933	15,567
11 / 175.6-166.8	853,789	565,948	235,218	142,576	62,524	34,818
10 / 166.8-157.0	195,798	116,746	5,816	1,668	65	14

Figure 2-9 shows the range of sediment yield (minimum, mean, maximum) by reach for material greater than 2 mm for all five scenarios. Figure 2-10 shows the range of sediment yield by reach for material greater than 8 mm for all 5 scenarios.

The sediment loads in the mainstem can generally be explained in the context of Lane's balance, which can be written as:

$$QS \propto Q_s d_{50}$$

where Q is flow rate, S is energy slope, Q_s is sediment supply, and d_{50} is the median bed particle diameter. The average energy slope and representative particles diameters in the Sacramento River are shown in figures 2-11and 2-12.

The most upstream reaches, reaches 20 - 23 are characterized by a high energy slope, and the sediment diameters are large because no sediment is supplied to these reaches. Therefore, the sediment transport rates through these reaches are low. Some tributaries enter upstream of Reach 19, but they contribute relatively minor amounts of gravel sized sediment. The slope also markedly decreases in Reach 19 and therefore, there is little sediment transport occurring in this reach.

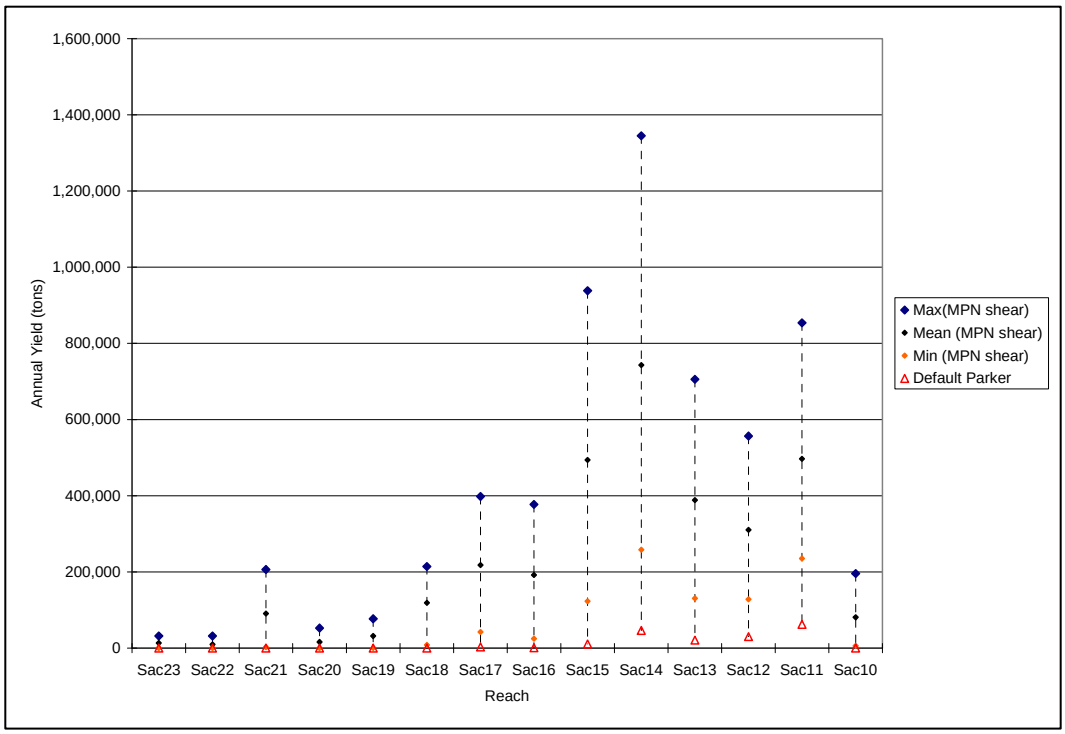

Figure 2-9. Range of sediment yield for material greater than 2 mm.

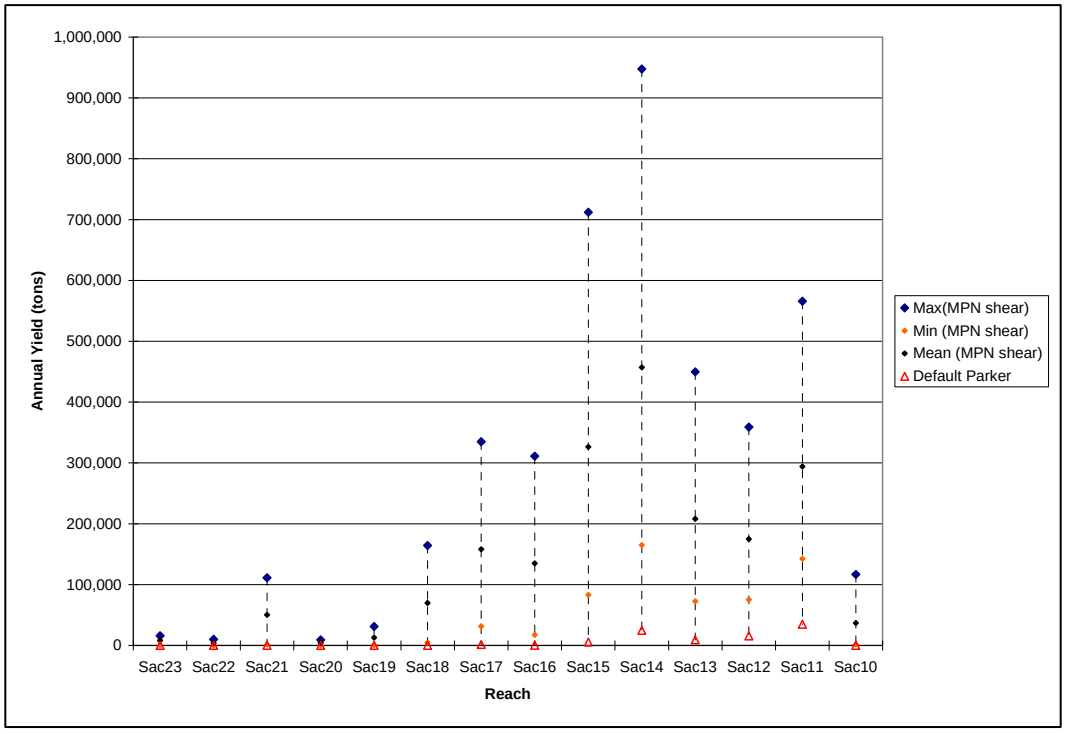

Figure 2-10. Range of sediment yield for material greater than 8 mm.

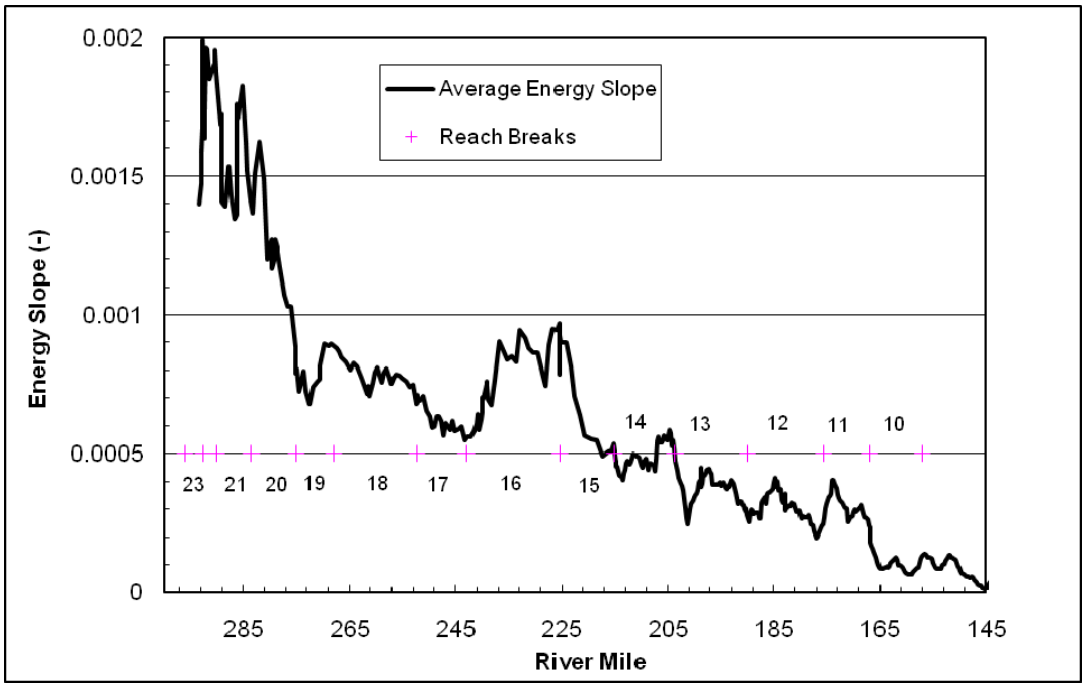

Figure 2-11. Energy slope in Sacramento River at 90,000 cfs.

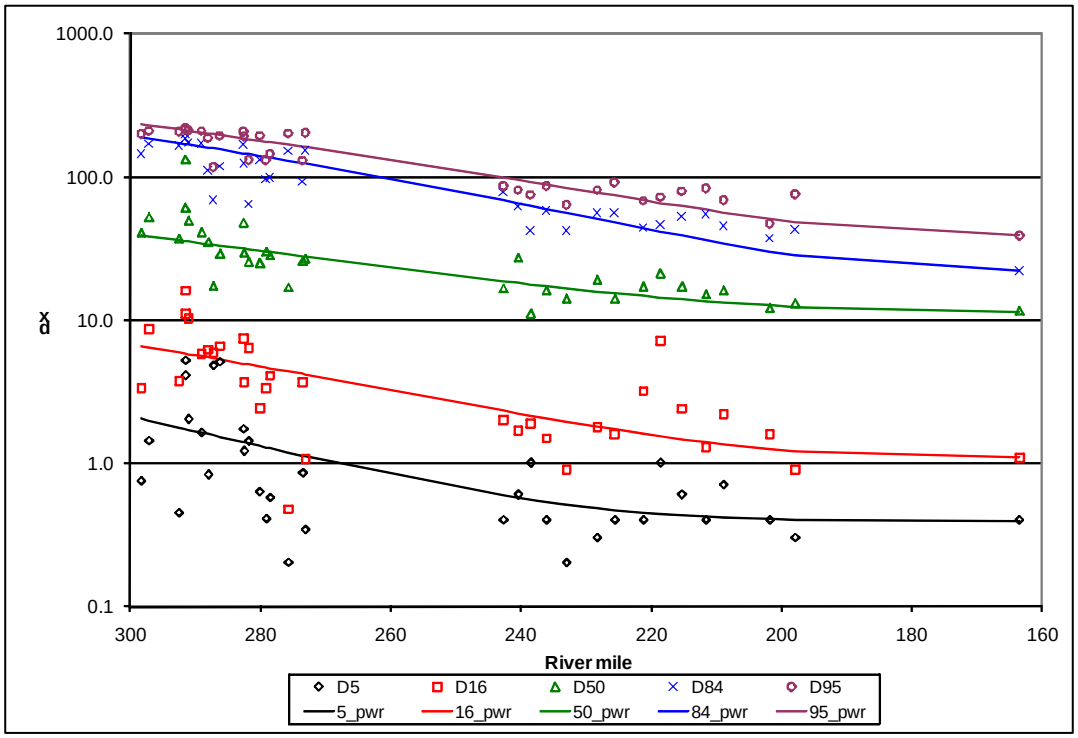

Figure 2-12. Representative bed material diameter in Sacramento River.

Tributary supply starts to be significant in Reach 18 with the addition of Cottonwood Creek' sediment load. The peak flows become greater, and the bed material becomes smaller. Due to these factors, even though the energy slope in Reach 18 is less than in Reaches 20 - 23, sediment transport rates are significantly higher in Reach 18.

Reach 17 is immediately upstream of Red Bluff Diversion Dam, and the energy slope of the river is significantly less in this reach than in Reach 18 and 16. However, the sediment transport capacities of Reaches 17 and 16 are approximately the same and greater than Reach 18. Increased transport capacities in these reaches is primarily due to additional tributaries that enter into Reach 17, such as Reeds, Dibble, and Red Bank, that contribute significant amounts of gravel sized sediment.

Sediment transport rates increase significantly in Reaches 15 and 14 because the bed material size is decreasing more rapidly from upstream to downstream than the energy slope. These two reaches are predicted to have the greatest transport rates of the reach from Keswick Dam to Colusa.

The transport rate in Reach 13 decreases significantly because the energy slope decreases significantly in this reach. Reach 13 begins at RM 203 and ends at RM 190, which is near the confluence with Stony Creek. The sediment transport rates continue to decrease in Reach 12 because of the continued decrease in energy slope.

Transport rates in Reach 11 increase because the energy slope remains relatively consistent, but the bed material decreases in size. However, it should be noted that very little bed material data were collected in Reaches 12 and 11. Therefore, the bed material had to be interpolated from adjacent reaches. Significant uncertainty is associated with the calculated sediment transport rates in these reaches.

The most-downstream reach of this assessment, Reach 10, shows a significant decrease in sediment transport capacity and also in energy slope. Moulton Weir is located in this reach, and this weir significantly decreases the peak flow in the Sacramento River.

2.3 Sediment Mass Balance in Main Stem

A quantitative estimate of the erosion and deposition occurring in each reach is made using a sediment budget where the incoming sediment to a reach (from upstream reach and tributaries) is compared to the outgoing sediment from a reach (assumed to equal the yield of that reach). Reach (*i*) would have the incoming sediment yield of the upstream reaches (*i*-1) and input from the tributaries in that reach. Figure 2-13 provides a schematic showing a mass balance for reach (*i*), and equation 2-1 is used to calculate the sediment balance for reach (*i*).

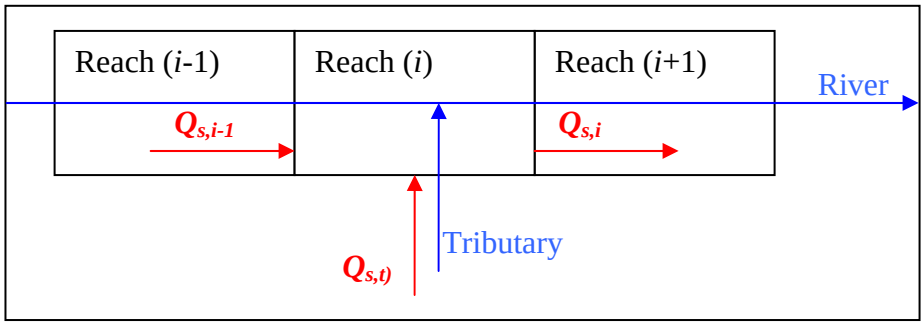

Figure 2-13. Schematic of mass balance calculations for reach (*i*).

$$\Delta V_i = \left(Q_{s,i-1} + Q_{s,t} - Q_{s,i} \right) \Delta t \qquad 2\text{-}1$$

Where:

ΔV (i) = weight (tons) of deposition in reach *i*
$Q_{s,i-1}$ = sediment load (tons/year) for the reach upstream of *i*
$Q_{s,t}$ = sediment load (tons/year) for tributary (t) in reach *i*
$Q_{s,i}$ = sediment load (tons/year) for reach *i*
Δt = time (year)

The mass balances were computed assuming the maximum, minimum, and average values resulting from the four scenarios in table 2-3. A mass balance assuming default Parker values was also computed. A positive sediment yield implies aggradation is possible for that reach, and a negative sediment balance implies degradation is possible.

The assumed upstream boundary condition is zero incoming sediment for Reach 23 (from Keswick Dam). The sediment budget assumes that sediment load from each upstream reach is at the upstream reach's transport capacity (that either there will be erosion in that upstream reach to increase sediment supply or that there will be deposition in that reach to decrease sediment supply). Reach 22 would have incoming sediment equal to the yield of Reach 23, no input from

tributaries (Appendix A, Table A-10), and sediment output equal to the yield as presented in table 2-6. These mass balance calculations continue in the downstream direction. The sediment budget was calculated for the range of sediment yields to produce a range of potential erosion or deposition. figures 2-14 and 2-15 present the mass balance calculations for historical hydrology by reach for material greater than 2 mm and greater than 8 mm, respectively. These values represent the upper (8mm) and lower (2mm) bounds of material likely to travel as bed load, which affects channel morphology and spawning habitat. Sediment sizes lower than this are expected to be transported as suspended load, which has a negligible effect on morphology.

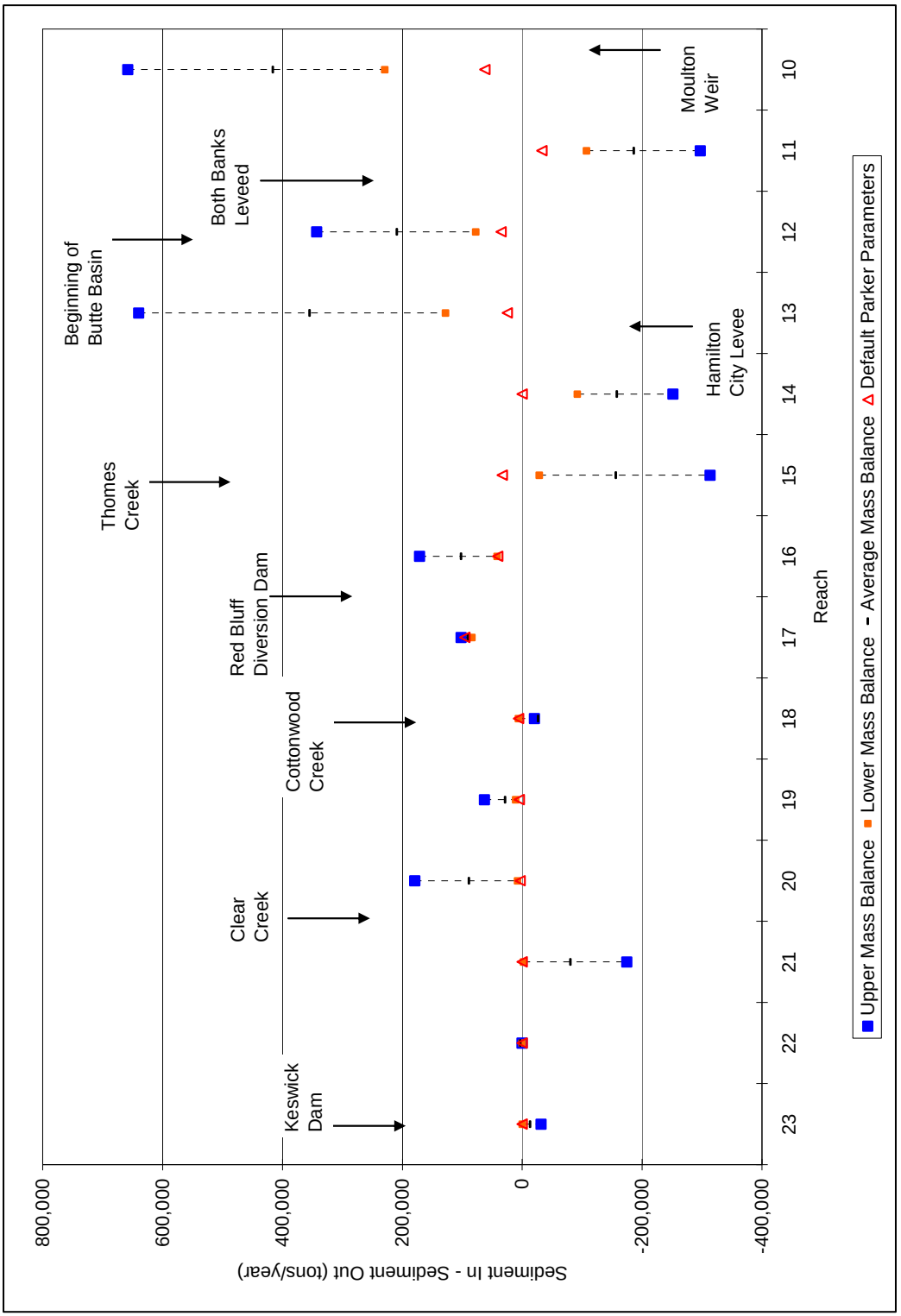

Figure 2-14. Mass balance of surface material greater than 2 mm based on historical hydrology.

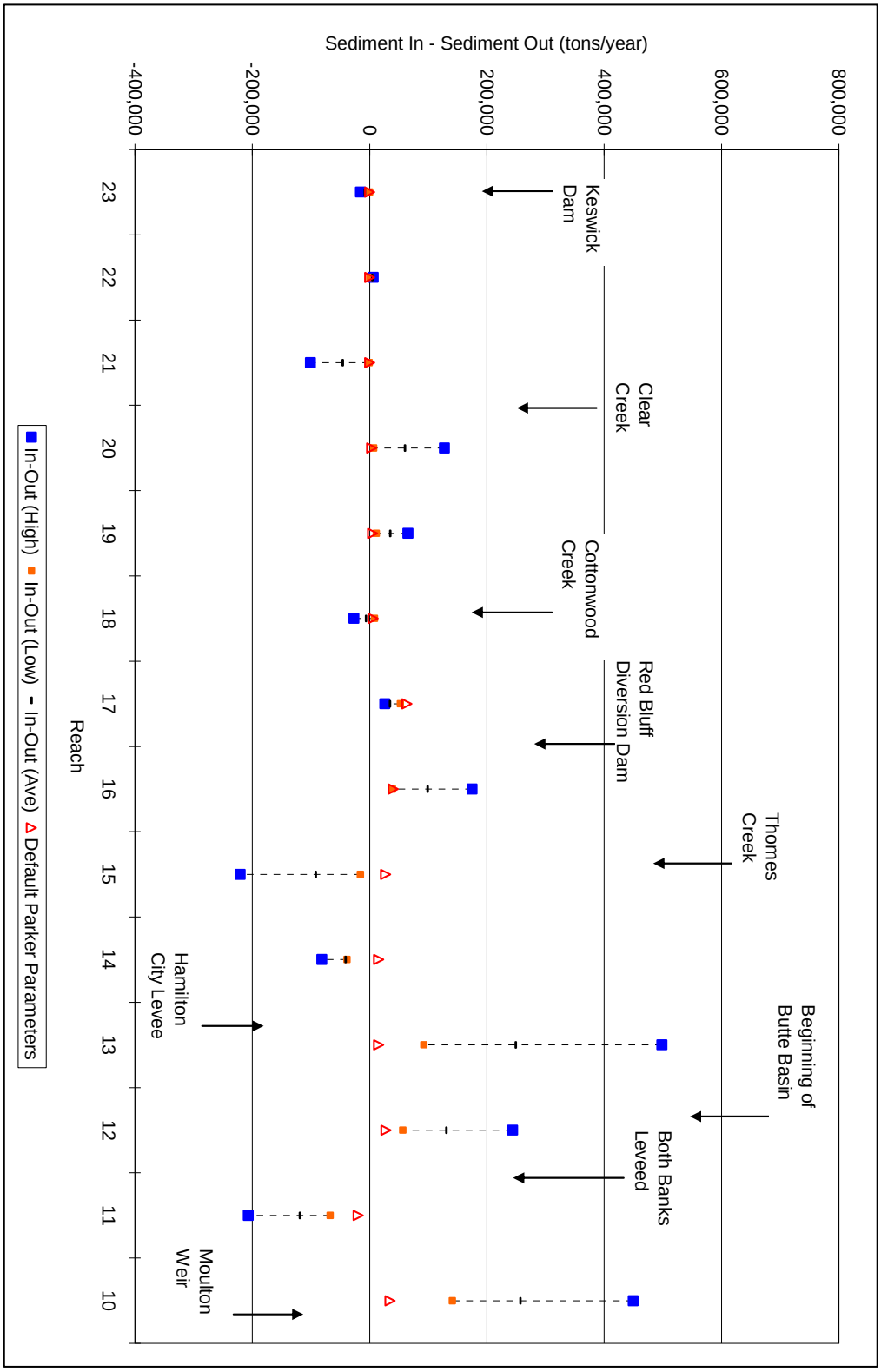

Figure 2-15. Mass balance of surface material greater than 8 mm based on historical hydrology.

2.4 Conclusions and Recommendations

2.4.1 Erosion and Deposition Patterns

The sediment mass balance can be used to provide a map of erosional and depositional reaches (figure 2-16). Based upon the results in figure 2-16, the reaches were classified as armored, slightly erosional, erosional, balanced, slightly depositional, or depositional. Armored indicates that the bed is essentially immobile. Erosion would have occurred in the past, but the sediment has been mined from the reach and the erosion process has stopped because the sediment remaining in the bed is large enough so that flows cannot mobilize it. Classifications of slightly erosional or slightly depositional indicate that there is a slight trend towards erosion or deposition in this reach, but that the uncertainty associated with the estimates did not conclusively prove that the reach is erosional or depositional. Balanced indicates that the computations showed that the sediment entering the reach was approximately balanced by the sediment transport capacity of the reach. Classifications of erosional or depositional indicate that the results of the capacity analyses strongly suggest a condition of degradation or aggradation.

Reaches 23 and 22 are immediately downstream of Keswick Dam and are essentially immobile, with very little sediment movement. No significant tributaries enter into these reaches, and the main channel moves very little sediment. Reach 21 also has very little bed load movement because the only significant tributary in this reach is Clear Creek, which supplies a small amount of sediment. Reach 21 is expected to be slightly erosional, with relatively small rates of erosion.

Reaches 20, 19, and 18 were predicted to be in balance. Some tributaries enter in these reaches, and the mainstem transport capacity increases accordingly.

Reaches 17 and 16 were predicted to be slightly depositional, but the rates of deposition were not large. Several tributaries enter into this reach that supply significant amounts of sediment. The current Sacramento River in these reaches may not be capable of transporting all of that material downstream. However, the rates of deposition would be difficult to monitor because they are less than 50,000 tons per year. Averaged over the 27 miles of river, the rate of deposition would be less than 0.2 inch per year, assuming a channel width of 600 feet.

Reaches 15 and 14 have large sediment transport capacities and are predicted to be slightly erosional. Similar to Reaches 17 and 16, however, the rates would be difficult to measure. Reach 13 shows more significant rates of deposition because of the decrease in energy slope in this reach.

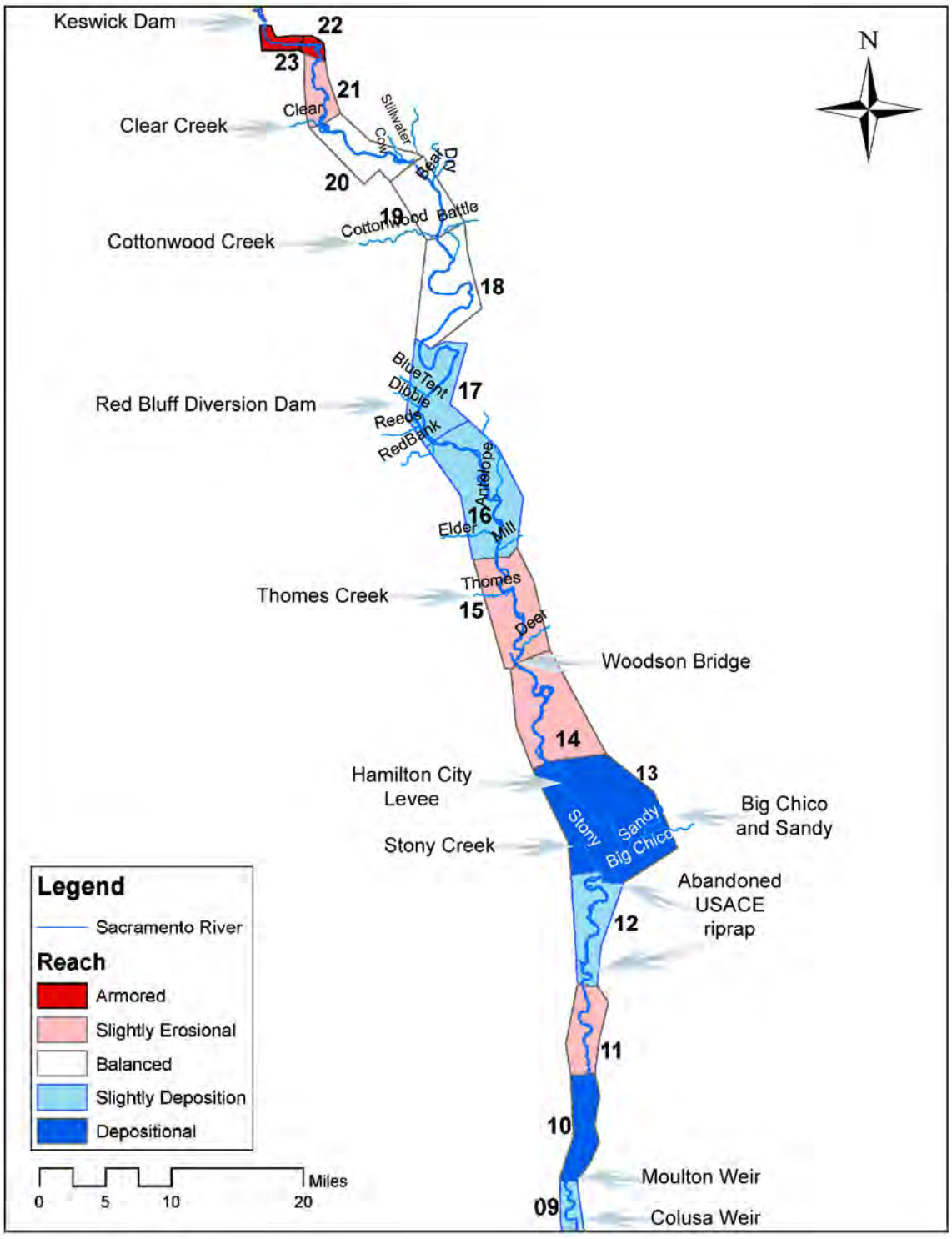

Figure 2-16. Erosional and depositional reaches as predicted by SRH-Capacity. Flow is to the south.

Reaches 12 and 11 may be affected by bank protection measures. Reach 11 is downstream from an effective grade control structure created from the abandoned bank protection at RM 178. The bank protection, without maintenance, did not keep the river from meandering. Currently, the river crosses the abandoned bank protection, which now may act as a grade control structure. There is also a constriction caused by State Highway 45, as well as levees occurring on both sides of the river at the upstream portion of Reach 11. This constriction may be causing a backwater condition in the lower portion of Reach 12, allowing sediment to settle. Therefore, the supply of sediment into Reach 11 may be reduced, causing erosion in this reach, thus also supplying Reach 10 with available sediment.

Reach 10 shows significant amounts of deposition because of the reduction in stream slope and the fact that Moulton Weir removes significant amounts of the peak flow.

2.4.2 Recommendations

There are many uncertainties in the current analysis. Bed material information is missing in several locations. Another difficultly is the lack of bed load information in the main stem or tributaries. The sediment transport formulas used in this study could be calibrated based upon measurements of bed load, which would significantly improve the certainty.

In spite of the uncertainties, most of the deposition and erosion rates are small relatively to the size of the river, but a few locations may warrant additional analysis. Reach 10 contains the Moulton Weir and the site of the proposed Delevan Diversion. Because the slope decreases in this reach and the weir reduces peak flows, deposition is likely to be an issue in the future. Future studies should collect new survey and bed material information. Comparison of historical surveys and aerial photographs with more recent data could be used to quantify deposition rates and calibrate the sediment transport models.

2.4.3 Model Use

The SRH-Capacity model can be used to simulate loads for the tributary and main stem under various scenarios with changing hydraulics, bed materials, and transport capacity functions. The model can be used to run a variety of simulations using different reference shear stresses, hiding factors, and transport equations. Estimates from the model can then be compared to observed data to determine appropriate equations and factors for the Sacramento River.

This information can then be used in other models, such as the Sedimentation River Hydraulics-One-Dimensional Sediment Transport Dynamics Model (SRH-1D) and the Unsteady and Unstructured Reynolds Averaged Navier-Stokes solver (U^2RANS), to provide better model results.

Chapter 3

Meander Modeling

Contents

Page

3. Meander Modeling 3-1
   - 3.1 Model Description 3-1
   - 3.2 Model Calibration Using Laboratory Data 3-2
     - 3.2.1 Input Data 3-4
     - 3.2.2 Calibration Process 3-6
     - 3.2.3 Model Calibration Not Incorporating Vertical Erosion 3-6
     - 3.2.4 Model Calibration With Raster Elevation Update and Bank Height Resistance Coefficient 3-8
   - 3.3 Calibration Using Field Data 3-12
     - 3.3.1 Data Preprocessing 3-12
     - 3.3.2 Model Calibration 3-14
   - 3.5 Conclusions 3-21

Figures

Page

3-1 Post-test and pre-test photos of the study channel, from USACE (1945) 3-3

3-2 Thalweg traces at periodic time intervals, from USACE (1945) 3-3

3-3 Centerlines for four time steps along with the valley axis of the channel 3-5

3-4 Calibration resulting in the first bend being modeled 3-6

3-5 Calibration resulting in the second bend being modeled 3-7

3-6 Calibration resulting in the third bend being modeled 3-7

3-7 Calibration resulting in the fourth bend being modeled 3-8

3-8 Calibration results with raster elevation update and bank height resistance coefficient 3-11

Figures

Page

3-9 Comparison of channel topography between laboratory model and computational model. The top picture is from USACE (1945). The bottom is simulated in SRH-Meander..... 3-11

3-10 SRH-Meander project reach 3-13

3-11 Flow discharge data at Vina Woodson Bridge at RM 219 (VIN)..... 3-15

3-12 Flow discharge data at Hamilton City gauge at RM 199.2 (HMC)..... 3-15

3-13 Flow discharge data at flow hydrograph from DWR gauge Ord Ferry at RM 184.2 (ORD) 3-16

3-14 Calibration result in reach 1..... 3-18

3-15 Calibration result in reach 2..... 3-19

3-16 Calibration result in reach 3..... 3-20

Tables

Page

3-1 Rating Curve 3-16

3-2 Summary of Parameters Used in Calibrating the SRH-Meander Model 3-17

3. Meander Modeling

The Sedimentation and River Hydraulics Meander Model (SRH-Meander) simulates river meandering processes and bank erosion. This chapter describes the model and calibration.

3.1 Model Description

Channel migration is an important process to maintain cottonwood forests because channel migration will create new bare surfaces on which cottonwoods can establish. Channel migration is also important for introducing woody vegetation into the river systems, which provides habitat for various aquatic species. Without channel migration, cottonwood forests would age, and little regeneration of the forest would occur. Also, little woody vegetation would be introduced into the river system.

SRH-Meander is a computer model that simulates the bed topography, flow field, and bank erosion rate in a curved river channel with an erodible bed. SRH-Meander can be used to predict channel migration in meandering rivers for infrastructure and maintenance concerns and for vegetation studies. In each time step, SRH-Meander:

1. Calculates the flow field based on either the standard step method, normal depth method, or a user input rating curve.

2. Computes the channel bank erosion rate

3. Updates the channel alignment with the erosion rate, including the instigation of a channel cutoff if it is needed

SRH-Meander uses methods first proposed by Johannesson and Parker (1989). It is a re-derivation of the analysis by Engelund (1974). The basic idea behind these analyses is to write the flow variables as a sum of two parts:

1. The solution to the case of flow in a straight channel

2. A deviation from the straight channel solution for the case of a slightly curved channel

The deviation is assumed to be linearly related to the maximum curvature of the channel. These perturbed flow variables are substituted into the three-dimensional (3D) flow equations. The equations are then simplified and grouped into the terms responsible for the straight channel flow solution and terms due to the channel curvature. The equations become ordinary differential equations and can be solved analytically or through relatively simple numerical methods. The

sediment transport rates are assumed to be a function of the local velocity and shear stress. The model is not intended to improve upon the sediment transport rates of the Sedimentation River Hydraulics Capacity Model (SRH-Capacity), and these calculations are only performed in this model as an intermediate calculation to the meander rates (figure 1-3).

Johannesson and Parker (1989) assume the bank erosion rates are related to the near-bank depth-averaged flow velocity, which is calculated by a small perturbation approach. The near bank depth-averaged flow velocity is decomposed into two components characterized by local curvature forcing and the free system (see Johannesson and Parker 1989 for further explanations of these concepts). Sun et al. (2001a, b) improved Johannesson and Parker's (1989) linearization theory to calculate bank erosion in river meanders by incorporating a multiple-size sediment transport equation. SRH-Meander adopted the Sun at al. (2001a, b) method. More information on SRH-Meander can be found in Huang and Greimann (2007).

SRH-Meander does not simulate these detailed physical processes and, therefore, relies upon user input to define when a cutoff would occur. SRH-Meander simulates channel cutoffs when the ratio of the length of channel to the length of the valley exceeds the user-specified threshold value for critical sinuosity. In the physical world, when the channel sinuosity becomes too large, the channel does not have enough energy to carry incoming flow and sediment, and the river abandons an existing portion of its length to find a new (shorter and steeper) path. Channel cutoffs were predicted in the study reach by calibrating the critical sinuosity at which the cutoff occurred. Cutoffs are a complex process that also depends on floodplain topography, vegetation, and other factors.

A straight line is used to link the two points of the channel during the cutoff. After the cutoff, points are redistributed along the channel at equal distances.

3.2 Model Calibration Using Laboratory Data

The following discusses calibration of SRH-Meander in a controlled laboratory study conducted by the United States Army Corps of Engineers (USACE) at the U.S. Waterways Experiment Station in Vicksburg, Mississippi. The results of the USACE laboratory study were published as A Laboratory Study of the Meandering of Alluvial Rivers (USACE 1945) and served as the source of information for this model calibration. The term "calibration process" in this discussion represents the adjustment of input parameters to match channel centerlines from the computer model to the resulting channel centerlines from the USACE's physical model in this laboratory study (USACE 1945).

The study itself consisted of a myriad of tests attempting to isolate and adjust individual variables to better understand channel migration response. This section refers to one test in particular in USACE (1945), titled "Effect of Not Feeding Sand at the Entrance." This test was selected for calibration because of the relatively large flume size, as well as the availability of presented data. The test was completed in a flume approximately 20 feet wide and 100 feet long, although data were only collected in the first 60 feet of the flume. The test ran for 160 hours. Thalweg traces were presented for the initial channel, after 35 hours, after 83 hours, and after the 160-hour test. Figure 3-1 shows overhead photographs from the study of the pre- and post-test (160-hour) channels. Figure 3-2 shows the channel alignments subsequently digitized for the laboratory calibration.

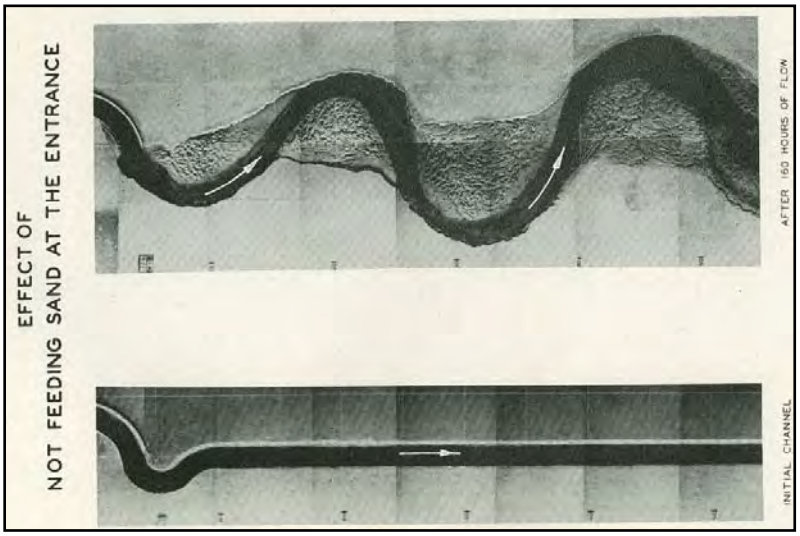

Figure 3-1. Post-test and pre-test photos of the study channel, from USACE (1945).

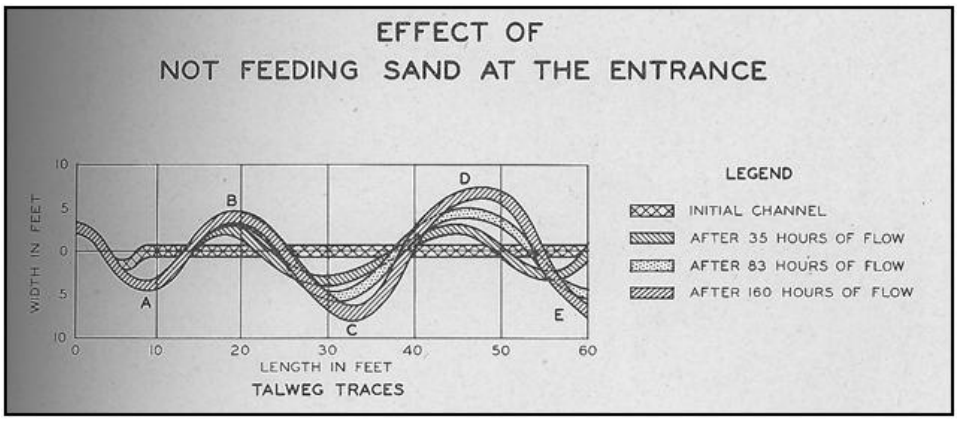

Figure 3-2. Thalweg traces at periodic time intervals, from USACE (1945).

3.2.1 Input Data

Data inputs for the SRH-Meander model are flow data, channel geometry (planform, profile, and cross sectional), channel roughness, bed material size, and bank erosion rates.

Flow data. The USACE (1945) reported a range of flows between 0.05 and 0.5 cubic feet per second (cfs). The authors were not able to determine the exact flow rates used during the experiments; however, the higher flow rates will have a dominating effect on the channel migration. During the calibration, several flow rates were simulated to achieve good agreement between the SRH-Meander output and the USACE flume study results. The flow rate of 0.5 cfs gave the best results for channel alignment and channel bed erosion, as determined through comparisons with the measured centerline.

Channel geometry. Initial conditions for the model included the profile and cross sectional geometry inputs; namely, a bed slope of 0.007 foot per foot, and a trapezoidal cross section with a 1.62-foot bottom width, a channel height of 0.23 foot, and a channel top width of 1.82 foot. The alluvium used as the bed and banks of the USACE (1945) study was reported in the form of two grain size distributions: a fine sand (d50 ~ 0.2 millimeters [mm]) comprised 80 percent of the channel material, and a silt (d50 ~ 0.045 mm) comprised the remaining 20 percent of the channel material. The lab data show that the channel widens during the no sediment feeding condition. However, the calibration process assumes a constant channel width. A channel bottom width of 3 feet was used in the calibration because that is near the final width at the end of the experiments. The USACE present the initial conditions and thalweg traces that were recorded after 35, 83, and 160 hours of flow. Figure 3-2 shows these traces.

USACE (1945) reported changes in planform geometry, cross sectional geometry, and profile geometry during the test. The SRH-Meander model assumes that the cross sectional geometry remains constant; therefore, the authors used channel conditions that were intended to represent average conditions during the entire test. The channel planform alignments, as shown in figure 3-2, were scanned and digitized using DigitizeIt software http://www.digitizeit.de/. These data were then extracted to ArcMap so that SRH-Meander could read the resulting shapefiles. Figure 3-3 presents an ArcMap layout of the digitized centerlines for the four time steps, along with the valley axis used for modeling purposes.

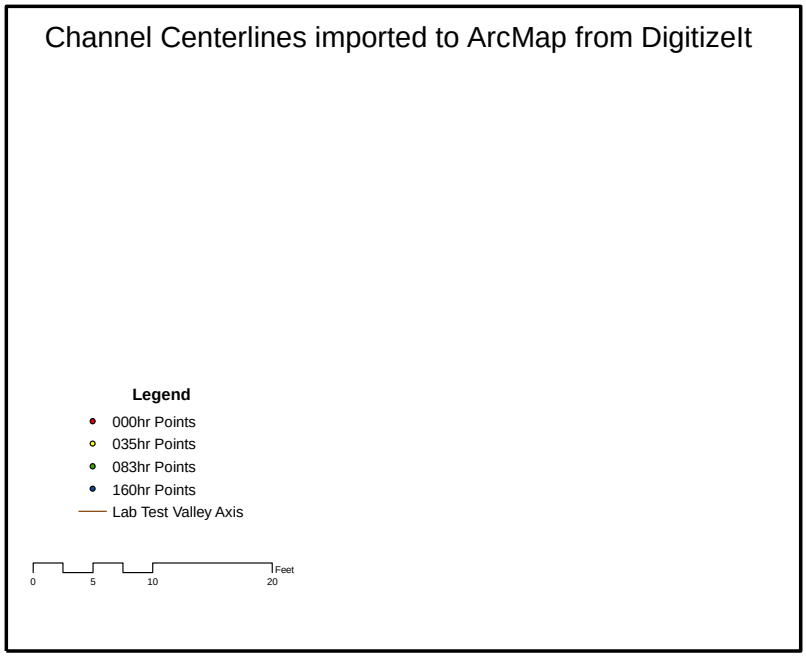

Figure 3-3. Centerlines for four time steps along with the valley axis of the channel.

Channel roughness (Manning's roughness coefficient). No estimate for channel roughness was provided in USACE (1945). Channel roughness could have been estimated based solely on grain size; however, as the channel is small relative to prototype channels, the effects of grain roughness may be more pronounced (scale effect) and a higher roughness would exist than that calculated using typical design equations. Thus, Manning's roughness coefficient was treated as a calibration parameter.

Bank erosion rates. Bank erosion coefficients were treated as input parameters requiring calibration. The SRH-Meander model uses polygons to spatially identify locations and associated erosion rates. Various erosion rates could be assigned at different sections of the channel; however, the bed and bank material were essentially uniform throughout the test section. Thus, a single erosion coefficient for the entire channel should be sufficient, with the exception of the flume entrance. USACE (1945) used nonerosive material at the entrance bend, so a polygon encompassing the entrance bend was given an erosion coefficient of approximately zero, and a second polygon was used for the portion of the channel that was allowed to meander. The erosion coefficient associated with the meander polygon was adjusted during the calibration process.

Results of USACE (1945) indicate that the bank erosion in the upstream bend stopped after the channel eroded and the slope flattened. The flattening of the slope reduced the velocity and the shear, thereby reducing the erosion of the banks.

SRH-Meander updates the terrain elevation and computes a new channel slope during simulations. Terrain elevation is updated by considering the mass balance between channel erosion/deposition, incoming sediment rate, outgoing sediment rate, and bank erosion/deposition. A bank-height resistance coefficient reduces the bank erosion in areas with high banks.

3.2.2 Calibration Process

Calibration parameters included model grid spacing, channel width, Manning's roughness coefficient, and the erosion and bank height resistance coefficients for the polygon encompassing the meandering portion of the channel.

3.2.3 Model Calibration Not Incorporating Vertical Erosion

The SRH-Meander model (without terrain elevation updates and a bank height resistance coefficient) was unable to reproduce a centerline alignment that matched the entire length of the published USACE results. A single set of coefficients could only match one bend at a time and only the amplitude. Figures 3-4 to 3-7 show the measured thalweg trace after 160 hours along with the four different resulting model centerlines and an indication of where they matched the lab test results (red circles).

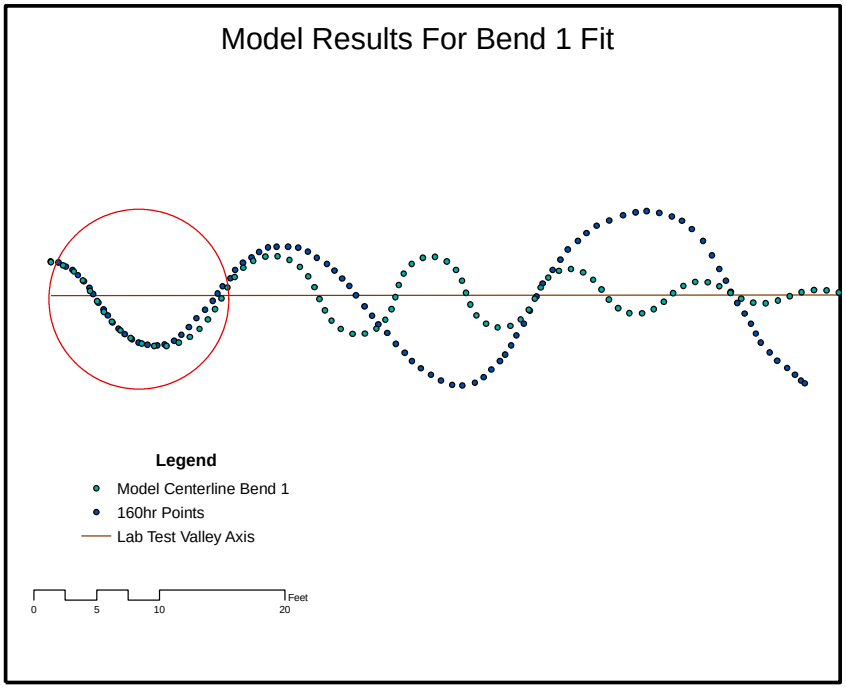

Figure 3-4. Calibration resulting in the first bend being modeled.

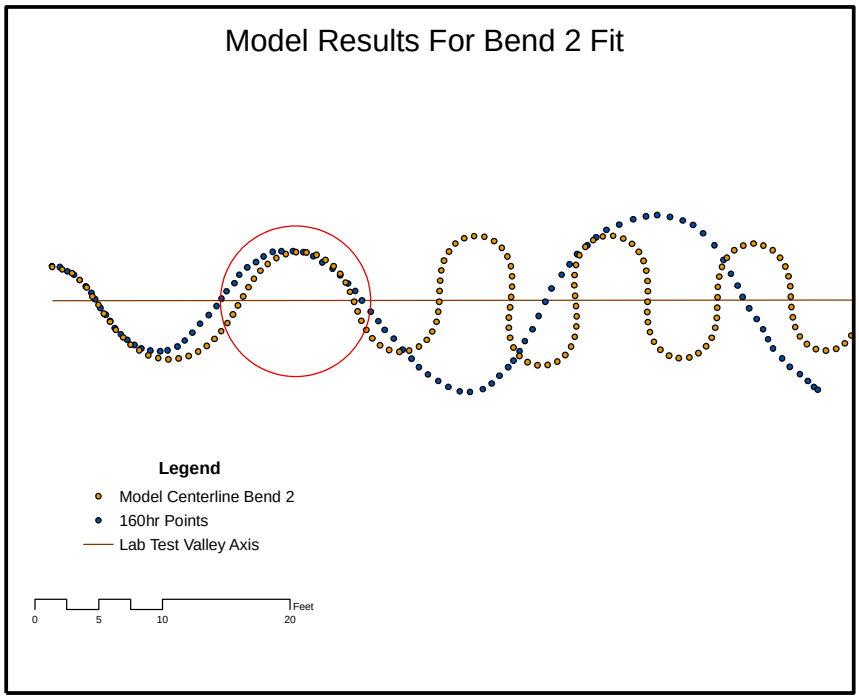

Figure 3-5. Calibration resulting in the second bend being modeled.

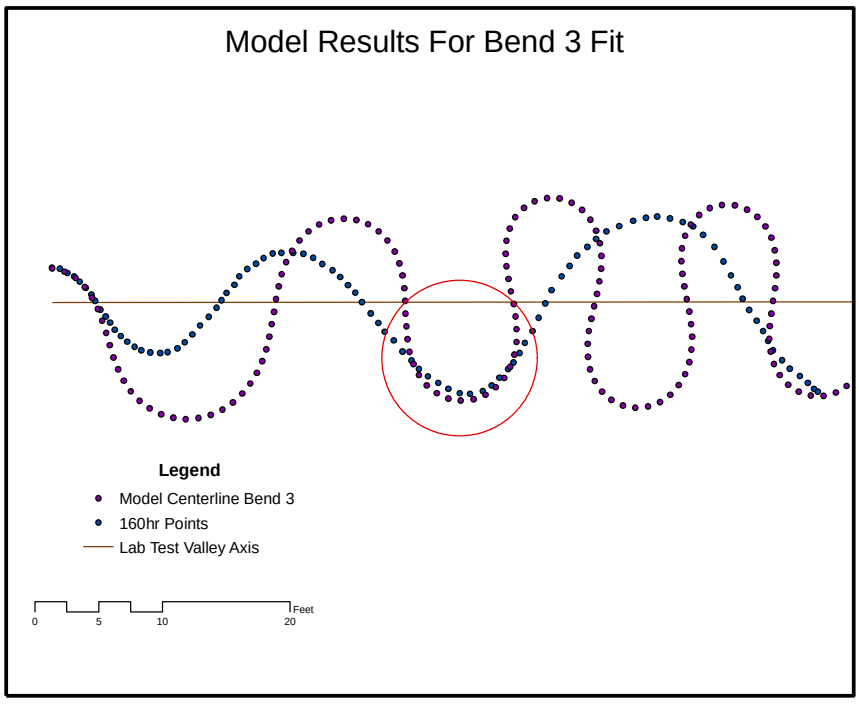

Figure 3-6. Calibration resulting in the third bend being modeled.

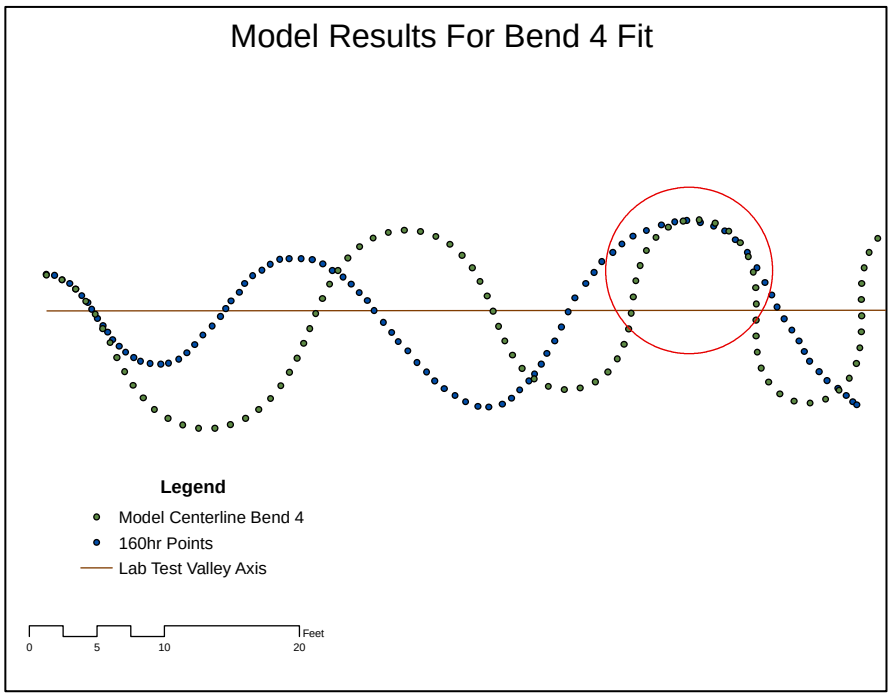

Figure 3-7. Calibration resulting in the fourth bend being modeled.

Matching the locations where the channel centerline crossed the valley axis was only possible for certain bends, but not for the whole reach. When meander wavelengths were accurate, amplitudes were not; conversely, when amplitudes were matched, meander wavelengths were inaccurate. Because there was significant vertical erosion during the experiment, the bank height increased and the slope decreased. Increasing the bank height would slow the bank erosion rates, and decreasing the slope would also slow the bank erosion rates. To simulate the vertical erosion, the model needed to incorporate sediment transport and a sediment budget. Without considering sediment budget, the model cannot predict erosion of the channel bed upstream and calculate the bank erosion resistance due to high bank height and low flow velocity. To remedy this limitation, the authors added the ability to compute a sediment budget into the meander model, as described in the next section.

3.2.4 Model Calibration With Raster Elevation Update and Bank Height Resistance Coefficient

This section describes the methods and calibration process to incorporate sediment budget into the meander model.

SRH-Meander computes a sediment mass balance between two cross sections. Spatial-delay and/or time-delay effects are important when there are rapid hydraulic changes in short reaches. To include these effects, SRH-Meander uses

the analytical solution from Han (1980) to calculate the sediment concentration as shown in equation 3-1:

$$C_i = C_i^* + (C_{i-1} - C_i^*) \exp\left\{-\frac{V_{di} W_i \Delta x}{Q_i}\right\} \quad 3\text{-}1$$

Where:

C = computed discharge weighted average sediment concentration
C_i^* = the computed sediment transport capacity concentration
Q_i = flow rate
V_{di} = deposition velocity
W_i = channel top width
Δx = reach length
i = cross-section index (increasing from upstream to downstream)

Equation 3-1 is employed for each of the particle size fractions. The volume of sediment deposition, ΔVs, in a reach can be calculated (for erosion ΔVs would be negative) as shown in equation 3-2:

$$\Delta V_s = (Q_{si-1} - Q_{si})\Delta t = (Q_{i-1} C_{i-1} - Q_i C_{si})\Delta t \quad 3\text{-}2$$

Where:

ΔV_s = change in sediment storage
Q_s = sediment transport rate
Δt = time step

The volume of deposition can also be geometrically approximated by equation 3-3:

$$\Delta V_s = A^n \Delta z_b - h_l s_l \Delta n_l + h_r s_r \Delta n_r \quad 3\text{-}3$$

Where:

Δz_b = bed elevation change
A = plan area of river bed
n_l, n_r = lateral location of left and right banks
s_l, s_r = length of left and right banks
h_l, h_r = height of left and right banks (if it is deposition, it is the bank height under water).

The SRH-Meander model assumes that channel cross section geometry remains unchanged during channel migration. If bank erosion is predicted on one side of the channel, deposition is predicted up to the water surface on the other side. Channel width at that flow rate remains constant. Because the bank height is explicitly simulated when elevations are being tracked, the bank height can now

be used in the bank erosion rate equation. The bank erosion rate is linearly related to the deviation in velocity from the mean velocity, and the bank resistance coefficient is linearly related to the dimensionless bank height as shown in equation 3-4:

$$E_b = (E_0 - Bh/H)u_b \qquad 3\text{-}4$$

Where:

E_b = rate of bank erosion [L/T]
E_0 = bank erosion constant [-],
B = bank height resistance coefficient [-]
h = bank height [L]
H = cross sectional water depth [L]
u_b = deviation from mean velocity at bank [L/T]

In the previous calibration, only E_0 was calibrated to the measured data and B was assumed to be zero. Figure 3-8 shows the thalweg trace after 160 hours with and without mass balance consideration in USACE (1945). With a mass balance method, the model predicted nonuniform development of bends. The bends increased in size from upstream to downstream. During the no-sediment feeding condition at the entrance, the channel deepened upstream. The upstream channel slope became so flat that the flow no longer had enough velocity and shear stress to erode the bank. Additionally, vertical erosion increased the channel bank height and decreased the bank erosion rate; however, the model did not predict the channel phase correctly when compared with bends observed from the laboratory test. When the end of the channel is calibrated to the laboratory data, the first, second, and third bends are all shifted in the downstream direction. However, the version of SRH-Meander that incorporates a sediment mass balance gave a much improved prediction over the version of SRH-Meander that does not consider a sediment mass balance. The model is still expected to have errors in predicting the exact amplitude and phase of the meander pattern, but by incorporating the sediment mass balance, the errors are significantly reduced.

Figure 3-9 visually compares the model terrain topography (with mass balance) after 160 hours with the photograph taken in the laboratory test. While there were no records of the terrain elevation from USACE (1945), results suggest that the model has the potential to predict the general flood plain topography after channel migration.

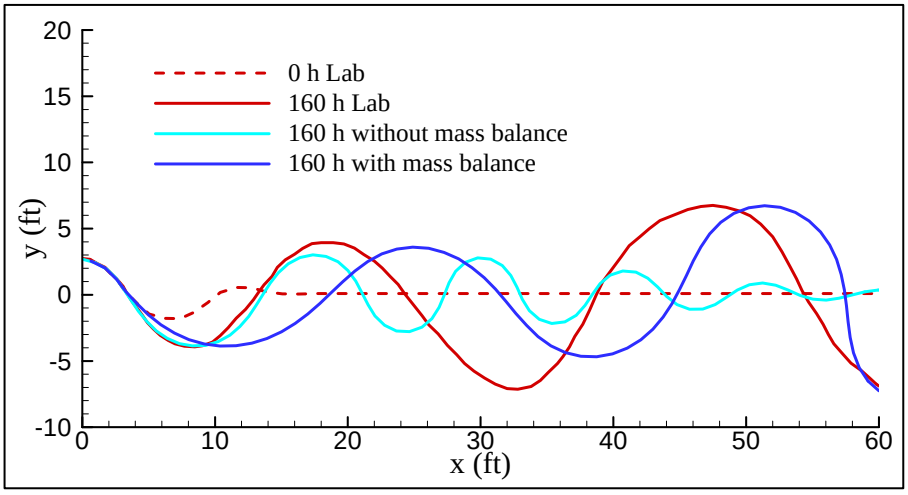

Figure 3-8. Calibration results with raster elevation update and bank height resistance coefficient (red lines are from USACE 1945, and blue lines are from SRH-Meander model simulation).

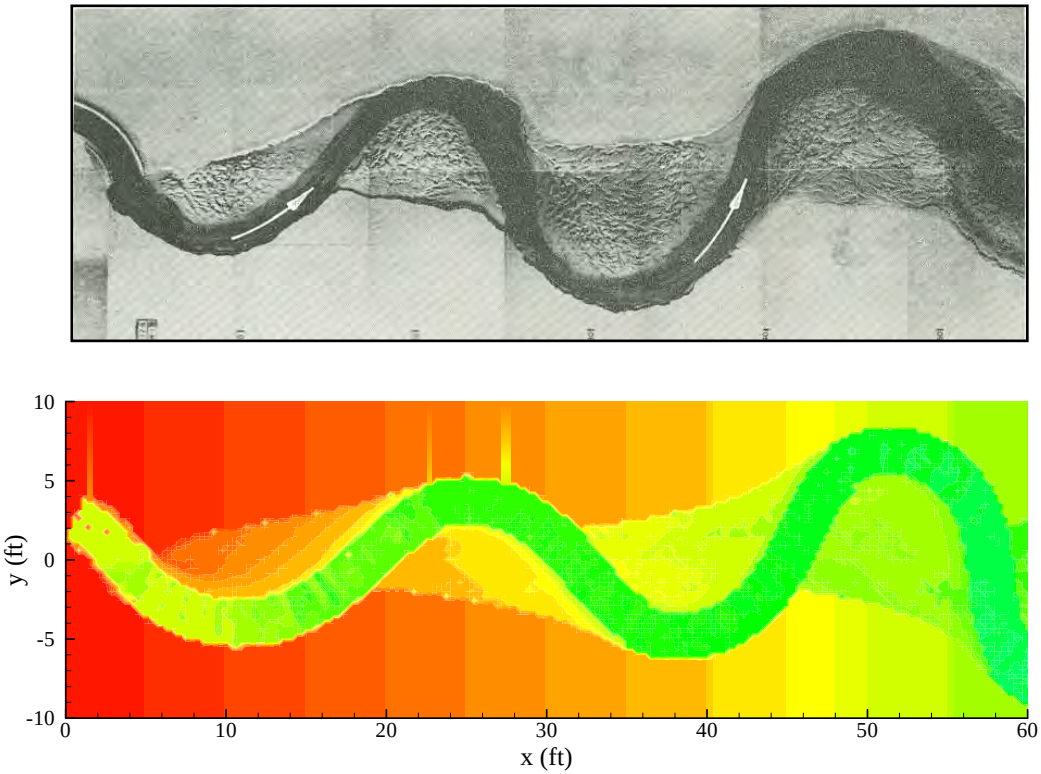

Figure 3-9. Comparison of channel topography between laboratory model and computational model. The top picture is from USACE (1945). The bottom is simulated in SRH-Meander. The ticks are in 10-foot increments.

3.3 Calibration Using Field Data

3.3.1 Data Preprocessing

To use SRH-Meander for prediction of channel migration in meandering rivers under various North of the Delta Offstream Storage (NODOS) alternative flow scenarios, it was necessary to calibrate the model to historic meander rates. As stated by Crosato (2007), "it is not possible to determine the erodibility coefficients a priori, based on bank properties, presence of vegetation, etc. . . [for real rivers without] . . . calibrating the erodibility coefficients on field observations." The period of record used for model calibration was October 1, 1976, to September 30, 1999. This interval was chosen based on the availability and quality of data. The model calibration includes 101 miles from Red Bluff at river mile (RM) 243 to Colusa at RM 142 (figure 3-10). Data collection for the SRH-Meander calibration of the Middle Sacramento River model runs is described below.

Flow data from gages operated by the State of California Department of Water Resources (CDWR) were used for model calibration. Mean daily flows from three CDWR gages were selected for the period October 1, 1976 to September 30, 1999:

The following CDWR gage data were used:

- Vina Woodson Bridge (VIN) upstream of Hamilton City at RM 219
- Hamilton City (HMC) between Hamilton City and Ord Ferry at RM 199.2
- Ord Ferry (ORD) downstream of Hamilton City at RM 184.2

Missing flow data in each record were reconstructed from available data of the same date from the other two gauge records. VIN was missing data from October 1, 1978, to January 1, 1993. HMC was missing data from January 1, 1981, to January 1, 2001. ORD was missing data before January 1, 1993.

The stream gage at Bend Bridge (just upstream of Red Bluff) provided a continuous record, and regression relationships were developed between the lower stream gages and Bend Bridge. In cases where data did not exist at the lower gages, data were derived from Bend Bridge regression relationships.

The USACE publication, Sacramento and San Joaquin River Basins, Comprehensive Study (USACE 2002), provided a longitudinal profile, cross section geometry, Manning's roughness coefficients, and bed material size for construction of a 1D hydraulics model. River planform geometry was determined from traces of active channels on CDWR aerial photographs and geographic information system (GIS) maps. Bank erosion rates were used as calibration parameters.

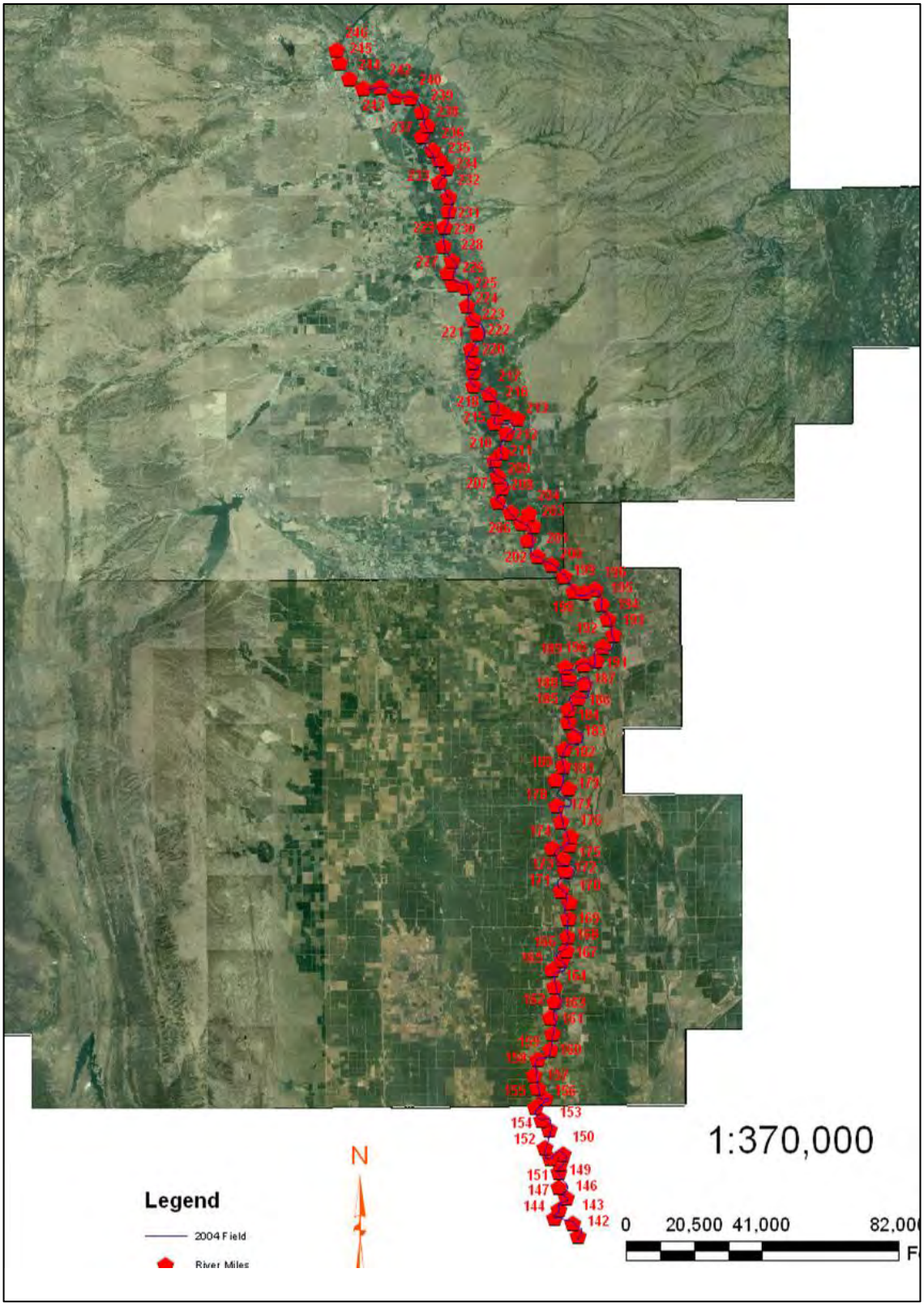

Figure 3-10. SRH-Meander project reach.

3.3.2 Model Calibration

SRH-Meander can ignore flows below a user input threshold. If the flow is below this threshold, it is assumed that no migration occurs. SRH-Meander also has an upper threshold above which the flow is assumed to go out of bank. The upper threshold is essentially a cap on the flow rate. The lower threshold was calibrated to be 35,000 cfs for the Sacramento River, and the upper threshold was set to 90,000 cfs, which is the average bank-full discharge for the reach based upon the HEC-RAS modeling.

Flow data can be entered in SRH-Meander as upstream incoming flow and lateral flow. Flow data from gauge VIN were used as incoming flow at Red Bluff. The difference between gauge flows at HMC and VIN was used as lateral flow input at gauge station HMC. The difference between flows from gauges ORD and HMC was used as lateral flow entering at gauge station ORD. We assumed that all tributaries between the gages would be represented by a single input. Flow regimes are presented in figure 3-11 (VIN), figure 3-12 (HMC), and figure 3-13 (ORD). Upper and lower limits of flow are only applied to the upstream incoming flow (VIN) and are shown in figure 3-11.

Calibration parameters were:

- **Critical sinuosity for cutoffs.** This is the critical sinuosity above which a meander cutoff is assumed to occur.

- **Model grid spacing.** Grid spacing does not reflect a physical process, but defines the distance between nodes of the modeled centerline, and scales with the reach-averaged channel width. The model grid spacing in meander models is typically a calibration parameter (Crosato, 2007).

- **Bank erosion coefficients.** The bank erosion coefficient (E_0) was calibrated for each eroding bend. The bank height resistance coefficient, B, was assumed to be zero.

Hydraulic geometry (i.e., flow velocity, top channel width, hydraulic radius, and energy slope for an average channel) was prescribed by a flow rating curve. The rating curve table was constructed from a HEC-RAS model with 1997 channel geometry (USACE 2002). The rating curve is presented in table 3-1.

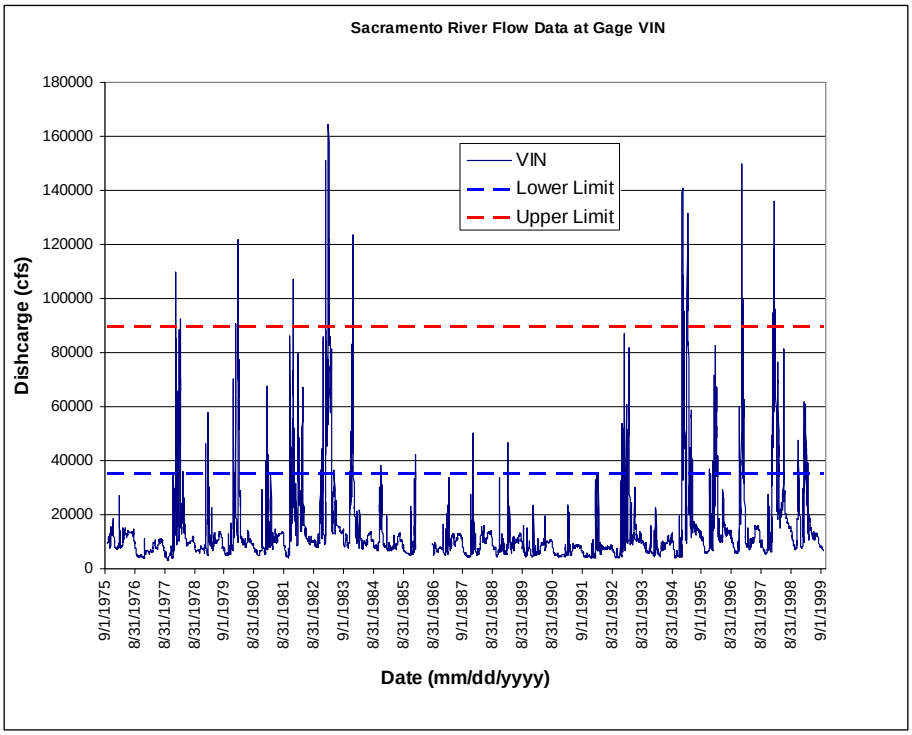

Figure 3-11. Flow discharge data at Vina Woodson Bridge at RM 219 (VIN).

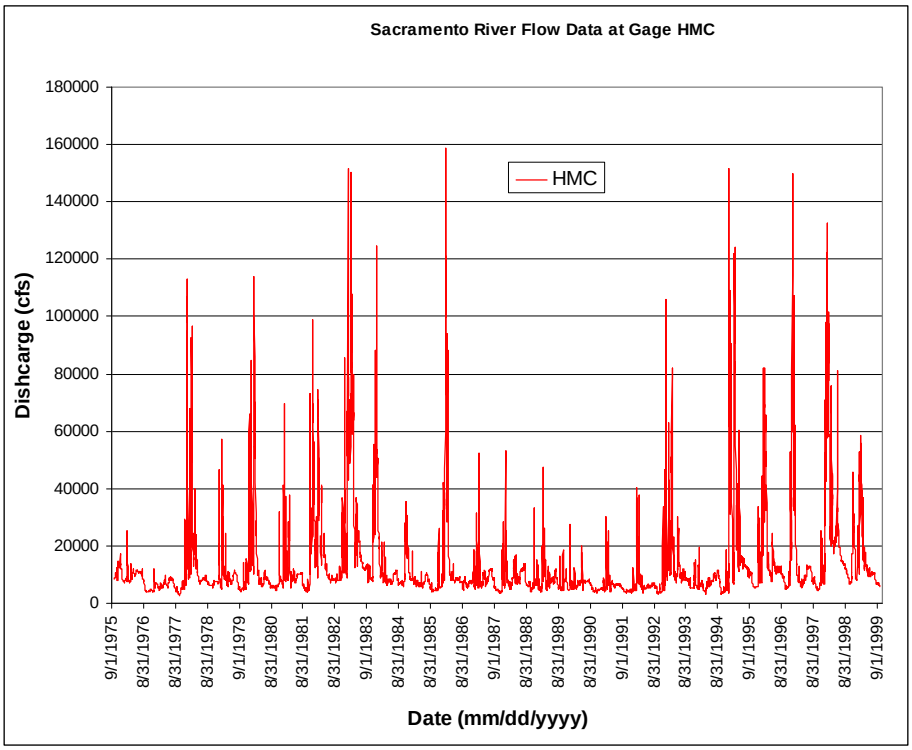

Figure 3-12. Flow discharge data at Hamilton City gauge at RM 199.2 (HMC).

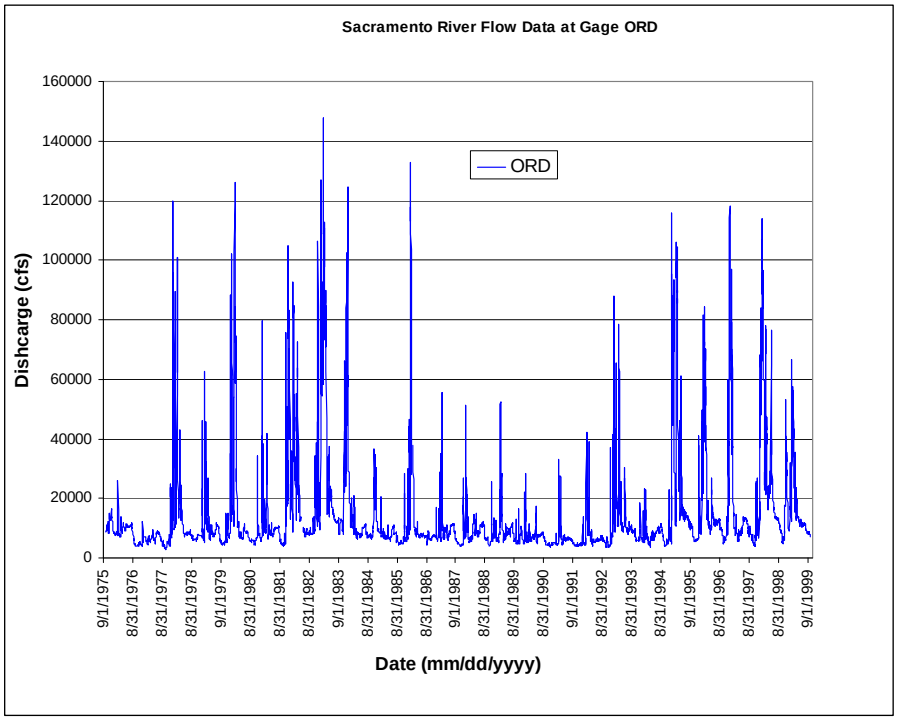

Figure 3-13. Flow discharge data at flow hydrograph from DWR gauge Ord Ferry at RM 184.2 (ORD).

Table 3-1. Rating Curve

Flow Rate (Q) (in m^3/s)	Velocity (V) (in m/s)	Friction Slope (S_f) (in m/m)	Depth (D) (in m)	Top Width (W) (in m)	Hydraulic Radius (H_r) (in m)
850	1.18	5.79E-04	2.77	271	2.76
991	1.23	5.63E-04	2.93	284	2.91
1,133	1.29	5.48E-04	3.07	292	3.05
1,274	1.33	5.40E-04	3.22	298	3.20
1,416	1.38	5.36E-04	3.35	303	3.33
1,557	1.40	5.43E-04	3.42	315	3.40
1,699	1.43	5.48E-04	3.51	324	3.49
1,841	1.46	5.53E-04	3.61	331	3.59
1,982	1.49	5.62E-04	3.70	338	3.68
2,124	1.51	5.68E-04	3.80	342	3.77
2,265	1.54	5.66E-04	3.89	350	3.87
2,407	1.56	5.68E-04	4.00	353	3.97
2,549	1.58	5.70E-04	4.09	356	4.06
2,690	1.60	5.71E-04	4.17	358	4.15

Note: m^3/s = cubic meters per second, m/s = meters per second, m/m = meters per meter, m = meters.

Calibration compares the output channel alignment (as measured from historical aerial photography) to the actual channel alignment at the end of the selected time interval. An iterative approach was taken in calibrating the model to match the field data. Erosion coefficients were adjusted, as necessary, until the modeled alignment sufficiently matched actual channel alignment. The critical sinuosity for cutoffs is also adjusted in each polygon defining the erosion coefficient so that the channel cutoff is reproduced.

Table 3-2 contains a summary of the calibrated parameters and predetermined parameters (parameters determined before calibration) that were used during calibration of the SRH-Meander model to the Sacramento River. Minimum, average, and maximum erosion coefficients are presented.

Table 3-2. Summary of Parameters Used in Calibrating the SRH-Meander Model

Predetermined parameters	**Manning's roughness coefficient (n)**	0.032
	Average Energy Slope (ft/ft)[1]	0.00056
	Bed Material Size (mm)	14
	Number of Polygons	542
Calibration parameters	**Grid Spacing (-)[2]**	0.6
	Critical Sinuosity for Cutoff (-)	2.3-4.5
	Minimum Erosion Coefficient (-)	8.90E-09
	Average Erosion Coefficient (-)	2.23E-05
	Maximum Erosion Coefficient (-)	1.40E-04

[1] ft/ft = feet per foot.
[2] (-) indicates a dimensionless parameter.

3.3.2.1 Calibration Results

Figures 3-14 through 3-16 display three examples of calibration results for three study reaches: the centerlines for the 1976 and 1999 channels as digitized from aerial photography, and the simulated SRH-Meander centerlines for 1999. The model calibrated moderately well, and the average absolute distance of model output coordinates to actual channel centerline was 88.1 feet for the study reach. These values are small, considering that the average channel top widths are 1,000 feet and the channel migrates up to 100 feet per year in some locations. The grid spacing was set to 0.6 times the channel width, which meets Crosato (2007) criteria for numerical meander models. The criteria specify that optimal distance between successive grid points should have the order of half the channel width.

In general, SRH-Meander was better at modeling changes in bend amplitude than at modeling bend translation (figure 3-14). Whether the model predicts translation versus amplification is primarily a function of the channel roughness input parameter combined with the calculated curvature of the centerline. Bed material size is relatively less important and results are not sensitive to small changes in its value. The Manning's roughness coefficient can only have a single value for the entire model as well as for the full range of flows used, which may

not reflect the actual channel roughness at all locations and flows. Calibrating one bend with a given curvature to amplify properly may mean that a subsequent bend with a similar curvature may not translate as observed. Because of the interactions between bends, it is difficult to calibrate all bends accurately.

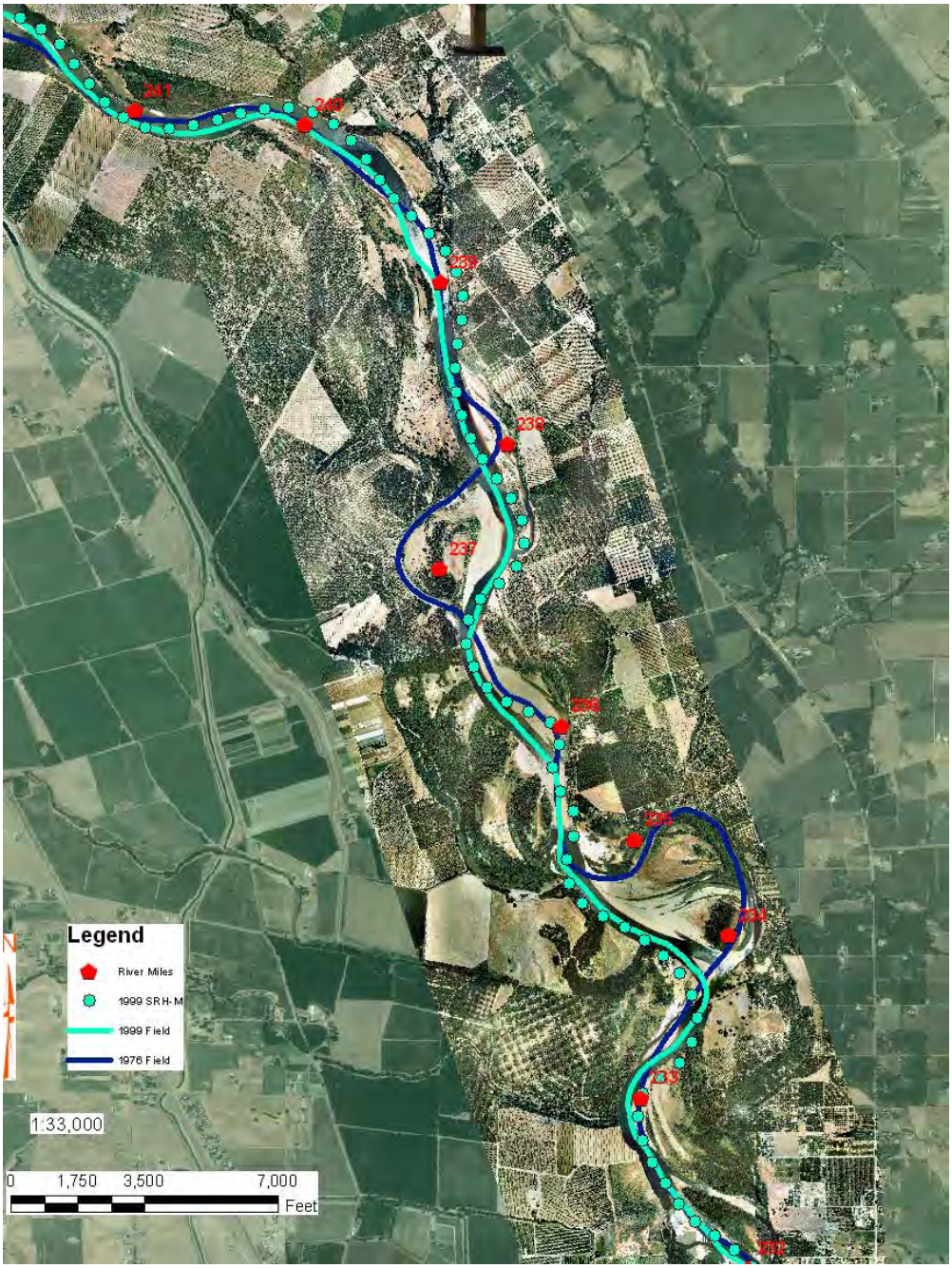

Figure 3-14. Calibration result in reach 1. Points represent simulated channel alignments in 1999. Lines represent measured channel alignments in 1976 and 1999.

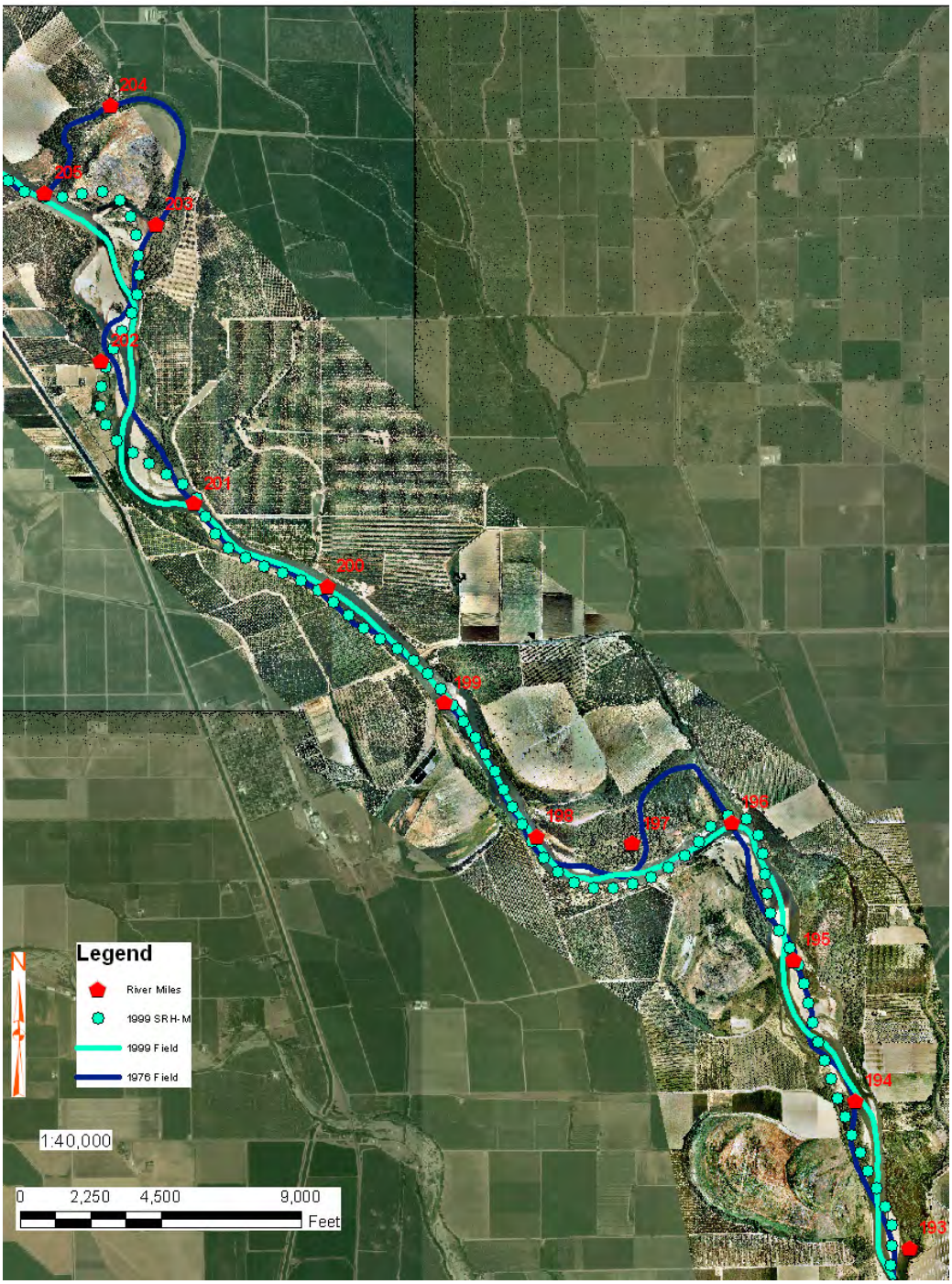

Figure 3-15. Calibration result in reach 2. Points represent simulated channel alignments in 1999. Lines represent measured channel alignments in 1976 and 1999.

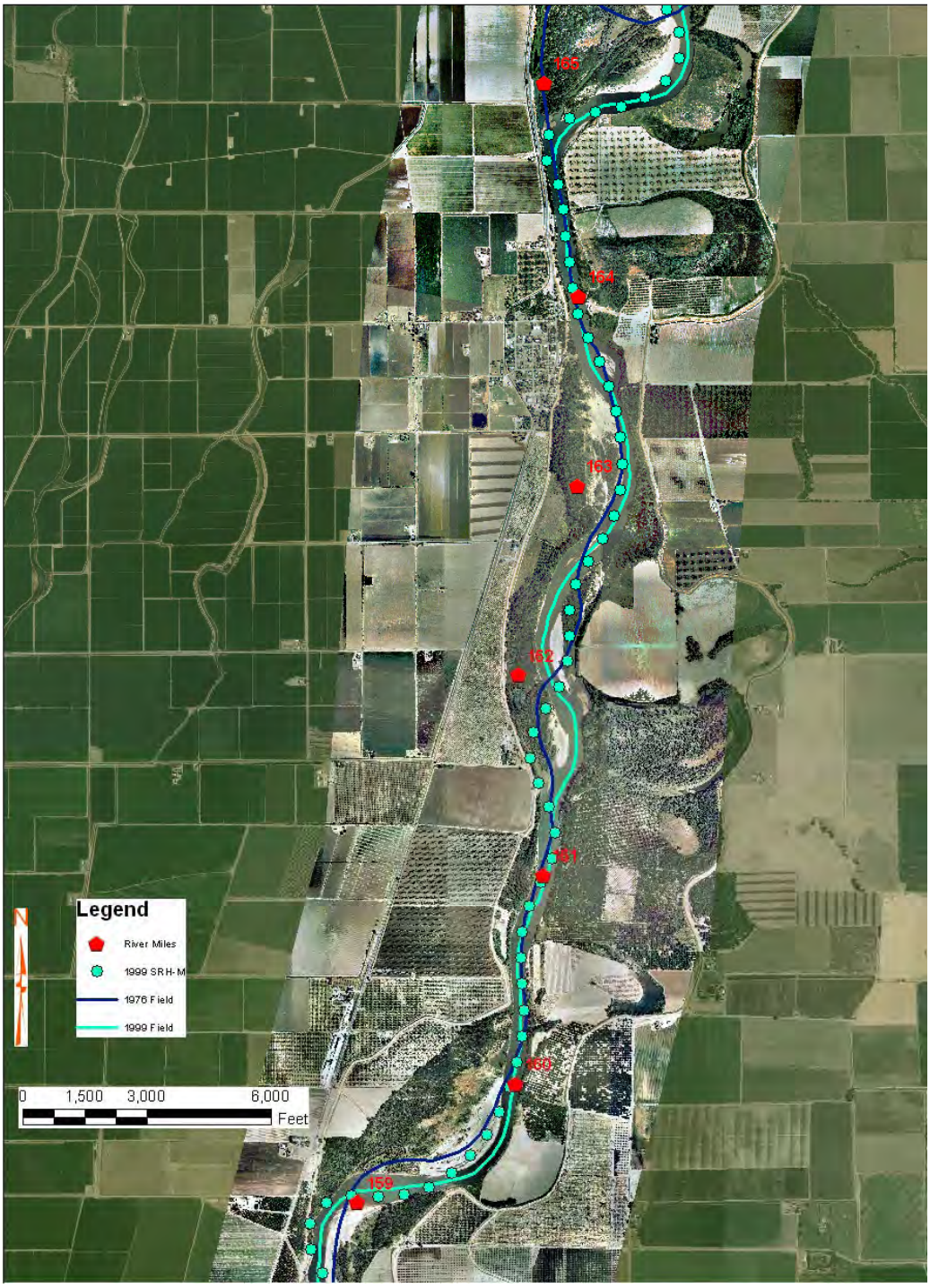

Figure 3-16. Calibration result in reach 3. Points represent simulated channel alignments in 1999. Lines represent measured channel alignments in 1976 and 1999.

3.5 Conclusions

SRH-Meander has proved generally capable of matching historical meander tendencies in the Sacramento River. It is able to estimate the future direction of channel migration. The model calculates the area that will be eroded and may be able to show changes to the terrain that result from meandering. The model can also estimate the bends where a channel cutoff is likely; however, it will not be able to estimate the exact time or specific method of cutoff. The model is also limited because it cannot consistently reproduce the down valley migration rates as accurately as the cross valley migration rates. SRH-Meander is limited in that each bend requires calibration of the erosion coefficients. Additional calibration and correlation of bank erosion coefficients to bank properties may help improve the model's predictive capabilities. Parameter sensitivity studies on channel roughness and bed material size will help define model uncertainties. It is, however, a state-of-the-art model and there are no other readily available models that resolve these issues.

In its current state, the model will be most useful in identifying the reaches that will be most active. It will also be useful in identifying locations where bank erosion could impact infrastructure in the near future. Finally, the model can be used to assess relative bank erosion rates across various flow and land management alternatives. Bank erosion is important to the regeneration of cottonwood forests, and therefore the model can be used to assess which reaches will most likely create sustainable cottonwood forests.

Chapter 4

Multidimensional Modeling

Contents

Page

4. Multidimensional Modeling 4-1

4.1 General Capability Description 4-1

4.1.1 U^2RANS 4-1

4.1.2. SRH-2D 4-2

4.2 Calibration Data for SRH-2D and U^2RANS 4-2

4.3 Verification and Validation for SRH-2D and U^2RANS 4-5

4.3.1 Velocity Data near RM 192.5 4-5

4.3.2 Mesh Development 4-5

4.3.3 Model Description 4-8

4.3.4 Results and Discussion for Verification and Validation 4-9

4.4 Mobile Bed Simulation for the 1986 Flood 4-18

4.4.1 Sediment Transport Data 4-18

4.4.2 Mesh Development 4-19

4.4.3 Sediment Classes 4-21

4.4.4 Initial and Boundary Conditions 4-21

4.4.5 Results and Discussion for Mobile Bed Simulation 4-25

4.5 Concluding Remarks 4-30

Figures

Page

4-1 Survey points (in red) for the river topography at RM 192.5 4-3

4-2 Bed elevation contours based on the TIN formed from all survey points 4-4

4-3 Bed elevation contours when extra topographic data are added at the left downstream bar 4-4

4-4 Plan view of all velocity measurement points (in red) at RM 192.5 4-5

Figures

Page

4-5 Solution domain and the 2D mesh for the SRH-2D simulation..... 4-6

4-6 A zoom-in view of the 2D mesh at the bar area 4-7

4-7 Bed elevation contours based on the 2D mesh 4-7

4-8 A 3D view of the bed for the bend at 192.5 RM; 1:10 vertical distortion 4-8

4-9 Comparison of measured and computed water depth at all velocity measurement points..... 4-10

4-10 Comparison of velocity vectors at all measurement points between measured and SRH-2D data 4-11

4-11 Comparison of velocity vectors at measurement points between measured and U^2RANS data..... 4-11

4-12 Comparison of velocity vectors at cross section 1 between measured and SRH-2D data 4-12

4-13 Comparison of velocity vectors at cross section 2 between measured and SRH-2D data..... 4-12

4-14 Comparison of velocity vectors at cross section 3 between measured and SRH-2D data..... 4-13

4-15 Comparison of velocity vectors at cross section 4 between measured and SRH-2D data..... 4-13

4-16 Comparison of velocity vectors at cross section 1 between measured and U^2RANS data..... 4-14

4-17 Comparison of velocity vectors at cross section 2 between measured and U^2RANS data..... 4-14

4-18 Comparison of velocity vectors at cross section 3 between measured and U^2RANS data..... 4-15

4-19 Comparison of velocity vectors at cross section 4 between measured and U^2RANS data..... 4-15

4-20 Comparison of relative velocity magnitude at cross section 1 4-16

4-21 Comparison of relative velocity magnitude at cross section 2 4-16

4-22 Comparison of relative velocity magnitude at cross section 3 4-17

4-23 Comparison of relative velocity magnitude at cross section 4 4-17

Figures

Page

4-24 Solution domain and the mesh used for SRH-2D simulation 4-20

4-25 Bed elevation contours based on the elevations represented by the mesh in figure 4-24 4-20

4-26 Flow hydrograph representing the 1986 floodflow recorded below Glen-Colusa Irrigation District (GCID) 4-21

4-27 The stage-discharge rating curve based on SRH±-1D simulation results 4-22

4-28 Partition of the solution domain into four gradation zones..... 4-23

4-29 The bed gradations used for each zone of the solution domain..... 4-24

4-30 Simulated velocity at the constant flow discharge of 4,431 cfs; results are used as the initial conditions..... 4-24

4-31 Net eroded (positive) and deposited (negative) depth in feet on January 18 and 31, relative to the bed elevation on January 1 ... 4-25

4-32 Net eroded (positive) and deposited (negative) depth in feet on March 31 and April 30, relative to the bed elevation on January 1 4-26

4-33 Inundation and velocity contours at various times 4-27

4-34 Net eroded (positive) and deposited (negative) depth, relative to January 1, 1986, at various times..... 4-28

4-35 Sediment sorting with D_{50} distribution at various time 4-29

Tables

Page

4-1 Sediment Diameters of Each Size Class for the Simulation..... 4-21

4-2 Table 4-2. The Surface Gradations at Selected Sample Locations Collected in 1981 4-23

4-3 Table 4-3. The Bed Gradations Used for Each Zone of the Solution Domain 4-23

4. Multidimensional Modeling

Sedimentation and River Hydraulics Two-Dimensional Model (SRH-2D) and the Unsteady and Unstructured Reynolds Averaged Navier-Stokes solver (U^2RANS) model help advance understanding and describe processes at river bends, including bar growth and cottonwood establishment. SRH-2D simulates lateral and longitudinal velocity, erosion, and deposition patterns within the Sacramento River. U^2RANS simulates lateral, longitudinal, and vertical velocity and flow patterns. This chapter describes verification and application for these two models. The verification study is limited to flow only, without sediment transport modeling.

SRH-2D and U^2RANS are not explicitly linked to the other models listed in this report. This chapter is intended to demonstrate an application to the Sacramento River. Further work would be necessary to link the results of SRH-2D and U^2RANS to other models and to develop meaningful conclusions for the entire river.

4.1 General Capability Description

4.1.1 U^2RANS

U^2RANS is a three-dimensional hydraulics (3D) model that is accurate, well verified, and validated. It has been successfully applied to many research and engineering projects. U^2RANS is a comprehensive, general-purpose model. Three-dimensional hydraulic flow models, such as U^2RANS, are accurate and mature tools which have been routinely used to address many hydraulic engineering problems such as:

- Flow hydrodynamics in pools and river reaches upstream of hydropower dams
- Detailed flow characteristics around hydraulic structures
- Hydraulic impact of different project alternatives
- Fish passage facility design and evaluation
- Thermal mixing zone determination
- Design optimization, reservoir/lake stratification, selective cold water withdrawal, etc.

The main limitation of 3D hydraulic flow models is that they are usually applied to a river reach less than 5 miles long due to their heavy requirement for computer power.

U^2RANS uses state-of-the-art, unstructured computational fluid dynamics technology to unify multi block structured mesh (quad or hex) and unstructured mesh (quad, triangle, tet, hex, wedge, pyramid, or hybrid) elements into a single platform, and combines two-dimensional (2D) and 3D solvers in a common framework.

4.1.2. SRH-2D

SRH-2D is a 2D, depth-averaged, hydraulic and sediment transport model for river systems and watersheds developed at the Bureau of Reclamation (Reclamation). SRH-2D may be used to simulate both a river system and/or a watershed.

SRH-2D is a comprehensive model that has been applied to many projects at Reclamation, with a mature hydraulic simulation capability (Lai 2009). U^2RANS does not allow the simulation of sediment transport and mobile beds, but SRH-2D is a coupled hydraulic and sediment transport model that has mobile bed modeling capability.

SRH-2D solves the 2D dynamic wave equations (i.e., the depth-averaged St. Venant equations). The sediment solver may be classified as the unsteady nonequilibrium and nonuniform method and is the most general of its class. SRH-2D modeling capability is comparable to some existing 2D models but SRH-2D contain some unique features. First, SRH-2D uses a flexible mesh that may contain arbitrarily shaped cells. In practice, the hybrid mesh of quadrilateral and triangular cells is recommended, although a mesh of purely quadrilateral or triangular elements may be used. A hybrid mesh may achieve the best compromise between solution accuracy and computing demand. Second, SRH-2D adopts very robust and stable numerical schemes with a seamless wetting-drying algorithm. The resultant outcome is that few calibration parameters are needed to obtain the final solution.

SRH-2D is particularly useful for problems where 2D effects are important. Examples include: flows with in-stream structures, through bends, with perched rivers, with lateral flow spills, and for multiple channel systems. A 2D model may also be needed if one is interested in local flow velocities and eddy patterns, point bar formation for bend flows, or lateral variations. SRH-2D may be a useful tool for the point bar formation and cottonwood recruitment study for particular sites on Sacramento River because it predicts erosion and deposition, as well as the sediment sorting.

4.2 Calibration Data for SRH-2D and U^2RANS

SRH-2D and U^2RANS are verified with the field measured flow data for the river near river mile (RM) 192.5 on the Sacramento River. Detailed river bathymetric

data, plus the velocity data at selected cross sections, are available for carrying out the flow verification study.

The point bar and main channel near RM 192.5 were surveyed in June 2005 to provide the river topographic data necessary for multidimensional simulation at the meander bend. The above and below water survey points are shown in figure 4-1. A triangular irregular network (TIN) was created so that bed elevation could be obtained and used to develop the elevation of the mesh points used by the numerical models. The bathymetric contours of the TIN, based on the surveyed data, are shown in figure 4-2.

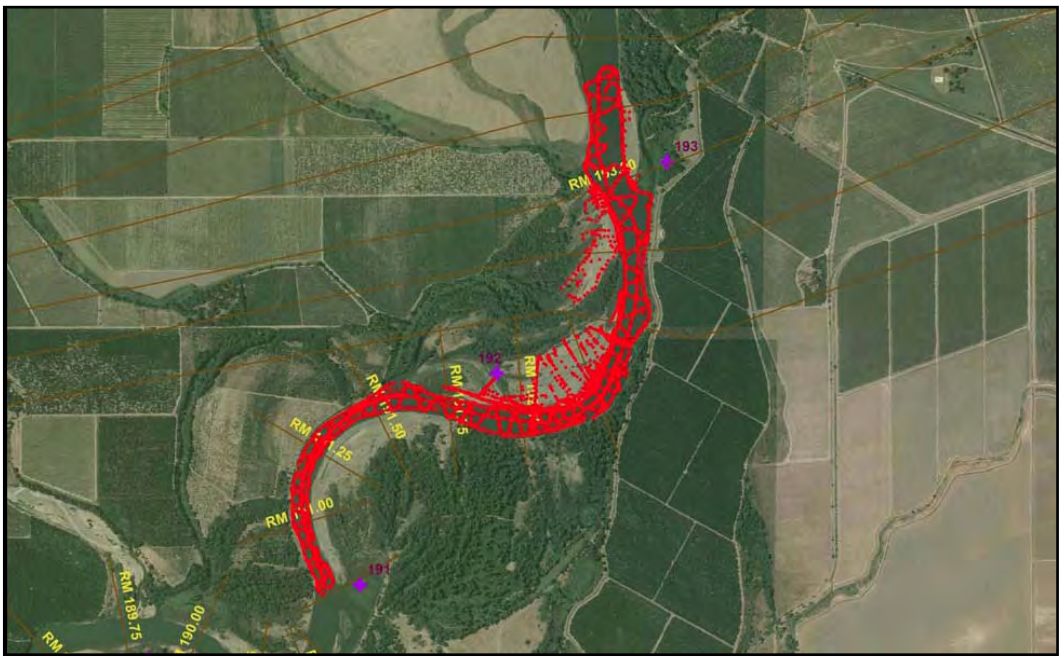

Figure 4-1. Survey points (in red) for the river topography at RM 192.5. Tan lines are survey cross sections (USACE, 2002).

Ground surveys were a combination of total station and real-time-kinematic global positioning system (RTK-GPS) survey techniques. The North American Datum of 1983 (NAD83) was used for horizontal control, and the vertical datum was the North American Vertical Datum of 1988 (NAVD88). The projection used was the California State Plane Projection Zone 2. Survey units were in feet.

Topographic data described above are sufficient for the verification study presented in this section as the flow extent for discharges less than 30,000 cubic feet per second (cfs) is fully contained by the coverage area of the data. For the mobile bed simulation discussed in Section 4.3, however, the flow inundation area is larger than the coverage area of the data. Extra points were manually added to represent the topography for the downstream left bar. Cross section surveys at the

cross sections shown in the figure 4-1 were available to determine the elevation of the point bar. Expanded topography is shown in figure 4-3.

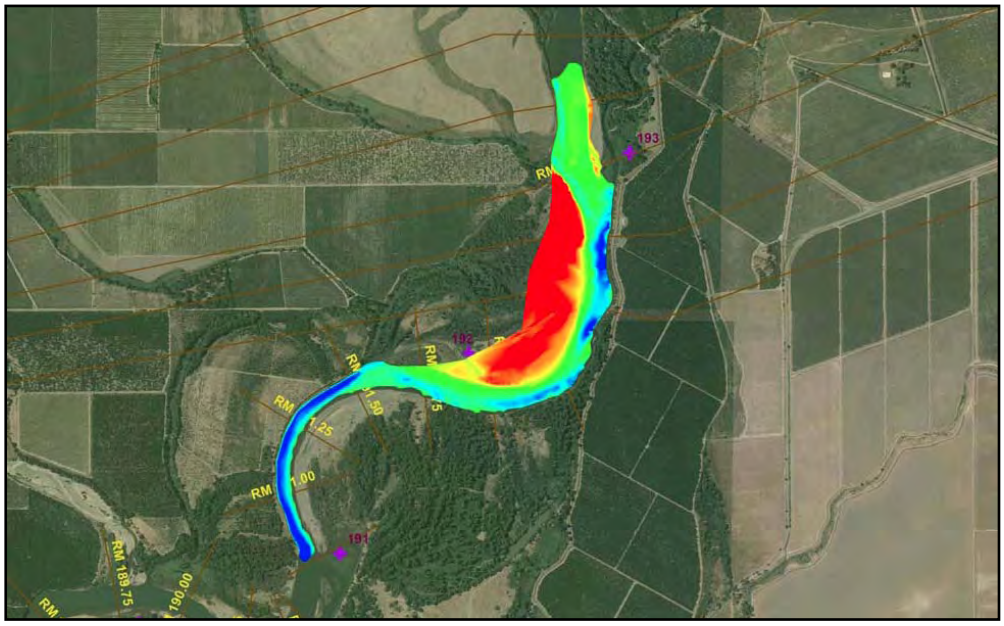

Figure 4-2. Bed elevation contours based on the TIN formed from all survey points.

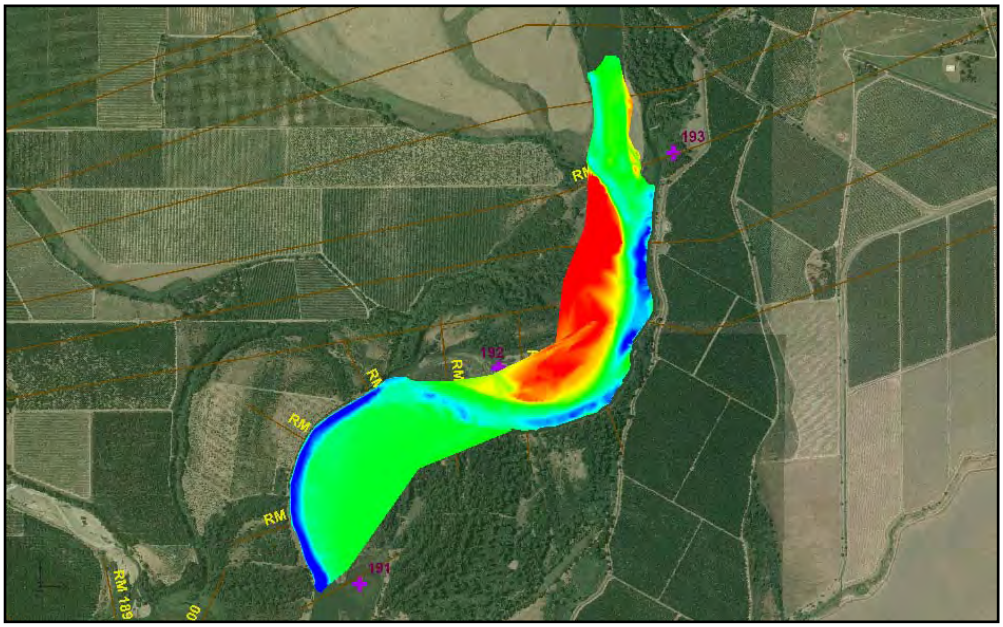

Figure 4-3. Bed elevation contours when extra topographic data are added at the left downstream bar.

4.3 Verification and Validation for SRH-2D and U^{2}RANS

This section focuses on verification and validation of both the SRH-2D and U^{2}RANS models for their ability to predict flow hydraulics. Field data, described in the previous section, are available for comparison.

4.3.1 Velocity Data near RM 192.5

Velocity data were collected on May 10, 2005 with an Acoustic Doppler Profiler (ADP) instrument. The survey team recorded 3D velocity vectors at several cross sections near RM 183 and 192.5. The average daily flow for that day at the U.S. Geological Survey (USGS) stream gauge 11377100 near Red Bluff (RM 245) was 24,600 cfs; and at USGS stream gauge 11389500 near Colusa (RM 145), the flow was 29,400 cfs.

The plan view of all velocity measurement points is shown in figure 4-4 (in red) at RM 192.5. Note that only the depth averaged velocity at these horizontal points is compared with the simulation.

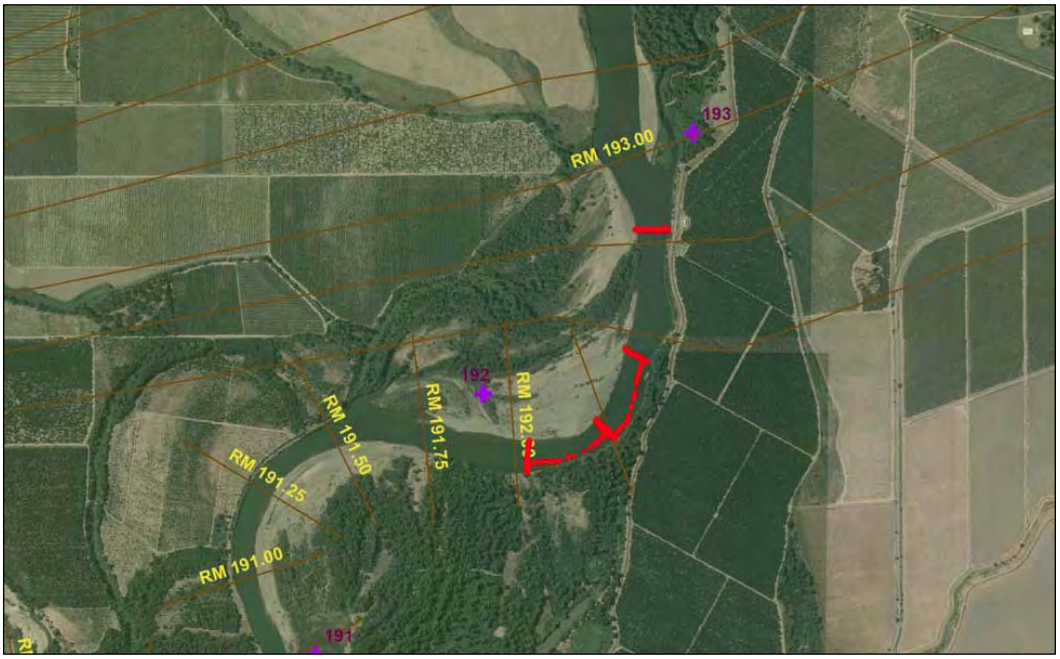

Figure 4-4. Plan view of all velocity measurement points (in red) at RM 192.5. Cross sections are labeled with RM.

4.3.2 Mesh Development

A 2D horizontal mesh is developed using the Surface-Water Modeling System (SMS) for SRH-2D hydraulic modeling (Aquaveo LLC 2010). The same mesh is

then used to develop a 3D mesh suitable for use by U^{2}RANS by extending each horizontal point from bed to water surface.

The solution domain and the zonal (polygonal) partitions are determined first. The solution domain consists of about 2.7 RMs and is limited to the coverage area of the topographic survey data (see figure 4-1). The polygonal partitions are less critical for the study because only the main channel is wetted and a constant Manning's roughness coefficient is used. The final solution domain and the generated mesh are shown in figure 4-5, and a zoom-in view of the mesh is displayed in figure 4-6. The 2D mesh has a total of 4,380 cells and 4,413 mesh points. The mesh extends approximately 3 miles and is between 600 and 1000 feet wide. The 3D mesh is obtained by using 16 mesh points to extend the 2D mesh points vertically from the bed to the water surface. The 3D mesh has a total of 65,790 cells and 70,608 mesh points.

It is important to be certain that the river topography is well represented by the mesh. The bed elevation contours, based on the 2D mesh and shown in figure 4-7, can be compared with the survey points data. This comparison shows that the topography has been well represented by the mesh. Figure 4-8 also shows a 3D view of the riverbed.

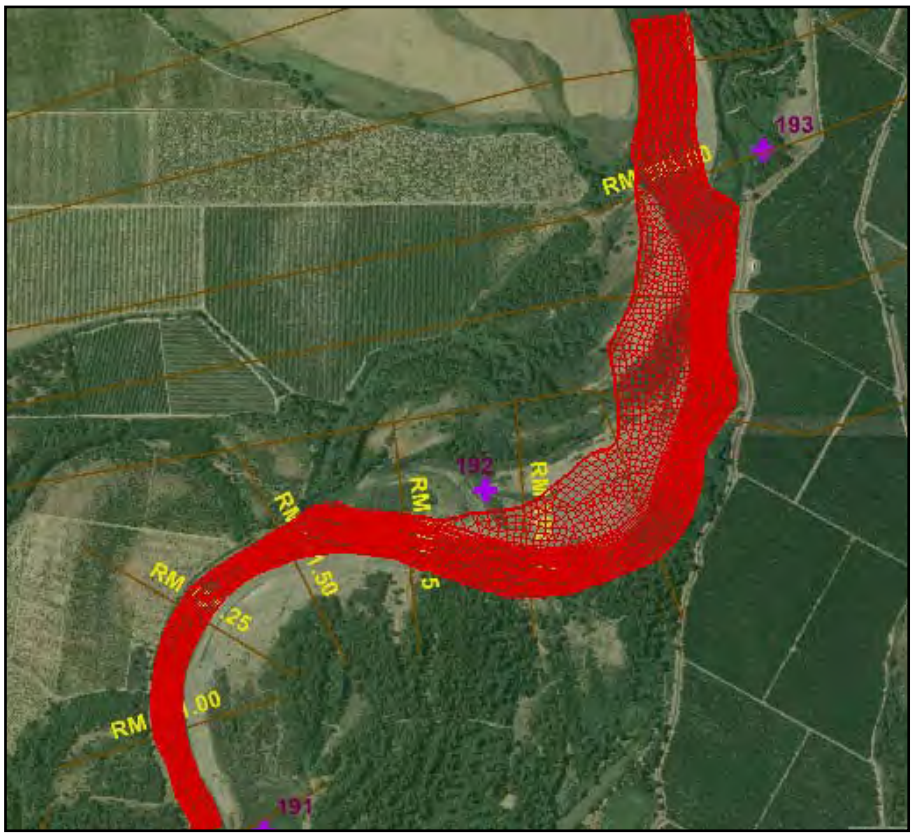

Figure 4-5. Solution domain and the 2D mesh for the SRH-2D simulation.

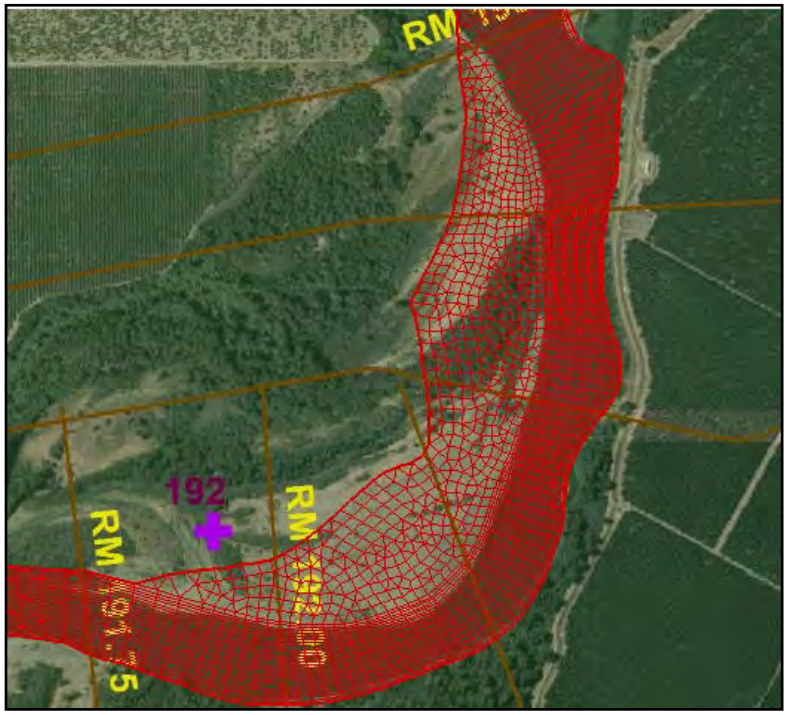

Figure 4-6. A zoom-in view of the 2D mesh at the bar area.

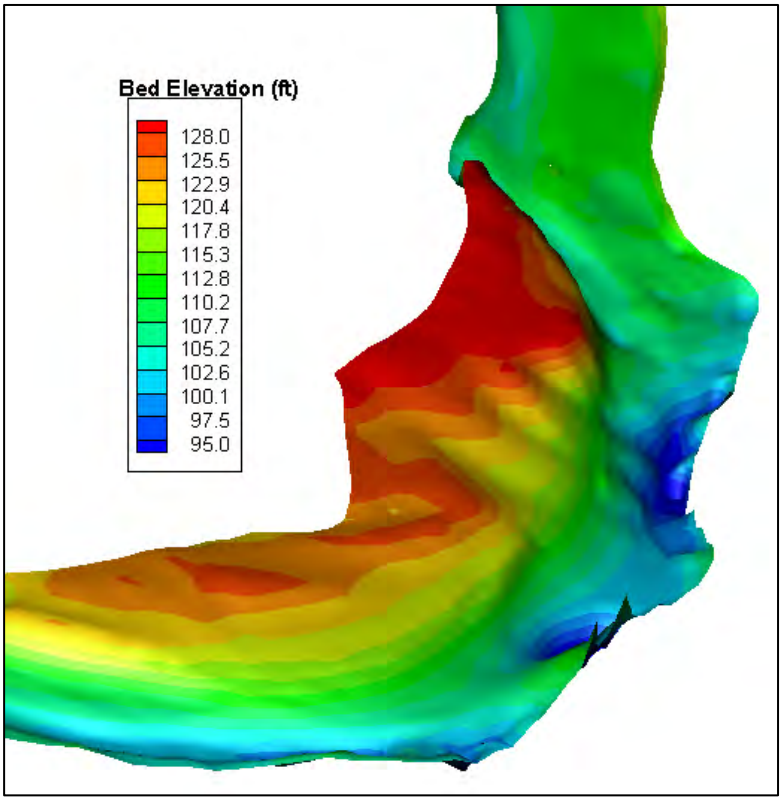

Figure 4-7. Bed elevation contours based on the 2D mesh.

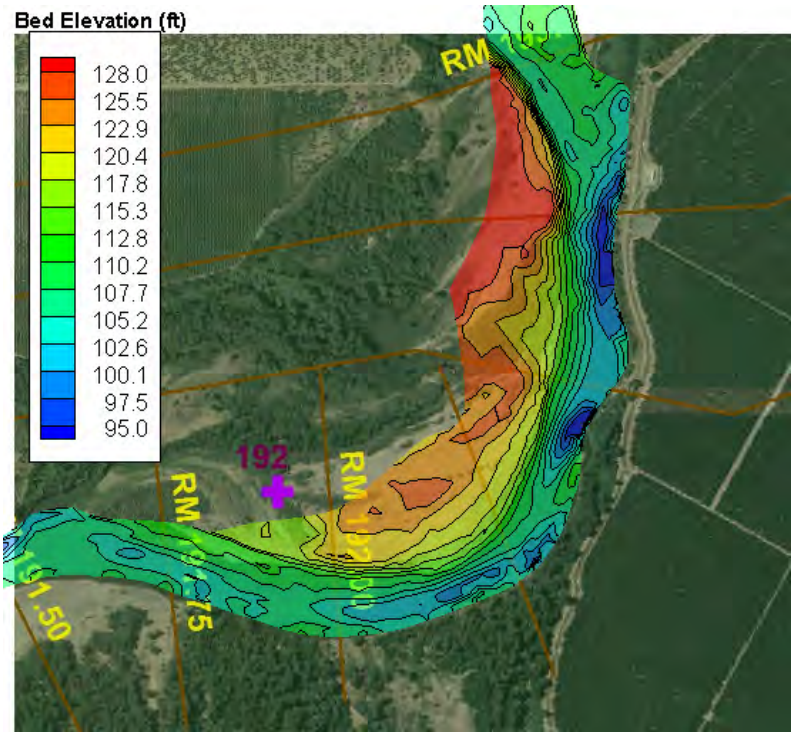

Figure 4-8. A 3D view of the bed for the bend at 192.5 RM; 1:10 vertical distortion.

4.3.3 Model Description

The SRH-2D model used the mesh discussed above. Flow enters at the upstream boundary. There is a large uncertainty in discharge based on the measured velocity (Reclamation 2005). Measured discharge ranges from 21,200 cfs to 29,400 cfs. Based on the post-analysis of simulation results, it was determined that the actual flow would be towards the higher end of the uncertainty range. Simulations used a flow discharge of 29,400 cfs, recorded at USGS stream gauge 11389500 near Colusa (RM 145).

The water surface elevation at the downstream end of the solution domain is needed for an exit boundary condition. This study used results from the Sedimentation River Hydraulics One-Dimensional Sediment Transport Dynamics Model (SRH-1D). SRH-1D simulated more than 100 miles of the Sacramento River. The predicted water surface elevation at the exit boundary of the solution domain from SRH-1D is approximately 116 feet. Comparison of the measured and simulated water depths later validated the downstream boundary.

The SRH-1D model used a Manning's roughness coefficient of 0.027 for the reach at the RM 192.5 meander bend. The SRH-1D model was calibrated to observed water surface measurement near the point bar. The same coefficient was used for the SRH-2D simulation and uniformly applied to the entire solution

domain. The U^{2}RANS 3D modeling required an effective roughness height, and a value of 0.024 meter was used, which is the median particle diameter of the bed.

4.3.4 Results and Discussion for Verification and Validation

Both SRH-2D and U^{2}RANS models were used to simulate the flow at the RM 192.5 bend. First, the water depths were compared at all measurement points shown in figure 4-9. The agreement between the predicted and measured results is good, particularly taking the uncertainty of the ADP measurement into consideration.

The velocity vector comparison between the simulation and the measured data is shown in figures 4-10 and 4-11. For further examination of the results, measurement points are divided into four cross sections as marked in figures 4-10 and 4-11. Velocity vector results are then compared at the four cross sections (shown as XS) from figures 4-12 to 4-19 for both SRH-2D and U^{2}RANS results. For figures 4-10 through 4-19, black arrows are the measured data and red arrows are the U^{2}RANS results. Not all points are displayed.

Further, the velocity magnitude between measured and predicted results is compared in figures 4-20 to 4-23 using the XY plots for the four cross sections. The only significant deviation between the 2D model and the measured velocity magnitude seems to be at cross section 3. The model does not pick up the switch of the velocity maximum from the left bank to the right bank between cross sections 2 and 3. The 3D model does simulate this switch accurately. Overall, the 2D model simulates the velocity direction and magnitude relatively well.

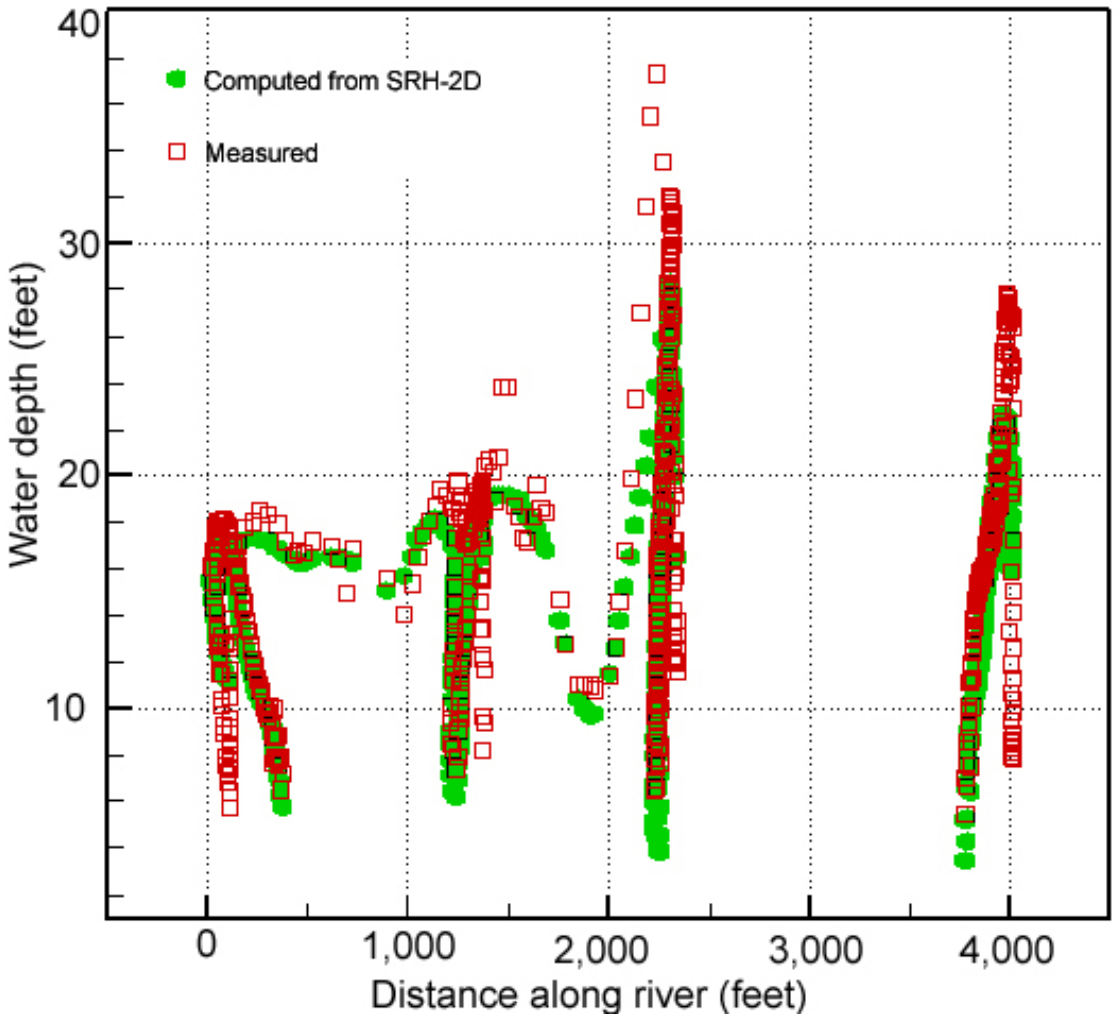

Figure 4-9. Comparison of measured and computed water depth at all velocity measurement points; distance along river is relative to the downstream-most measured point.

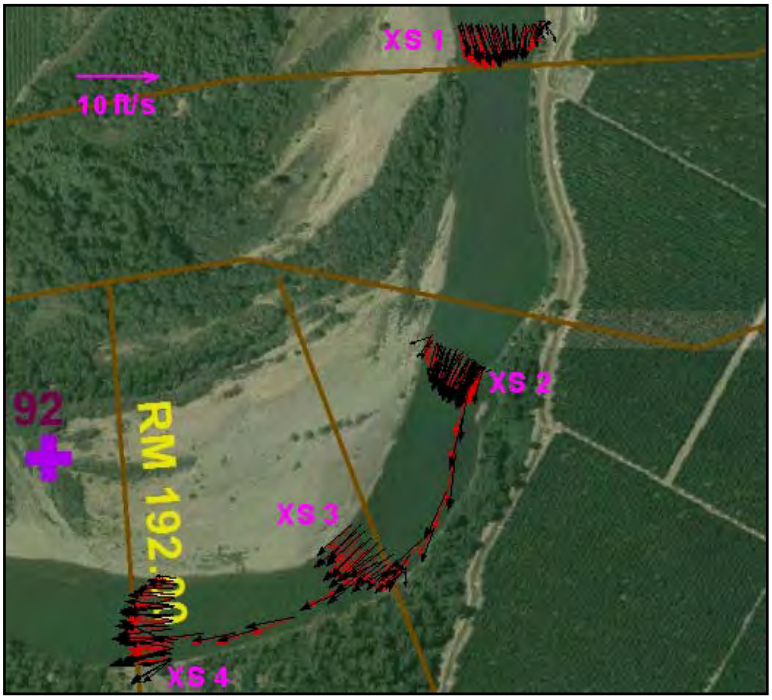

Figure 4-10. Comparison of velocity vectors at all measurement points between measured and SRH-2D data. Black arrows are computed and red arrows are measured.

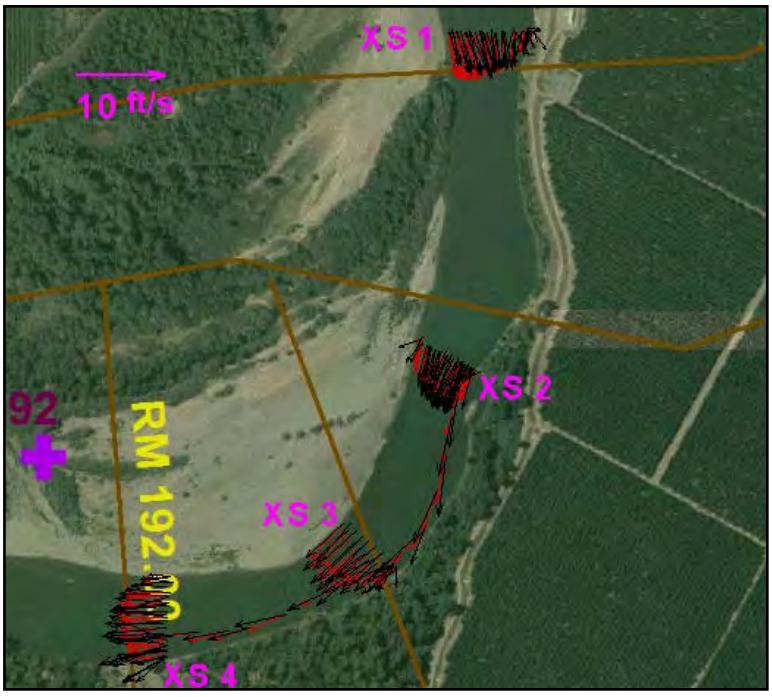

Figure 4-11. Comparison of velocity vectors at measurement points between measured and U^{2}RANS data. Black arrows are computed and red arrows are measured.

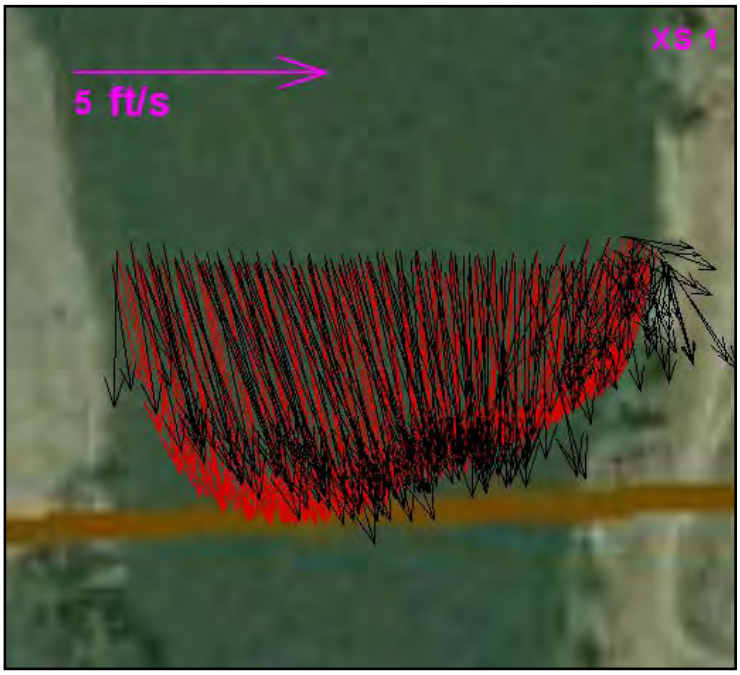

Figure 4-12. Comparison of velocity vectors at cross section 1 between measured and SRH-2D data. Black arrows are computed and red arrows are measured.

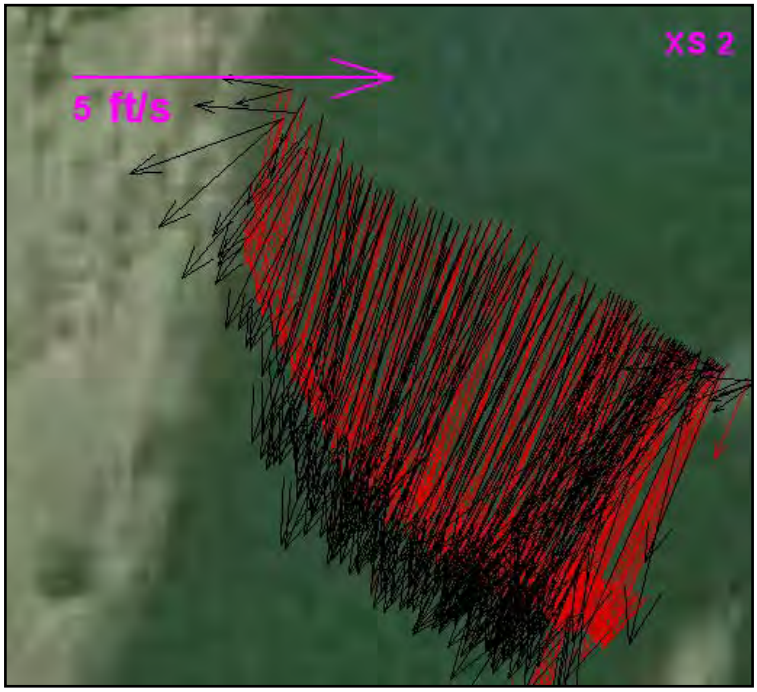

Figure 4-13. Comparison of velocity vectors at cross section 2 between measured and SRH-2D data. Black arrows are computed and red arrows are measured.

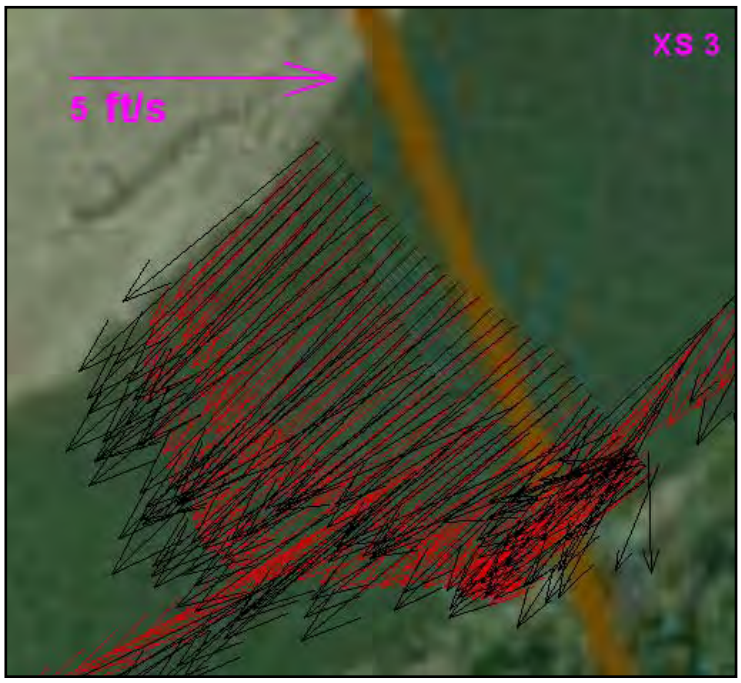

Figure 4-14. Comparison of velocity vectors at cross section 3 between measured and SRH-2D data. Black arrows are computed and red arrows are measured.

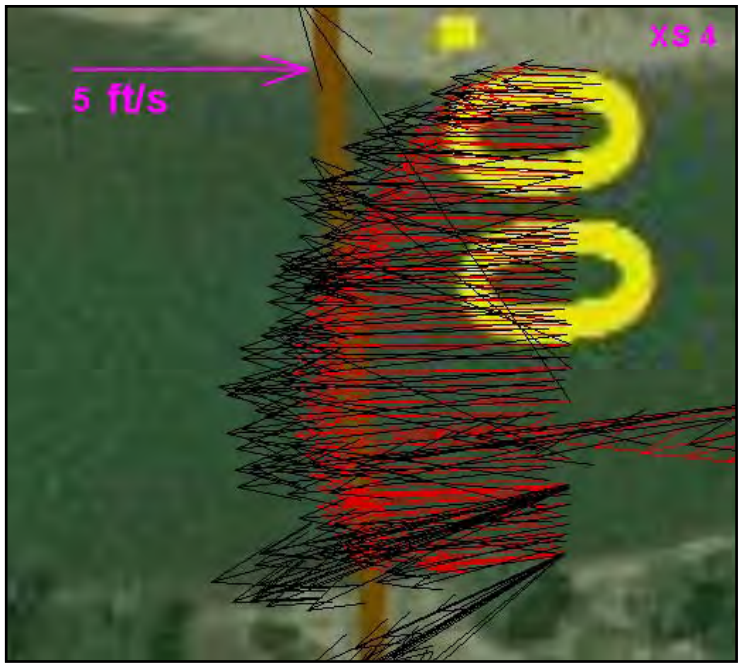

Figure 4-15. Comparison of velocity vectors at cross section 4 between measured and SRH-2D data. Black arrows are computed and red arrows are measured.

Figure 4-16. Comparison of velocity vectors at cross section 1 between measured and U^{2}RANS data. Black arrows are computed and red arrows are measured.

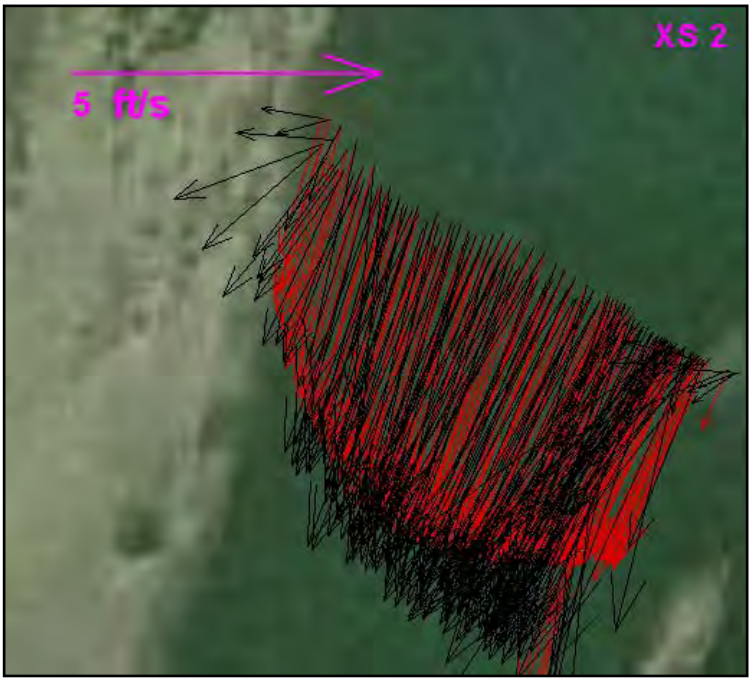

Figure 4-17. Comparison of velocity vectors at cross section 2 between measured and U^{2}RANS data. Black arrows are computed and red arrows are measured.

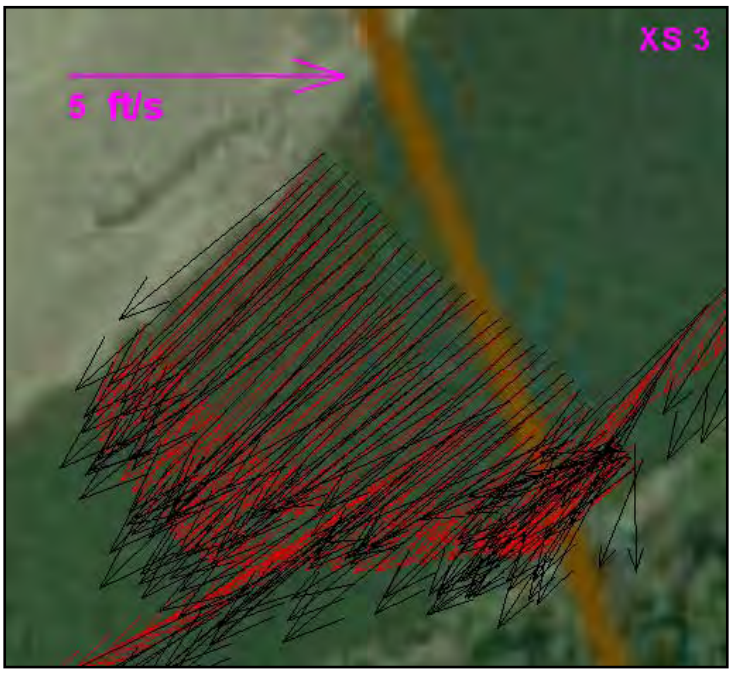

Figure 4-18. Comparison of velocity vectors at cross section 3 between measured and U^{2}RANS data. Black arrows are computed and red arrows are measured.

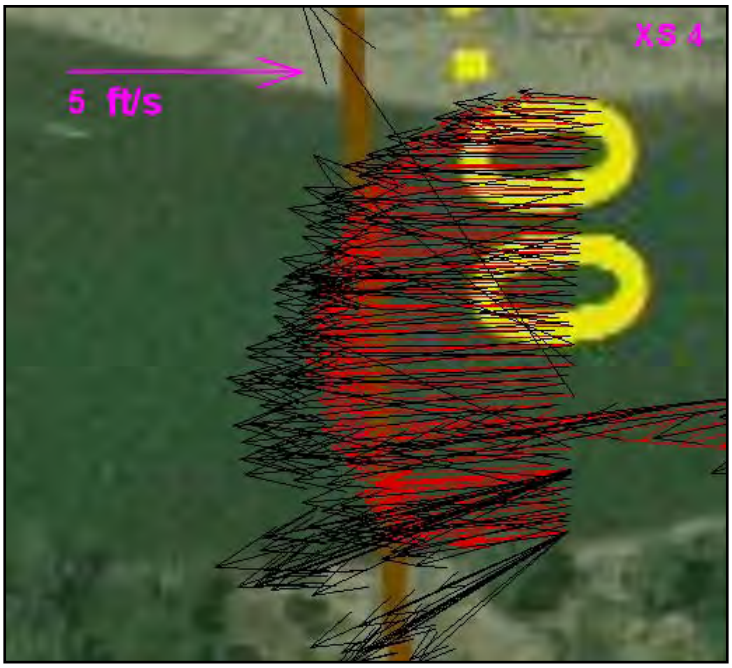

Figure 4-19. Comparison of velocity vectors at cross section 4 between measured and U^{2}RANS data. Black arrows are computed and red arrows are measured.

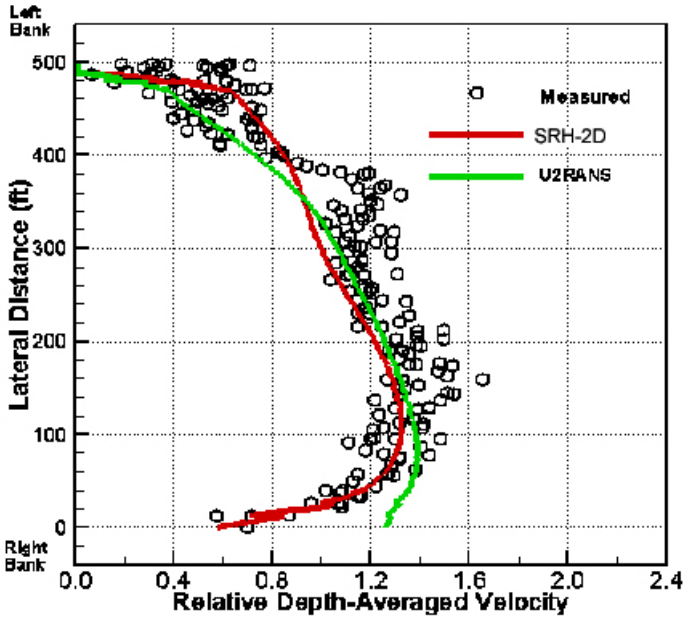

Figure 4-20. Comparison of relative velocity magnitude at cross section 1. Depth-averaged velocity is scaled by the mean velocity, and lateral distance is relative to the rightmost measurement point on the cross section.

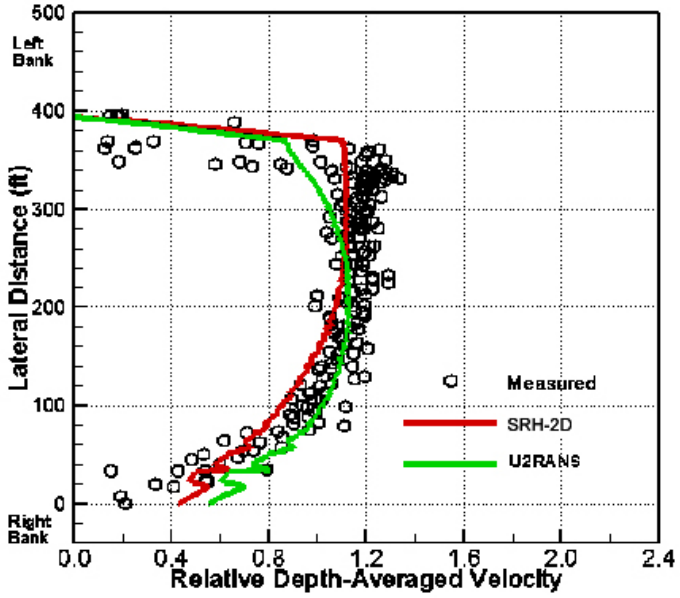

Figure 4-21. Comparison of relative velocity magnitude at cross section 2. Depth-averaged velocity is scaled by the mean velocity, and lateral distance is relative to the rightmost measurement point on the cross section.

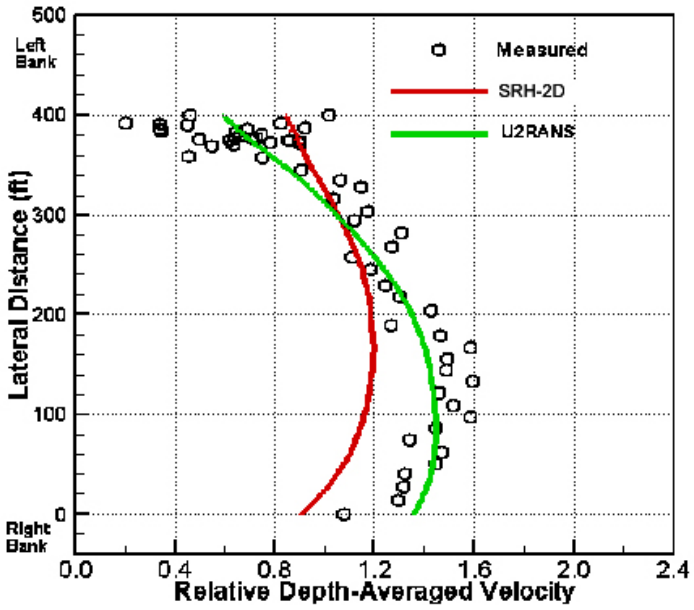

Figure 4-22. Comparison of relative velocity magnitude at cross section 3. Depth-averaged velocity is scaled by the mean velocity, and lateral distance is relative to the rightmost measurement point on the cross section.

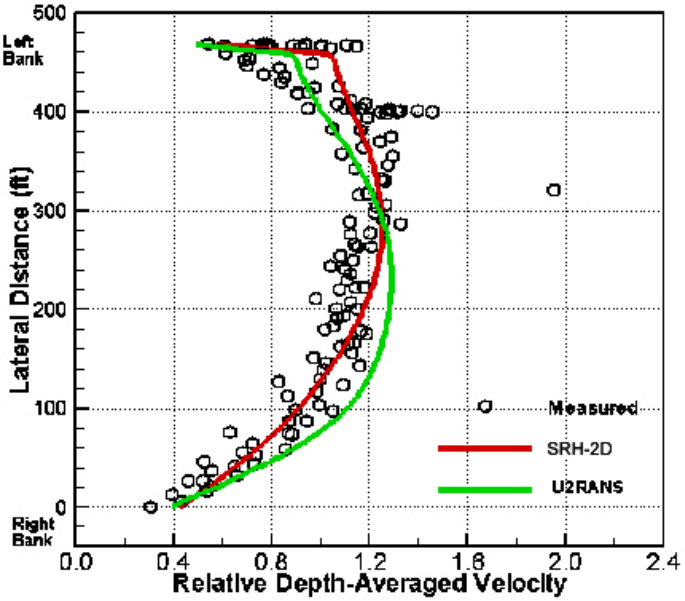

Figure 4-23. Comparison of relative velocity magnitude at cross section 4. Depth-averaged velocity is scaled by the mean velocity, and lateral distance is relative to the rightmost measurement point on the cross section.

When comparing the measurements with the simulated value, note that turbulence causes considerable variation in velocity over time. The variation in velocity due to turbulence is roughly proportional to the friction velocity. The constant of proportionality varies based upon the channel geometry and roughness, but it is around 2 or greater (Nezu and Rodi 1986). For this section, the friction velocity based on the average friction slope is approximately 0.3 foot per second (ft/s) as computed from a Hydrologic Engineering Centers River Analysis System (HEC-RAS) model of the river. Therefore, the turbulent velocity fluctuations could be 0.6 ft/s or greater. To obtain a true time-averaged velocity at a point, many velocity profiles over a long time period need to be recorded. The velocity measurements at a given point should be thought of as a possible velocity at a point, not the true average velocity at a point. At any given instance in time, the velocity can vary about the mean by approximately 0.6 ft/s.

4.4 Mobile Bed Simulation for the 1986 Flood

This section illustrates the capabilities of the SRH-2D model and demonstrates that SRH-2D can be used for sediment transport and other modeling questions relevant for this project.

SRH-2D has been verified and validated with a number of laboratory datasets and one validation was reported in the conceptual model report (Reclamation 2006b). Hydraulic flow has been validated as discussed in Section 4.2 of this report. Although SRH-2D has been verified on previous projects,[1] no sediment data are available to verify the model on the Sacramento River. Therefore, results should be considered preliminary and are for demonstration purposes only.

4.4.1 Sediment Transport Data

Sediment transport in a river depends on many variables such as flow hydraulics, bed gradation, and upstream sediment supply. The bed gradation may change from its initial state as sediment particles are removed or deposited on the bed. Flow hydraulics and fractional sediment transport rates change due to the adjusting bed gradations. In general, the water column and the riverbed may be divided into four vertical layers:

- **Suspended Load:** a layer in the water column where sediment particles are hydraulically entrained. This movement is labeled as “suspended load” (including wash load).

- **Bed Load:** a layer near the bed where sediment particles roll, slide, or saltate.

[1] See papers on the SRH-2D Web site http://www.usbr.gov/pmts/sediment/model/srh2d/

- **Active Layer:** a layer on the top surface of a bed where sediment exchange occurs between the substrate and water.

- **Subsurface Layer:** one or more bed layers underneath the active layer.

Bed material load transport is addressed for this project. Bed material load consists of the particles present in the substrate in significant quantities. The bed material load combines suspended load and bed load, but it neglects the wash load fraction of suspended load.

Sediments are assumed to be noncohesive and nonuniform, and they are divided into a number of sediment size classes. Each sediment class is routed through the river and subject to interaction and exchange with the particles on the bed. The nonuniform (or multi-size) approach is necessary to simulate armoring and sorting. Each sediment size class obeys the mass conservation equation for nonequilibrium transport. The sediment transport capacity formula is used to provide a limit for the equilibrium rate, but the rate itself is solved by the nonequilibrium mass equations. The model can automatically determine if the sediment transport is supply limited or capacity limited. In this study, the Parker (1990) sediment transport capacity equation is used to compute the fractional sediment transport capacity. This equation was originally developed for gravel transport but was later found to be applicable to sand and gravel mixture (Andrews 2000). The Parker equation is particularly suited to the multi-size simulation due to inclusion of a hiding effect.

4.4.2 Mesh Development

The solution domain and the mesh for the sediment simulation are the same as those of the flow simulation presented in Section 4.2, except for adding an area representing the downstream left bar. The reason for this addition is that simulated flow discharges as high as 100,000 cfs inundate a larger extent of the solution domain. The expanded solution domain is still too small to contain the 100,000 cfs flood, but no measured topographic data exist for the larger area. Because the larger flows are for demonstration purposes only, no additional data were collected.

The solution domain and the mesh are displayed in figure 4-24 and may be compared with the mesh in figure 4-5. Also, the bed elevation contours, represented by the mesh, are shown in figure 4-25. It may be compared with figure 4-3, in which elevation contours are from the survey data only. The mesh accurately represents the topography.

The mesh in figure 4-24 uses both quadrilateral and triangular cells and consists of 4,856 mesh cells and 4,556 mesh points.

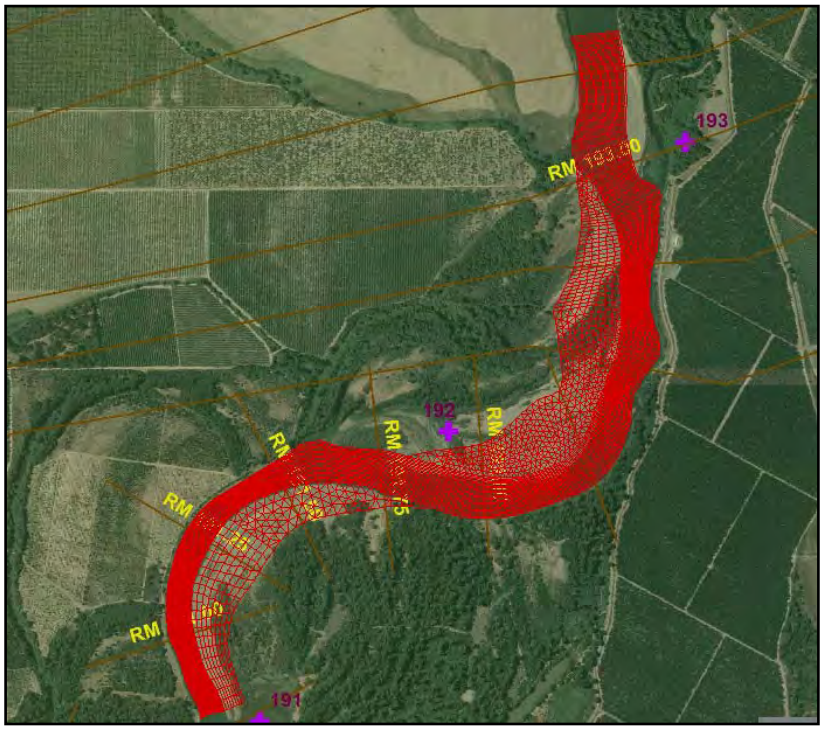

Figure 4-24. Solution domain and the mesh used for SRH-2D simulation.

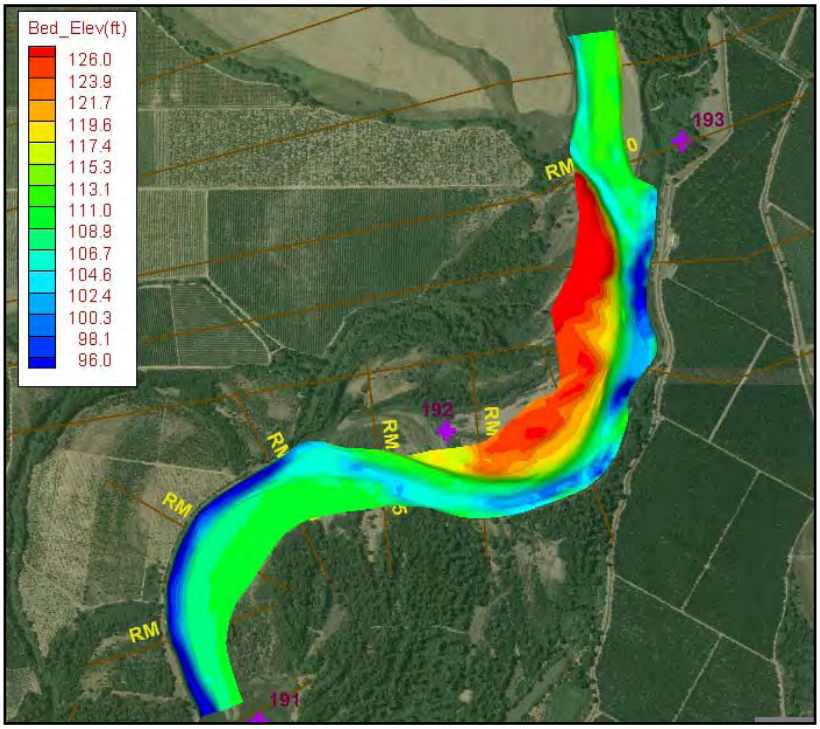

Figure 4-25. Bed elevation contours based on the elevations represented by the mesh in figure 4-24.

4.4.3 Sediment Classes

In this study, the sediment mixture was divided into nine sediment size classes as listed in table 4-1. The classes 1-3 represent sands, class 9 is used to represent the nonerodible bed, and the remaining classes represent gravels.

Table 4-1. Sediment Diameters of Each Size Class for the Simulation

Size Class No.	1	2	3	4	5	6	7	8	9
Lower d(mm)	.0625	0.25	1	2	4	10	60	100	300
Upper d(mm)	0.25	1	2	4	10	60	100	300	10,000

Note: mm = millimeters

4.4.4 Initial and Boundary Conditions

The 1986 flood was used as the flow through the simulated reach. Figure 4-26 shows the 1986 floodflows through the simulated reach. The hydrograph starts from January 1, 1986, and ends on April 30, 1986; therefore, a time-accurate unsteady simulation is carried out there for 4 months (150 days) using SRH-2D. The flow reaches its highest discharge on February 19, with a value of 103,190 cfs.

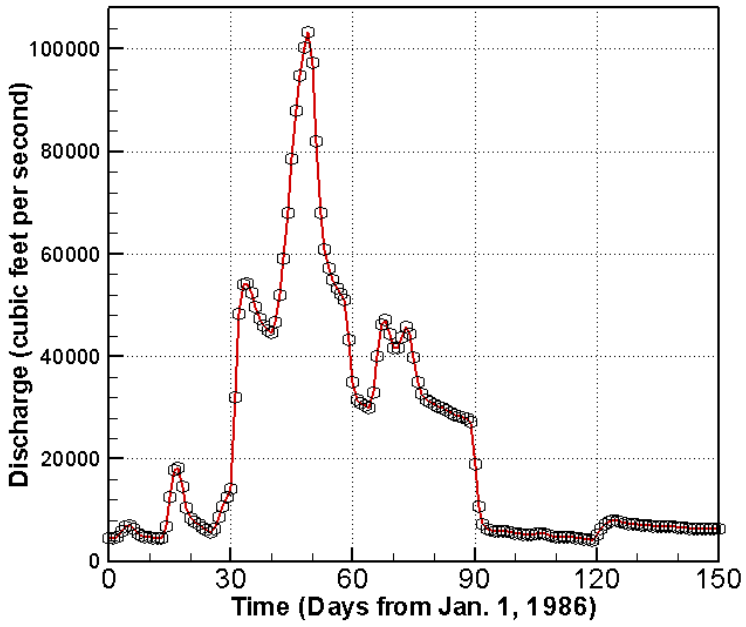

Figure 4-26. Flow hydrograph representing the 1986 floodflow recorded below Glen-Colusa Irrigation District (GCID).

The hydrograph (discharge) is applied as the boundary condition at the upstream boundary. The downstream boundary requires a water surface elevation. Due

to the unsteady nature of the flows, the water elevation is not constant and varies with flow. This study used a stage-discharge rating curve from the SRH-1D model results. The rating-curve data at the exit boundary of the current model are shown in figure 4-27.

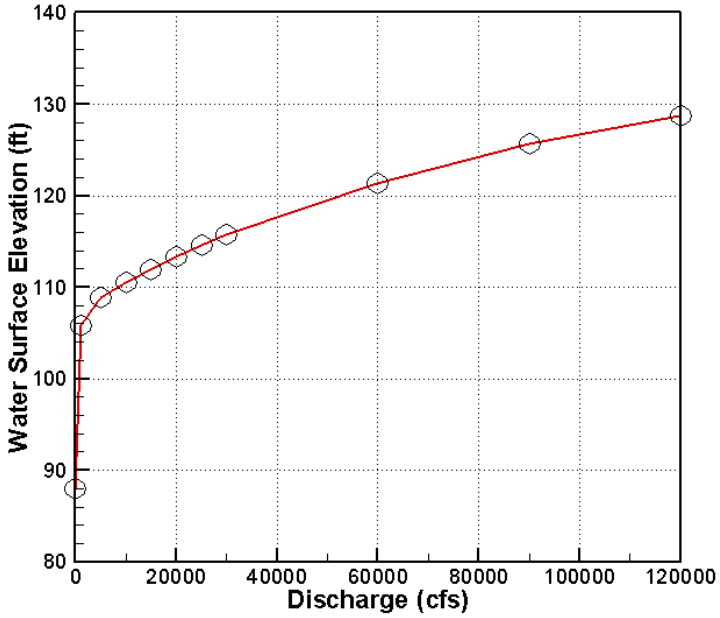

Figure 4-27. The stage-discharge rating curve based on SRH±-1D simulation results.

Two additional data sets are needed for the mobile bed simulation:

- **Sediment gradation on the bed.** There are limited bed gradation data available for the river reach under study. The information used is from the data that the U.S. Army Corps of Engineers collected in 1981 (Water Engineering and Technology [WET] 1988). The data provides the bed gradation at a number of locations within or near the simulated reach listed in table 4-2. There is large scatter in the data, and the lateral locations of the sample points are unknown. More sediment samples are recommended for the site if a more accurate simulation is sought. Four bed material zones are delineated as shown in figure 4-28, and different bed gradations may be assigned to different zones. The gradation of each zone is estimated from the data in table 4-2 and is shown in table 4-3 and figure 4-29. The sediment is assumed to be finer on the downstream end of the point bar than the upstream end. In particular, the upstream end of the bar had a D_{50} of 20 mm, the middle portion of the bar had a D_{50} of 6 mm and the downstream portion of the bar had a D_{50} of 1 mm, or sand-sized. Additionally, the Manning's roughness coefficient is also assigned for each zone: 0.028 for the main channel and 0.025 for the remaining zones.

- **Sediment supply at the inlet boundary.** For the sediment supply at the inlet boundary, the "capacity" method is used; that is, the sediment supply is equal to the computed sediment transport capacity.

Table 4-2. The Surface Gradations at Selected Sample Locations Collected in 1981 (WET 1988)

River Mile	D_{16} (mm)[1]	D_{35} (mm)	D_{50} (mm)	D_{84} (mm)	D_{95} (mm)
197.7	0.43	2.18	5.94	35.7	53.33
190.8#1[2]	0.25	4.0	8.76	22.11	28.51
190.8#2	0.25	0.30	0.34	0.45	0.5
189.4#1	1.26	9.28	20.16	73.52	107.63
189.4#2	0.71	6.46	11.5	24.51	29.8
189.3#3	0.19	0.29	0.33	0.46	0.66

[1] mm = millimeters
[2] # is the survey point on the RM.

Table 4-3. The Bed Gradations Used for Each Zone of the Solution Domain

Zone Name	D_{16} (mm)	D_{35} (mm)	D_{50} (mm)	D_{84} (mm)	D_{95} (mm)
Main channel	2.0	10.0	60.0	100.0	200.0
Bar – upstream	1.0	9.0	20.0	70.0	105.0
Bar – middle	0.5	2.0	6.0	35.0	50.0
Bar – downstream	0.1	0.5	1.0	3.0	8.0

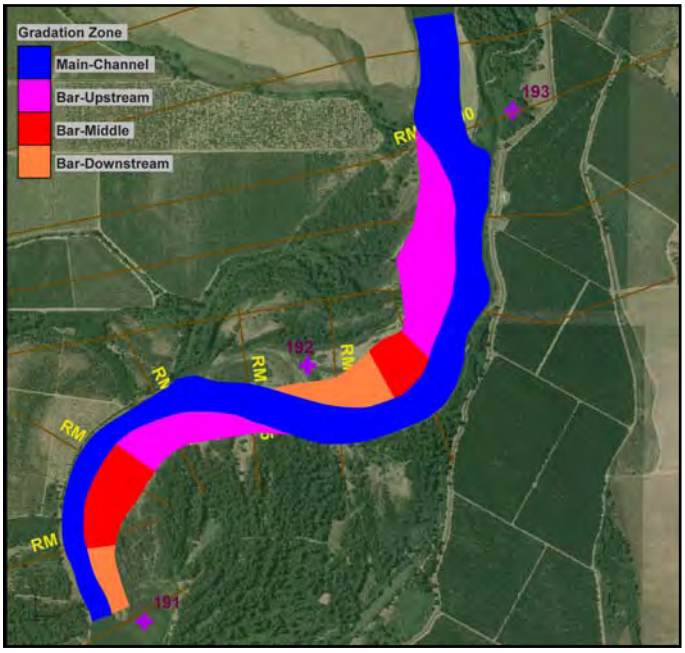

Figure 4-28. Partition of the solution domain into four gradation zones.

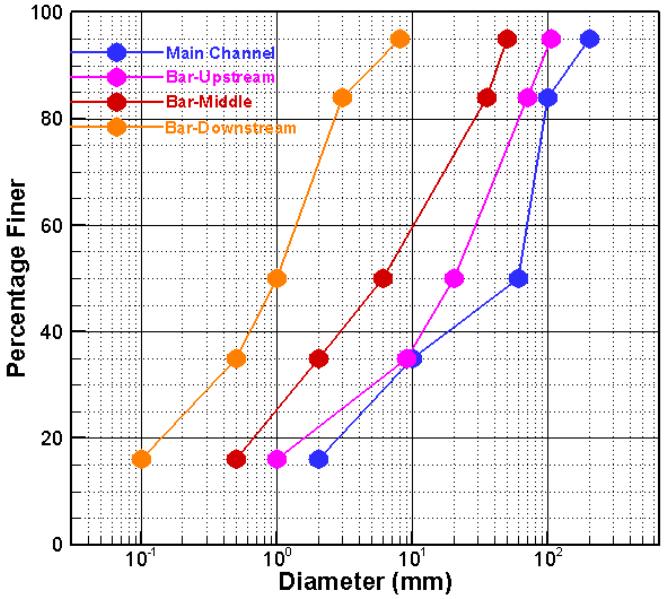

Figure 4-29. The bed gradations used for each zone of the solution domain.

For the initial condition at the beginning of the simulation, a separate steady state flow simulation was performed with a constant flow discharge of 4,431 cfs (the water elevation at the exit of the solution domain is fixed at 108.42 feet). These conditions correspond to the daily average flow on January 1, 1986. The steady state solution on January 1, 1986, is used as the initial condition, and the predicted velocity is shown in figure 4-30.

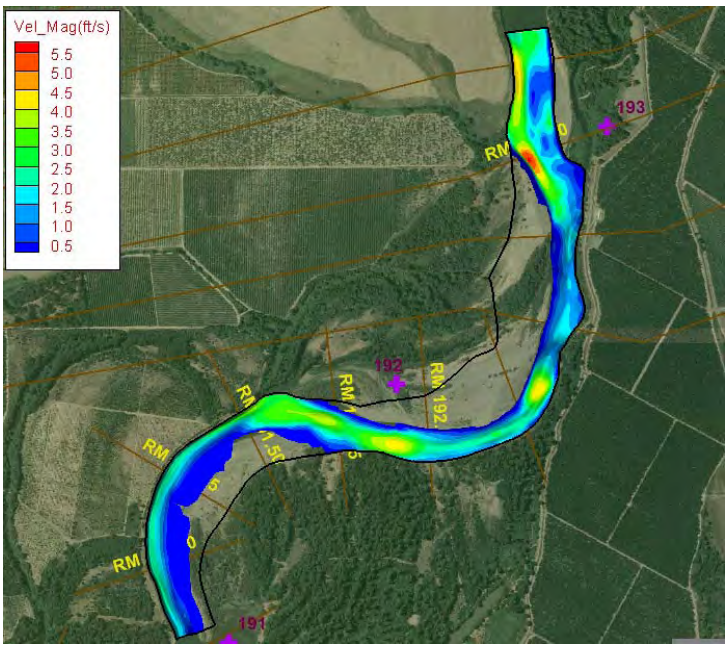

Figure 4-30. Simulated velocity at the constant flow discharge of 4,431 cfs; results are used as the initial conditions.

4.4.5 Results and Discussion for Mobile Bed Simulation

The mobile bed simulation period spanned from January 1 to April 30, 1986. A large amount of data was generated, and discussion below focuses on a few important observations. This simulation is intended as a demonstration of the mobile bed model.

The bed change due to erosion and deposition was less than 0.2 feet for the majority of the reach for flows below 20,000 cfs. Only higher flows are responsible for the bed evolution. This may be seen by comparing plots of the predicted net eroded and deposited depth. The flow discharge is below 20,000 cfs before January 31 and after March 31 (figure 4-26). Figure 4-31 shows that the erosion and deposition is small throughout January, while figure 4-32 shows that the erosion/deposition is negligible in the month of April. January 18 is chosen to display results, as the flow is 18,242 cfs. On March 31, the daily discharge is 27,092 cfs. Because little sediment moves under low flows, using higher flows only for sediment models would provide an accurate simulation of sediment movement.

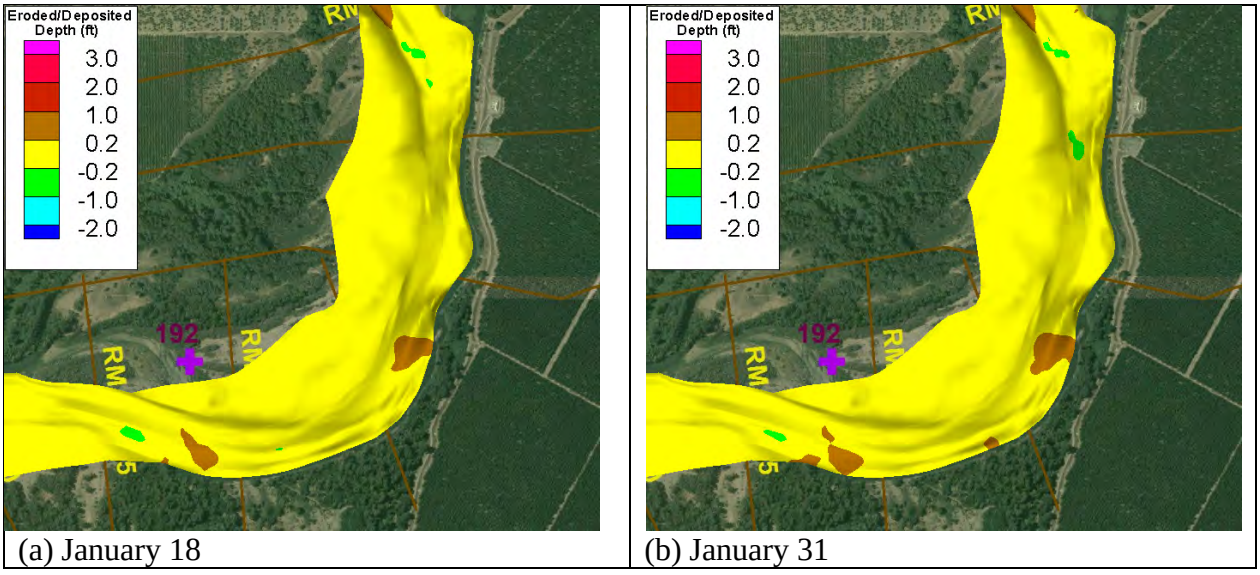

(a) January 18 (b) January 31

Figure 4-31. Net eroded (positive) and deposited (negative) depth in feet on January 18 and 31, relative to the bed elevation on January 1.

.

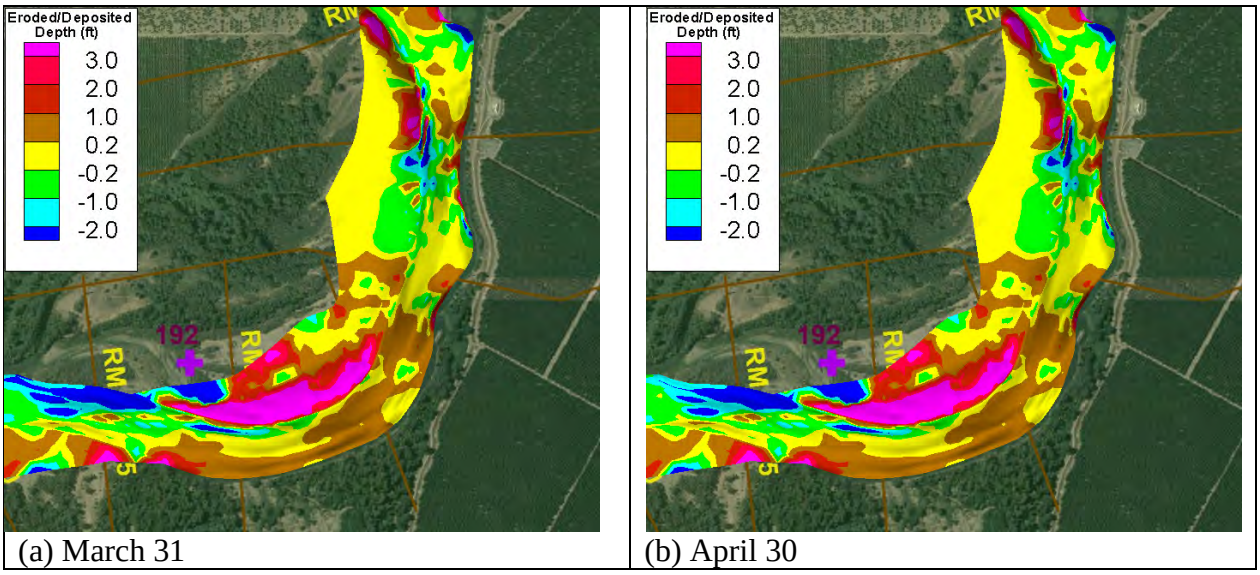

Figure 4-32. Net eroded (positive) and deposited (negative) depth in feet on March 31 and April 30, relative to the bed elevation on January 1.

Figure 4-33 shows inundation along with the flow velocity at different times. Results of inundation, as well as velocity, water depth, bed stress, and water elevation are available. These results may be used to evaluate the cottonwood survival and growth. The point bar at RM 192.5 is mostly dry before January 31, but the bar starts to become wetted in February as the flood begins. Water reaches the highest depth on February 19, where about 50 percent of the point bar has a water depth about 12 feet, accompanied by high velocity. During retreat of the flood, the water depth is decreases, and a portion of the bar returns to a dry condition as shown in the plot on February 28. On March 31, almost the entire bar is dry. There is a rich set of information available from the model, which may be used to assess the cottonwood growth on the point bar. If a specific area of the point bar is identified for seeding and growth of cottonwood, information about the wetting and drying, along with the duration and the magnitude, are available from the model. The survival model (Sedimentation and River Hydraulics One-Dimensional Sediment Transport and Vegetation Dynamics Model [SRH-1DV]) may use these results to assess the cottonwood "drowning" and survival potential (see Chapter 6).

The depth of scouring and deposition, as well as the sediment size distribution (or sorting), are also important for cottonwood survival. Scour will remove the young trees immediately, and deposition may potentially bury geminated plants. Also, gravels would hinder and even halt tree growth, while finer sediments would promote the growth. The simulated depth of net erosion and deposition on the point bar is shown in figure 4-34, and the sediment size distribution is displayed in figure 4-35 for selected times.

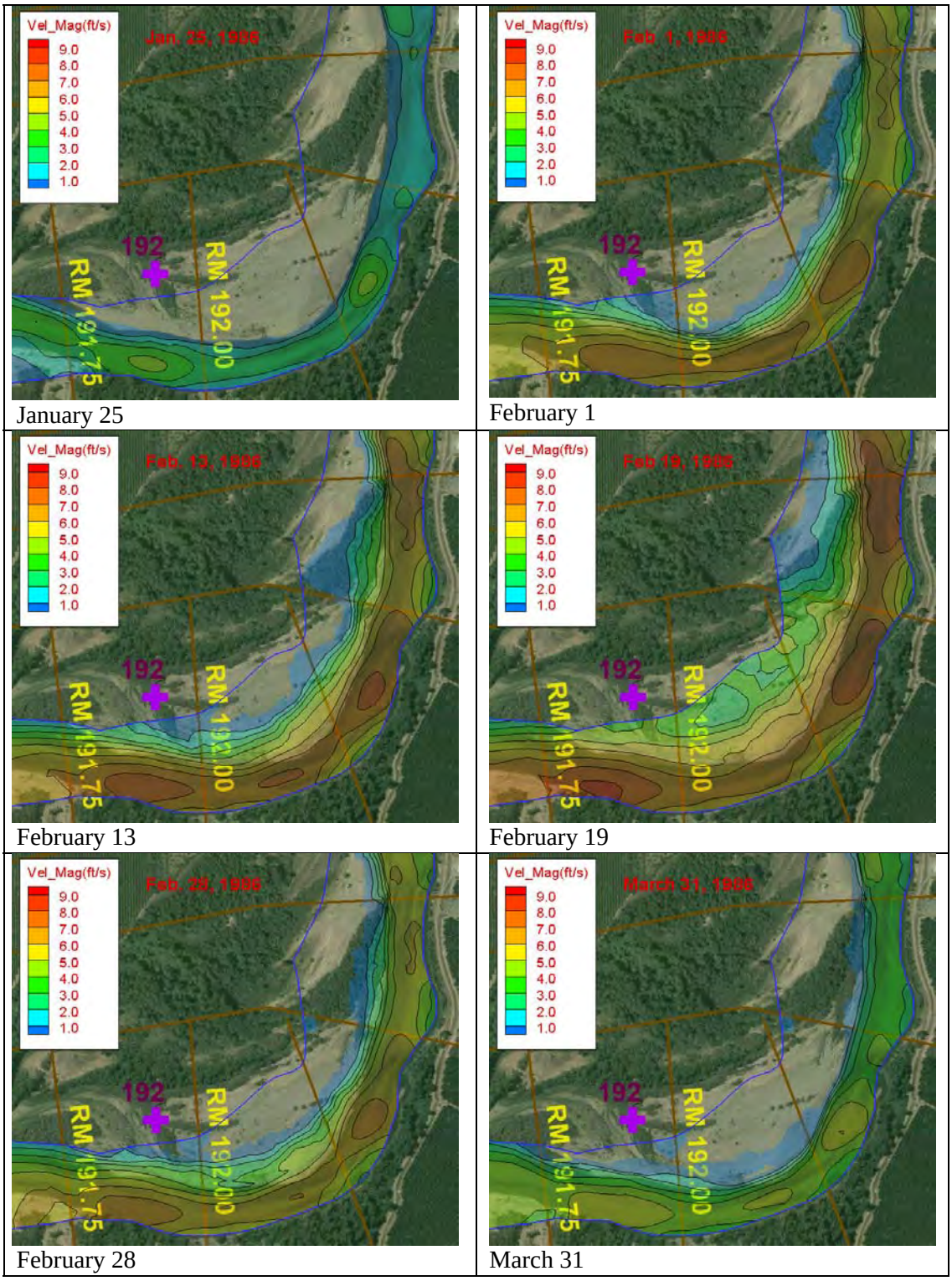

Figure 4-33. Inundation and velocity contours at various times.

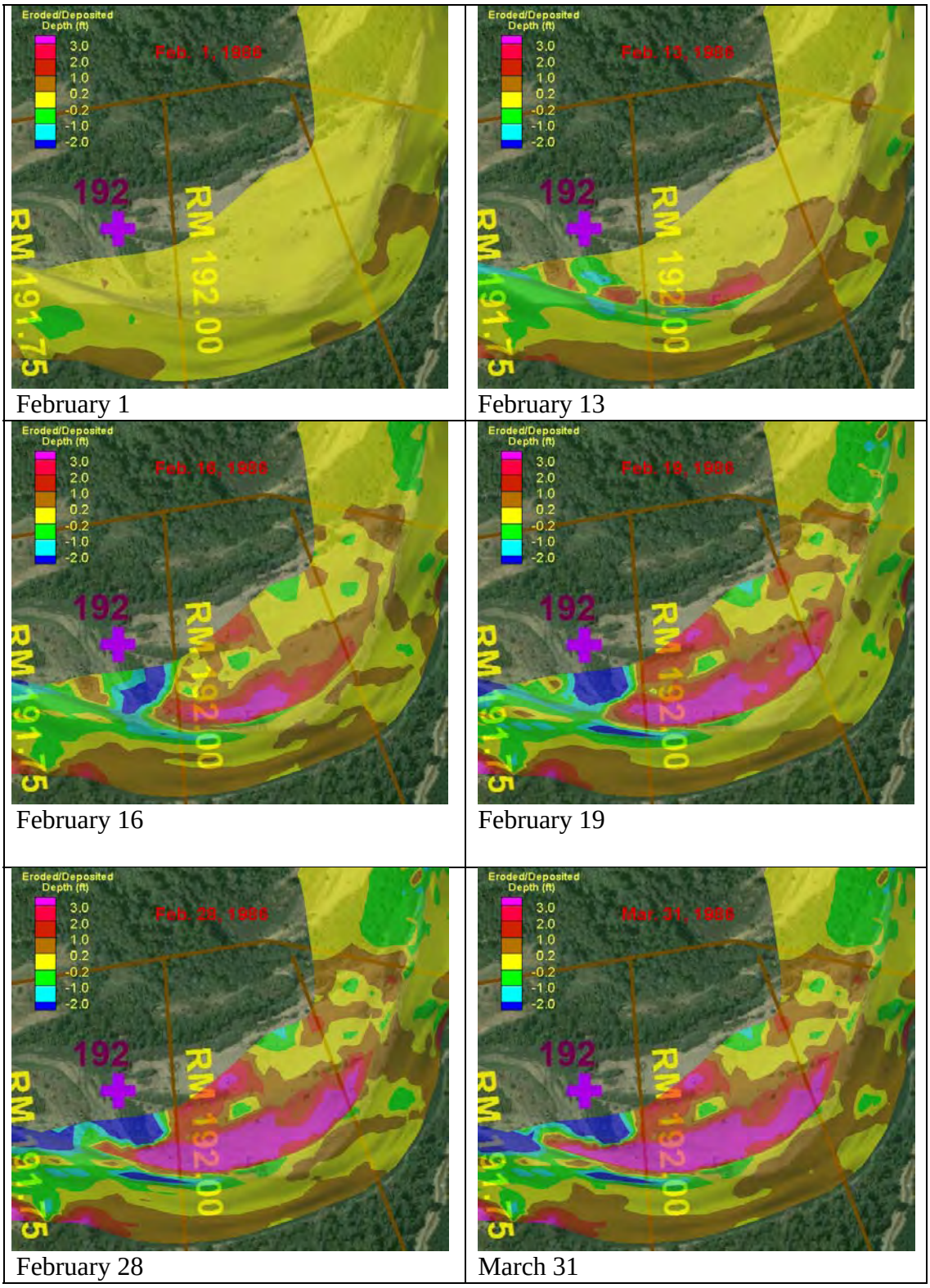

Figure 4-34. Net eroded (positive) and deposited (negative) depth, relative to January 1, 1986, at various times.

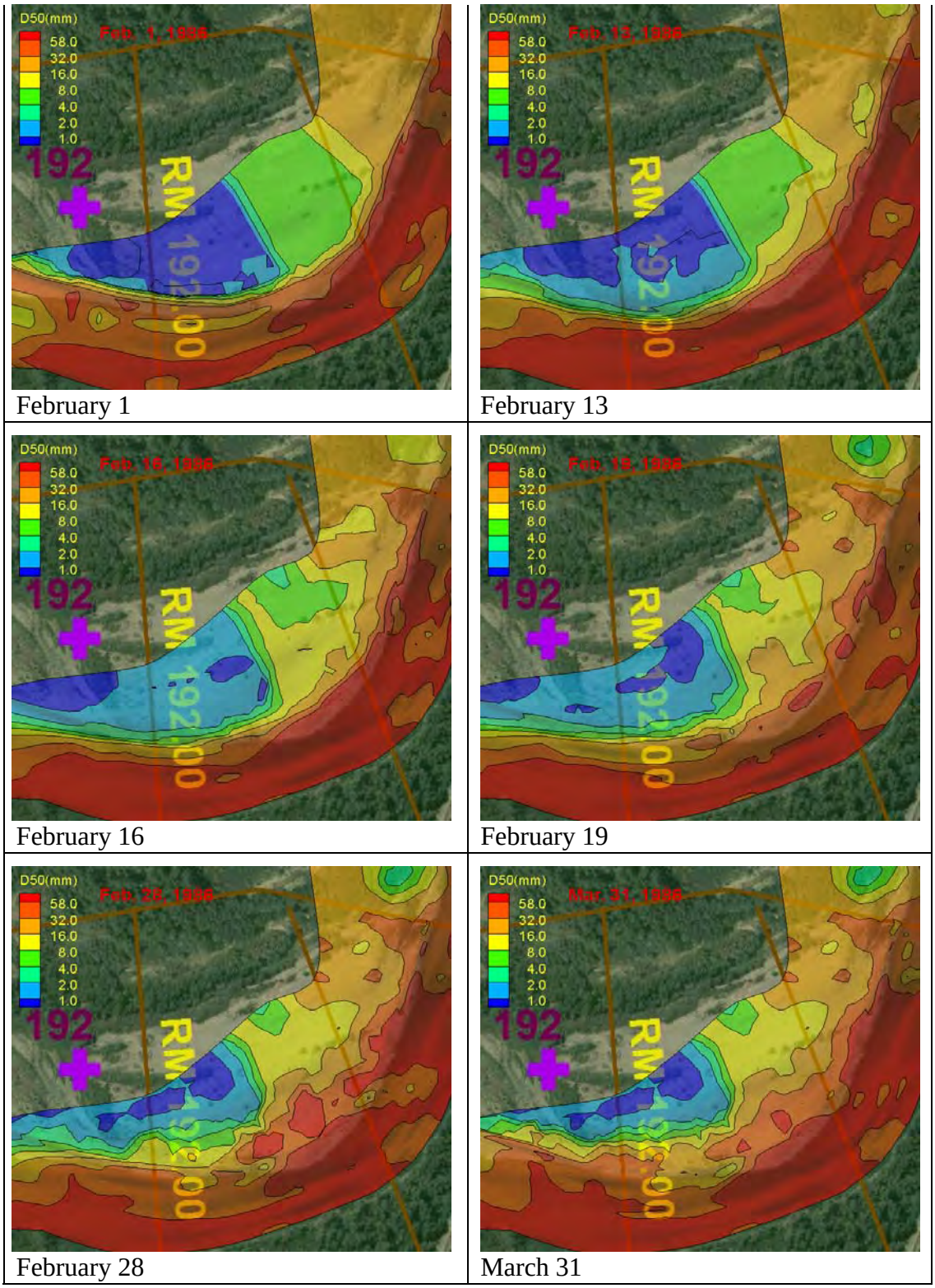

Figure 4-35. Sediment sorting with D_{50} distribution at various times.

The model predicted that most of the bar experienced erosion during the 1986 flood. The most severe erosion was at the point bar area close to the main channel. On February 19, the scour depth of the bar near the main channel was about 5 feet. Deposition occurred towards the downstream end of the bar. An examination of the sediment size distribution shows that the 1986 flood made the upstream portion of the bar coarser but the downstream portion of the bar remained sandy. Laterally, coarser sediments are near, and finer sediments are away from the river. The predicted distribution of the sediment sizes at the point bar at RM 192.5 is qualitatively consistent with Reclamation engineer's observations during the field trip in June 2005 and conceptual models of point bar evolution.

To increase the models' applicability and usefulness, two additional tasks are recommended:

- Collect more sediment data so that the initial bed gradation may be obtained and the data are available for model validation

- Carry out a validation study with the collected sediment data and then apply the model to provide the data needed by the riparian model, SRH-1DV

4.5 Concluding Remarks

As presented here, the SRH-2D simulation contributes to understanding of cottonwood establishment and survival studies and could be applied to the Sacramento River.

The model has other applications than those discussed in this chapter and can be used to supply information for other investigations, including detailed flood studies and ecological studies. On studies that require more detailed information than average channel values, we can use SRH-2D to supply information for simulating processes, including hydraulics, bed features, and erosion and deposition.

As discussed in section 4.4, the next steps to improve model effectiveness for sediment transport computations are to:

- Collect more sediment data on existing bed gradations
- Carry out a validation study on the bed gradations on a system-wide basis

Chapter 5

RHEM

Contents

Page

5. RHEM 5-1

5.1 Controlled Seedling Growth Experiments 5-1

5.1.1 Experiment Design 5-1

5.1.2 Experiment Results and Discussion 5-3

5.2 Model Algorithms 5-5

5.2.1 Plant Growth 5-5

5.2.2 Root Growth 5-8

5.2.3 Plant Transpiration 5-11

5.3 Calibration 5-14

5.4 Validation 5-17

5.4.1 River Mile 192.5 – Sand 5-17

5.4.2 River Mile 192.5 – Gravel 5-19

5.4.3 Validation Results 5-19

5.5 Determining the Parameters for SRH-1DV 5-20

5.6 Concluding Remarks 5-24

Figures

Page

5-1 Left: Photograph looking north, showing the tops of 12 rhizopods located on the southern end of the rhizopod system. An additional 18 rhizopods are located on the north side of the entryway. Right: Seedlings in the T1 (top) and T5 (bottom) treatments after 62 days of growth 5-3

5-2 Seedling survival during controlled water table decline experiments 5-4

5-3 Daily average reduction in potential transpiration due to drought stress. 5-17

Figures

Page

5-4 Soil water characteristics for gravel and sand soils located on Sacramento River point bar at RM 192.5. Matric head is the negative of the soil water pressure head. 5-18

5-5 Comparison of ET reduction factor due to drought stress for seedlings grown on sand and gravel at RM 192.5 on the Sacramento River during 2006. 5-20

5-6 ET reduction factor for various daily water table decline rates for the sand sediment type. 5-22

5-7 Recovery of ET reduction factor for different rates of daily water table elevation increase. 5-22

5-8 Desiccation and recovery rates for sand and gravel sediment as a function of water table decline rate. 5-23

Tables

Page

5-1 Grain Size Analysis for Sand Used in Controlled Experiments..... 5-23

5-2 Soil Physical Properties and Fitted van Genuchten Parameters for Sand Used in Controlled Experiments..... 5-2

5-3 Total Average Per-Plant Biomass (mg)..... 5-4

5-4 Total Average Maximum Root Depth (cm) 5-4

5-5 Model Parameters Set Using Field Observations..... 5-14

5-6 Observed and RHEM Simulated Per-Plant Biomass (mg) at H4 (Note: all T4 plants were dead by H4) 5-16

5-7 Observed and RHEM Simulated Maximum Root Depth (cm) at H4 (Note: all T4 plants were dead by H4) 5-16

5-8 van Genuchten (1980) Parameters Used to Characterize Gravel and Sand Gradation Soils from Sacramento River Point Bar at RM 192.5. 5-18

5-9 Observed and Modeled Plant Growth Values for a Seedling on Sand Sediment Located at RM 192.5 (June 1-August 16, 2006)... 5-19

5. RHEM

The Riparian Habitat Establishment Model (RHEM) simulates unsaturated ground water flow and detailed bioenergetics of individual cottonwood. The Mid-Pacific Region of the Bureau of Reclamation (Reclamation) and the Stockholm Environment Institute (SEI) developed this model. It is a modified version of the variably saturated flow code HYDRUS 2-D[1] (Simunek et al., 1999). The model simulates individual cottonwood seedling growth, while incorporating the effects of sediment gradation and hydraulic properties, water table depth, and atmospheric conditions. This chapter describes:

- *Controlled seedling growth experiments used to determine the parameters for RHEM algorithms*
- *Model calibration and validation*
- *Application of the model to develop the parameters for the Sedimentation and River Hydraulics One-Dimensional Sediment Transport and Vegetation Dynamics Model (SRH-1DV)*

5.1 Controlled Seedling Growth Experiments

Controlled experiments were conducted to determine the numerous cottonwood seedling growth parameters for RHEM, including growth rate, root-shoot allocation, and water stress thresholds.

5.1.1 Experiment Design

A system of 30 rhizopods[2] was constructed on the University of California at Davis campus. Each rhizopod consisted of a 45-centimeter (cm) diameter polyvinyl chloride (PVC) tube, open on one end, 154 cm long, and filled with a medium to coarse sand with a similar gradation to that found along the Sacramento River on the downstream portion of the point bar at river mile (RM) 192.5 (tables 5-1 and 5-2). Additional tubes were installed in each rhizopod for controlling the water table, observing soil moisture, and extracting intact seedlings. The rhizopods were placed in a pre-existing, rectangular, concrete lined pit. A wooden cover over the pit, which had cutouts for each rhizopod, minimized the exposure of the rhizopod sides to solar radiation (figure 5-1).

[1] HYDRUS 2-D is a software package for simulating water, heat, and solute movement in two- and three-dimensional variably saturated media. See: http://www.pc-progress.com/en/Default.aspx?hydrus-3d

[2] An apparatus constructed to grow tree seedlings under a precise rate of reduction in water table elevation.

Table 5-1. Grain Size Analysis for Sand Used in Controlled Experiments

Sieve Size (mm)	% Mass Retained
4	0.04
2	12.76
1	20.84
0.5	25.33
0.25	27.84
0.13	10.40
0.063	2.17
<0.063	0.62

Note: mm = millimeters

The experiment consisted of five treatments: T1, T2, T3, T4, and T5. Each treatment had 5 replicates, and each treatment had an "evaporation" rhizopod in which no seedlings were planted (5 treatments x 5 replicates + 5 evaporation = 30 rhizopods). These rhizopods were used to measure the rate of bare soil evaporation.

Table 5-2. Soil Physical Properties and Fitted van Genuchten Parameters (van Genuchten 1980) for Sand Used in Controlled Experiments

Parameter	Value
Bulk density	1.81 grams/cm^3
Saturated water content	27.7%
Saturated hydraulic conductivity	5.21 x 10^{-3} cm/d
α	0.04 cm^{-1}
n	3.84
θ_r	5.5%

Note: cm^3 = cubic centimeters, cm/d = centimeters per day

At the beginning of the experiment, the water table was maintained at 5 cm below the soil surface, and cottonwood seeds collected from the Sacramento River were sown. Treatments began 10 days after germination (June 28, 2008) and continued until the end of the experiment. Each treatment subjected the cottonwood seedlings to a different level of water stress. In treatments T1 – T4, the water table was lowered at a rate of 1, 2, 3, and 4 cm/d, respectively. In treatment T5, the seedlings were irrigated twice a day, and the rhizopod was allowed to freely drain.

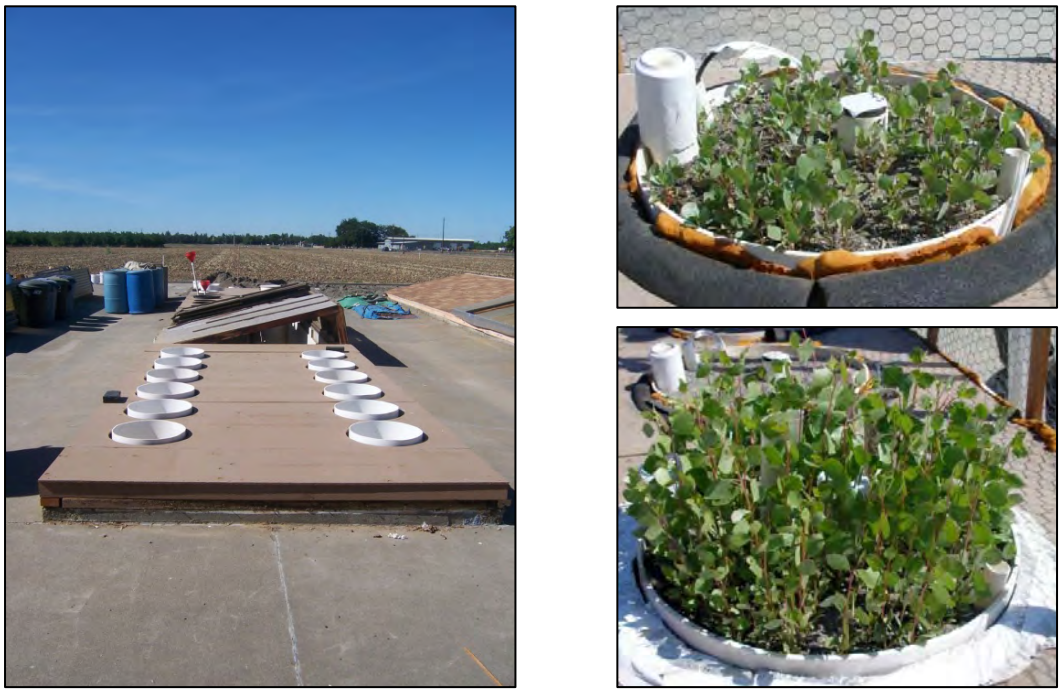

Figure 5-1. Left: Photograph looking north, showing the tops of 12 rhizopods located on the southern end of the rhizopod system. An additional 18 rhizopods are located on the north side of the entryway. Right: Seedlings in the T1 (top) and T5 (bottom) treatments after 62 days of growth.

Each harvest consisted of the extraction of three individual plants from each rhizopod. After each harvest, plant samples were processed to measure total dry biomass, shoot biomass, root biomass, leaf area, maximum root depth, and root distribution in 10-cm-deep increments. The initial harvest (H1) took place on June 27, 9 days after germination (June 18, 2008).

Treatments T1, T2, and T3 were continued for a total of 40 days, during which an additional three harvests were made of individual seedlings (H2 – H4), which occurred on July 9, July 16, and July 28. Treatment T4 had complete plant death by 27 days after germination. Treatment T3 had complete plant death by H4, 40 days after germination. Treatments T1, T2, and T5 were still alive at H4.

5.1.2 Experiment Results and Discussion

Differences between treatments were observed in overall biomass production, root depth, and plant survival (figure 5-2 and tables 5-3 and 5-4). Plants in all treatments grew at nearly the same rate through H2; however, by H3, the plants in T5 had grown larger than the others, and the plants in T4 were smaller. By H4, the plants in T5 had more biomass than plants in T1 and T2: 60 percent and 40 percent, respectively. The T4 plants had died, and the last surviving T3 plants had a biomass that was only 50 percent of the T1 plants' biomass.

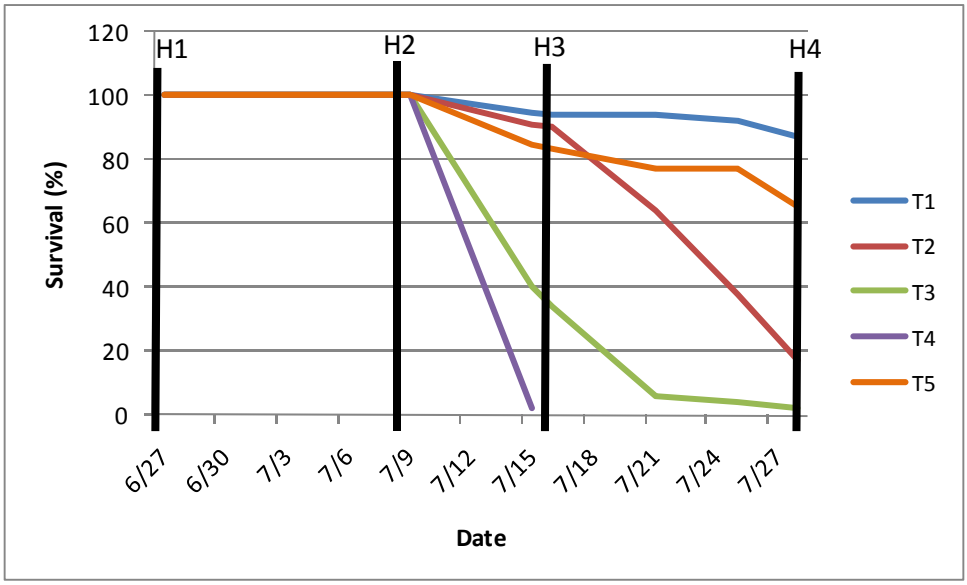

Figure 5-2. Seedling survival during controlled water table decline experiments. T1 = 1 cm/d, T2 = 2 cm/d, T3 = 3 cm/d, T4 = 4 cm/d, and T5 was irrigated twice daily and allowed to freely drain. Germination was June 18 and the 40th day (H4) is July 28.

Table 5-3. Total Average Per-Plant Biomass (mg)

Harvest/Date	T1	T2	T3	T4	T5
Germination/June 18					
H1/June 27	2.64	3.14	2.28	2.59	2.51
H2/July 9	10.66	12.06	9.23	13.04	12.00
H3/July 16	22.84	25.02	22.52	10.70	36.86
H4/July 28	31.51	36.22	16.54	[1]	52.31

Note: mg = milligrams
[1] By H4, the T4 plants had died.

Table 5-4. Total Average Maximum Root Depth (cm)

Harvest/Date	T1	T2	T3	T4	T5
H1/June 27	9.00	8.50	7.50	7.50	7.50
H2/July 9	17.00	21.00	16.00	26.67	19.00
H3/July 16	38.00	44.00	34.00	20.00	38.00
H4/July 28	44.29	59.09	40.00	[1]	43.13

[1] By H4, the T4 plants had died.

The different total biomass values observed between treatments are explained by a combination of water logging and drought stress. In the beginning of the experiment, the sediments were equally saturated in all treatments, and the similar

biomass values recorded for H1 reflect this. Treatments were started 2 days after H1. By H2, there was still little difference between the treatments in terms of average plant biomass. However, the root depth was greatest for T4, as those plants attempted to grow into the moist sediment above the rapidly declining water table. By H3, the plants in T5 were clearly growing at the most rapid rate. This was due to the combination of good root aeration caused by draining the T5 rhizopods and an ample supply of water from the twice-daily irrigations. In contrast, the T1 and T2 plants had access to ample water but were experiencing waterlogging stress caused by the relatively slow water table decline rates. Plants in T3 and T4 were stressed by a lack of water, and no T4 plants survived beyond H3. By H4, the plants in T5 were continuing their relatively rapid growth. Plants in T3 were severely stressed by lack of water and almost completely dead. The plants in T2, while having produced more biomass than T1 plants, were suffering from drought stress by H4, and survival was rapidly declining (figure 5-2). Results of the study illustrate the extreme sensitivity of cottonwoods to water table decline, and the impacts of both desiccation and inundation on biomass and survival. Natural cottonwood survival is limited by soil moisture retention, the rate of water table decline, and potential precipitation.

5.2 Model Algorithms

To develop a computer model capable of simulating seedling growth, stress, and death, a set of algorithms was developed based on relationships defined in the literature and observations made during the experiment described above. Plant growth in RHEM is represented by a series of equations used to simulate dry matter or biomass production, the partitioning of growth between above ground biomass, or canopy, and below ground root biomass, and the depth distribution of roots. Equations for potential and actual transpiration are used to estimate seedling water stress. Due to the importance of root zone water availability for the survival of cottonwood seedlings, particular attention was devoted to the distribution of root growth within the root zone. Initial conceptualization of this model was derived from Adiku et al. (1996). The model assumes that potential stressors such as nutrients, heat, and shading are not a factor. Only stresses caused by an excess or lack of water are considered.

5.2.1 Plant Growth

The first step in computing seedling growth is the calculation of potential growth assuming no water stress (Neitsch et al. 2005), as shown in equation 5-1:

$$\frac{d(Wg_{\max}(t))}{dt} = eS(1-e^{-kL}) \qquad 5\text{-}1$$

Where:

$Wg_{\max}(t)$ = the dry matter per unit area under ideal conditions in kilograms per square meter (kg m^{-2})

e = the radiation use efficiency in kilograms per mega-joule (kg MJ^{-1})

S = the incident radiation in mega-joules per square meter per second (MJ m^{-2} s^{-1})

k = the light extinction coefficient in meters per square meters (m m^{-2})

L = the leaf area in square meters (m^2)

The radiation use efficiency is reduced under high vapor pressure deficit conditions using the relationship (Neitsch et al. 2005) shown in equation 5-2:

$$e = \begin{cases} e_{vpd=1} - \Delta e_{dcl}\,(vpd - vpd_{thr}), vpd > vpd_{thr} \\ e_{vpd=1},\ vpd \le vpd_{thr} \end{cases} \quad \text{5-2}$$

Where:

$e_{vpd=1}$ = the radiation use efficiency when the vapor pressure deficit is 1 kilopascal (kPa)

Δe_{dcl} = the rate of decline in the radiation use efficiency per unit decrease in the vapor pressure deficit in kilograms per mega-joule per kilopascal (kg MJ^{-1} kPa^{-1})

vpd = the vapor pressure deficit (kPa)

vpd_{thr} = the threshold vapor pressure deficit above which the plant will have a reduced radiation use efficiency (kPa)

The actual growth rate is calculated as the potential growth rate limited by a factor that is a function of the degree of water stress, as shown in equation 5-3:

$$\frac{d(Wg_a(t))}{dt} = f_g \frac{d(Wg_{\max}(t))}{dt} \quad \text{5-3}$$

Where:

$Wg_a(t)$ = the actual dry matter per unit area (kg m^{-2})

f_g = a growth reduction function based on the ratio of actual transpiration (T_a) to potential transpiration (T_p) where T_r is the threshold value of T_a/T_p. This ratio serves as a sign of drought stress, since T_a is reduced relative to T_p as soil moisture conditions become limiting.

For T_a/T_p values less than 1.0, growth is limited as shown in equation 5-4.

$$f_g = \begin{cases} 1.0, \frac{T_a}{T_p} = 1.0 \\ T_a/T_p, \frac{T_a}{T_p} < 1.0 \end{cases} \quad \text{5-4}$$

Once actual biomass production is calculated, biomass is partitioned to either the shoot or root system. Greenhouse observations have shown that cottonwood seedlings divert more energy to root growth when soil moisture conditions are limiting (Kranjcec et al. 1998). In this model, dry matter growth is partitioned between roots and shoots as a function of the ratio T_a/T_p as shown in equation 5-5a (shoots) and 5-5b (roots).

$$\frac{d(Ws_a(t))}{dt} = (1 - RMRatio)\frac{d(Wg_a(t))}{dt} \quad \text{5-5a (shoots)}$$

$$\frac{d(Wr_a(t))}{dt} = [RMRatio]\frac{d(Wg_a(t))}{dt} \quad \text{5-5b (roots)}$$

Where:

$Ws_a(t)$ = the actual shoot dry matter (kg m^{-2})

$Wr_a(t)$ = the actual root dry matter (kg m^{-2})

The root-mass-ratio (RMRatio) is a partitioning factor and a function of T_a/T_p as calculated in equation 5-6.

$$RMRRATIO = \begin{cases} RMR_{max}, & \frac{T_a}{T_p} < T_{mrc} \\ RMR_{max} - \frac{\frac{T_a}{T_p} - T_{mrc}}{T_{src} - T_{mrc}} \left(RMR_{max} - RMR_{min} \right), & T_{mrc} \le \frac{T_a}{T_p} \le Tsrc \\ RMR_{min}, & \frac{T_a}{T_p} > T_{src} \end{cases} \quad 5\text{-}6$$

Where:

T_{src}, T_{mrc} = threshold values for defining the minimum and maximum RMRatios.

At T_a/T_p values greater than the threshold T_{src}, the RMRatio is equal to a minimum value, RMR_{min}. For decreasing values of T_a/T_p less than T_{src}, plant growth is increasingly allocated to the roots until a maximum RMRatio value is reached at the threshold value of T_{mrc}. For T_a/T_p values less than T_{mrc}, the RMRatio is equal to the maximum value, RMR_{max}.

Once the shoot biomass is calculated, a relationship between shoot biomass and leaf area can be used to calculate the change in leaf area relative to plant growth, as shown in equation 5-7.

$$L(t) = f_L W s_a(t) \quad 5\text{-}7$$

Where:

L = leaf area (m^2)

f_L = a factor that converts shoot biomass to leaf area (m^2 leaf area/kg m^{-2})

5.2.2 Root Growth

Root front is the deepest point of the roots. After the simulated plant biomass is partitioned into roots and shoots, the root front is extended, the new root mass is distributed over the root zone, and the root mass is converted into root length for eventual use in the calculation of actual transpiration.

The root front velocity (how fast the root grows) of cottonwood seedlings varies according to changing soil moisture conditions (Amlin and Rood 2002). Under conditions of drought stress, seedlings will increase the root front velocity. Presumably, this is an effort by the plants to grow roots into sediment with more available water. In coarse soils (gravels and cobbles), ample supplies of soil water are only available in the zone of capillary rise[3] close to the water table. In coarse soils, this zone is relatively thin; whereas in finer grained soils (fine sand

[3] The zone of capillary rise is defined as the region of the soil profile in which soil pores are completely filed by water but where the capillary pressure is less than atmospheric.

and silts), the zone is thicker. Results from the experiment described above indicate that seedlings extend the root front at a rate of 1 to 3.5 cm/d. Additionally, it was observed that roots can grow up to 15 cm below the water table. These two phenomena are captured in the root front velocity algorithm (equation 5-8):

$$\frac{d(D_r(t))}{dt} = V_r \; f_{vr}(\Psi) \qquad 5\text{-}8$$

Where:

$D_r(t)$ = the depth of the root zone (cm) at time t

V_r = the root front velocity in centimeters per hour (cm/h)

f_{vr} = a root front velocity reduction factor that is a function of the pressure head at the root front

Ψ = pressure head

The root front velocity is a function of the degree of water stress as calculated in equation 5-9.

$$V_r = \begin{cases} V_{r\max}, & \frac{T_a}{T_p} < T_2 \\ V_{r\max} - \frac{\frac{T_a}{T_p} - T_2}{T_1 - T_2}\left(V_{r\max} - V_{r\min}\right), & T_2 \le \frac{T_a}{T_p} \le T_1 \\ V_{r\min}, & \frac{T_a}{T_p} > T_1 \end{cases} \qquad 5\text{-}9$$

The root front velocity reduction factor limits root growth into sediments below the water table as calculated in equation 5-10.

$$f_{vr} = \begin{cases} 1.0, & \Psi < \text{DBWT} \\ 0.0, & \Psi \ge \text{DBWT} \end{cases} \qquad 5\text{-}10$$

Where:

DBWT = pressure head value (expressed as depth below the water table) above which root growth ceases (cm)

Next, the root growth is distributed within the root zone. Adiku et al. (1996) address this issue with a model that predicts root growth as a function of the overall increase in root biomass and the moisture distribution with depth, as shown in equation 5-11.

$$\frac{d(Wr_A(z,t))}{dt} = Wr_A(z,t)P_r[1-\frac{Wr_A(z,t)}{Wr_{Am}}]E_f(S_\theta) \qquad 5\text{-}11$$

Where:

$Wr_A(z,t)$ = the root mass per unit area (kg m^{-2}) at depth z and time t

Wr_{Am} = the maximum root mass of the plant (kg m^{-2})

P_r = the net root proliferation rate per second (s^{-1})

$E_f(S_\theta)$ = a function that limits root growth as a function of soil moisture where S_θ is the soil saturation.

E_f serves as a proxy for soil strength, which increases as soil moisture declines and, therefore, limits root extension as determined in equation 5-12.

$$E_f = \begin{cases} 0.0, & S_\theta < S_L \\ \frac{S_\theta - S_L}{S_c - S_L}, & S_L \le S_\theta \le S_c \\ 1.0, & S_\theta > S_c \end{cases} \qquad 5\text{-}12$$

Where:

S_L and S_c = threshold values of soil saturation. Root extension ceases for soil moisture values lower than S_L and is at its maximum for values greater than S_c.

Adiku et al. (1996) present a method for solving equation 5-11 without specifying the net root proliferation rate, P_r. Using this method, the right-hand side of equation 5-11 is solved for each depth increment (assuming that P_r is constant with depth and time). These values are then divided by the sum of values for all depth increments in the root zone, thereby creating a weighting factor used to distribute the total root growth over the depth increments and allowing for cancellation of P_r, as shown in equation 5-13.

$$\Delta Wr_{A_i}^{t} = \frac{Wr_{A_i}^{t-1}[1-\frac{Wr_{A_i}^{t-1}}{Wr_{Am}}]E_f(S_{\theta i}^{t-1})}{\sum_{j=1}^{N} Wr_{A_j}^{t-1}[1-\frac{Wr_{A_j}^{t-1}}{Wr_{Am}}]E_f(S_{\theta j}^{t-1})} \Delta Wr_a^{t} \qquad 5\text{-}13$$

Where:

ΔWr_{Ai}^{t} = the change in root mass per unit area at depth increment *i* during time step *t*

Wr_{Ai}^{t-1} = the root mass per unit area at depth increment *i* during the previous time step

$S_{\theta i}^{t-1}$ = the soil saturation in soil depth increment i during the previous time step

N = the total number of depth increments in the root zone for j =1, 2, 3…N.

Finally, the increase in root dry matter per unit area, ΔWr_{Ai}^{t}, is converted to root length per unit area for each depth increment in the root zone by multiplying by specific root length, c (in meters per kilogram [m kg^{-1}]), which is calculated as a function of the soil moisture conditions, as shown in equation 5-14.

$$\frac{d(R_{A,i}(t))}{dt} = c(\theta_i(t))\frac{d(Wr_{a,i}(t))}{dt} \qquad 5\text{-}14$$

Where:

$R_{A,i}(t)$ = the total root length per unit area (m m^{-2}) for root zone layer *i*

The value of specific root length, c (in m kg^{-1}), varies as a function of soil saturation in root zone layer i, as calculated in equation 5-15:

$$c = S_\theta * (c_{\max} - c_{\min}) + c_{\min} \qquad 5\text{-}15$$

Where:

c_{max} = the maximum value of the specific root length

c_{min} = the minimum value of the specific root length

5.2.3 Plant Transpiration

Potential transpiration by a seedling is estimated using equation 5-16, which is a modified version of the Penman-Monteith equation (Zhang et al. 1997).

$$T_p^t = L_A(t)\frac{sR_n + 0.93\rho_{air}C_pD/r_b}{\lambda[s + 0.93\gamma(2 + \bar{r}_s/r_b)]\rho_{H_20}} \qquad 5\text{-}16$$

Where:

T_p^t = the transpiration rate per unit leaf area in grams per square meter per second (g $m^{-2}s^{-1}$)

λ = the latent heat of vaporization of water in joules per gram (J g^{-1})

L_A = the total leaf area of the tree canopy (m^2)

s = the slope of the saturation vapor pressure curve in kilopascals per degree centigrade (kPa $^oC^{-1}$)

R_n = the net radiation absorbed per unit leaf area in watts per meter squared (W m^{-2})

ρ_{air} = the density in kilograms per cubic meter (kg m^{-3}) of air at constant pressure

C_p = the specific heat capacity in joules per kilogram per degree Kelvin (J kg^{-1} $^oK^{-1}$) of air at constant pressure

D = the saturation vapor pressure deficit of the air (kPa)

r_b = the leaf boundary layer resistance in seconds per meter (s m^{-1})

γ = the psychometric constant (kPa $^oC^{-1}$)

$\bar{r}_s$ = the minimum stomatal[4] resistance (s m^{-1})

ρ_{H_20} = the density of water in grams per cubic meter (g m^{-3})

The RHEM approach sets the stomatal resistance at a minimum value based on observations made during the experiment of unstressed plants.

Maximum transpiration limited by the root's ability to uptake water is calculated using equation 5-17:

$$T_a{}^t_R = \sum_{i=1}^{N} T_a{}^t_{Ri} = \sum_{i=1}^{N} q_r R_{A,i}^{t-1} RW(\theta_i^{t-1}) \qquad 5\text{-}17$$

Where:

[4] Note that stomata are pores in the leaf and stem epidermis used for gas exchange.

T_{aR}^{t} = the root limited maximum transpiration rate for time step t (m^3 H_20 m^2 s^{-1})

q_r = the maximum uptake of water per unit root length per unit time (m^3 H_20 m^{-1} root t^{-1})

RW = a dimensionless factor that limits transpiration as a function of soil moisture content during the previous time step

T_{aRi}^{t} = the root limited maximum transpiration for depth increment *i*.

The RW function (as calculated using equation 5-18) limits transpiration when pressure head, Ψ, is either below a threshold value, P_2, (water limiting) or above a threshold value, P_1 (water logging) (Feddes et al. 1978; Simunek et al. 1999). For values of h below the wilting point (h_{WP}), transpiration ceases.

$$RW = \begin{cases} 0.0, & \Psi < P_3 \\ \frac{\Psi - P_3}{P_2 - P_3}, & P_3 \le \Psi \le P_2 \\ 1.0, & P_2 \le \Psi \le P_1 \\ \frac{\Psi - P_1}{P_0 - P_1}, & P_1 \le \Psi \le P_0 \\ 0.0, & \Psi > P_0 \end{cases} \qquad 5\text{-}18$$

During initial simulations using the model described in equation 5-18, it was discovered that the waterlogging stress parameters P_0 and P_1 limit transpiration when the water table is close to the soil surface, due to the high water content caused by the capillary rise of water from the water table. This conflicted with observations of seedlings growing and transpiring with roots in saturated sediment. It was assumed that seedlings are able to grow under these conditions due to oxygen diffusion from the atmosphere into the near surface sediments. To mimic this effect, the constraint on transpiration imposed by the P_0 and P_1 parameters was relaxed in the top 8 cm of soil. Within these soil layers, the seedlings were allowed to transpire up to 8.8×10^{-4} cm/h, which is based on the calculated value for potential evapotranspiration (ET) on June 29, 2008, of the controlled growth experiments. Observations made during the experiments indicate that the plants grew well during the initial 11 days of growth, and roots extended to 8 cm deep by June 29. During this period, the water table was 5 cm deep. On June 29, visual observations indicated that the plants were in distress and, for that reason, the water table decline treatments were started. In summary, based on these observations, the authors assume that oxygen diffusion into the near surface sediments allows a maximum of 8.8×10^{-4} cm/h of transpiration using water from the top 8 cm of sediment.

The actual transpiration is calculated by comparing the maximum transpiration that can be supported by the roots, Ta_R^t, to the potential atmospheric transpiration

demand, Tp^t, for the current time step. When $Ta_R{}^t$ is greater than or equal to Tp^t, the transpiration is partitioned into the root zone depth increments using equation 5-19a.

$$Ta_i = Tp^t / Ta_R{}^t \, (Ta_{Ri}{}^t) \qquad 5\text{-}19a$$

Otherwise, the transpiration in each root zone depth increment is given by equation 5-19b:

$$Ta_i = Ta_{Ri}{}^t \qquad 5\text{-}19b$$

5.3 Calibration

The first step in calibration was to set all parameters to values observed during the controlled experiments. These included most of the parameters in the model (table 5-5). The next step was to run the model and determine if HYDRUS 2-D[5] was solving properly. This process required adjusting the time step controls and the minimum allowable pressure head at the soil surface (hCritA), which is used to calculate the atmospheric flux boundary condition. For finer-grained soils, this value is often on the order of -10,000 cm; however, as sand was modeled in this case, using such small values resulted in numerical instability. Using recommendations found on the HYDRUS 2-D user forum, a pressure head with a water content equivalent to a small fraction of the pore space was used. The value used was -50 cm.

Table 5-5. Model Parameters Set Using Field Observations

Variable	Value	Equation	Variable	Value	Equation
$e_{vpd=1}$	0.003 kg MJ^{-1}	5-2	Δe_{dcl}	0.0008 kg MJ^{-1} kPa^{-1}	5-2
vpd_{thr}	1.0 kPa	5-2	RMR_{max}	0.57	5-6
RMR_{min}	0.41	5-6	T_{mrc}	0.5	5-6
Tsrc	0.9	5-6	f_L	0.015 m^2 leaf area/kg m^{-2}	5-7
Vr_{min}	0.075 cm/h	5-9	Vr_{max}	0.235 cm/h	5-9
DBWT	15 cm	5-10	c_{max}	300,000 m kg^{-1}	5-15
c_{min}	100,000 m kg^{-1}	5-15			

[5] A Microsoft Windows based modeling environment developed by the U.S. Salinity Laboratory, U.S. Department of Agriculture (USDA), Agricultural Research Service (ARS), Riverside, California.

The next step of the process was to adjust parameters relating to waterlogging, drought stress, and root growth until simulated values matched observed values. This was done in several steps:

1. The potential growth parameters from equation 5-2, $e_{vpd=1}$, Δe_{dcl}, vpd_{thr} were set using literature values. The light extinction coefficient, k, was adjusted so that simulated total plant biomass for T5 equaled the observed value at H4. The calibrated value was 0.64, which is very close to the commonly used value of 0.65 (Neitsch et al. 2005). During this step, the observed biomass for T5 was the target, based on the assumption that plants in this treatment grew at nearly the potential rate.

2. The waterlogging parameters P_0 and P_1 from equation 5-18 were adjusted until the simulated biomass value for T1 matched the observed value at H4. These values were set at -18 and -21 cm, respectively. These parameters were adjusted using the plants in T1 as the target because this treatment had the largest amount of waterlogging stress due to it having the slowest rate of water table decline. These values are within the range for coarse sand suggested by other researchers (Bartholomeus et al. 2008).

3. The drought stress parameters P_2 and P_3 from equation 5-18 were adjusted until the simulated biomass value for the plants in T2 matched the observed value for H4. These values were set at -39 and -42 cm, respectively.

4. The root growth parameters T_1, T_2, S_c, and S_L from equations 5-9 and 5-12 were adjusted until the root front velocity and root mass depth distribution matched the observed values from all treatments. Their values were 0.95, 0.85, 0.25, and 0.1, respectively.

Results from the calibration show the model simulated the observed biomass and maximum root depth values from H4 (tables 5-6 and 5-7). All values were within 5 percent of the observed values for T1, T2, and T5, which were the calibration targets. These treatments were used as calibration targets for biomass production because they survived the duration of the experiment and represented unstressed plants (T5), waterlogging stressed plants (T1), and drought stressed plants (T2). The simulated values for T3, which were not a calibration target, were less accurate, with the biomass value overpredicted by 20 percent and the maximum root zone depth overpredicted by 89 percent. The inaccuracy in the root depth suggests the root front velocity algorithm (equation 5-8) does not contain some necessary features. The root front extension rate, while initially increasing during periods of drought stress, may be limited during periods of severe stress, which would explain the relatively low observed value at H4.

Table 5-6. Observed and RHEM Simulated Per-Plant Biomass (mg) at H4 (Note: all T4 plants were dead by H4)

	T1	T2	T3	T4	T5
Observed	31.51	36.22	16.54		52.31
Simulated	30.94	34.68	19.81		52.52

Table 5-7. Observed and RHEM Simulated Maximum Root Depth (cm) at H4 (Note: all T4 plants were dead by H4)

	T1	T2	T3	T4	T5
Observed	44.29	59.09	40.00		43.13
Simulated	41.78	59.56	75.56		44.87

As the main purpose of the RHEM is to predict cottonwood seedling survival under drought stress, the accuracy of the calibrated model can also be judged by comparing predicted drought stress to observations of seedling stress and death. To do this, a plot was made of an average daily ET reduction factor, which represents the value of T_a/T_p when drought stress reduces the transpiration below potential (figure 5-3). From this plot, it can be seen that the simulated plant in T4 experienced drought stress starting July 7, 2008. By July 15, the stress factor had reached a value of less than 0.4. This coincides with the observed death of all seedlings in T4 (figure 5-2). The drought stress factor in T3 reached a value of 0.4 by July 28, which corresponds with the observation of complete plant death for this treatment (figure 5-2). The simulated plant in T2 started to experience drought stress on July 14. This stress increased through the end of the month and this corresponds with the decreasing plant survival observed for T2 (figure 5-2). This agreement between simulations and observations of drought stress and seedling death provides confidence that the model is simulating these processes well.

There is some variation in the ET reduction factor and some periods where the ET reduction factor increases because of varying climatic factors and there are periods where the water table is relatively constant or increasing. The plant can begin to recover during these periods.

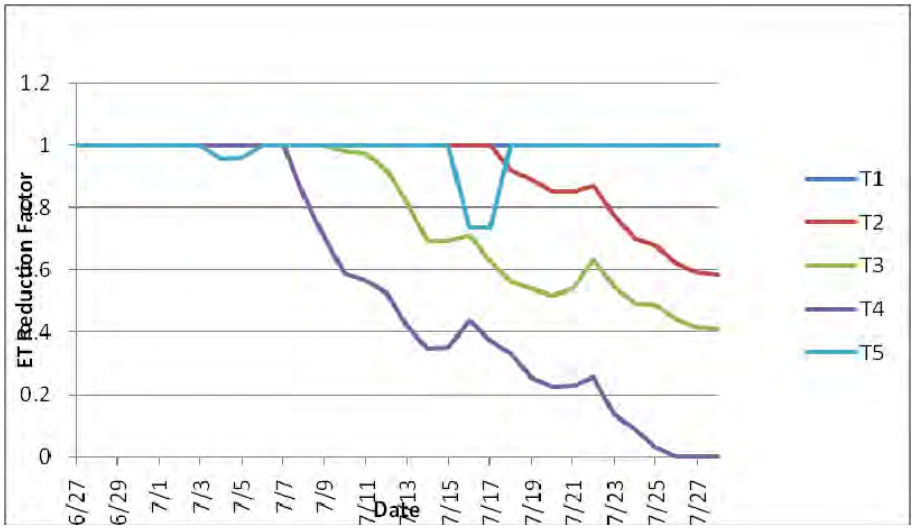

Figure 5-3. Daily average reduction in potential transpiration due to drought stress.

5.4 Validation

To validate the calibration of the cottonwood seedling growth model, simulations were compared with observations made by the authors during 2006 of seedling growth and death on a point bar located at RM 192.5 on the Sacramento River. The motivation for analyzing the differences in survival of cottonwood seedlings on these two sediment types was based on the findings of a higher rate of establishment on finer grained sediments such as silt and sand (Wood 2003).

Observations were made at two locations on the point bar with different sediment gradations:

- Location 1. Downstream end of the point bar where an eddy formed during high flow events and deposited fine sand and silt
- Location 2. Midpoint of the bar on coarse sediment consisting mostly of cobbles and gravel

At both locations, observation wells were installed and instrumented to record the water table depth on an hourly basis. The sites were visited periodically, and visual observations were made of seedling location, height, degree of stress, and death.

5.4.1 River Mile 192.5 – Sand

At Location 1 (with fine sand sediment), soil samples were collected and a laboratory analysis was conducted to determine the soil hydraulic properties. The

soil water retention curve and associated van Genuchten parameters are presented in figure 5-4 and table 5-8.

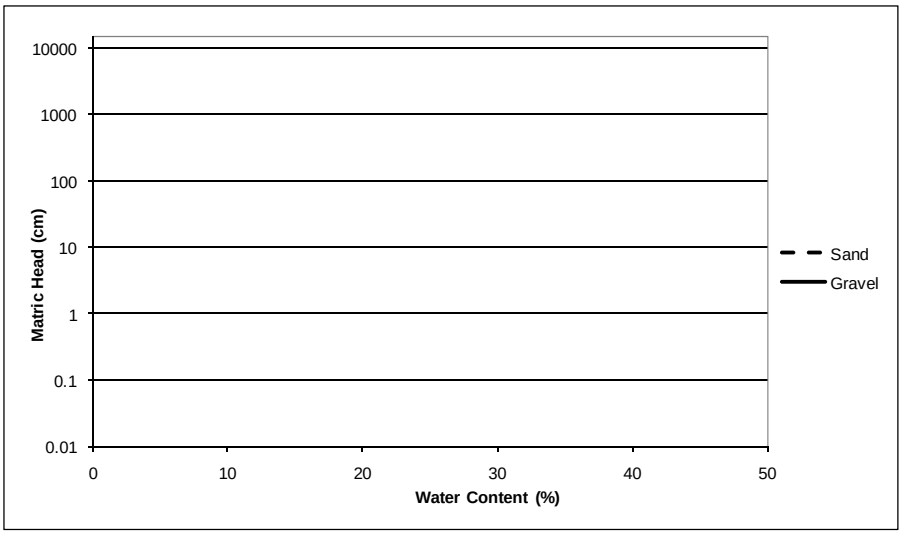

Figure 5-4. Soil water characteristics for gravel and sand soils located on Sacramento River point bar at RM 192.5. Matric head is the negative of the soil water pressure head.

Table 5-8. van Genuchten (1980) Parameters Used to Characterize Gravel and Sand Gradation Soils from Sacramento River Point Bar at RM 192.5.

	Residual volumetric water content	Saturated volumetric water content	Constants In the water retention model		Saturated flow hydraulic conductivity
	θ_r	θ_s	α (1/cm)	n	K_s (cm/d)[1]
Gravel	0.02	0.153	1.00	2.1	500
Sand	0.057	0.41	0.124	2.28	350

[1] cm/d = centimeters per day

The observed seedling at this location germinated around June 1, 2006. Seventy-six days later, on August 16, 2006, the seedling was harvested. Roots were harvested by driving a 2-inch pipe centered on the plant into the sediment, and then pulling it out of the soil. The sample was processed to determine dry root biomass, shoot biomass, leaf number, and root front depth. Leaf area was estimated visually to be approximately 50 to 75 square centimeters (cm^2).

During the growth of this seedling, the water table elevation was observed using a pressure transducer installed in a well located approximately 1.5 meters from the plant. Weather data including solar radiation, wind velocity, temperature, and relative humidity were obtained from the California Irrigation Management Information System (CIMIS) station located in Orland, California (station No. 61).

5.4.2 River Mile 192.5 – Gravel

The sediment in this location was a mix of cobbles up to 7 cm in diameter and gravel and very coarse sand. The measured porosity was 15 percent. Due to the coarseness of this sediment, it was not possible to measure the soil moisture release curve; therefore, the curve presented in figure 5-4 and table 5-8 is an estimate based on the assumption that gravel has larger values of α and K_s and smaller residual water content (θ_r) compared to sand (Idaho National Engineering and Environmental Laboratory 2001). Also, due to the coarseness of the sediment in this location, intact plant samples were not collected. Similar to the location on fine sediments, an observation well was installed to provide measurements of water table depth in the vicinity of the seedlings. Weather data were obtained from CIMIS station No. 61.

The observed seedlings at this location germinated within days of June 8, 2006. By July 12, the seedlings were 3 to 8 cm in height but showed a lack of vigor—presumably due to water stress. By July 26, the seedlings were very stressed, with approximately 50 percent of the seedlings reported dead. Subsequent observations through August 25 indicate that the remaining seedlings continued to grow to a height of 5 to 10 cm but remained stressed. On September 7, it was reported that nearly all the seedlings were dead. By October 3, all the seedlings were reported dead.

5.4.3 Validation Results

The RHEM simulation predicted a smaller seedling than that observed on the sand at RM 192.5 (table 5-9). Total biomass of the simulated seedling was 62 percent less than the observed value. The observed root mass ratio (root mass/plant mass) was 0.37. The modeled root mass ratio was somewhat higher (0.41). The large difference between the observed and simulated values for biomass may be because only a single seedling was collected from this cohort, which contained 100+ seedlings. Observations made on August 25, 2006, indicate that seedlings in this cohort ranged from 10-20 cm in height, which suggests there was a large range in total biomass among individual plants. On the gravel sediment, the simulated seedling was smaller and had a total biomass of 279 mg and a leaf area of 24 cm^2 on August 16. This is in general agreement with recorded observations that indicate, on August 25, the cohort of seedlings on the gravel sediment was half the height (5-10 cm) of the seedlings on the sand sediment.

Table 5-9. Observed and Modeled Plant Growth Values for a Seedling on Sand Sediment Located at RM 192.5 (June 1-August 16, 2006)

	Plant Mass (mg)	Shoot Mass (mg)	Root Mass (mg)	Leaf Area (cm^2)	Root Zone Depth (cm)
Observed	915	571	344	50-75[1]	75
Modeled	345	202	143	30	74

[1] Estimated value

While the comparison of biomass production indicates that RHEM may not be highly accurate with respect to plant size, validation results shows that RHEM is able to accurately predict root zone depth and seedling mortality resulting from dessication. This is of more importance to the application described in this document, as the analysis goal is to determine the survival of seedlings under various water management schemes. Comparisons of the ET reduction factor caused by drought stress show that the seedling on the gravel reached a value of 0.4 on August 27 and perished on August 29 (figure 5-5). This simulation result agrees with observations made in the field, which recorded that seedlings on the gravel sediment were alive on August 25 but were nearly all dead by September 9.

In contrast, the seedlings on the sand sediment were reportedly stressed but alive. The cause of the seedling death on the gravel was likely a rapid drop in the Sacramento River stage, which resulted in a water table decline of 5 cm/d for a period of 4 days. This rapid drop in river stage started on August 23. In RHEM, the reduction factor was reduced to less than 0.4 on August 27. The fact that the simulated seedling died 4 days after the initiation of the stress suggests that the measured seedling managed to transpire at nearly the full rate for a few days using water remaining in the soil after the water table lowered.

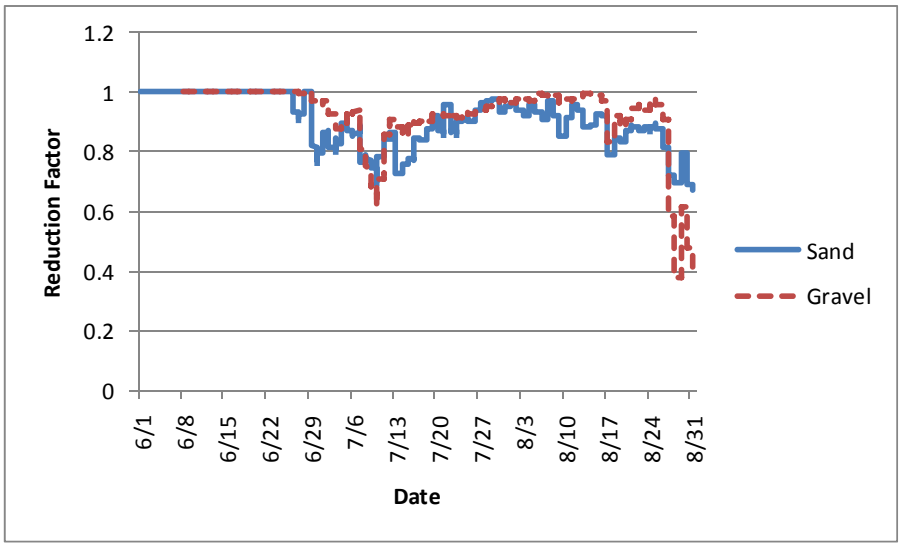

Figure 5-5. Comparison of ET reduction factor due to drought stress for seedlings grown on sand and gravel at RM 192.5 on the Sacramento River during 2006.

5.5 Determining the Parameters for SRH-1DV

The ultimate goal of the research and modeling effort described here was to provide information useful for Reclamation's SRH-1DV model, which will be

used to study the establishment of cottonwood seedlings along a 100-mile reach of the Sacramento River. To provide usable information about seedling survival, a series of numerical experiments was conducted using RHEM code, in which the effect of different water table decline rates on simulated seedling survival was simulated. These numerical experiments were conducted using the soil physical properties for sand and gravel sediments found on the point bar at RM 192.5. Both sand and gravel were studied in order to explore the differences in seedling survival between the two sediment types.

Numerical experiments were conducted using a fixed set of atmospheric boundary conditions and a range of water table decline rates. Experiments were devised to simulate both the imposition of drought stress caused by a falling water table and the reduction or recovery from stress caused by a rising water table. The stress caused by the falling water table was termed "desiccation," and the reduction in stress caused by the rising water table was termed "recovery."

A single day of hourly atmospheric variables was repeated during the entire simulation in order to remove variations in the results caused by changes in the weather. June 15, 1994, was chosen from the CIMIS Station No. 61 historical record because it represented one of the largest daily average rates of reference evapotranspiration (ETo) for the station. This was done to represent the maximum stress possible on the simulated seedlings. In these experiments, the plant's ability to deal with water stress was tested after the plants had 32 days to establish. This was done based on observations by California Department of Water Resources (CDWR) and the authors suggesting that fatal drops in river stage occurred later in the summer after the plants had some time to develop (Morgan and Henderson 2005). For the desiccation experiments, the water table was held at a constant depth of 5 cm for the first 3 days as the plant germinated and established its root system. During the second period (14 days), the water table was lowered at a rate of 1 cm/d. For the third period (15 days,) the water table was lowered at a rate of 0.5 cm/d. Following this third period, the experiment was initiated, and the water table was lowered a fixed amount every day until plant death occurred.

A plot of the ET reduction factor for the plants on the sand sediment shows how the plants responded to the different water table decline rates (figure 5-6). The plants took longer to perish with slower water table decline rates. For instance, the plant perished in 20 days with a 2-cm/d water table decline and in only 3.3 days with an 8-cm/d water table decline.

For the recovery experiments, the water table was held at a constant depth of 5 cm for the first 3 days as the plant germinated and established its root system. During the second period (14 days), the water table was lowered at a rate of 1 cm/d, and during the third period (15 days), the water table was lowered at a rate of 0.5 cm/d. For the plants on the sand sediment, the water table was then lowered

7 cm/d for 8 days in order to stress the plants to near death. For the gravel sediment, after the third period, the water table was lowered 4 cm/d for 3 days, and then held constant for 1 day. This resulted in enough drought stress on the plants that the ET reduction factor was reduced to 0.44 for the sand and 0.46 for the gravel. In both cases, the experiment was started, and on the following days, the water table elevation was increased at a fixed rate. The ET reduction rate for the sand sediment is shown in figure 5-7. Recovery took longer for lower rates of water table increase. In one example, the plant fully recovered in 15.4 days for the 2-cm/d increase in water table elevation under an ET reduction factor equal to 1.0. The plant fully recovered in 3.4 days with the 10-cm/d increase in water table elevation.

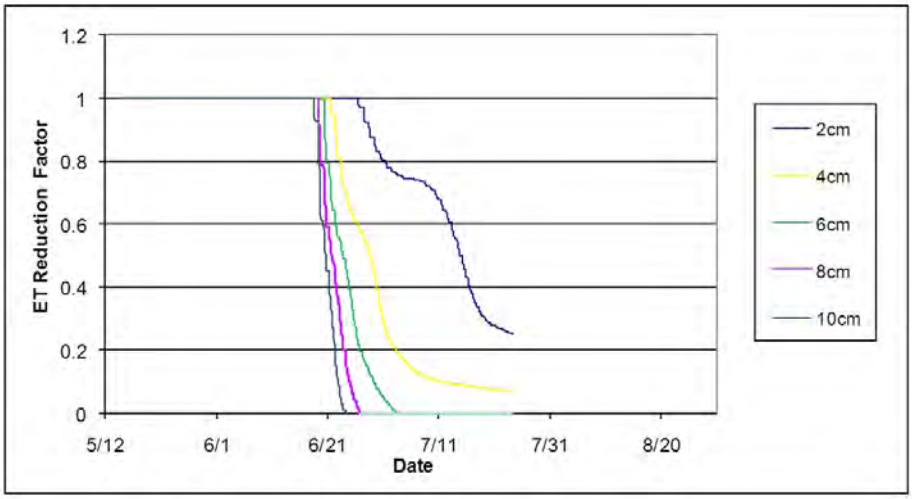

Figure 5-6. ET reduction factor for various daily water table decline rates for the sand sediment type.

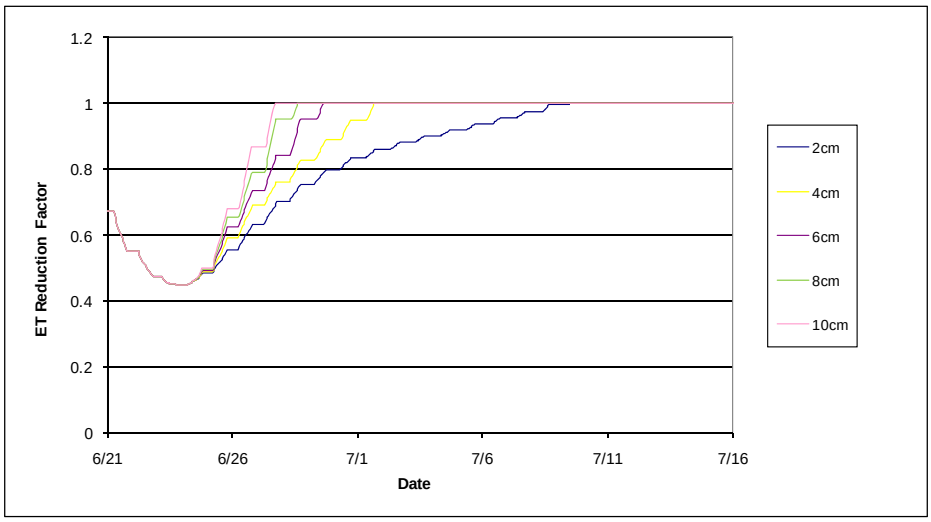

Figure 5-7. Recovery of ET reduction factor for different rates of daily water table elevation increase.

A comparison of the desiccation and recovery rates for sand and gravel sediment is presented in figure 5-8. An example of how to interpret this graph is that cottonwood seedlings growing in the sand sediment will take over 6 days to die if the water table drops at 5 cm/d. On gravel sediment, the plants will take about 3 days to die at the same rate of water table decline. Differences in these values were expected due to the differences in the soil hydraulic properties. The sand sediment has a greater water holding capacity in the root zone above the capillary rise zone than the gravel sediment. Both root growth and water holding capacity of the soils would result in more water available for plant use within the soil profile. For water table decline rates of 2 cm/d and less, the ability of the roots to grow deeper at a similar rate resulted in much less stress and little difference between the sediment types. It is interesting to note that recovery rates (e.g., where the water table decline rate is less than 0) are nearly identical for both sediment textures. This is probably due to the rapid rate of water movement in the soil types as the water table rises.

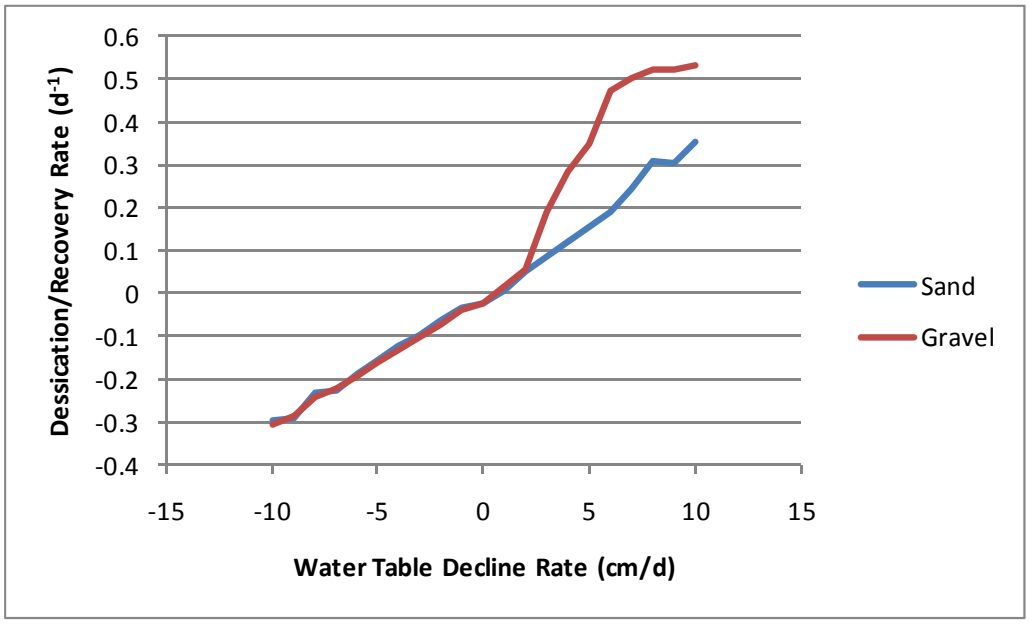

Figure 5-8. Desiccation and recovery rates for sand and gravel sediment as a function of water table decline rate.

The RHEM model for predicting cottonwood desiccation mortality, based on plant stress and recovery in sand or gravel soils, was incorporated into the final runs of the sediment transport and vegetation growth model, SRH-1DV. Stress rates on seedling cottonwood plants are tracked within SRH-1DV and the young plants are removed when the rates shown in figure 5-8 are exceeded. SRH-1DV is described in detail in Chapter 6.

5.6 Concluding Remarks

The controlled field experiments and modeling described above provide a detailed analysis of cottonwood seedling growth and survival when moisture is limited. The RHEM is able to simulate seedling growth with a reasonable degree of accuracy using the calibration data set. RHEM is also able to predict seedling survival when the plants are moisture limited using the validation data set, which was based on limited observation data. However, results from the validation suggest that some aspects of the algorithms need further refinement to accurately predict seedling growth parameters. In particular, the root front velocity algorithm may need to be redesigned to account for severe water stress and reduce the maximum root front velocity in this situation. The numerical experiments studying the effect of different water table decline rates show a significant difference in the ability of seedlings to survive on sand versus gravel sediment. This conclusion is in agreement with observations made by others (Wood 2003), and this study provides a quantification of those differences useful for modeling seedling survival on the Sacramento River. The RHEM model has been incorporated into the Sacramento River SRH-1DV model to compute desiccation mortality for young cottonwood plants.

Chapter 6

One-Dimensional Modeling (SRH-1DV)

Contents

Page

6. One-Dimensional Modeling (SRH-1DV) 6-1
- 6.1 Ground Water Module 6-2
- 6.2 Vegetation Module 6-3
  - 6.2.1 Establishment Module 6-4
  - 6.2.2 Growth Module 6-7
  - 6.2.3 Mortality Module 6-7
  - 6.2.4 Vegetation Types 6-10
  - 6.2.5 Use 6-12
- 6.3 Input Data 6-12
  - 6.3.1 Flow Data 6-13
  - 6.3.2 Geometry Data 6-13
  - 6.3.3 Sediment Data 6-18
  - 6.3.4 Ground Water Parameters 6-23
  - 6.3.5 Vegetation Parameters 6-23
- 6.4 Calibration of Flow and Ground Water Modules 6-36
- 6.5 Calibration of Sediment Module 6-39
- 6.6 Cottonwood Calibration with Field Data 6-40
  - 6.6.1 2005 Data 6-41
  - 6.6.2 2006 Data 6-43
- 6.7 Calibration of Multiple Vegetation Types with Vegetation Mapping 6-45
  - 6.7.1 Methodology for Computing Mapping Values 6-47
  - 6.7.2 Methodology for Computing Modeled Values 6-48
  - 6.7.3 Results of Multiple Vegetation Calibration 6-49
- 6.8 Multiple Vegetation Application to Sacramento River 6-51
  - 6.8.1 Vegetated Area From a Multiple Vegetation Simulation 6-52
  - 6.8.2 Plant Germination 6-55
  - 6.8.3 Hydrologic Regime and Desiccation 6-56
  - 6.8.4 Inundation 6-58
  - 6.8.5 Maximum Extent of Invasive Riparian Plants 6-60
- 6.9 Summary and Conclusions 6-61

Figures

		Page
6-1	Flowchart for the Vegetation Module	6-4
6-2	Flowchart for the Establishment Module.	6-6
6-3	Flowchart for the Growth Module	6-7
6-4	Flowchart for the Mortality Module.	6-8
6-5	Comparison of CDWR (1991) and USACE (2002) river mile designations with overlap from RM 182 to RM 183	6-15
6-6	Comparison of CDWR (1991) and USACE (2002) river mile designations with overlap from RM 190 to RM 194	6-16
6-7	Bed slope and energy grade line at a flow of 20,000 cfs.	6-17
6-8	Stream profile from RM 80 to RM 215 (from HEC-RAS 3.1). The water surface elevations at flows of 20,000 and 90,000 cfs are shown.	6-18
6-9	Sediment load at USGS gage on Sacramento River at Hamilton City	6-19
6-10	All available USGS bed load measurements along project reach	6-21
6-11	Gravel bed load data in project reach	6-22
6-12	Comparison between simulated and measured river stage at CDWR RM 183. The flow rate and simulated average bed elevation are also shown.	6-38
6-13	Comparison between simulated and measured river stage at CDWR RM 192.5. The flow rate is also shown.	6-38
6-14	Comparison between simulated and measured ground water elevation at CDWR RM 192.5.	6-39
6-15	Comparison between measured and predicted gravel bed load transport near Hamilton City Bridge (RM 199).	6-40
6-16	Seed release characteristics at CDWR study sites RM 183 and 192.5	6-41
6-17	Seedling dispersal patterns in 2005. Note gravel sized material at RM 183.	6-42
6-18	Simulated area of cottonwood recruitment at RM 183 and RM 192.5 compared to measured seedling density.	6-43
6-19	Simulated elevation above low water (6,000 cfs) of cottonwood recruitment, compared to measured elevations of recruitment in 2006. Site has gravel soil on a point bar at RM 192.5	6-44

Figures

Page

6-20 Simulated elevations above low water (6,000 cfs) of cottonwood recruitment compared to measured elevations in 2006. Site has sandy soil on a point bar at RM 192.5 6-44

6-21 Illustration of trimming GIS coverage to match land area. 6-48

6-22 Total vegetated area computed by SRH-1DV every 4 months (on 1 day in October, February, and June) for 8 years. 6-52

6-23 Existing vegetation by cross section location in June 2007 (year 8): cottonwood (brown), mixed forest (green), Gooding's black willow (blue), narrow leaf willow (orange), and invasive species (red); as predicted by SRH-1DV 6-53

6-24 2007 vegetation mapping at RM 186 to RM 190. Giant reed (red) are located in flood plain at complex channels of near migrating bends. 6-54

6-25 New plants, 0 to 1 year, by river mile and vegetation type in October 2000, year 2. 6-55

6-26 New plants, 0 to 1 year, by river mile and vegetation type in October 2007, year 8. 6-56

6-27 Daily flows at 5 stations for an 8-year period as input to SRH-1DV. 6-56

6-28 Total acres of desiccated plants for 8 years of simulation by river mile and vegetation type. 6-57

6-29 Flow regime at Keswick and at RM 237.6 shown with total acres of desiccation for each vegetation type presented over time for 8 years of simulation. The upper chart shows the hydrologic regime (gage data) and the lower chart shows the acres of desiccation. 6-58

6-30 Total plant mortality from inundation with respect to time, shown with Figure 6-29 and 2 flow regimes (gage at Keswick and RM 237.5). 6-59

6-31 SRH-1DV simulation from October 2007 (8th year) with unlimited availability of seed and propagules where germination of invasive plants is not restricted to downstream locations. Peak not shown is over 700 acres. 6-60

Tables

		Page
6-1	Description of Ground Water Input Parameters for SRH-1DV	6-3
6-2	List of Active Stream Gages on Sacramento River.....	6-14
6-3	Manning's Roughness Coefficients Used in the SRH-1DV Model. (Roughness coefficient values are listed at locations where values change.)	6-17
6-4	Bed Material Distribution Averaged from USACE Samples between RM 140 to RM 226	6-18
6-5	Size Distribution for Incoming Sediment Load	6-20
6-6	Ground Water Parameters for Simulation	6-23
6-7	VIV Records Used in the 1999 to 2007 Simulation Matching Existing Mapped Vegetation to Initial Vegetation Conditions in the Model.....	6-25
6-8	Vegetation Parameters for Model Simulation	6-28
6-9	Desiccation Rate of Cottonwoods for Sand and Gravel Soils.....	6-36
6-10	Model Sediment Parameters Used in the SRH-1DV Simulation...	6-40
6-11	Comparison of Vegetation Mapping Classification Systems Used for the Sacramento River in 1999 and 2007.....	6-46
6-12	Comparison of Changes in Area Simulated by Vegetation Modeling to Changes in Area Measured from Vegetation Mapping Between 1999 (Year 1) and 2007 (Year 8).....	6-50
6-13	Vegetation Divisions Based on Individual Vegetation Types with More than 50 Acres per Cross Section.....	6-54
6-14	A Comparison of Vegetation Coverage Under Two Scenarios of Invasive Plant Establishment	6-61

6. One-Dimensional Modeling (SRH-1DV)

Sedimentation and River Hydraulics One-Dimensional Sediment Transport and Vegetation Dynamics Model (SRH-1DV) simulates flow hydraulics, sediment transport, and vegetation establishment and survival of the entire study area (Red Bluff to Colusa). This chapter describes the:

- *Development of the SRH-1DV ground water module (Section 6.1)*
- *Development of the SRH-1DV vegetation module (Section 6.2)*
- *Determination of the input data (Section 6.3)*
- *Calibration of the SRH-1DV flow module (Section 6.4)*
- *Calibration of the SRH-1DV sediment module (Section 6.5)*
- *Calibration and validation of SRH-1DV cottonwood plant growth (Section 6.6)*
- *Calibration of SRH-1DV multiple vegetation growth (Section 6.7)*
- *Application of the model to the Sacramento River (Section 6.8)*

SRH-1DV incorporates results from the previous described models to provide quantifiable predictions of vegetation establishment, growth, and survival for each location in the study area. Inter-related processes of flow, sediment transport, and plant development are assessed on a daily basis. SRH-1DV cannot provide the detailed predictions in a horizontal plane of a multidimensional model; however, this one-dimensional (1D) model is capable of computing plant growth over the longitudinal extent of the study area and over an extended period of years.

As illustrated in figure 1-3 in Chapter 1, daily flows from the CALSIMII/Upper Sacramento River Daily Operations Model (USRDOM) analysis, tributary sediment loads from the Sedimentation and River Hydraulics Capacity Model (SRH-Capacity), and vegetation parameters from the Riparian Habitat Establishment Model (RHEM) are inputs to the SRH-1DV Sacramento River model. Results from the multidimensional models and results from the Sedimentation and River Hydraulics Meander Model (SRH-Meander) are incorporated into interpretation and conclusions from SRH-1DV modeling.

SRH-1DV is an extension of the Sedimentation and River Hydraulics One-Dimensional Sediment Transport Dynamics Model (SRH-1D), a 1D flow and sediment transport model developed by the Technical Service Center (TSC) (Huang and Greimann 2007). SRH-1DV was written to include ground water and vegetation simulation.

The flow module of SRH-1DV can compute steady or unsteady water surface profiles. SRH-1DV is a cross section based model comparable to the Hydrologic Engineering Centers River Analysis System (HEC-RAS) model, as it uses similar hydraulic computation methods. The sediment module of SRH-1DV can compute sediment transport capacity and resulting vertical bed changes. Multiple sediment sizes can be analyzed using several different transport functions. Details of the numerical solution of the flow model, sediment transport algorithms, and channel representation can be found in Huang and Greimann (2007).

6.1 Ground Water Module

The ground water module within SRH-1DV is a cross-section based saturated flow model that solves the equation 6-1:

$$\frac{\partial z_g}{\partial t} = \frac{\partial}{\partial y}\left(K \frac{\partial z_g}{\partial y} \right) \qquad 6\text{-}1$$

Where:

z_g = Ground water elevation
K = Saturated flow hydraulic conductivity
y = Direction along the cross section.

Ground water levels are a function of the river water elevation and a soil permeability coefficient. The module solves for the ground water levels, and assumes no ground water interaction between cross sections. Therefore, the ground water solutions obtained from SRH-1DV will only be applicable near the river, i.e., generally within the alluvial soils of the floodplain. The boundary conditions imposed in the model are:

1. A known water surface elevation wherever the water surface intersects the cross section

2. No flux boundary conditions at the cross section end points

The user can enter separate saturated hydraulic conductivities for the left and right overbanks. It is also possible to enter a known flux or fixed water surface boundary condition but this was not done for the presented simulations.

The required ground water input records for SRH-1DV are listed in table 6-1.

Table 6-1. Description of Ground Water Input Parameters for SRH-1DV

Record	No. of Fields	Variable Descriptions
GMT	1	GTYPE: type of ground water simulation performed (0=none, 1 = cross section based saturated flow)
GH2	N	G_XLOC: Number of locations where saturated hydraulic conductivity values for left and right floodplains are given
GHC	3	HC_L: Hydraulic conductivity of left floodplain HC_R: Hydraulic conductivity of right floodplain HCAP: Height of capillary fringe

6.2 Vegetation Module

Concepts for the vegetation module of SRH-1DV were taken from the vegetation model developed in the Central Platte River Habitat Recovery Program. The original vegetation component of that model was developed primarily by Simons and Associates and is documented in Bureau of Reclamation (Reclamation) (2006a). Within SRH-1DV, the vegetation routines were entirely rewritten, and many new concepts have been introduced.

The vegetation module SRH-1DV is intended to be generic and applicable to a variety of species. Most of the data used to support the model have been collected on cottonwoods; however, the processes included in the model should be valid for a wide variety of plant species. The model offers a highly parameterized simulation of vegetation that relies upon parameters that need to be determined by field and laboratory studies for each species simulated.

A test of the model in the simulation of cottonwood establishment at the point bar scale is described in Section 6.6. The model is applied to several plant types or communities and calibrated using vegetation mapping in 1999 and 2007. This work is described in Section 6.7. An application of the model to the Sacramento River is described in Section 6.8.

The vegetation module SRH-1DV is composed of three submodels of plant processes:

1. Germination (establishment)
2. Growth
3. Removal (mortality)

The model uses the same cross section representation as the one dimensional SRH-1D model or HECRAS model. Plant establishment, growth, and removal are computed at each point within a cross section independently of other portions at each time step. The overall vegetation flowchart of SRH-1DV is given in figure 6-1.

Vegetation Model within SRH-1DV

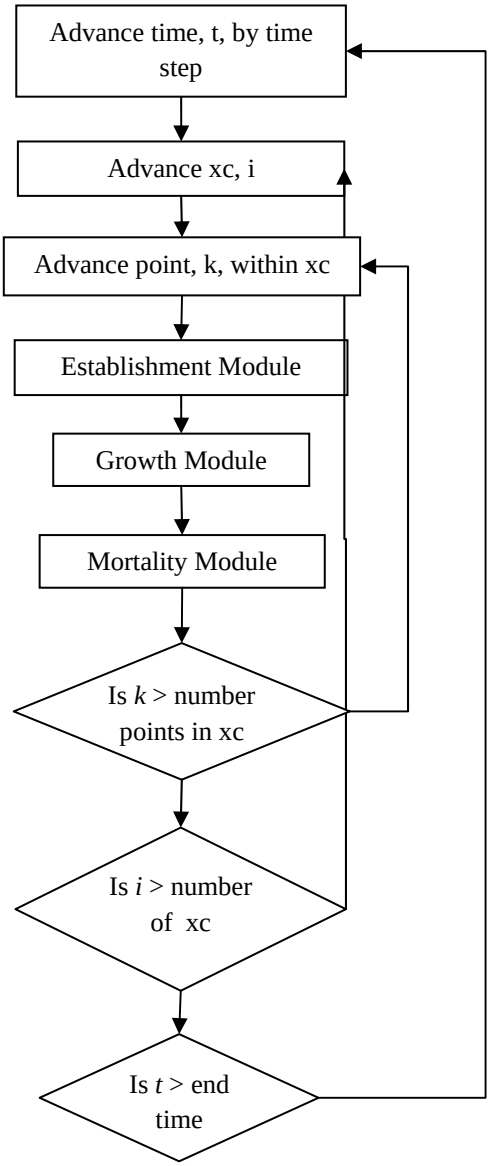

Figure 6-1. Flowchart for the Vegetation Module. "xc" is cross section.

6.2.1 Establishment Module

The Establishment Module simulates the germination process. Two main types of germination are simulated: germination due to air dispersal and germination due to water dispersal. Established plants can also expand to adjacent points through lateral spread of roots.

6.2.1.1 Air Dispersal

If air dispersal is being simulated, a plant is assumed to germinate if three criteria are satisfied:

1. Available space
2. Available seeds
3. Moist soil

The "available space" criterion is met if no other vegetation is present at that location that would outcompete the plant. At every point in a cross-section, a plant type can establish if all of the following conditions are met:

- An older plant of the same type is not already growing at that point
- Competition rules for other established plants do not prevent germination
- The plant type is tolerant of existing shade conditions at that location

For example, if there are five plant-types in the model, all five plant types can potentially establish at a single point at one time. However, an older plant and a new plant of the same type cannot grow at the point. Also, all competition stipulations between plant types and shading conditions for that plant type must be met at that location. Plants specified as non-tolerant of shade cannot establish when overhung by the canopy of a plant at the same or adjacent point. Competition, shading and multiple plant types were model developments added after initial development work with cottonwood.

The "available seeds" criterion determines whether or not seeds are available to germinate. Start and end days for seed germination are user specified. The date must be between the start and end date for seed germination for a plant to establish. It is assumed that an unlimited number of seeds are available between the start and end dates, regardless of the presence or absence of mature plants.

The "moist soil" criterion determines if the soil has enough soil moisture for the seed to begin germination. For each plant type, the user enters a distance above the ground water table in which germination is allowed. Also, the user enters a specified number of days and a distance above the ground water table where the seed is allowed to germinate. This accounts for the time that the soil remains moist after the river stage recedes.

6.2.1.2 Water Dispersal

Plant seeds or regenerative plant fragments can also be dispersed by water. If water dispersal is being simulated, then if a plant is present at a cross section, seeds are assumed to be dispersed at a user-defined distance downstream if the depth of water at the location of the plant exceeds a user-defined value. At each time step, the water depth at a particular plant's location is compared against the

user-specified value. If the depth exceeds that value, then the seed is released to the downstream cross sections and that seed can germinate at the cross section points nearest to the water surface elevation. The time period of germination is limited to a user-specified period.

6.2.1.3 Lateral Root Spread

Plant types, including narrow leaf willow and arundo, can be identified in the vegetation input file as being able to expand through lateral growth of roots. These plants can colonize closely spaced adjacent points in the cross section or even closely spaced adjacent cross sections. Before plants can spread laterally to an adjacent point or cross section, root growth must exceed 50 percent of the distance between points. Lateral spread to an adjacent cross section is rare since cross section spacing is commonly greater than extension of the plant for the period considered. Lateral root spread rate is specified for each plant type in the input file. Figure 6-2 shows the decision tree for vegetation establishment within the Establishment Module.

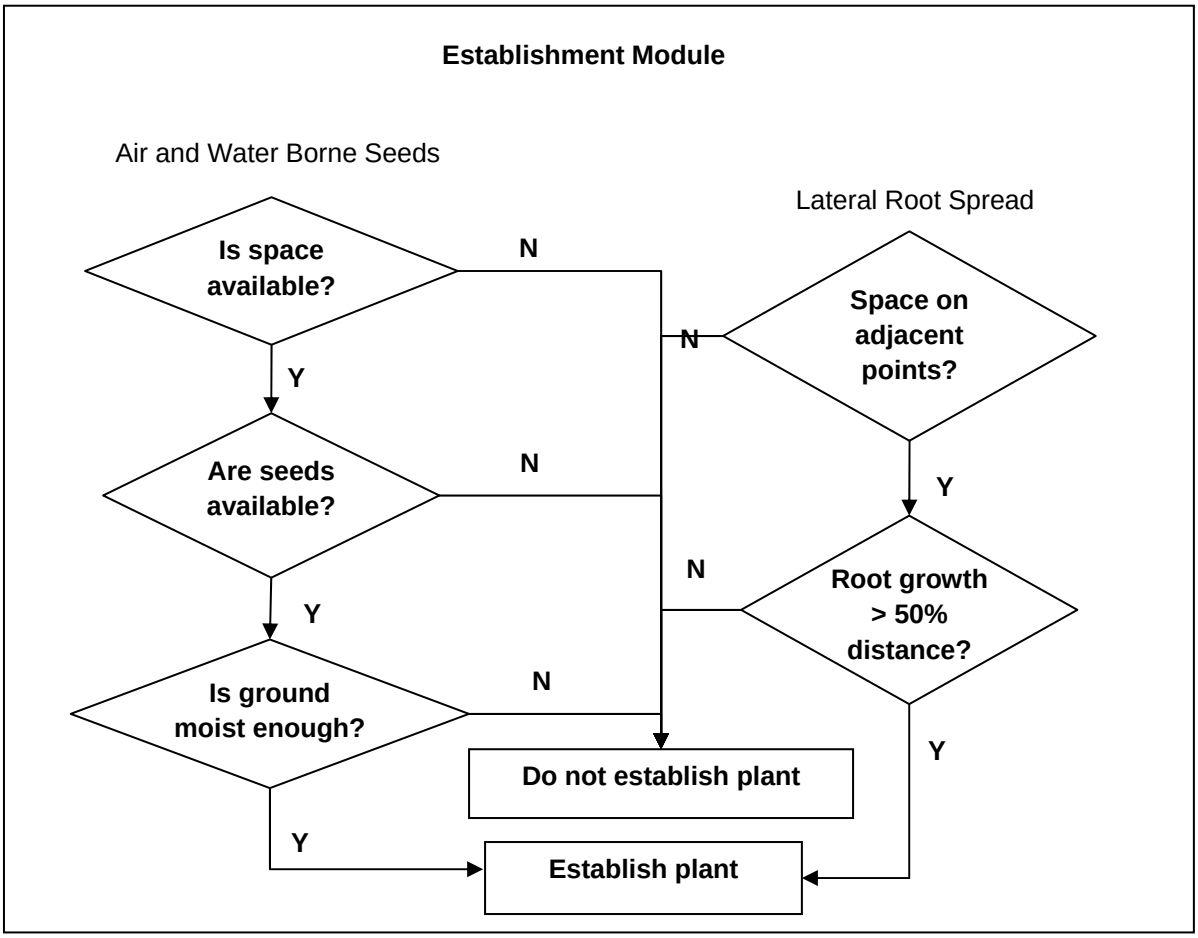

Figure 6-2. Flowchart for the Establishment Module.

6.2.2 Growth Module

The Growth Module calculates vertical growth of the root (depth), stalk (height), and canopy (width). User-specified growth rates for the roots, stalks, and canopy are based upon the month and age of the plant; that is, a growth rate can be assigned for each month of the first year, and then different growth rates can be assigned for each subsequent year of plant life. Root growth is computed at the specified rates until reaching a user-specified depth with respect to the ground water table. Stalk growth and canopy width are also computed and tracked in the Growth Module until the plant reaches an assigned maximum height or width for the vegetation type. Figure 6-3 shows the flowchart for the Growth Module.

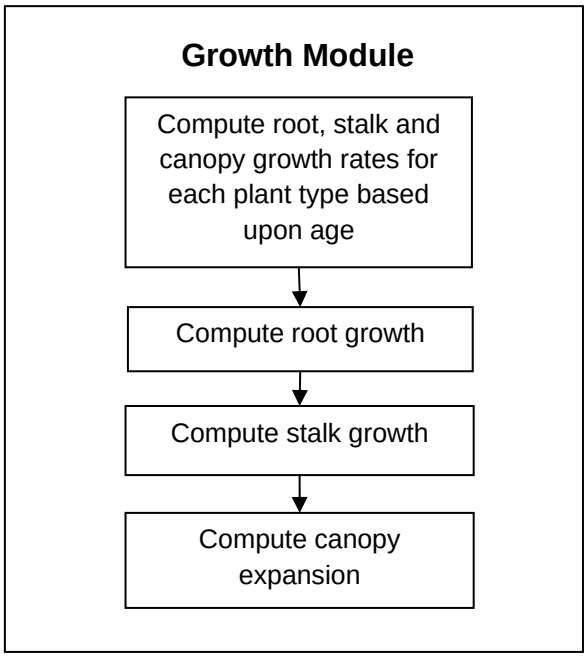

Figure 6-3. Flowchart for the Growth Module.

6.2.3 Mortality Module

The Mortality Module calculates whether the plant survives each time step. Figure 6-4 shows the decisions and flowchart for the Mortality Module. There are multiple ways a plant may die in this study, and thus be removed from the module:

1. **Desiccation.** If a plant experiences too much stress due to lack of water, then the plant will die.

2. **Senescence (Age).** The plant becomes older than the user-specified maximum age.

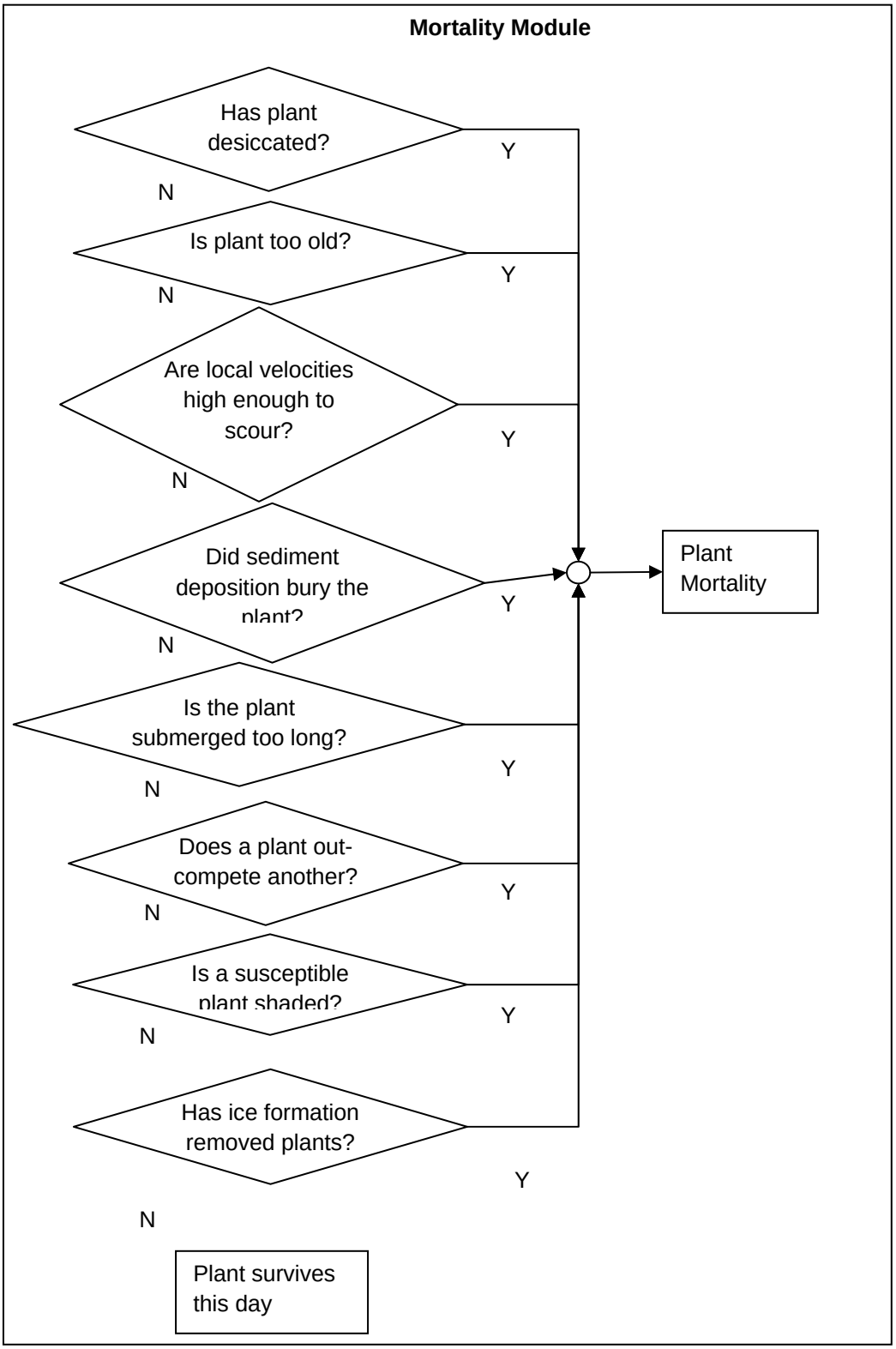

Figure 6-4. Flowchart for the Mortality Module.

3. **Scour.** The local flow velocity at the plant becomes larger than a user-specified value.

4. **Inundation.** Flows exceed the root crown by an assigned depth and flow duration.

5. **Burial.** Sediment deposited at the site of the plant exceeds the plant height by a user-specified depth.

6. **Competition.** Assigned rules define competition between plants.

7. **Shading.** A susceptible plant is under the canopy of another plant.

8. **Ice Removal.** The formation of ice or movement of ice during breakup can remove a number of new plants.

6.2.3.1 Desiccation

Two methods are used to predict desiccation, both of which depend on the relative location of the root and capillary fringe. The capillary fringe is assumed to be a constant distance above the ground water elevation for a particular cross section. The ground water elevation is calculated as described in the Ground Water Module section. One method assumes that desiccation occurs when the root is separated from the capillary fringe for a user-specified number of days. The other method tracks a "water stress" variable. When the value of that variable exceeds a user-specified value, then desiccation occurs. This water stress method was developed from the Stockholm Environment Institute (SEI) laboratory studies and development of the RHEM.

Time of Separation. The "time of separation" method tracks the relative elevation of the plant root and the capillary fringe. When a plant is a user-specified distance above the capillary fringe of the water table for more than the number of days specified, the critical time of separation is reached. The critical time of separation can also be a function of the plant age. The user can vary each plant's resistance to desiccation with age.

Water Stress. The other method of desiccation tracks a water stress parameter, which can increase or decrease every time step depending upon whether the plant is experiencing or recovering from water stress. The user enters a desiccation table of water stress values (desiccation rates) versus water table change where a negative desiccation rate indicates recovery. If the water table is declining faster than the root can grow, the desiccation rate is positive and the plant will eventually die. However, if the water table rises or stabilizes, the desiccation rate is negative. The relationship between rate of desiccation and the water table for each plant type is a function of soil type. The program has one relationship for sand and one for gravel. Soil type for every location is specified by the cross section, or specified by the Geographic Information System (GIS) polygon in the ground water input file.

6.2.3.2 Senescence

Removal due to age occurs when the plant becomes older than the user-specified age. The age of death is set for each plant type. All plants of the same type and age will die concurrently on the day the specified age is reached.

6.2.3.3 Scour

Removal due to scour occurs when the local scour velocity at the plant becomes larger than a user-specified value–the "critical scour velocity." This critical scour velocity value can be assigned for various ages for each plant type.

6.2.3.4 Burying

Removal due to burying occurs when sediment deposited at the site of the plant exceeds the plant height by an assigned value.

6.2.3.5 Inundation

Removal due to inundation occurs when flows exceed the root crown by an assigned depth and duration.

6.2.3.6 Competition

Competition is implemented through a matrix for each plant type, containing rules between each plant type based on plant age. For example, a new cottonwood seedling could be prevented from establishing if 3-year-old grass, a 2-year-old invasive plant, or an agricultural plant of any age is already present at the point. Although two plant types could be established at the same point, the dominant plant could eliminate the second plant at a user-specified age. For example a 3-year-old invasive plant can eliminate any age of grass or a 0, 1, or 2 year-old cottonwood.

6.2.3.7 Shading

Plants can be prevented from growing in areas that are shaded. A canopy growth function was added to the growth module to track locations of shade. The shaded area around each plant is determined based on age of the plant and growth rate of the canopy specified by month. During simulation, the model computes if the plant at a point is shaded by other vegetation at that point or shaded by vegetation on adjacent points. The user can enter the age at which the plant becomes shade tolerant.

6.2.3.8 Ice Scour

Young plants can be removed by ice processes during the seasons of river ice formation and breakup. This mortality requires daily air temperatures for input.

6.2.4 Vegetation Types

Two calibration studies for the vegetation model were performed. First, many of the cottonwood values were calibrated with field data. The model was then expanded with multiple vegetation types and calibrated a second time. In the second study, vegetation mapping was used to provide verification of cottonwood

values and calibration of additional vegetation types. Both calibration studies are described in later sections in this chapter.

Fremont cottonwood was the original plant simulated with the SRH-1DV model. Six plant types were added to the initial cottonwood model: mixed forest (mxf), Gooding's black willow (gbw), narrow leaf willow (nlw), herbaceous (herb), invasive riparian plants (inv), and managed and cultivated plants (ag). These plant types combined with Fremont cottonwood (ctw) were selected to represent the range of riparian communities of the Sacramento River. A designation of no-grow (nogr) areas was also used in both studies to mark developed lands where growth does not occur. Some plant types represent a single species, and others represent multiple species or a community that shares similar germination, growth, and mortality characteristics. Descriptions of the eight vegetation plant types are:

1. **Fremont cottonwood** (*Populus Fremontii*) (ctw). A fast growing, flood and drought tolerant plant found in the flood plain of the river.

2. **Mixed forest** (mxf). Contains woody species that can be found in the flood plain. If there is a group of cottonwoods within an area dominated by different species of low density the area is classified as cottonwood and not as mixed forest. Normally, species in this category are less tolerant of inundation, although they are still found in the flood plain. Oregon ash (*Fraxinus latifolia*), box elder (*Acer negundo*), California sycamore (*Platanus racemosa*), and valley oak (*Quercus lobata*) can be included and are described with generic values for parameters including germination season and growth rates.

3. **Gooding's black willow** (*Salix goodingii*) (gbw).

4. **Narrow leaf willow** (*Salix exigua*) (nlw). Although parameters are based on requirements for narrow leaf willow, this category is also representative of other riparian shrubs. These plants tolerate inundation and grow roots quickly, but root depth is relatively shallow in comparison to woody species.

5. **Herbaceous** (herb). The desiccation mortality has been turned off for this vegetation type, so these plants can grow in both riparian and upland areas. Mainly used to represent low ground cover as a mechanism to prevent germination of other plants, when specified.

6. **Invasive riparian plants** (inv). Represent vegetation that, although rarely found on the Sacramento, has had an impact on habitat or geomorphic conditions in other rivers within a short span of 5 to 10 years. Parameters for this vegetation type are based on Giant reed (*Arundo donax*), although a few mapped locations of tamarix (*Tamarix ramosissima*) (also known as

saltcedar) have been included. Giant reed is characterized by shallow root systems and a high tolerance for inundation of the roots. The plant is spread by waterborne propagules.

7. **Managed and cultivated plants** (ag). A separate plant type is assigned to remove cultivated and managed lands from the computations. Unlike riparian plants, these areas are not dependent primarily on flow levels from the river and can include fields, orchards, vineyards, and pastures. A plant may be assigned as a managed and cultivated plant, but germination, growth, and removal are not simulated.

8. **Developed lands** (nogr). Areas that do not support native vegetation due to development are designated as no-grow areas. Like managed and cultivated plants, no plant germination, growth or removal is simulated. These areas include roads, urban development, and commercial sites

6.2.5 Use

SRH-1DV has been developed as a general program applicable to different regions and climates. Airborne seeds was used for establishing plants in the cottonwood calibration model and all three establishment methods, including airborne seeds, waterborne propagules and lateral root spread, were applied in the multiple vegetation model. Root and stalk growth were used in the cottonwood simulation, and canopy growth was added later for multiple vegetation simulations. The ice mortality was not applied in either the cottonwood or multiple vegetation models. Senescence and burial mortalities were applied to the cottonwood study only, and competition and shading mortalities were applied to the multiple vegetation study only.

6.3 Input Data

Required data for SRH-1DV include daily flow data; cross section geometry for the study reach; sediment data for bed, banks, and sediment sources; ground water parameters; and vegetation parameters. A primary source of input data was the U.S. Army Corp of Engineers (USACE) Comprehensive Study of the Sacramento and San Joaquin Basins (2002).

This section describes the input data used to perform three simulations:

1. Cottonwood establishment from May to Oct in 2005
2. Cottonwood establishment from May to Oct in 2006
3. Growth of multiple vegetation types from 1999 to 2007

6.3.1 Flow Data

The flow record for the Sacramento River can be obtained from several gaging stations along the river (table 6-2). In this table, the identifications for each gaging station, as given by both the California Department of Water Resources (CDWR) and the U.S. Geological Survey (USGS) are shown. The Hydrological Unit Classification Identification (HUC ID) is assigned by USGS for each gage. Each of these gages has a continuous record of daily average flows for the Sacramento River.

6.3.2 Geometry Data

SRH-1DV requires cross sectional data, similar to other 1D hydraulic models. Both the Sacramento District of the USACE and the CDWR supplied the geometry data. Cross sections were obtained from integrating bathymetric boat survey data at wetted locations and photogrammetry surveys of dry terrain. Both surveys occurred in 1997 (USACE 2002). USACE cross sections were spaced approximately one-quarter mile apart and extended from river mile (RM) 80 to RM 215. Early work with SRH-1DV included only USACE sections from RM 145 to RM 215; however, CDWR cross sections were added between RM 130 and RM 145 and between RM 215 and RM 250. Simulations calibrated to cottonwood field studies included CDWR and USACE cross sections between RM 145 and RM 300, and simulations for calibration of multiple vegetation types to vegetation mapping included cross sections between RM 143 and RM 250.

CDWR references to river mile are based on 1991 mapping and can vary by more than 1 mile from the USACE (2002) river mile designations. Cross sections from the USACE study and CDWR (1991) river mile locations are compared in figures 6-5 and 6-6. USACE designations are used at locations where the two data sets overlap.

Positions of levees, overbank locations, and Manning's roughness coefficient values were also supplied by USACE (2002). Table 6-3 lists SRH-1DV Mannings roughness coefficient values.

A plot of the streambed slope and energy grade line based on USACE cross sections is presented in figure 6-7. The energy grade line was computed from a HEC-RAS simulation at a flow of 20,000 cubic feet per second (cfs). The energy slope generally decreases in the downstream direction from RM 215 to RM 140. Downstream of RM 140, the energy slope is generally constant. A plot of the minimum bed elevation (thalweg) is shown in figure 6-8. The jagged profile indicates an existing pool-riffle system, generally desirable for channel migration and most fishery habitats. Water depth in the pools can exceed water depth in the riffles by 20 feet or more.

Table 6-2. List of Active Stream Gages on Sacramento River

USGS ID	CDWR ID	Station Name	HUC1 ID	Latitude	Longitude	Drainage Area (mi^2)	Begin Date	Operator
11342000	DLT	Sacramento R A, Delta, CA	18020005	40.93959397	-122.4172351	425	10/1/1944	USGS and CDWR
11370500		Sacramento R A, Keswick, CA	18020101	40.6009835	-122.4444553	6,468	10/1/1938	USGS
11377100	BND	Sacramento R, AB Bend Bridge NR, Red Bluff, CA	18020103	40.28848836	-122.1866645	8,900	10/1/1891	USGS and CDWR
11383730	VIN	Sacramento River at Vina-Woodson Bridge	18020103	39.90932465	-122.0930417		4/13/1945	USGS and BOR2
11383800	HMC	Sacramento River at Hamilton City	18020103	39.75154874	-121.9955356	10,833	4/21/1945	USGS
11388700	ORD	Sacramento River at Ord Ferry	18020104	39.6282165	-121.9944222			CDWR
11389500	COL	Sacramento R A, Colusa, CA	18020104	39.21405663	-122.0002508	12,090	4/11/1921	CDWR
11390500	WLK	Sacramento R BL Wilkins Slough NR, Grimes, CA	18020104	39.00989476	-121.82469	12,915	10/1/1938	CDWR
11425500	VON	Sacramento R A, Verona, CA	18020109	38.77434584	-121.5982928	21,251	10/1/1929	CDWR
11391020	FRE	Sacto R at Fremont Weir (crest 33.5 feet)	18020104	38.75990254	-121.6677393		12/18/1973	USGS and CDWR
11426000	YBY	Sacramento Weir Spill to Yolo Bypass NR, Sacramento, CA	18020109	38.60684926	-121.5552347		1/1/1943	USGS and CDWR
11447650	FPX	Sacramento R A, Freeport, CA	18020109	38.45601954	-121.5013437		10/1/1948	USGS

Note that hyperlinks go to USGS National Water Information System.
[1] HUC = Hydrological Unit Classification
[2] BOR = Bureau of Reclamation

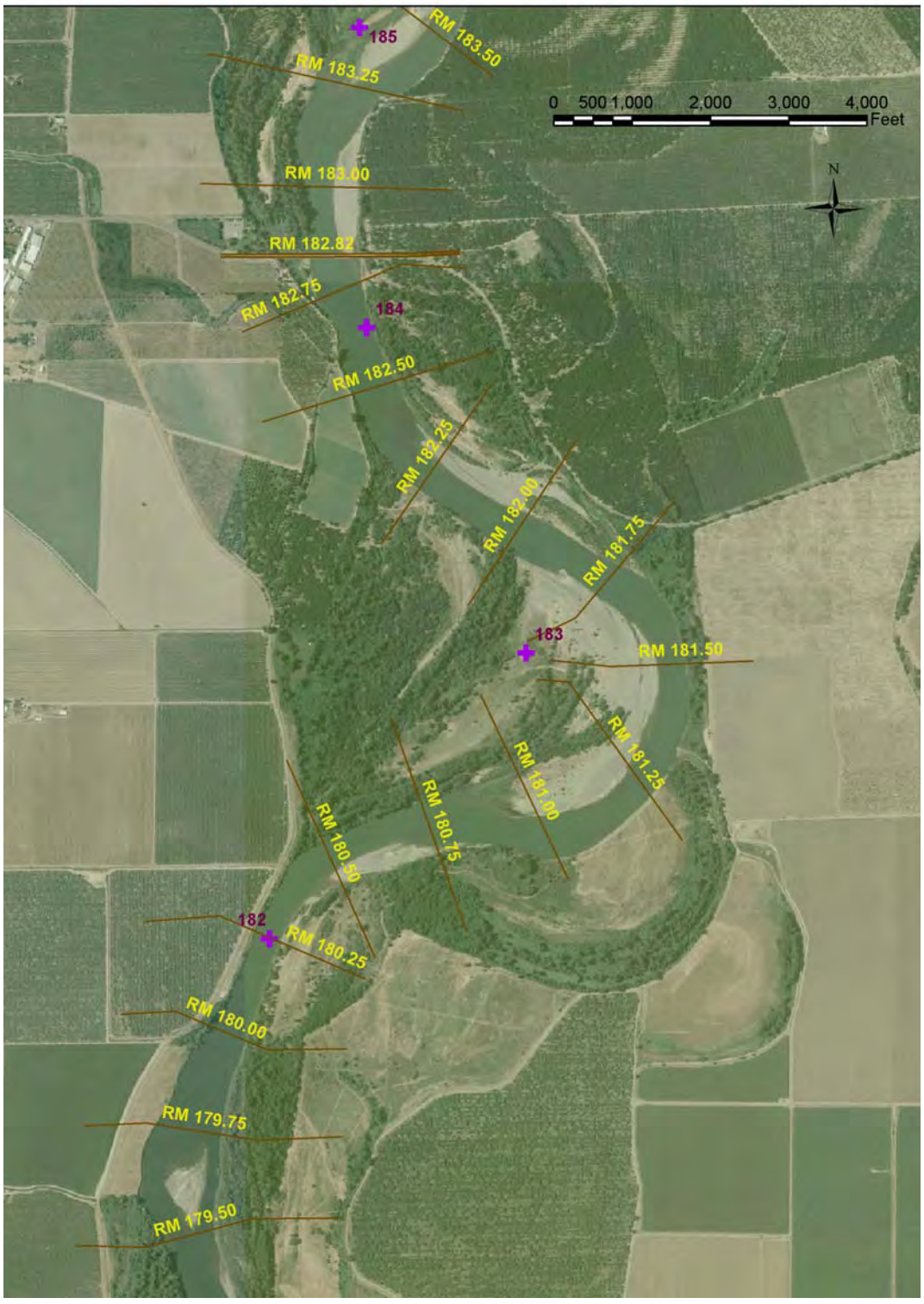

Figure 6-5. Comparison of CDWR (1991) and USACE (2002) river mile designations with overlap from RM 182 to RM 183. CDWR (1991) river mile designations are shown as purple crosses. Cross sections are from USACE (2002) study.

Figure 6-6. Comparison of CDWR (1991) and USACE (2002) river mile designations with overlap from RM 190 to RM 194. CDWR (1991) river mile designations are shown as purple crosses. Cross sections are from USACE (2002) study.

Table 6-3. Manning's Roughness Coefficients Used in the SRH-1DV Model (Roughness coefficient values are listed at locations where values change.)

River Station RM	Manning's Roughness Coefficient		
	Left Overbank	Channel	Right Overbank
215.50	0.200	0.032	0.200
202.25	0.200	0.032	0.200
202.00	0.150	0.030	0.150
193.00	0.150	0.030	0.150
192.75	0.060	0.027	0.060
182.82	0.060	0.027	0.060
182.75	0.100	0.027	0.100
166.77	0.100	0.027	0.100
166.76	0.029	0.028	0.029
157.50	0.029	0.028	0.029
157.25	0.047	0.040	0.047
146.50	0.047	0.040	0.047
146.25	0.035	0.035	0.035
119.75	0.035	0.035	0.035
119.50	0.045	0.045	0.045
118.98	0.045	0.045	0.045
118.75	0.030	0.030	0.030
80.38	0.030	0.030	0.030

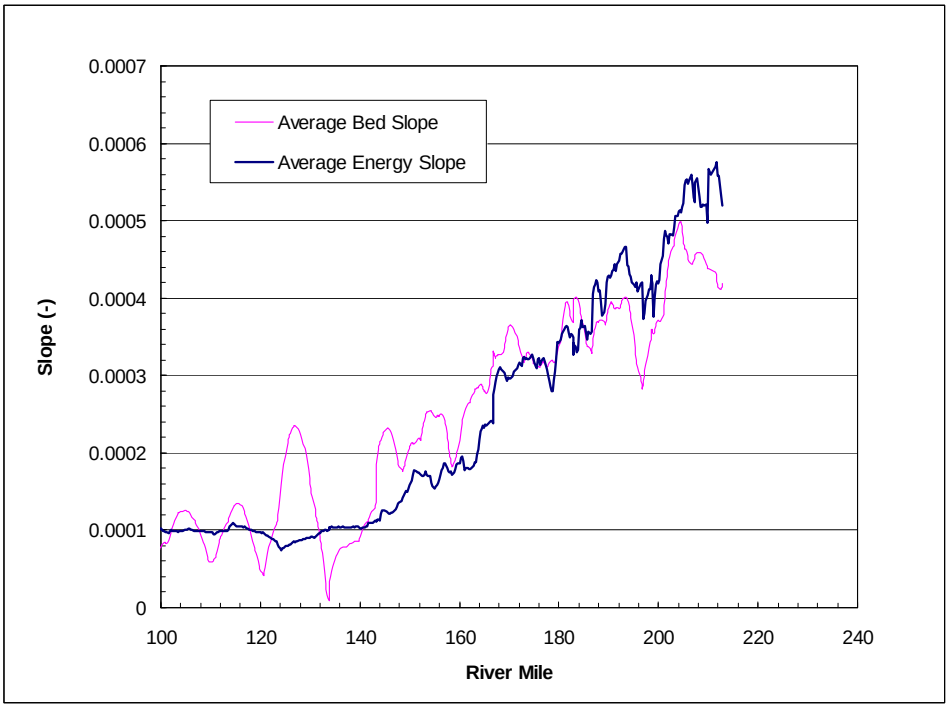

Figure 6-7. Bed slope and energy grade line at a flow of 20,000 cfs.

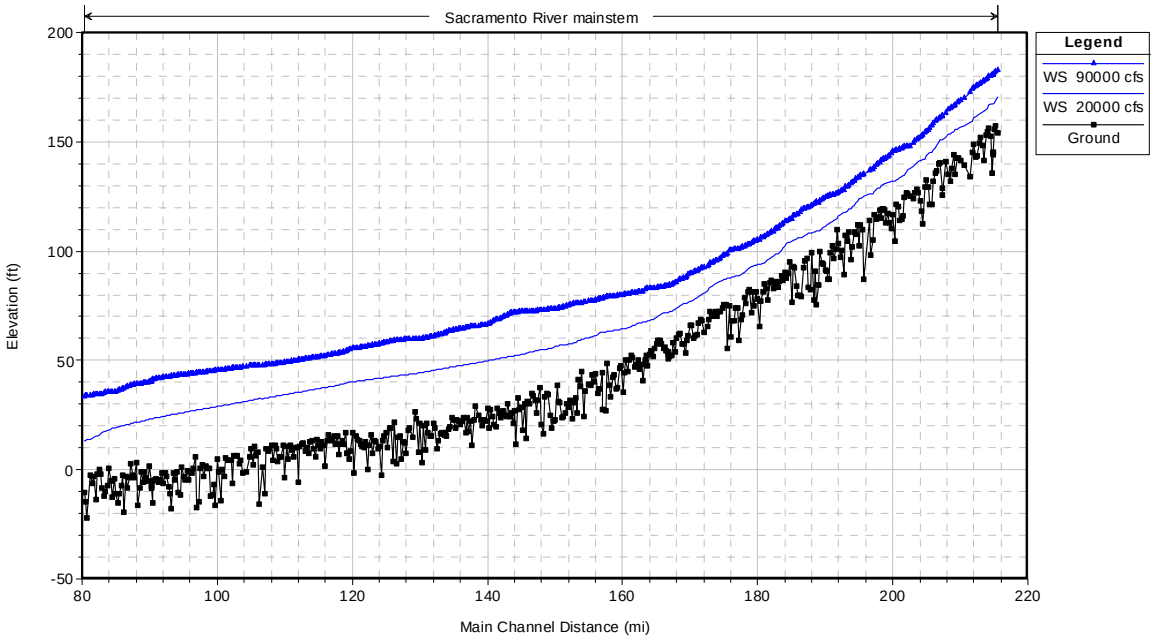

Figure 6-8. Stream profile from RM 80 to RM 215 (from HEC-RAS 3.1). The water surface elevations at flows of 20,000 and 90,000 cfs are shown.

6.3.3 Sediment Data

Size gradation of the riverbed material helps define transport characteristics of the bed (table 6-4). Bed material data used in the SRH-1D model were obtained by averaging all bed material samples that the USACE measured from RM 140 to RM 226. There is some variation of the bed material throughout the reach, but The bed material does change throughout the reach and future simulations will describe this more exactly.

Table 6-4. Bed Material Distribution Averaged from USACE Samples Between RM 140 to RM 226

Diameter (mm)[1]	0.125	0.25	0.5	1	2	4	8	16	32	64
% Passing	11.5	12.5	14.4	18.3	26.0	38.5	52.7	70.5	95.2	100

[1] mm = millimeters

USGS-recorded sediment load data from 1976 to 1979 are available from the Hamilton Stream Gage on the Sacramento River (USGS Gage No. 11383800). A simple power function was fitted to the suspended and bed load data as shown in equation 6-2:

$$Q_s = aQ^b \qquad 6\text{-}2$$

Where:

Q_s = Total sediment load in tons per day (tons/d)

Q = Discharge in cfs.

a = Constant coefficient for the power function of 3E-7

b = Constant coefficient for the power function of 2.45.

Figure 6-9 provides a plot of the suspended and bed load measurements. The fraction within each size class for various flow rates was also determined from the USGS data. Linear regression was used to determine the fraction within each size class as a function of flow rate. Results used in SRH-1D and then incorporated into SRH-1DV are shown in table 6-5.

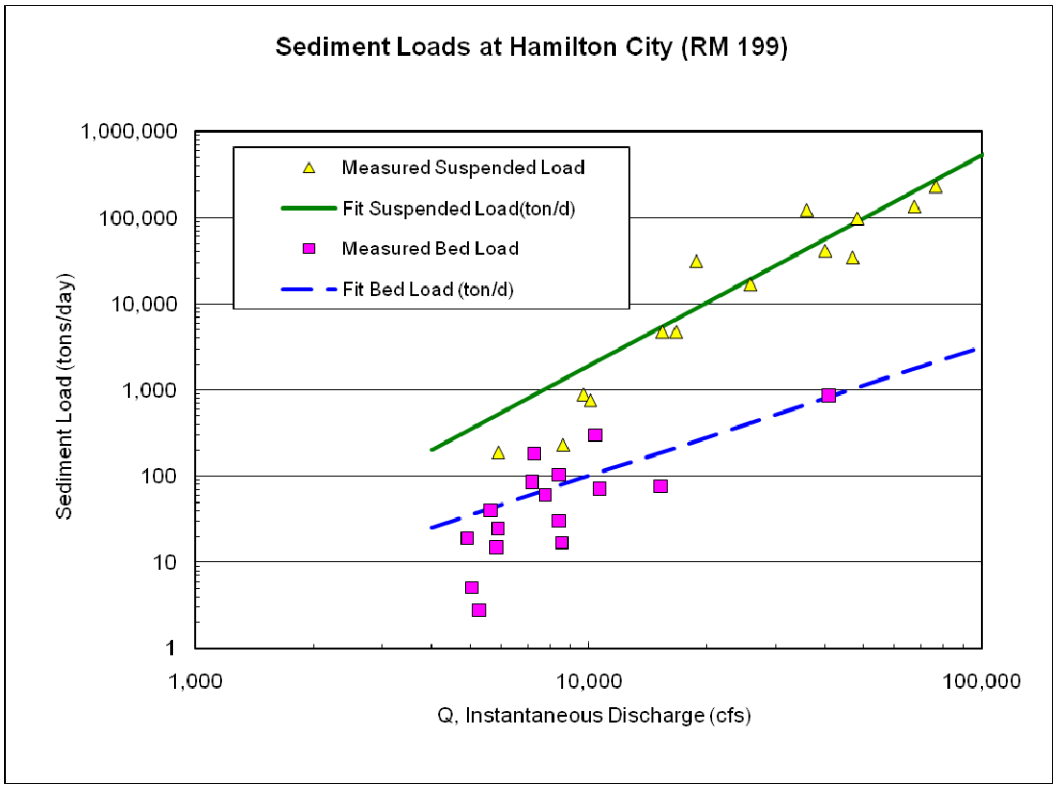

Figure 6-9. Sediment load at USGS gage on Sacramento River at Hamilton City.

Table 6-5. Size Distribution for Incoming Sediment Load

Lower diameter (mm)	0.0002	0.063	0.125	0.25	0.5	1	2	4	8	16	32
Upper diameter (mm)	0.063	0.125	0.25	0.5	1	2	4	8	16	32	64
Flow (cfs)	Percent in size class (%)										
4,000	63.82	13.55	9.62	8.98	3.213	0.442	0.114	0.000	0.020	0.195	0.047
6,400	66.25	14.06	9.81	7.01	2.255	0.291	0.081	0.021	0.042	0.135	0.046
10,200	67.65	14.36	10.10	5.81	1.584	0.187	0.059	0.039	0.058	0.093	0.046
16,400	68.19	14.47	10.55	5.27	1.116	0.117	0.044	0.052	0.069	0.066	0.047
26,200	67.88	14.40	11.26	5.35	0.777	0.071	0.034	0.062	0.077	0.048	0.047
41,900	66.61	14.12	12.39	6.08	0.508	0.041	0.028	0.068	0.083	0.036	0.048
67,100	64.06	13.55	14.18	7.66	0.257	0.022	0.024	0.073	0.088	0.028	0.049
107,400	59.66	12.58	17.04	10.4	0.046	0.008	0.019	0.068	0.081	0.021	0.044

Note that shading is provided for easier reading.

As a comparison, all available USGS bed load data along the main stem of the Sacramento were analyzed. A major shortcoming of available bed load data is that there are only two bed load measurements above 20,000 cfs, and the highest flow sampled was 40,900 cfs (figure 6-10). Data for bed loads with diameter greater than 2 mm (gravel) are shown in figure 6-11.

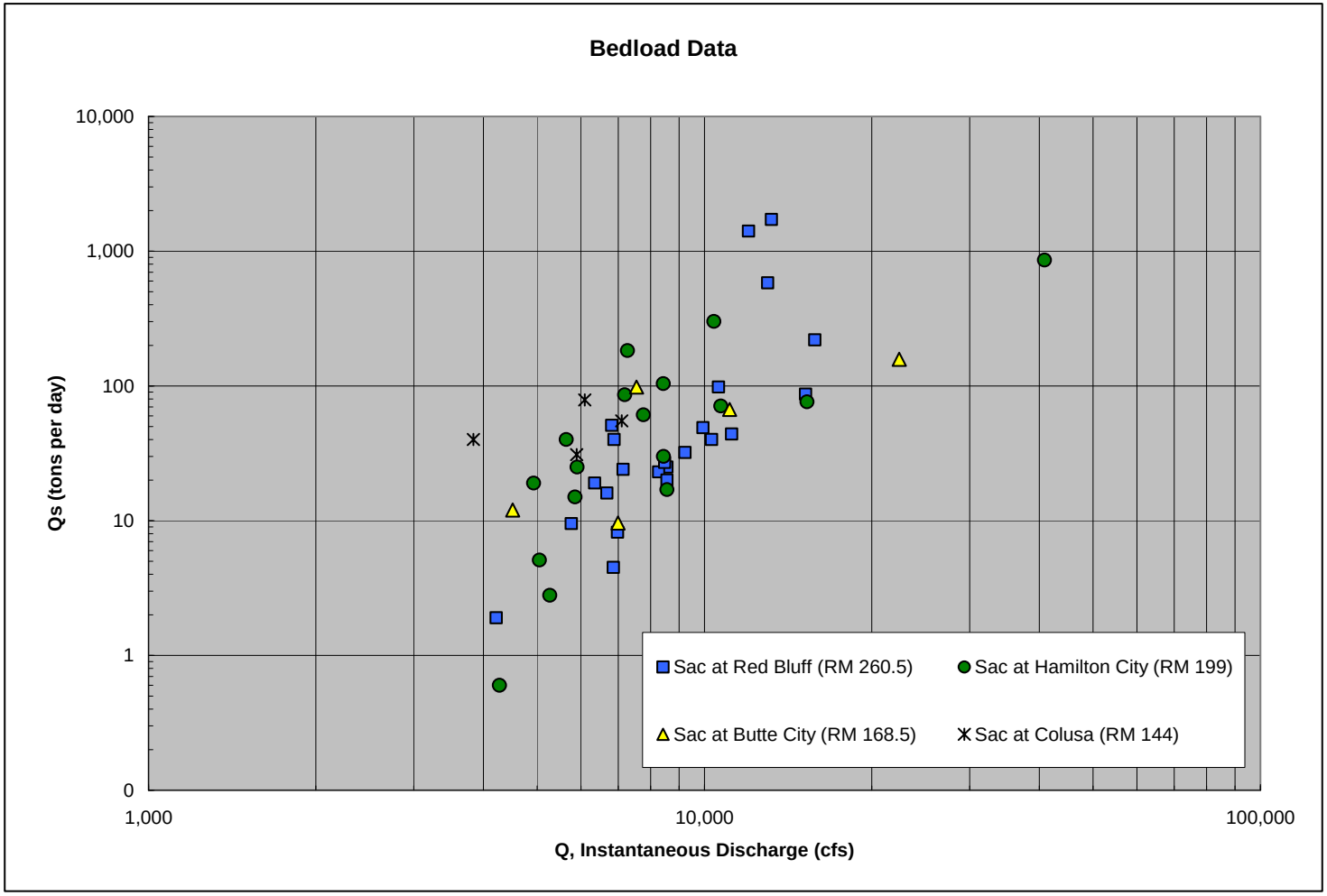

Figure 6-10. All available USGS bed load measurements along project reach.

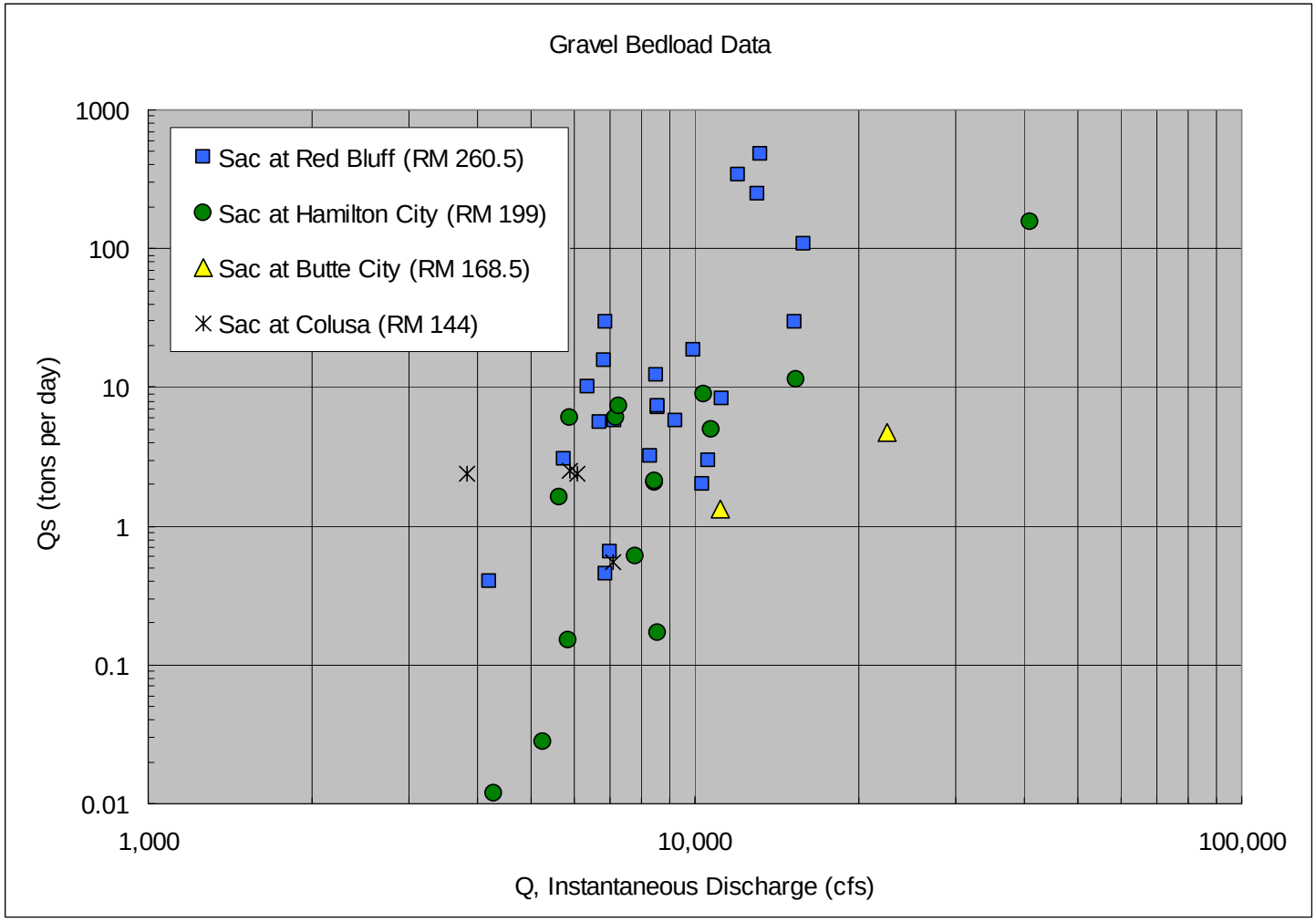

Figure 6-11. Gravel bed load data in project reach.

6.3.4 Ground Water Parameters

Ground water parameters are assigned by cross section, similar to sediment inputs. The model assumes that each cross section is independent of the other cross sections and that no water flux is allowed at the cross section endpoints. Saturated hydraulic conductivity was calibrated based upon well data (CDWR 2005). Ground water parameters are shown in table 6-6.

Table 6-6. Ground Water Parameters for Simulation

For all cross sections within x feet downstream	200,000
Left and right hydraulic conductivity (K) ft/day	1.0E+05
Height of capillary fringe (Sand 0.8, Gravel 0.11)	0.80 or 1,1
Drop velocity(ft/day)	0.50
Ground water minimum height (hmin)	20.00
Ground water maximum height (hmax) (for ground behind levees)	1

The height of the capillary fringe was based upon the data presented in Chapter 5. To the authors' knowledge, no systematic measurement of capillary height has occurred on the Sacramento River. If the substrate is sandy, a value of 0.8 feet is used. If the substrate is primarily gravel, a value of 0.11 feet is used. During dry periods with no flow in the channel, the minimum ground water elevation (hmin) can be influenced by ground water flow conditions outside the boundaries of the model. These conditions are generalized by assigning a lower limit (hmin) to ground water elevation for lands within the model. A second limit, hmax, is assigned to the water surface on lands behind levees. Unless the levee is breached, surface water depth behind a levee is influenced more by drainage patterns of adjacent lands than by the surface water of the river. The three dimensional (3D) drainage patterns cannot be adequately described within the boundaries of the model, so a general maximum depth of flooding behind levees is assigned. Both hmin and hmax are values in feet with respect to the ground elevation.

6.3.5 Vegetation Parameters

A vegetation file is entered into SRH-1DV in addition to flow, sediment, and geometry files. Vegetation parameters are presented in two groups. The first group includes general input parameters and initial conditions, while the second group contains germination, growth, and mortality parameters specific to each vegetation type. Sources for some of the parameters are included in this section.

6.3.5.1 General Parameters and Initial Conditions

The records and fields for general parameters and initial vegetation conditions of the model are outlined in Appendix B, table B.1. One set of general parameters

is needed for each simulation. The VIN,[1] VIT and VIV records are used when GIS vegetation mapping is available to assign existing vegetation conditions to model cross sections at the start of the simulation. A VIN record identifies a file with a table of mapped polygons (csv file) constructed from a GIS file of polygons (shp file). The shp file contains labels, areas, and other information associated with each vegetation polygon. The VIT record identifies the list containing names of vegetation communities in the csv file, and the VIV file defines the initial age and density of vegetation communities associated with each GIS polygon. Table B.2 in Appendix B documents the information used for General Input Records in the model simulations.

Values for VIV records are presented separately in table 6.7. If GIS mapping is available, VIV records are used to assign established vegetation to each model cross section at the start of the simulation. After initialization, the model tracks growth of the assigned plants, in addition to computing new vegetation (germination) when conditions are suitable. Every VIV record translates a mapped community, to the modeled vegetation types. For example, the GIS shapefile may contain 30 mapped categories of land use, which are translated into the 8 modeled vegetation types using the VIV records.

For each mapped community, the VIV records associates the GIS identifier, the age, and the density. The ability to assign density of each plant type to represent a mapped community is an improvement to the computing process added after the cottonwood study. Density is input as a decimal representing the percent of points in the mapped polygon. For a density of 0.1 or 10 percent, the associated age and type of vegetation is assigned to 1 point out of every 10 points in the mapped polygon. A vegetation type excluded from a mapped community were assigned an age of 0. Areas described as “Riparian Scrub” may have sparsely located grasses, occasional shrubs, and a rare tree. All riparian scrub polygons were assigned points:

- 1-year grass at 6 out of 10 points
- 3-year willow at 3 out of 10 points
- 10-year cottonwood at 1 out of 10 points

All other vegetation types in the riparian scrub VIV record were assigned an age of 0.

Descriptions of the mapped communities and aerial photos were used to match communities with vegetation types, and to assign average densities and representative ages to vegetation types.

[1] Note that VIN is not the Vina Woodson Bridge, but a database record identifier.

Table 6-7. VIV Records Used in the 1999 to 2007 Simulation Matching Existing Mapped Vegetation to Initial Vegetation Conditions in the Model. Note that shading indicates entries for vegetation (age followed by density) where 1 is 100 percent of density.

	Cotton-wood		Mixed Forest		Gooding's Black Willow		Narrow Leaf Willow		Herba-ceous		Invasive		Managed and Cultivated		Developed Lands	
Modeled Vegetation Types	ctw		mxf		gbw		nlw		herb		inv		ag		nogr	
1999 GIS Classifications	age	D	age	D	age	D	age	D	age	D	age	D	age	D	age	D
Barren and wasteland	0	1	0	1	0	1	0	1	0	1	0	1	0	1	0	1
Berry shrub	0	1	0	1	0	1	0	1	0	1	0	1	1	1	0	1
Citrus and subtropical	0	1	0	1	0	1	0	1	0	1	0	1	1	1	0	1
Cottonwood forest	40	1	0	1	0	1	0	1	0	1	0	1	0	1	0	1
Deciduous fruits and nuts	0	1	0	1	0	1	0	1	0	1	0	1	1	1	0	1
Disturbed	0	1	0	1	0	1	0	1	0	1	0	1	0	1	0	1
Field crops	0	1	0	1	0	1	0	1	0	1	0	1	1	1	0	1
Giant reed	0	1	0	1	0	1	0	1	0	1	3	1	0	1	0	1
Grain and hay crops	0	1	0	1	0	1	0	1	0	1	0	1	1	1	0	1
Gravel	0	1	0	1	0	1	0	1	0	1	0	1	0	1	0	1
Herb land	0	1	0	1	0	1	0	1	1	0.5	0	1	0	1	0	1
Idle	0	1	0	1	0	1	0	1	0	1	0	1	1	1	0	1
Industrial	0	1	0	1	0	1	0	1	0	1	0	1	0	1	1	1
Marsh	0	1	0	1	0	1	0	1	0	1	0	1	0	1	0	1
Mixed forest	0	1	40	1	0	1	0	1	0	1	0	1	0	1	0	1
Native vegetation	0	1	0	1	0	1	0	1	0	1	0	1	1	1	0	1
Open water	0	1	0	1	0	1	0	1	0	1	0	1	0	1	0	1
Pasture	0	1	0	1	0	1	0	1	0	1	0	1	1	1	0	1

Table 6-7. VIV Records Used in the 1999 to 2007 Simulation Matching Existing Mapped Vegetation to Initial Vegetation Conditions in the Model. Note that shading indicates entries for vegetation (age followed by density) where 1 is 100 percent of density.

	Cotton-wood		Mixed Forest		Gooding's Black Willow		Narrow Leaf Willow		Herba-ceous		Invasive		Managed and Cultivated		Developed Lands	
Modeled Vegetation Types	ctw		mxf		gbw		nlw		herb		inv		ag		nogr	
1999 GIS Classifications	age	D	age	D	age	D	age	D	age	D	age	D	age	D	age	D
Residential	0	1	0	1	0	1	0	1	0	1	0	1	0	1	1	1
Rice	0	1	0	1	0	1	0	1	0	1	0	1	1	1	0	1
Riparian scrub	0	1	0	1	5	0.1	2	0.3	1	0.5	0	1	0	1	0	1
Riparian vegetation	0	1	0	1	20	0.5	5	1	0	1	0	1	0	1	0	1
Semi-agricultural	0	1	0	1	0	1	0	1	0	1	0	1	1	1	0	1
Tamarix	0	1	0	1	0	1	0	1	0	1	2	1	0	1	0	1
Truck and berry crops	0	1	0	1	0	1	0	1	0	1	0	1	1	1	0	1
Urban	0	1	0	1	0	1	0	1	0	1	0	1	0	1	1	1
Urban commercial	0	1	0	1	0	1	0	1	0	1	0	1	0	1	1	1
Urban landscape	0	1	0	1	0	1	0	1	0	1	0	1	0	1	1	1
Urban vacant	0	1	0	1	0	1	0	1	0	1	0	1	0	1	1	1
Valley oak	0	1	40	1	0	1	0	1	0	1	0	1	0	1	0	1
Vineyards	0	1	0	1	0	1	0	1	0	1	0	1	1	1	0	1
Water surface	0	1	0	1	0	1	0	1	0	1	0	1	0	1	0	1

D = density

6.3.5.2 Parameters by Vegetation Type

Germination, growth and mortality parameters are entered for each vegetation type. The vegetation type is identified by the VVN record, followed by the parameters associated with that type. For eight vegetation types, there would be eight sets of parameters. Record and field names for each parameter can be found in Appendix B, table B.3. Table 6-8 lists the parameters used for the main vegetation types in the final simulations.

6.3.5.3 Selection of Vegetation Parameters

Parameters in the SRH-1DV vegetation file were often found in journal articles on site studies of mature plants or laboratory investigations of new seedlings. Cottonwood desiccation values based on plant stress were developed specifically for the model from plant desiccation studies in the SEI laboratory. Federal and state plant libraries on the internet were also used as resources in selecting representative parameters for less studied aspects of plant growth. Occasionally a range of values for a specific plant could be found from multiple sources, but the range in values often appeared related to regional and climatic factors. Verification and sensitivity simulations helped to identify influential parameters that were addressed further in model calibration studies using field or mapping data. Calibration helped define parameters within the range of values initially considered. Calibration studies with 2005 and 2006 cottonwood field data and also based on GIS mapping data from 1999 to 2007 are presented in later sections. In this section references for select vegetation parameters are presented, and also unique aspects of some parameters are briefly discussed.

Germination

MDY, Begin and End Date of Dispersal Season. Several journal articles report on germination seasons for frequently studied plants including Fremont cottonwood, Gooding's black willow, and narrow leaf willow. Dates appear to vary with the region and climate, supporting the hypothesis that the germination season is tied to hydrology and air temperature (Stillwater Sciences 2006). Airborne seed dispersal season selected for cottonwood was May 1 to July 1. These dates were based on a seed dispersal survey conducted by the CDWR (2005).

One of the most variable parameters is seed dispersal season for mixed forest. Mixed forest includes Oregon ash (*Fraxinus latifolia*), box elder (*Acer negundo*), California sycamore (*Platanus racemosa*), and valley oak (*Quercus lobata*), although other woody species may be grouped in this mapping community. These woody species share similar traits like water and shade tolerance but have wider variation in germination seasons. Valley Oaks germinate from acorns and the root can begin growing in December several months before the shoot appears, giving the taproot a 3 foot start on growth towards the water table (see http://phytosphere.com/oakplanting/acorns.htm).

Table 6-8. Vegetation Parameters for Model Simulation

	Fremont Cottonwood (ctw)	Mixed Forest (mxt)	Gooding's Black Willow (gbw)	Narrow Leaf Willow (nlw)	Invasive Plants (inv)	Upland Grass (herb)
GERMINATION						
MMT. Plant colonizes by airborne seed, water-borne propagules, and/or lateral root spread	Air	Air	Air	Air and Lateral Root	Water and Lateral Root	Air
MDY. Begin and end day of dispersal season	120 to 180	135 to 160	144 to 162	129 to 273	90 to 210	0 to 150
Airborne Seed Dispersal						
MPR. Days required for germination	0.5	1	0.5	1.5	na	1
MPR. Maximum dry days allowed before germination	2	2	2	2	na	45
MPR. Height above ground water table moist enough for germination	1	0.5	1	1	na	200
MPR. Depth below ground water germination still occurs (feet)	0.1	0.01	0.2	0.2	na	0.01
Water Dispersed Propagules						
MPW. Critical depth (feet)	na	na	na	na	1	na
MPW. Travel distance (feet)	na	na	na	na	25,000	na
MPW. Seed survival (days)	na	na	na	na	6	na
Spread by Lateral Root Extension						
MLT. Lateral root spread rate at age (year), rate (feet per day)	na	na	na	0, 0.07	0, 0.08	na
				1, 0.11	1, 0.10	na
MLT. Season of root spread	na	na	na	Feb-Nov	Mar-Nov	na
Maximum height of establish above low water (feet)	na	na	na	25	15	na

Table 6-8. Vegetation Parameters for Model Simulation

	Fremont Cottonwood (ctw)	Mixed Forest (mxt)	Gooding's Black Willow (gbw)	Narrow Leaf Willow (nlw)	Invasive Plants (inv)	Upland Grass (herb)
GROWTH						
GCP. Canopy Spread, age (yr) and rate (ft/day)	0, 0.002	0, 0.002	0, 0.002	0, 0	0, 0	0.0
	2, 0.005	2, 0.005	2, 0.005	na	na	na
	15, 0.008	15, 0.008	15, 0.008	na	na	na
	45, 0.002	45, 0.002	45, 0.002	na	na	na
GCP. Season of growth	Mar-Nov	Mar-Nov	Mar-Nov	na	na	na
GCM. Max radius (feet)	10	15	10	0.1	0.1	0.1
GRT. Root Growth Rate, age (year) and rate (feet per day)	0, 0.066	0.03	0, 0.0656	0, 0.065	0, 0.1	0, 0.0042
	6, 0.011	0.01	6, 0.01	na	na	na
GRT. Season of growth	Mar-Nov	Mar-Nov	Mar-Nov	Mar-Nov	Mar-Nov	Sept-Jan
GRS. Max depth of root below water table before stops (feet)	0.01	0.01	0.1	0.2	0.2	0.01
GRS. Max depth below ground (feet)	24	20	22	8	5	0.5
ROUGHNESS						
RAM. Age and Manning's n roughness coefficient	0, 0.04	0, 0.04	0, 0.04	0, 0.04	0, 0.04	0, 0.04
	5, 0.06	5, 0.06	5, 0.06	5, 0.07	5, 0.07	5, 0.45
	30, 0.08	30, 0.08	30, 0.08	30, 0.01	30, 0.1	30, 0.45
MORTALITIES						
CMP. Competition X plant age (* = any age), Y plant, and Y plant age			0.1, ctw, 24	0.1, ctw, 24		0.1, ctw, 6
			0.1, mxf, 24	0.1, mxf, 24		0.1, mxf, 6
					0.1, nlw, 1	0.1, gbw, 6
X plant at specified age (i.e. 1rst column is ctw) dies if Y plant has reached	0.1, herb, 3	0.1, herb, 3	0.1, herb, 3	0.1, herb, 3	0.1, herb, 3	0.1, nlw, 1
	0.1, inv, 2	0.1, inv, 2	0.1, inv, 2	0.1, inv, 2		0.1, inv, 1

Table 6-8. Vegetation Parameters for Model Simulation

	Fremont Cottonwood (ctw)	Mixed Forest (mxt)	Gooding's Black Willow (gbw)	Narrow Leaf Willow (nlw)	Invasive Plants (inv)	Upland Grass (herb)
specified age.					1, nlw, 3	1, nlw, 2
			2, mxf, 40	2, mxf, 40		
			2, mxf, 40	2, mxf, 40		
	2, inv, 3	2, inv, 3	2, inv, 3	2, inv, 3		2, inv, 3
	*, ag, 0.01	*, ag, 0.01	*, ag, 0.01	*, ag, 0.01	*, ag, 0.01	*, ag, 0.01
	*, nog, 0.01	*, nog, 0.01	*, nog, 0.01	*, nog, 0.01	*, nog, 0.01	*, nog, 0.01
CSH. Age when shade tolerant (years)	1	0.1	1	1	3	99
SVC. Scouring - age (yr), critical velocity (ft/second)	0, 2	0, 2	0, 2	0, 2	0, 3	0, 5
	1, 2.5	1, 2.5	1, 3	1, 3	1, 4	1, 3
	2, 3	2, 3	2, 4	2, 4	2, 5	2, 4
	3, 4	3, 4	3, 5	3, 5	3, 6	na
	4, 5	4, 5	4, 8	4, 6	na	na
	5, 6	5, 6	na	na	na	na
DTM. Inundation - age (years), time (days), depth (ft)	0, 15, 0.5	0, 12, 0,25	0, 18, 0.5	0, 18, 0.5	0, 18, 0.5	0, 5, 0.1
	1, 30, 1	1, 25, 1	1, 35, 1	1, 35, 1	1, 35, 1	1, 12, 0.1
	2, 30, 2	2, 25, 2	2, 35, 2	2, 35, 2	2, 35, 2	na
	3, 60, 2	3, 50, 2	3, 70, 2	3, 70, 2	3, 70, 2	na
	4, 120, 2	4, 90, 2	4, 150, 2	4, 150, 2	4, 150, 2	na
	5, 150, 2	5, 120, 2	5, 180, 2	5, 180, 2	5, 180, 2	Na
YMT. Desiccation Method root depth or cumulative stress	cumulative stress	root depth	root depth	root depth	root depth	Na
YTM. Desiccation – Root Depth Method	na	0, 3, 0.1	0, 2, 0.1	0, 2, 0.1	0, 5, 0.5	Na
	na	1, 7, 0.1	1, 5, 0.1	1, 5, 0.1	1, 10, 0.5	Na

Table 6-8. Vegetation Parameters for Model Simulation

	Fremont Cottonwood (ctw)	Mixed Forest (mxt)	Gooding's Black Willow (gbw)	Narrow Leaf Willow (nlw)	Invasive Plants (inv)	Upland Grass (herb)
age (yr), time (days), and height above capillary fringe for desiccation (ft)	na	2, 14, 0.1	2, 11, 0.1	2, 11, 0.1	2, 20, 0.5	Na
	na	3, 28, 0.1	3, 25, 0.1	3, 25, 0.1	3, 50, 0.5	Na
	na	6, 60, 0.1	6, 50, 0.1	4, 25, 0.1	na	Na
	na	na	na	5, 25, 0.1	na	Na
	na	na	na	29, 50, 0.1	na	Na
YWT. Desiccation – Cumulative Stress Method water table decline (ft/day), stress (sand), stress (gravel)	-3.2800, -1.510, -1.510	na	na	na	na	Na
	-0.0328, -0.018, -0.021	na	na	na	na	Na
	0.000, -0.012, -0.013	na	na	na	na	Na
	0.0328, 0.005, 0.009	na	na	na	na	Na
	0.0656, 0.030, 0.032	na	na	na	na	Na
	0.0984, 0.051, 0.115	na	na	na	na	Na
	3.2800, 1.990, 5.900	na	na	na	na	Na
YMN. Months drying is allowed	Nov-Mar	Nov-Mar	Nov-Mar	Dec-Jan	Dec-Feb	Jan-Dec

Oregon ash produces airborne seeds in September and October that are viable for a year (Niemiec et al. 1995). Box elder also produces airborne seeds in the fall that are dispersed throughout the winter producing a range of germination periods. Initially, a wide season was selected to represent the main woody species; however, this season was reduced to June 15 through July 10 during calibration to more closely represent the areas of GIS mapped vegetation. The longer germination season was producing excess areas of mixed forest in the model. The first contributing explanation for this poor fit is that the woody species within this vegetation type could have been better represented by reorganizing into two or three different vegetation types. A second potential explanation is presented by authors of the GIS mapping study who caution against comparing values to their mixed forest mapping community when treated independent of other woody species like cottonwood.

Giant reed can germinate from propagules carried downstream during high flows, or can expand to new locations through rhyzoid growth. Spencer and Ksander (2001) determined that new shoots emerged and survived at 57.2 degrees F and 68 degrees Fahrenheit but could not emerge from rhizome sections at 44.6 degrees F. Shoots first appeared in a Davis, California, experiment in late March when the average daily temperature was 52.7 degrees F, and continued to emerge until November. These values were used as a guide for invasive vegetation seed dispersal season.

MPR, Germination Parameters. These parameters include:

- Time required for seed germination
- Maximum time allowed for germination from soil wetting
- Capillary fringe area for germination
- Height above ground water surface that germination can occur

In a study of cottonwood establishment and survival, Borman and Larson (2002) found that the cottonwood seedling crop would fail if the surface dried within several days after germination. The initial seedling root growth was slow, and the surface soil needed to be damp for the first 1 to 3 weeks after germination. Germination usually occurred between 8 and 24 hours after a cottonwood seed fell on a moist surface. Cottonwood seed germination is assigned a value of 12 hours in this model.

The maximum number of days between germination and the time when the water table is within a specified distance of the ground surface is also a required model input. The maximum number of days is set to 2 days, which assumes the soil will dry out 2 days after the river recedes below the specified elevation. Height above the ground water surface is set to the capillary fringe height. The capillary fringe

height is approximately 1 foot, although this may vary in the reach. Germination is assumed not to occur below the ground water table.

Growth Parameters

GST, Stalk Growth Rate. The stalk growth rate table assigns stalk growth rate by plant age for each month of the year. Stalk growth rate is not relevant to other computations in the model, but the rate does control the appearance of the stalk in the cross-section window during the simulation. These values have not been presented in the parameter table.

GSM, Maximum Height of Stalk. When the maximum plant height is reached, the plant stops growing. This value is primarily used for graphical observations of cross sections during the simulation and is inconsequential to the results presented in this report. Varying stalk heights and colors allow the observer to distinguish between plant types, but like the stalk growth rate table, these values have not been included in the parameter table.

GRT, Root Growth Rate. Values for root growth rate are assigned by plant age for each month of the year. If root growth can be sustained at the same rate as the drop in water table elevation, the roots can continue to supply the plant with moisture from the ground water. Values for cottonwood root growth used in the model were based on several published investigations. Morgan (2005) and Cederborg (2003) observed the average growth rate for roots to be approximately 0.5 centimeters per day (cm/d) with a maximum of 1.4 cm/d. Roberts et al. (2002) reported an average rate of 2.2 cm/d, with a maximum rate of 3.2 cm/d. In the dessication study at the SEI laboratory (Chapter 5), it was found that seedlings could generally sustain a water table drop of 0.5 cm/d indefinitely. These results indicate that 0.5 cm/d is a root growth rate that does not exert stress on the plant. A plant can have faster root growth rates for a period of time, but this rate of growth expends plant energy reserves and exerts stress on the plant, eventually causing mortality. Therefore, the root growth parameter is best thought of as a "no stress" root growth value.

GRS, GRT, Maximum Depth of Root Below Water Table Before Growth Stops. The depth below the ground water table where the root growth stops was assumed to be 0.1 foot for Fremont cottonwood and Gooding's black willow. Narrow leaf willow and invasive plants have better coping mechanisms for inundation so their roots are allowed to extend to 0.2 foot below the water surface before growth stops.

GRS, GRT Depth, Maximum Depth of Root Growth. Maximum root depth is one of the most sensitive parameters in the model for defining survival between different vegetation types. In addition to ground water and moisture availability, a second factor for root depth is soil type, with densely compacted soils or rock restricting the extension of roots and aeration, and a third factor is aeration since

roots need oxygen to transpire. It is assumed, however, that maximum depths can be attained in the alluvial soils being modeled. Aeration is addressed with inundation tracking described under plant mortality. Therefore, the primary factor defining root depth in the model is ground water depth.

The root depth parameter, GRT_Depth, represents different root structures with taproots, rather than laterally spreading roots. Lateral root growth is also represented as a plant colonizing mechanism under model germination. Rhizomes of the invasive plant giant reed tend to grow laterally, and narrow leaf willow roots, to a lesser extent, also grow laterally. Lateral root growth development occurring with tap root development for woody species may reduce plant reliance on the ground water table. The growth of a taproot appears to be most prominent in young plants up to about 6 years. Although streamflow and subsequently ground water often respond promptly to rainfall, SRH-1DV does not directly account for precipitation in the analysis of plant survival. Stress on plants is based on proximity to ground water. Subsequently, calibration studies can indicate root depths to be used in the model and may represent the deepest values reported in the literature. Zimmermann's (1969) investigation on plant ecology in Southeastern Arizona presents root depths for cottonwood, black willow, sycamore, and alder growing in areas where ground water is generally less than 40 feet below the surface, but older trees might depend at least part of the year on moisture in the alluvium. Actual root depths reported were 7+ feet for cottonwood, 7 feet for black willow and 15+ feet for Hackberry. Horton et al., (2001) reported that Fremont cottonwood was commonly found in areas where ground water was 0.5 to 4 meters deep. Gooding's black willow is more shallow-rooted than Fremont cottonwood (Stromberg, et al., 1991, 1996, Stromberg, 1993). Adjusted root depths for native plants in this model after calibration are: Fremont cottonwood, 24 feet; mixed forest, 20 feet; Gooding's black willow, 22 feet; and narrow leaf willow, 8 feet.

Tamarix has deep roots (Zimmerman 1969 and Horton et al. 2001), but other invasive plants like giant reed and phragmites have shallow rhizomes that are easily undercut in secondary flows similar to wetland plants like California bulrush or cattail. The single vegetation type for invasive plants as used in this study is representative of giant reed and other shallow rooted plants, but this vegetation type is not a good representation of tamarix. The calibrated root depth for invasive plants in the Sacramento model is 5 feet.

Mortality Parameters

DTM, Death by Inundation. Inundation mortality occurs when the root crown of a cottonwood is submerged by a specified depth and for an extended period of time. The threshold time of inundation and the depth of inundation above the root crown can be entered as a function of age. Hosner (1958) found that plains cottonwood seedlings will survive 8 days of inundation, but most die after 16 days. After a few years of growth, cottonwoods may become more resistant to

drowning; however, prolonged inundation will still kill most plants, and inundation of more than a few weeks will stress cottonwoods (Neuman et al. 1996). In a study by Stromberg et al. (1993), inundation of saplings (<1 cm at 1 meter [m] height, and <1 yr), pole trees (<1- 10 cm at 1 m height), and large trees (>10 cm at 1 m height) were examined in the Sonoran desert where 2-yr, 5-yr, and 10-yr floods had occurred. Flow depths varied from 0.4 to 2.1 m. Gooding's black willow had greater rates of survival than Fremont cottonwood. Survival of poles and saplings declined sharply when depths exceeded 1.5 m and ranged from 30 percent to 78 percent for saplings, 73 percent to 93 percent for pole trees and was 100 percent for mature trees. Auchincloss et al. (2010) determined that Fremont cottonwood seedlings had 78 percent and 50 percent survival for one week and two week submergence of seedlings. Mortality increased linearly for seedlings based on days of complete submergence at a rate calculated by equation 6-3.

$$\% \text{ mortality} = 4.6 + (2.5 * x) \qquad 6\text{-}3$$

Where:

x = number of days submerged

Auchincloss et al. (2010) also reported that greater depths of submergence were more detrimental than shallow depths of submergence. In addition, seedlings had greater survival rates in colder water fluctuating between 11 and 18 degrees Celsius in contrast to temperatures of 18 to 24 degrees Celsius.

YMT, Type of Desiccation Simulation. There are two types of desiccation mortalities that can be selected: a root depth method and a cumulative water stress method. Water stress values apply specifically to young cottonwood plants and have not been developed for other vegetation types or ages. The root stress method was used in the cottonwood study and the water stress method was developed during multi-vegetation studies.

YTM, Desiccation by Root Depth. The root depth method depends on separation between the root tip and the capillary zone of the water table for a specified number of days to determine when desiccation will occur. Fremont cottonwood and Gooding's black willow have drought-coping mechanisms as adult plants which increase the plants resilience to drought stress. Horton et al.(2001) report on the canopy dieback mechanism that allows plants to reduce water consumption through branch sacrifice during dry periods. Giant reed is assigned a high resilience (more days before removal) in this simulation because of its rhizome development that allows the plant to extend laterally to a water source. Narrow leaf willow is less tolerant of drought than Fremont cottonwood.

YWT, Desiccation by Cumulative Water Stress. The second method, based on water stress of young plants, was added following laboratory desiccation studies

of cottonwood plants conducted by SEI (Chapter 5). Cumulative stress imposed on the young plant (measured as a desiccation rate) is tracked until a user-specified water stress is reached and the plant is removed. Desiccation rates for the water stress method are provided for two soil types. These values were developed based on the RHEM studies presented in Chapter 5. Desiccation rate values for cottonwoods in sand and gravel soil types are shown in table 6-9. Plants are assumed to die from desiccation when the stress parameter exceeds a user specified value. In the study conducted by SEI, cottonwoods generally perished when the water stress parameter exceeded 0.6.

Table 6-9. Desiccation Rate of Cottonwoods for Sand and Gravel Soils

	Desiccation Rate (d-1)	
WT decline (ft/d)	Sand	Gravel
-3.280	-1.510	-1.510
-0.0328	-0.018	-0.021
0.000	-0.012	-0.013
0.0328	0.005	0.009
0.0656	0.030	0.032
0.0984	0.051	0.115
3.280	1.990	5.900

YMN, Months Desiccation is Allowed. This record can be used to assign dormant months when desiccation will not harm the plant.

IMT, Ice Scour Mortality. This process is not simulated in this study.

AMT, Mortality by Senescence. Plants that reach a maximum age are removed from the model. Mortality by Senescence is not simulated in the Sacramento model due to the relatively short time period (7 years or less) of the simulations.

6.4 Calibration of Flow and Ground Water Modules

Following development of the initial code and input files, three aspects of the model were calibrated: the flow and ground water modules, the sediment transport module, and the cottonwood establishment, growth and survival module. For calibration of the flow and ground water module, data collected by CDWR were used. CDWR's Red Bluff office collected water surface elevations and ground water elevations near CDWR RM 192.5 and CDWR RM 183 during the spring and early summer of 2004 and 2005. They also collected information on cottonwood seedling dispersal and cottonwood establishment at this location. Data collection is described in CDWR (2005). The water surface elevations were

collected near the cross section at RM 192.5, and ground water wells were located on the point bars at RM 192.5 and RM 183.

Flow records used were obtained from CDWR-operated gaging stations. Gaging station No. A02630, Sacramento River at Hamilton City (HMC), located at RM 199, was the reference discharge site correlated to RM 192.5 in this calibration. Gaging station No. A02570, Sacramento River at Ord Ferry (ORD), located at RM 184 was the reference discharge site for RM 183 in this calibration. Water surface elevations at RM 183 and RM 192.5 (measured by CDWR in 2005) were compared to SRH-1DV simulated water surface elevations (figures 6-12 through 6-14).

In the comparison to measured water surface elevation at RM 192.5, an average of the water surfaces at the modeled cross sections upstream (192.5) and downstream (192.25) of the measured site were used. The modeled water surface at RM 182 was compared to the measured water surface elevation at RM 183.

The primary calibration parameter for hydraulic simulation is the roughness coefficient of the river channel. In this case, Manning's roughness coefficient had previously been calibrated and reported by USACE (2002). USACE values are listed in table 6-3. The agreement between the measured and predicted water surface elevations was excellent for the flows below 20,000 cfs, and therefore modification of the values reported in the USACE study was unnecessary. Additional data collected at high flows would be valuable to testing the model at higher discharges.

Ground water data at RM 192.25 were used to calibrate the saturated hydraulic conductivity parameter. Ground water wells were located closest to river station 192.25. Well # 4 was located approximately 1000 feet from the edge of low water and Well #3 was located approximately 500 feet from the edge of low water. The simulated and measured ground water levels at approximately 1,000 feet from the water edge are shown in figure 6-14. Ground water levels respond very quickly to river stage changes, indicating a high hydraulic conductivity for soils near the river. Calibration resulted in a large hydraulic conductivity of 200,000 feet per day (ft/d), which is an expected value for gravel, which is the dominant particle size on the upper portion of the point bar at RM 192.5 (Freeze and Cherry 1979).

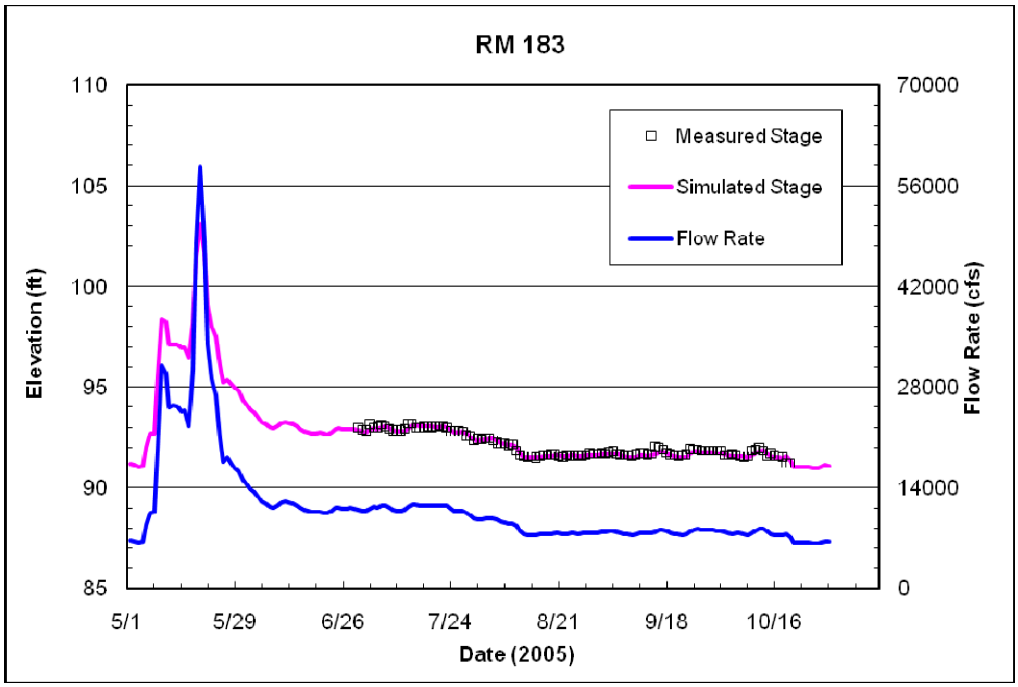

Figure 6-12. Comparison between simulated and measured river stage at CDWR RM 183. The flow rate and simulated average bed elevation are also shown.

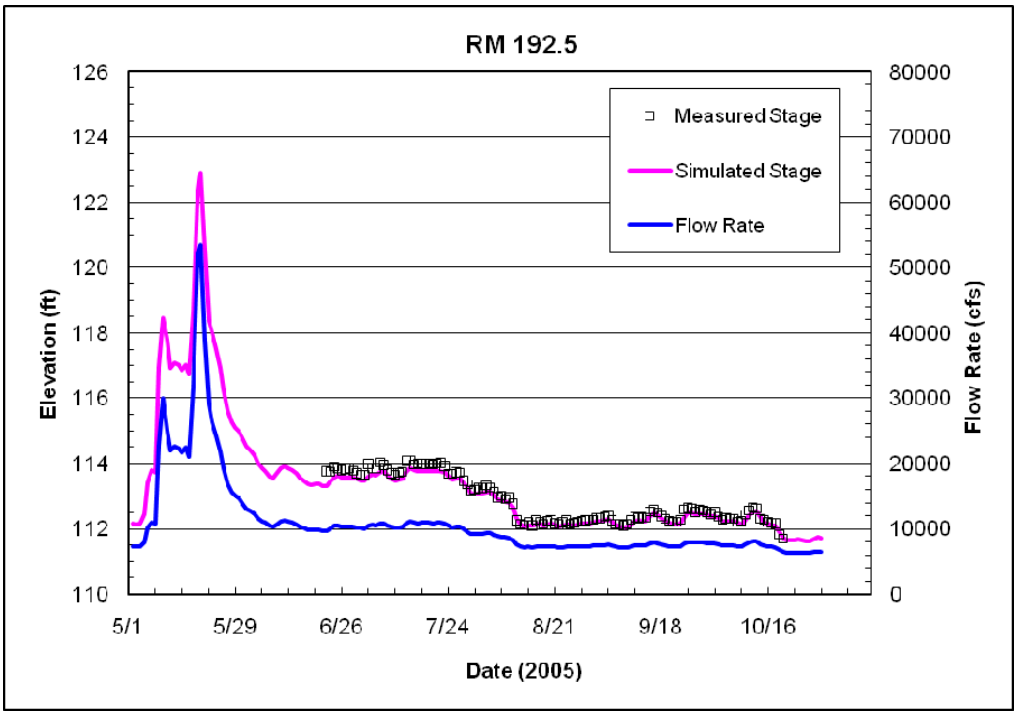

Figure 6-13. Comparison between simulated and measured river stage at CDWR RM 192.5. The flow rate is also shown.

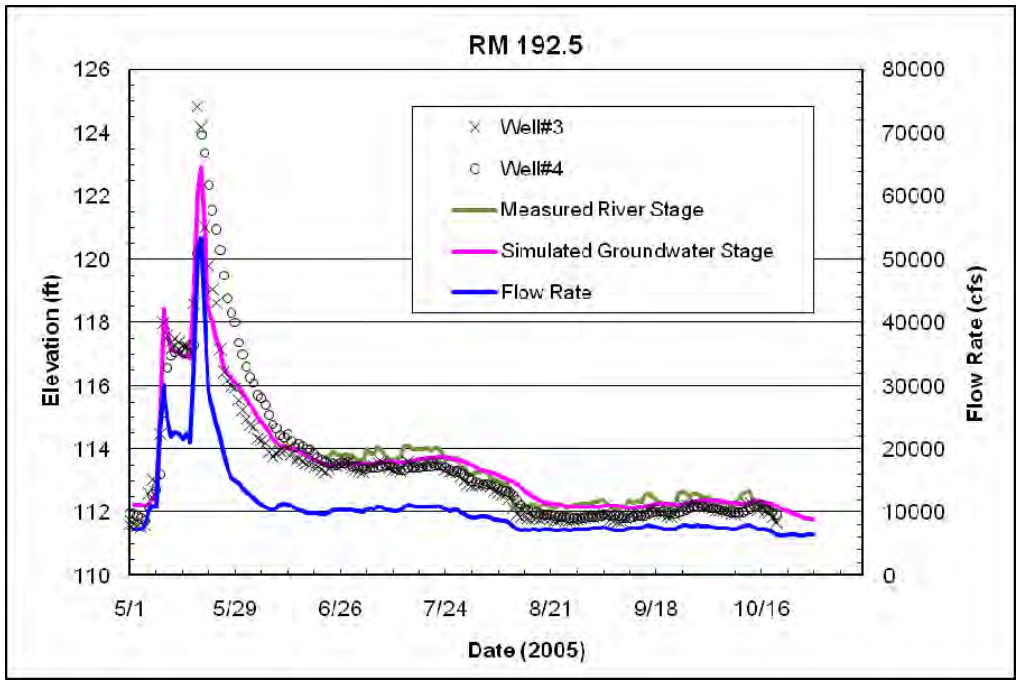

Figure 6-14. Comparison between simulated and measured ground water elevation at CDWR RM 192.5.

6.5 Calibration of Sediment Module

Limited historical geometry information is available for the Sacramento River. One-dimensional sediment transport models have a limited ability to simulate bed elevation changes in the Sacramento River because large lateral adjustments also participate in the mass balance. In general, sediment transport models can only directly model vertical changes and have limited capability to simulate horizontal changes. The horizontal changes in the river are typically much larger than the vertical changes and overwhelm vertical adjustment; however, 1D sediment transport models can be useful as a tool to compare the predicted sediment loads to the measured sediment loads.

Table 6-10 shows the sediment parameters used in the SRH-1D simulation. Parker's (1990) surface-based bed load formula was chosen to represent sediment transport. Predicted gravel transport was compared against measured transport for a range of flows (figure 6-15). Limited bed load data are available, particularly at high flows; therefore, it is difficult to determine the accuracy of the predicted bed load transport. This is the same transport formula used in the analysis of SRH-Capacity.

Table 6-10. Model Sediment Parameters Used in the SRH-1DV Simulation

Parameter	Value
Time step	0.5 hours
Active layer thickness	1 foot
Transport formula	Parker

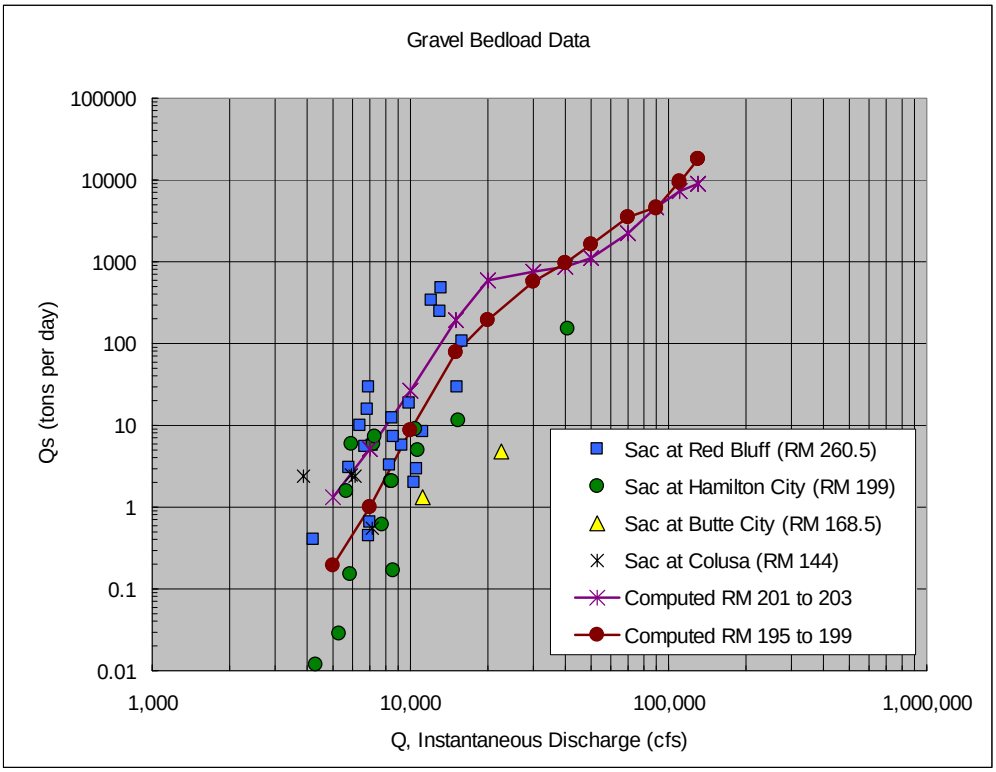

Figure 6-15. Comparison between measured and predicted gravel bed load transport near Hamilton City Bridge (RM 199).

6.6 Cottonwood Calibration with Field Data

Following calibration of the flow and ground water modules, and calibration of the sediment module, a calibration study of cottonwood growth was performed to improve the validity of the SRH-1DV model results. CDWR monitored the establishment and growth of cottonwoods on the point bars at RM 192.5 and RM 183 in 2005, and at RM 192.5 in 2006. These data were used to calibrate cottonwood growth parameters in the vegetation module of SRH-1DV. The upstream area of the point bar at RM 192.5 is mainly composed of gravel soil, and the downstream area of the point bar is mainly composed of sandy soil. The cross sections where cottonwood data are collected on RM 183 are comprised of primarily of gravels.

6.6.1 2005 Data

CDWR (2005) collected data for calibration of cottonwood establishment and survival in the vegetation module. In addition to monitoring water stage and ground water levels, described in the previous section, seedling survival was monitored at two point bars, located at RM 183 and 192.5, during the summer of 2005. The cottonwood seedling dispersal is shown in figure 6-16. The plot shows the dispersal of cottonwood seeds at RM 192 and RM 183 for several different cottonwood plants. Photographs shown in figure 6-17 document the desiccation of the cottonwood due to a decrease in Sacramento River flow.

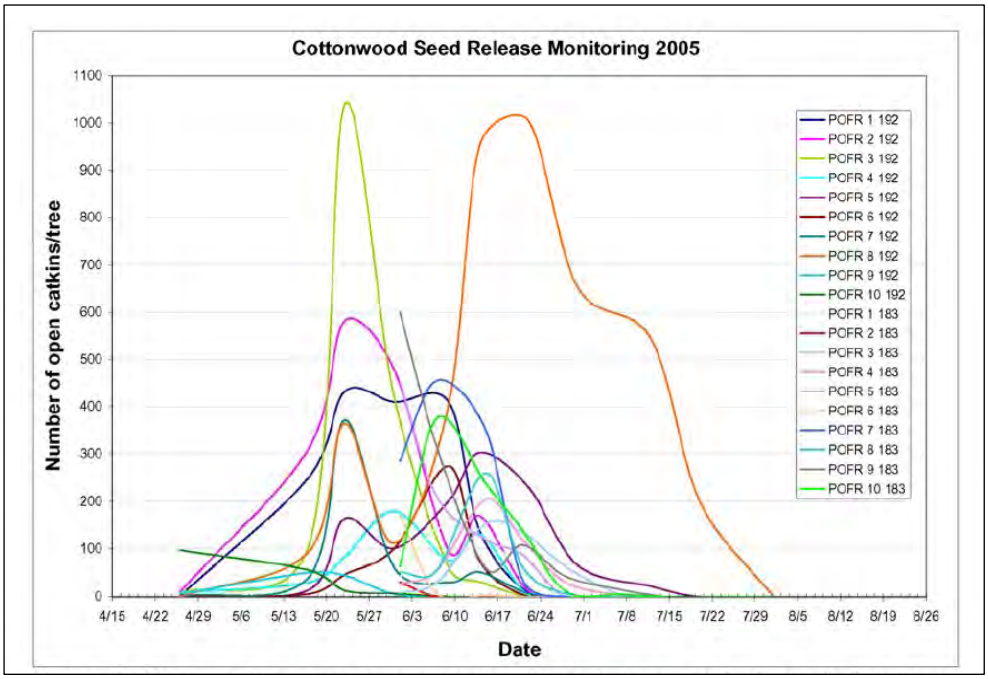

Figure 6-16. Seed release characteristics at CDWR study sites RM 183 and 192.5. Catkins are a strand of tiny, inconspicuous and short lived flowers on cottonwoods. (Figure 5 from CDWR [2005]).

Vegetation parameters were calibrated to match the documented mortality of cottonwood seedlings at these locations. The primary calibration parameter was the cottonwood root growth rate. For all simulations, a root growth rate of 0.5 cm/d is used. A range of values was tested between 0.024 and 2 cm/d, but a value of 0.5 cm/d fit the data the best. Because the bed material at RM 183 and 192.5 at the transects shown in figure 6-17 in primarily gravel, the gravel desiccation parameters are used.

A comparison between the simulated seedling area and the measured seedling density is given in figure 6-18. SRH-1DV does not currently predict the density

of vegetation, only the presence or absence of a particular vegetation type. Therefore, we were only able to compare the measured densities over time to the predicted areal coverages over time.

Figure 12. Seedlings before July 28th (left) were very healthy. The right photo, taken on August 23rd at RM 183, shows dehydrating seedlings following a recession exceeding root growth capabilities.

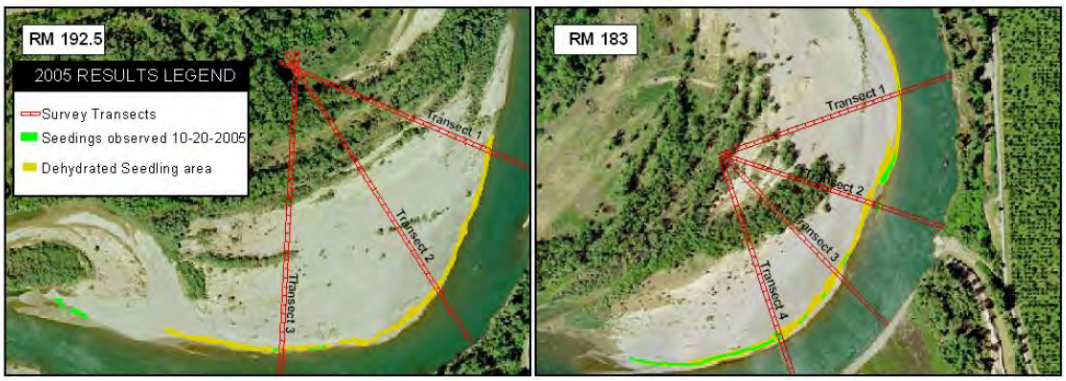

Figure 13. The study site aerial photographs show the dehydrated areas that were very healthy in July before the recession. The remaining seedlings that were still observed on October 20th were limited to an average 2 seedlings/m^2.

Figure 6-17. Seedling dispersal patterns in 2005. (Figures 12 and 13 taken from CDWR [2005]). Note gravel sized material at RM 183. m^2 = per square meter.

The model reproduced the establishment of the cottonwoods following the high flows in mid-May and the desiccation of those cottonwoods following the decrease in flow from approximately 11,500 cfs to 7,500 cfs in early August (figure 6-18).

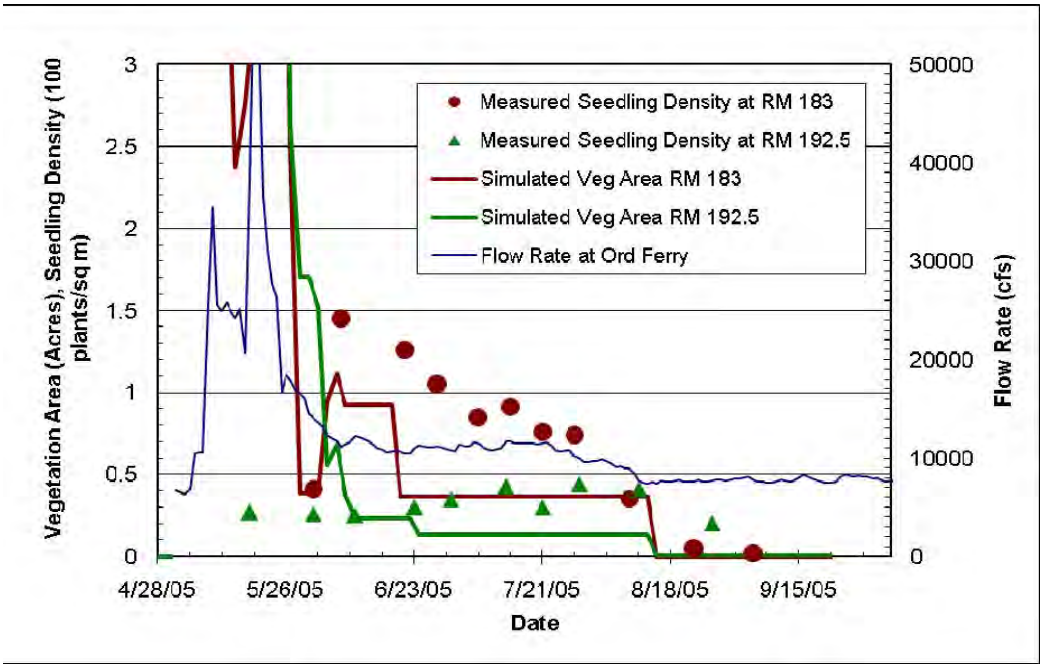

Figure 6-18. Simulated area of cottonwood recruitment at RM 183 and RM 192.5 compared to measured seedling density.

6.6.2 2006 Data

CDWR also collected vegetation data in 2006 at two cross sections, one at RM 192.25 and one at RM 192 (Henderson 2006, CDWR, personal communication). The soil at RM 192.25 was predominantly gravel while the soil at RM 192 was primarily sandy. CDWR tracked the minimum and maximum elevations of the cottonwood seedlings, with respect to low water, in the upstream part of the point bar. The 2006 season had more successful cottonwood germination than the 2005 season, particularly in the sandy soil.

The authors simulated the minimum and maximum elevations of recruitment above low water elevation in both the gravel and sandy soils using SRH-1DV. The same vegetation parameters calibrated to the 2005 data were applied. The only difference between RM 192.25 and 192 was the soil type, which changes the desiccation rate, as stated in table 6-9.

The comparison between the measured and simulated elevation of 2006 cottonwood establishment above low water is shown in figure 6-19 for gravel soil and in figure 6-20 for sandy soil. The model accurately tracks the final elevation of seedling establishment for both the gravel and sandy soils. However, the model does not track the gradual decrease in the minimum and maximum elevation of the cottonwoods from May 27 until July 20. After that date, the model simulates the surviving height of seedlings accurately.

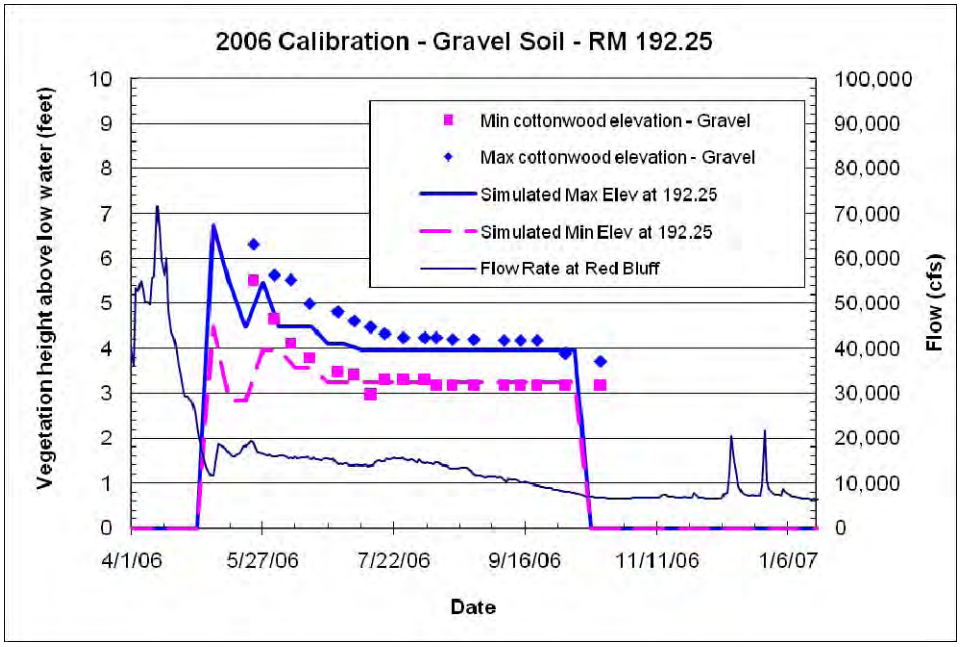

Figure 6-19. Simulated elevation above low water (6,000 cfs) of cottonwood recruitment, compared to measured elevations of recruitment in 2006. Site has gravel soil on a point bar at RM 192.5. Measured and simulated values are compared to daily flow at the Red Bluff CDWR gage.

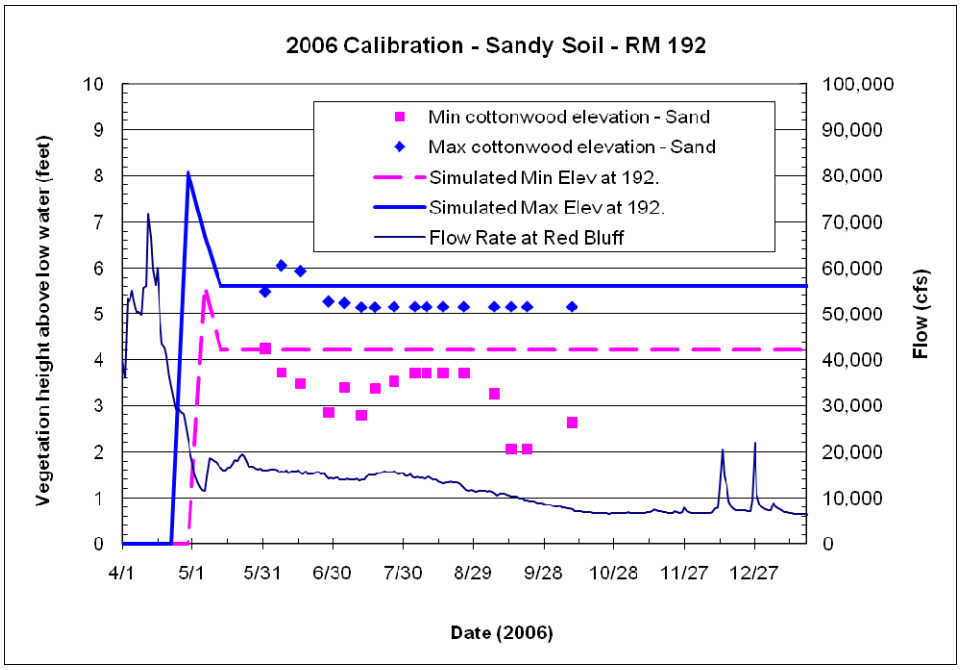

Figure 6-20. Simulated elevations above low water (6,000 cfs) of cottonwood recruitment compared to measured elevations in 2006. Site has sandy soil on a point bar at RM 192.5. Measured and simulated values are compared to daily flow at the Red Bluff CDWR gage.

The model predicts that the cottonwood seedlings desiccate in the gravel sediment around September 23. This date corresponds to the date when measured elevations above low water begin to decrease. Although measured values are not displayed past mid October in figure 6-19, the seedlings eventually all desiccated in the gravel sediment at this location in 2006.

Model results shown in figure 6-20 indicate that the seedlings in the sandy soil survive until the fall, which is in agreement with field measurements. The measured minimum elevation of cottonwood seedlings in the sandy soil decreases on September 14, indicating additional recruitment in September. The model assumes that recruitment cannot occur past July 1 and, therefore, it does not represent the lowering of the minimum elevation on September 14, 2006. The reasoning for decreases in the measured minimum elevation at such a late date in the year is uncertain.

6.7 Calibration of Multiple Vegetation Types with Vegetation Mapping

A second calibration of the SRH-1DV vegetation module was completed using two sets of GIS vegetation mapping (1999 and 2007) for the Sacramento River. Both sets of vegetation mapping include flood plain areas adjacent to the mainstem river in the Ecological Management Zone (EMZ) from RM 144 to RM 245. Changes in vegetated area between 1999 and 2007 mapping were compared to changes in vegetated area computed by SRH-1DV for the same period. This second calibration also served as a verification of Fremont cottonwood (ctw) values, in addition to calibrating the more recently added vegetation types: mixed forest (mxf), Gooding's black willow (gbw), narrow leaf willows (nlw), and invasives (inv).

The 2007 mapping of the Sacramento River by the Geographical Information Center (GIC) at California State University, Chico, is an update of the 1999 vegetation mapping. The methodology for preparing the 2007 mapping update is reported in Nelson, Carlson, and Funza (2008) and in Viers, Hutchinson, and Stouthamer (2009). 2007 alliances or communities of vegetation were reorganized from the 1999 alliances in the California Native Plants Society (CNPS) classification system. Table 6-11 shows the relationship between the two classification systems.

Table 6-11. Comparison of Vegetation Mapping Classification Systems used for the Sacramento River in 1999 and 2007

CNPS 1999		GIC 2007	
Type	**Abbreviation**	**Type**	**Abbreviation**
Berry scrub	BS	Blackberry scrub	BS
Disturbed	D	Not used	
Giant reed	GR	Giant reed	GR
Gravel and sand bars	G		GB
GV cottonwood riparian forest	CF	Fremont cottonwood	CW
GV mixed riparian forest	MF	CA walnut	BW
	MF	CA sycamore	CS
	MF	Box elder	BE
GV riparian scrub	RS	Mixed willow	MW
	RS	Riparian scrub	RS
	RS	Gooding's willow	GW
Herbland cover	HL	CA annuals	CA
	HL	Introduced perennials	PG
Open water	OW	Open Water	OW
Tamarix	TA	Not used	
Valley freshwater marsh	M	Bulrush/cattail	BC
	M	Floating leaf	FL
	M	Ludwigia peploides	LP
Valley oak	VO	Valley oak	VO

An evaluation of the second mapping effort and the ability to detect change between the two mapping sets is discussed in three papers: Viers and Hutchinson (2008a), Viers and Hutchinson (2008b), and Viers, Hutchinson, and Stouthamer (2009), available from the Sacramento River Web site, http://www.sacramentoriver.org/sacmon/. Conclusions from this evaluation were that the mapping efforts were useful, but problems exist with accuracy in some categories when comparing between the two years. Some difference may result from a change in the classification structure, and others may be due to typical problems with photos including distortion, angle, and clarity when using digital methods to classify vegetation types:

> *. . . overall association between map classifications was statistically marginal with an overall accuracy rate of 39% between the two mapping efforts. We expect divergence, precisely because of landscape change in the intervening period of time: however there is clear class confusion between the two data sets. (Viers and Hutchinson [2008b])*

Findings in Viers and Hutchinson (2008c) include:

> *Cottonwood: Some 50% of the points which occurred in Cottonwood in 1999 remained cottonwood in 2007. However, of the points considered cottonwood in 2007, only 26% were considered cottonwood in 1999, with the majority (49)% occurring in mixed forest. . . .*
>
> *Valley Oak: . . . for valley oak in the 2007 map, 62% of random points were considered mixed forest in 1999, indicating a possible underestimate in 1999. . .*
>
> *Giant Reed: There is substantial confusion between these classes across time. In effect, only 8% of giant reed remained giant reed between the two time periods, , ,*
>
> *. . . the other problematic vegetation types are covered in Viers and Hutchinson. These are primarily the overarching classes of Mixed Riparian Forest (MF) and Riparian Scrub (RS). Mixed Riparian Forest included box elder, black walnut, and California sycamore, among many types. Riparian Scrub includes a little of everything, such as willow, blackberry, and elderberry.*

Most of the uncertainty appears to stem from forest designations, including cottonwood and valley oak, and efforts to aggregate woody species. Viers and Hutchinson (2008b) comment: "In principle, all forested types could be lumped to evaluate change in forest cover with high confidence." Viers and Hutchinson also caution on direct comparisons of riparian scrub and its aggregation and on accuracy of giant reed comparisons, although they thought the trends appeared reasonable. These recommendations impact the selection of classifications for a comparison between mapped and modeled results, and they help to explain uncertainties in results as described in the succeeding sections.

6.7.1 Methodology for Computing Mapping Values

Vegetation mapping from 1999 and 2007 were overlain in ArcGIS 9,2 ArcMap3 version 9.3.1. In most cases, the 1999 mapping had more coverage because it included agricultural lands. Polygons outside the 2007 coverage were trimmed from the 1999 coverage to produce similar areas. Some differences between the coverages remain because polygons were only trimmed if there was a large area outside the limits of the 2007 coverage (figure 6-21).

Areas identified as restoration plots in the 2007 coverage were also removed for this calibration. Many, if not all, of these sites were identified as agricultural lands in the 1999 mapping, and changes to areas that are restoration land in 2007 may have resulted from management practices. The current version of SRH-1DV

[2] ArcGIS is an authoring system for data, maps, globes, and models.
[3] ArcMap is a program used primarily to view, edit, create, and analyze geospatial data.

links river flow and river sediment conditions but does not replicate management actions of mechanically removing vegetation or irrigating vegetation.

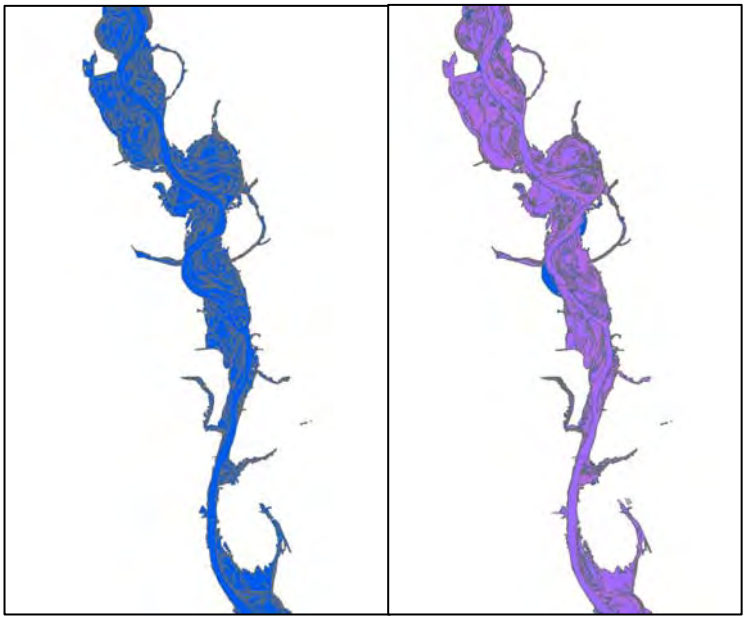

Figure 6-21. Illustration of trimming GIS coverage to match land area. 2007 mapping on left (blue) is overlying 1999 coverage on right (overlap is lavender).

Acreage for each polygon was computed in attribute tables from the 1999 layer and the 2007 layer. Polygon acreage for each year was also summed by classification. Classifications were then reorganized to be consistent between mapping years and to be comparable to model results.

6.7.2 Methodology for Computing Modeled Values

Vegetation within the model SRH-1DV was organized by vegetation type, which could be a single species or a group of species with similar establishment, growth, and mortality characteristics. There were eight types selected to represent conditions in the floodplain of the Sacramento River: Fremont cottonwood (ctw), mixed forest (mxf), Gooding's black willow (gbw), narrow leaf willow (nlw), grass (herb), invasive (inv), cultivated land (ag), and a designation of no grow (nog).

Multiple types can be assigned to a single cross section point with the exception of a no grow designation (nogr), which excludes other vegetation types at a point. The 1999 vegetation classifications were translated to individual points in a cross section by combining vegetation types and plant densities at cross section points within a polygon. For example, a point in a mapped riparian scrub polygon may

be assigned as just grass, grass and a narrow leaf willow, just narrow leaf willow, or have no assigned vegetation.

The primary measure of vegetation in the model is vegetated area for each vegetation type. Vegetated area is computed for each point with a plant. Width of vegetated area is determined as half the distance between the adjacent points on the left and right. Length of the vegetated area is half the distance upstream to the next cross section plus half the distance downstream to the next cross section. For example, a point on a cross section that is spaced 20 feet from the adjacent point on river right and 10 feet from the adjacent point on river left has a width of 15 feet. Assuming the upstream cross section is 300 feet distant and the downstream cross section is 100 feet, the length of vegetated area is 200 feet. Vegetated area of narrow leaf willow defined by a plant on that point is 3,000 square feet.

If a cottonwood seedling is also growing at the same point in the model, 3,000 square feet are also attributed to cottonwood vegetated area. As a result of this double-counting, a summation of vegetated area from all vegetation types can be a larger value than actual channel area.

Because of the large amount of output produced, predicted vegetated area was recorded on only 3 days for every year (1 day each in October, February, and June). The dates are equally spaced (365.25/3) and represent the condition of vegetation in the winter, late spring and at the end of the growth season. An average value was computed for the 3 days and used for a comparison between years. Predictions of vegetated area will not always match the mapped area. For more direct comparison between the predicted and mapped changes in vegetated area, the average value for year 8 was divided by the average value for year 1, and the ratio from the model simulations were compared to the ratio from vegetation mapping.

6.7.3 Results of Multiple Vegetation Calibration

Polygons from the 1999 mapping were input to SRH-1DV to describe existing conditions, and in this calibration, the difference between 1999 and 2007 polygons from mapping are compared to the differences in vegetation output by SRH-1DV in the first year and 8th year of the model simulation as shown in table 6-12.

Three vegetation types: grass (herb), cultivated and managed lands (ag), and developed lands (nogr) are not presented or used for calibration. Grass (herb) germination and growth are not linked to the water table in the SRH-1DV model so that natural processes that cover both riparian and upland bare ground can be represented. The remaining two land categories in the vegetation module, cultivated and managed areas (ag) and a development (nogr) designation, are used similarly to remove non-applicable lands from vegetation growth computations.

As applied in these simulations, it is not productive or defendable to calibrate the three categories of grass, managed lands, or developed lands.

Table 6-12. Comparison of Changes in Area Simulated by Vegetation Modeling to Changes in Area Measured From Vegetation Mapping Between 1999 (Year 1) and 2007 (Year 8). Shaded columns are consolidations of previous categories, tan cells are comparable values for calibration.

Model	Year	ctw	mxf	Forests	gbw	nlw	Ripar-ian Vege-tation	Ripar-ian Scrub	Ripar-ian	Giant Reed or Invasive
Model (sand)	Year 1 average	5,295	8,768	14,063	2,226	1,355			3,580	1
	Year 8 average	6,109	8,018	14,127	2,693	2,136			4,829	3
	Year 1/ Year8	1.15	0.91	1.00	1.21	1.58			1.35	2.63
Mapping	Year 1 average	3,971	7,187	11,158			2,176	2,145	4,322	77
	Year 8 average	5,020	5,972	10,993			2,017	4,018	6,036	131
	Year 1/ Year 8	1.26	0.83	0.99			0.93	1.87	1.40	1.71

6.7.3.1 Cottonwood and Other Forests

Mapping results show a large increase in cottonwood and a decrease in mixed forests from 1999 to 2007; however, a caution against aggregating woody species accompanies this information. When forest areas are combined as recommended by Viers and Hutchinson (2008b), the results indicate no change in forest cover. Model results are shown for sandy soils. Values for sandy soils were used to validate cottonwood values and to calibrate mixed forest values (mxf), Gooding's black willow (gbw), and narrow leaf willow (nlw). Predicted increases in cottonwood are smaller than mapped values; however, most cottonwood parameters were previously calibrated to field data and not adjusted here. Mixed forest predictions remain the same, similar to mapped values. The simulated change for all woody species is an increase of 6 percent. The compared values are shaded tan.

6.7.3.2 Riparian

Mapped riparian areas are classified as riparian scrub and riparian vegetation or mixed willow. Modeled riparian vegetation is classified as Gooding's black willow (gbw) and narrow leaf willow (nlw). The combined categories of riparian are intended to be equivalent and comparable between the mapped and simulated values, as shown in tan in table 6-12. Gooding's black willow combined with narrow leaf willow is used to represent the combined mapping classifications of riparian scrub and riparian vegetation. Mapping results have large increases in

riparian scrub and a decrease in riparian vegetation. The combined mapping results (as recommended by Viers and Hutchinson [2008b]) have a 40-percent increase, similar to the combined modeling results that predict a 36-percent increase for riparian lands.

6.7.3.3 Invasive Vegetation

Map results and simulation results are similar for the mapped classification of giant reed and the modeled classification of invasives (predominantly giant reed) with both methods predicting a 71- to 81-percent increase. There is some uncertainty, however, associated with the area of coverage. Giant reed coverage from mapping studies has more than 10 times the model area of invasives in the first year. Ratios of year 8 to year 1 are very similar; however, the discrepancy in land area is an aspect to be further investigated.

6.7.3.4 Conclusions

Narrow leaf willow and Gooding's black willow appear to be successful indicators of riparian lands in model simulations. Model simulations of cottonwood forest and mixed forests also compare well with mapped results when combined, but it is difficult to confirm cottonwood model predictions with the 1999 and 2007 data sets due to the uncertainties noted about mapped cottonwood areas. Results of giant reed calibration could be described as encouraging; however, additional studies on the simulation of giant reed are recommended. Finally, a comparison of spatial distributions of model plant species and distribution of mapped communities, although not a one-to-one comparison, may be a beneficial next step in verifying model results.

6.8 Multiple Vegetation Application to Sacramento River

After the flow and ground water calibration, the sediment calibration, the cottonwood calibration and the calibration of the multiple vegetation types, the Sacramento model simulation from 2000 to 2007 (multiple vegetation types) was analyzed for additional insights on the patterns of vegetation change. A sand soil assumption was used for the full length of the study area in this analysis. The model simulation provided detailed information on changes in vegetation coverage that cannot be deduced from the two sets of vegetation mapping. For example, mapping results inform on changes in areal extent of vegetation classifications and the location of these changes. Modeling provides the same information on vegetation types but also tracks plant ages and the type, age and area of plant mortalities. Also the simulation can be used to predict the specific time when changes in vegetation occur, within the 8-year time period of this mapping study.

6.8.1 Vegetated Area From a Multiple Vegetation Simulation

Vegetated area composed of cottonwood (ctw), mixed forest (mxt), Gooding's black willow (gbw), narrow leaf willow (nlw), and riparian invasive plants (inv) is generally increasing in response to the 8 years of hydrologic regime simulated (figure 6-22), but the R2 value is poor.

Mixed forest and cottonwood account for much of the vegetation in a representation of both existing and new vegetation with respect to river mile location (figure 6-23). Acres of narrow leaf willow and Gooding's black willow are similar.

Vegetation divisions based on individual vegetation types with more than 50 acres per cross section are listed in table 6-13. More cottonwood is available in the downstream end of Reach 1, the upstream end of Reach 2, the upstream end of Reach 6, and throughout Reach 7. Based on a definition of less than 50 acres per vegetation type, there is no dominant vegetation type or preponderance of vegetation in Reaches 1, 3, 5 and 8. A subarea of Reach 1 is the exception, where there are 90 acres of new or existing cottonwood at RM 146. Locations of high acreage can represent an established colony of mature plants or can represent locations where younger plants have recently established. More detail can be determined by looking at plant age in addition to plant type. Figure 6-23 provides insight into locations that favor one plant type over another or locations that better support all plants tracked by the model.

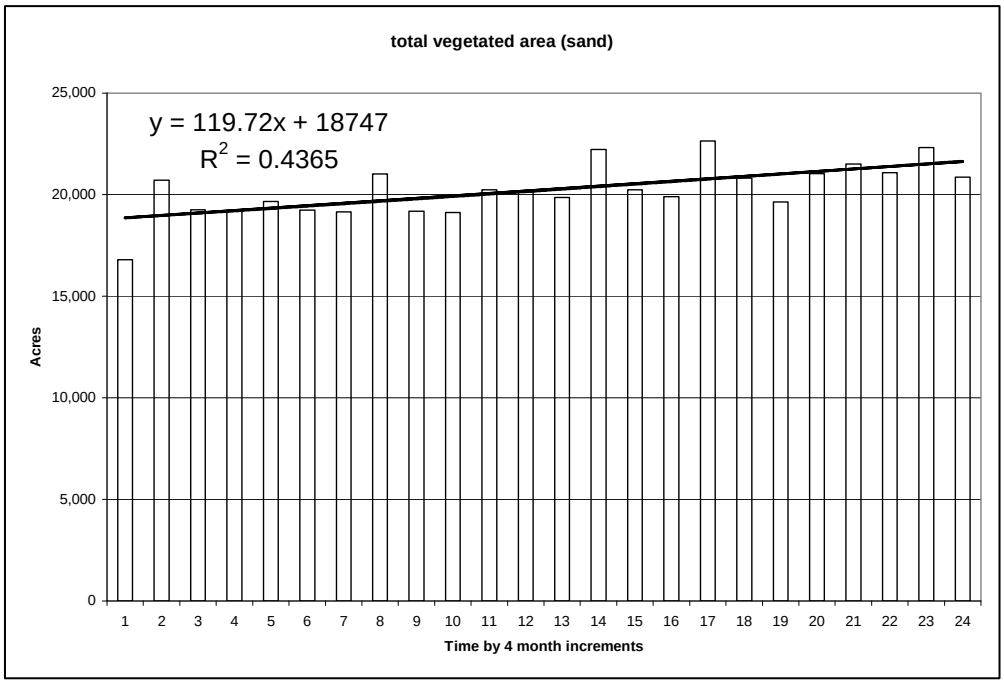

Figure 6-22. Total vegetated area computed by SRH-1DV every 4 months (on 1 day in October, February, and June) for 8 years.

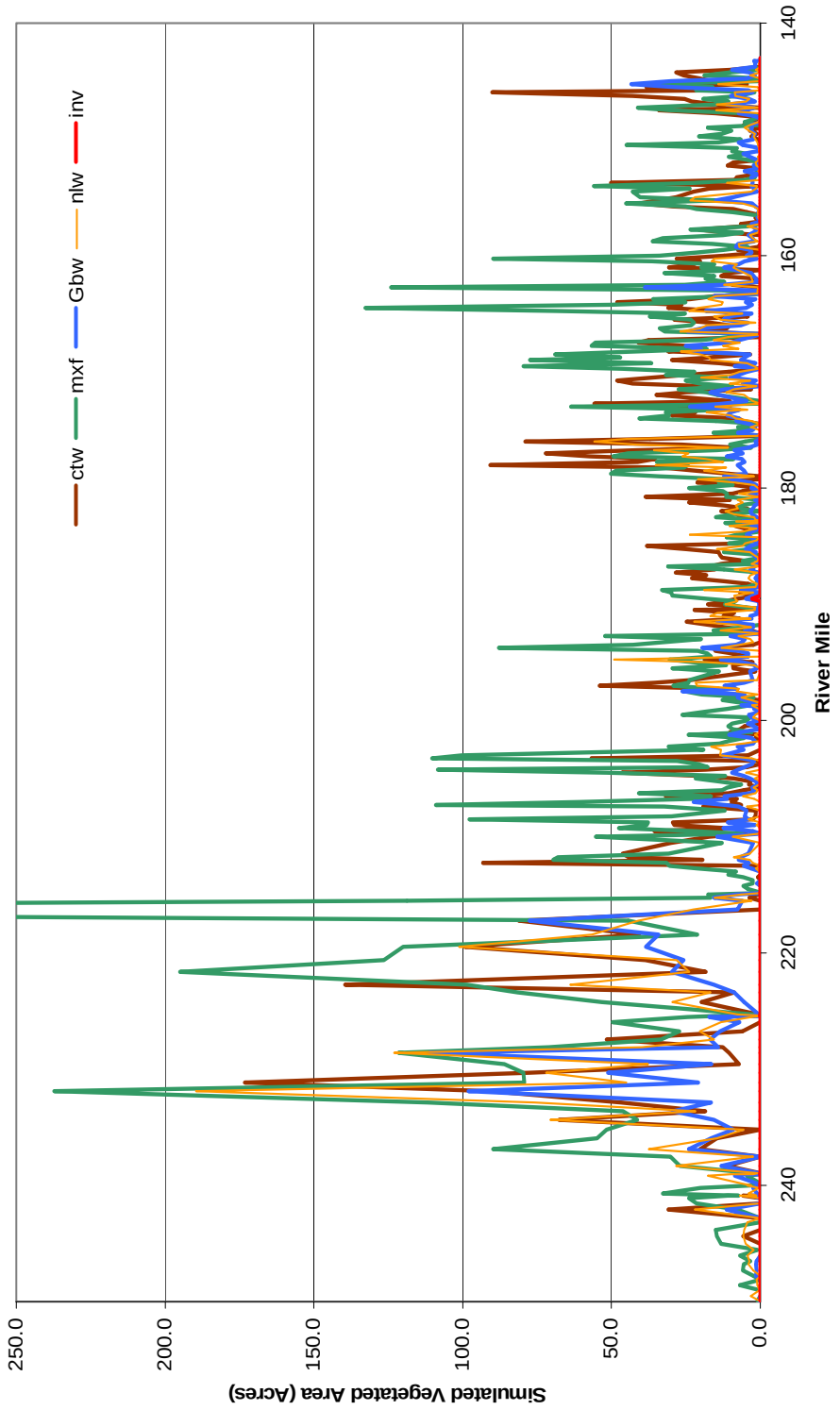

Figure 6-23. Existing vegetation by cross section location in June 2007 (year 8): cottonwood (brown), mixed forest (green), Gooding's black willow (blue), narrow leaf willow (orange), and invasive species (red); as predicted by SRH-1DV.

Table 6-13. Vegetation Divisions Based on Individual Vegetation Types with More than 50 Acres per Cross Section

RM of vegetation divisions	Vegetation Reach	Vegetation Coverage (>50 acres per type)
143 to 160	1	No (exception: RM 146)
160 to 178	2	Yes
178 to 193	3	No
193 to 197	4	Yes
197 to 203	5	No
203 to 215	6	Yes (exception: RM 212 to RM 215)
215 to 237	7	Yes (division with most vegetation)
237 to 250	8	No

Narrow leaf willow and riparian invasive plants have relatively shallow root systems that commonly restrict the plants to narrow strips of coverage along the banks of the river. Acreage is low, except at locations of complex planform and meander migration bends where wider flood plains and low benches can be colonized. Invasive plants also appear to establish at locations where the channel is shallow and less erosive, and plants are not readily undercut. Figure 6-24 shows giant reed locations from 2007 vegetation mapping. Invasive plants like giant reed are difficult to erode unless undercut. The scour parameters for this plant would normally be higher than willow (more resistant to velocity), but are set at lower values than willow to represent plant removal resulting from secondary, 3D scour patterns that can undercut these shallow rooted plants.

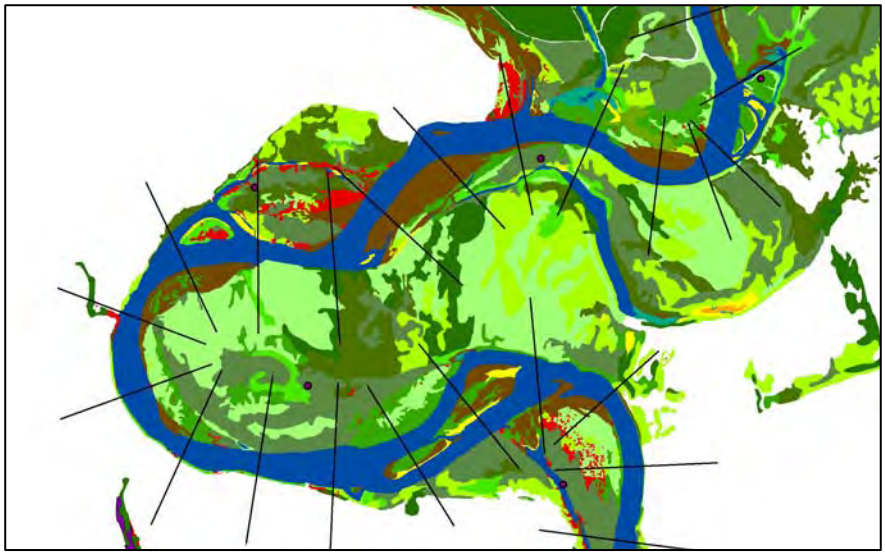

Figure 6-24. 2007 vegetation mapping at RM 186 to RM190. Giant reed (red) are located in flood plain at complex channels of near migrating bends.

6.8.2 Plant Germination

Figures 6-25 and 6-26 present the total acres of new vegetation (seedlings 0 to 1 year). Seedlings for all vegetation types are compared between October of year 2 and October of year 8. Little new vegetation established between RM 250 and RM 240, consistent with results shown in figure 6-23. Vegetation acreage increased between RM 240 and RM 235 and remained high downstream to RM 205. Little vegetated area was predicted between RM 180 and RM 205. Acreage of newly established vegetation was predicted to increase again between RM 180 and RM 160. Locations with more vegetation are normally found at river sites with more complexity. About half as much new vegetation is predicted in year 8 (figure 6-26), compared to year 2 (figure 6-25), but there could be more 1- and 3-year-old vegetation from the high peak flows that occurred in previous years.

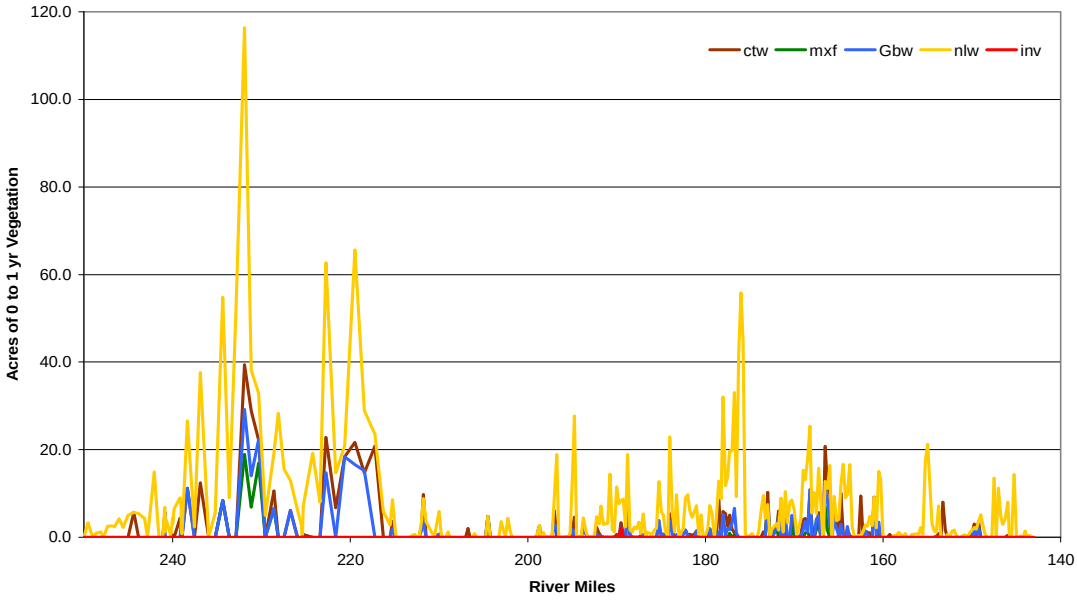

Figure 6-25. New plants, 0 to 1 year, by river mile and vegetation type in October 2000, year 2.

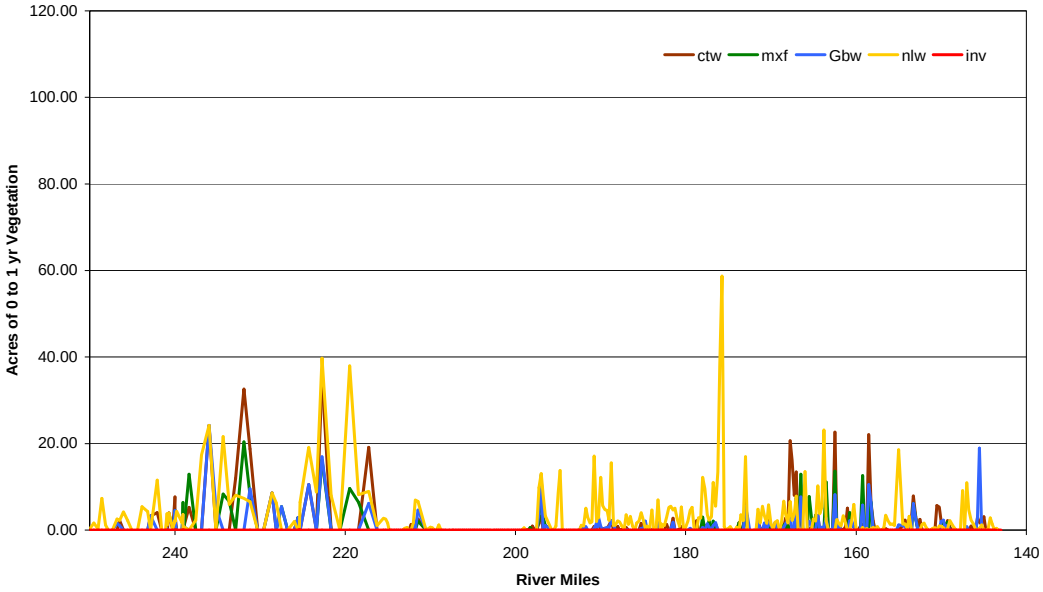

Figure 6-26. New plants, 0 to 1 year, by river mile and vegetation type in October 2007, year 8.

6.8.3 Hydrologic Regime and Desiccation

A continuous base flow, high peak flows that push water onto overbank areas, slow drawdown rates allowing root growth to match the rate of ground water decline, back-to-back peaks increasing overbank wetting, and repeat peaks during seed dispersal windows are desirable flow regime characteristics that promote vegetation. The hydrologic regimes from SRH-1DV calibration runs are shown in figure 6-27. The smallest peak flows occur in 2007 and 2000, and the largest peaks occur in the years 2005 and 2006. Multiple peaks in 2006 re-wet low overbank areas.

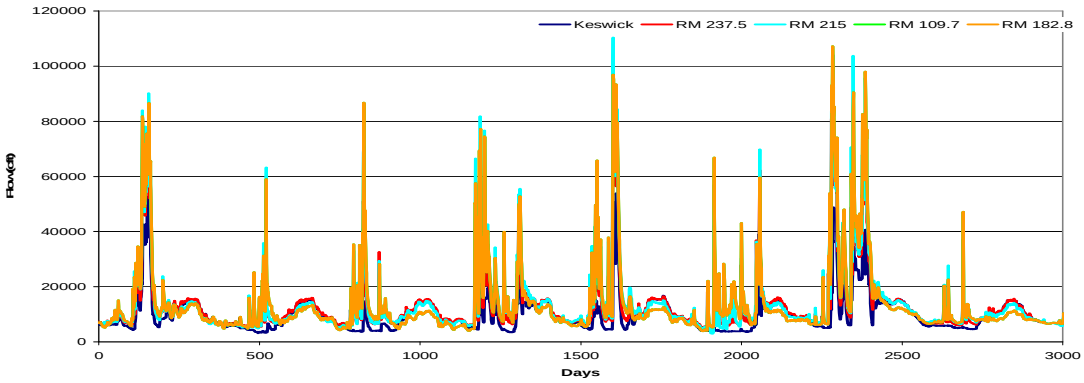

Figure 6-27. Daily flows at 5 stations for an 8-year period as input to SRH-1DV.

Following the flow regime chart is a chart of total acres of plants removed by desiccation (figure 6-28). The pattern for acres removed by desiccation is similar to the presence of total vegetated acres along the river (figure 6-23). River locations characterized by the greatest predicted vegetated area also have more acres of plants removed by desiccation. A large value for acres of plants removed can represent the removal of plants from a large area during a single flow event or the repeated removal of a small coverage throughout the study period.

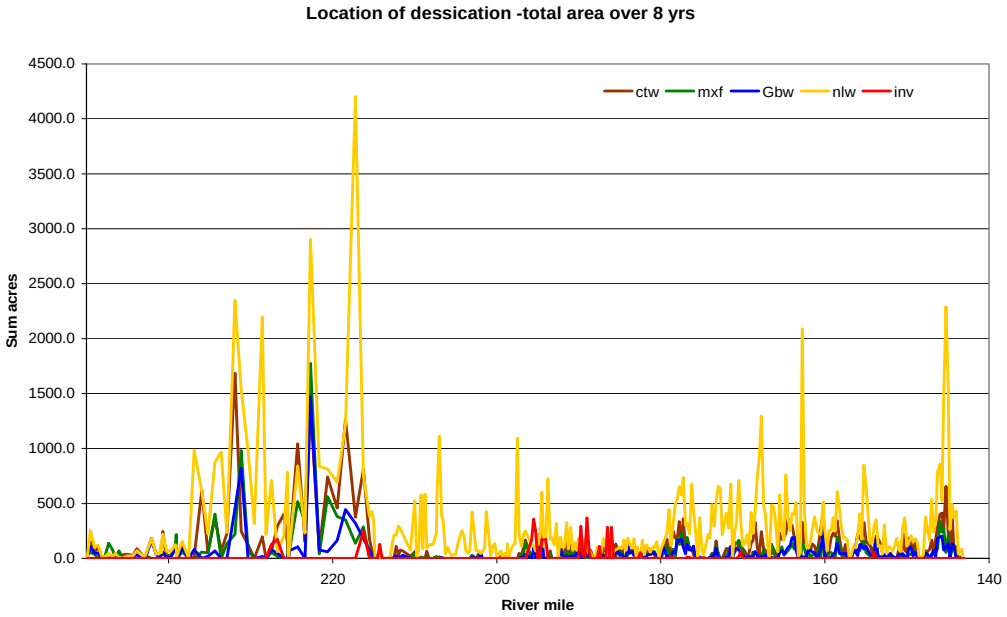

Figure 6-28. Total acres of desiccated plants for 8 years of simulation by river mile and vegetation type.

Desiccation removes more narrow leaf willow (nlw) plants than other vegetation types in this simulation. Narrow leaf willow could be susceptible to desiccation due to a shallow root system that can hinder access to ground water. A large tolerance assigned to narrow leaf willow for seed germination near the water line and a long germination season to replicate the lateral spread of plants by root extension and propagules could also contribute to a high value for mortality. A large quantity of narrow leaf willows are removed upstream of RM 215. Flow regimes for two gages upstream of this location are shown in figure 6-29.

Desiccation over time for the same period is also presented in figure 6-29. Narrow leaf willow (nlw), cottonwood (ctw), mixed forest, and Gooding's black willow (gbw) are predicted to be removed during a dry period in 2004 that follows a peak flow in the winter of 2004-2005 that did not exceed 40,000 cfs .A similar flow period in 2001 caused an increase in narrow leaf willow desiccation but did not result in an increase in predicted desiccation of other vegetation types.

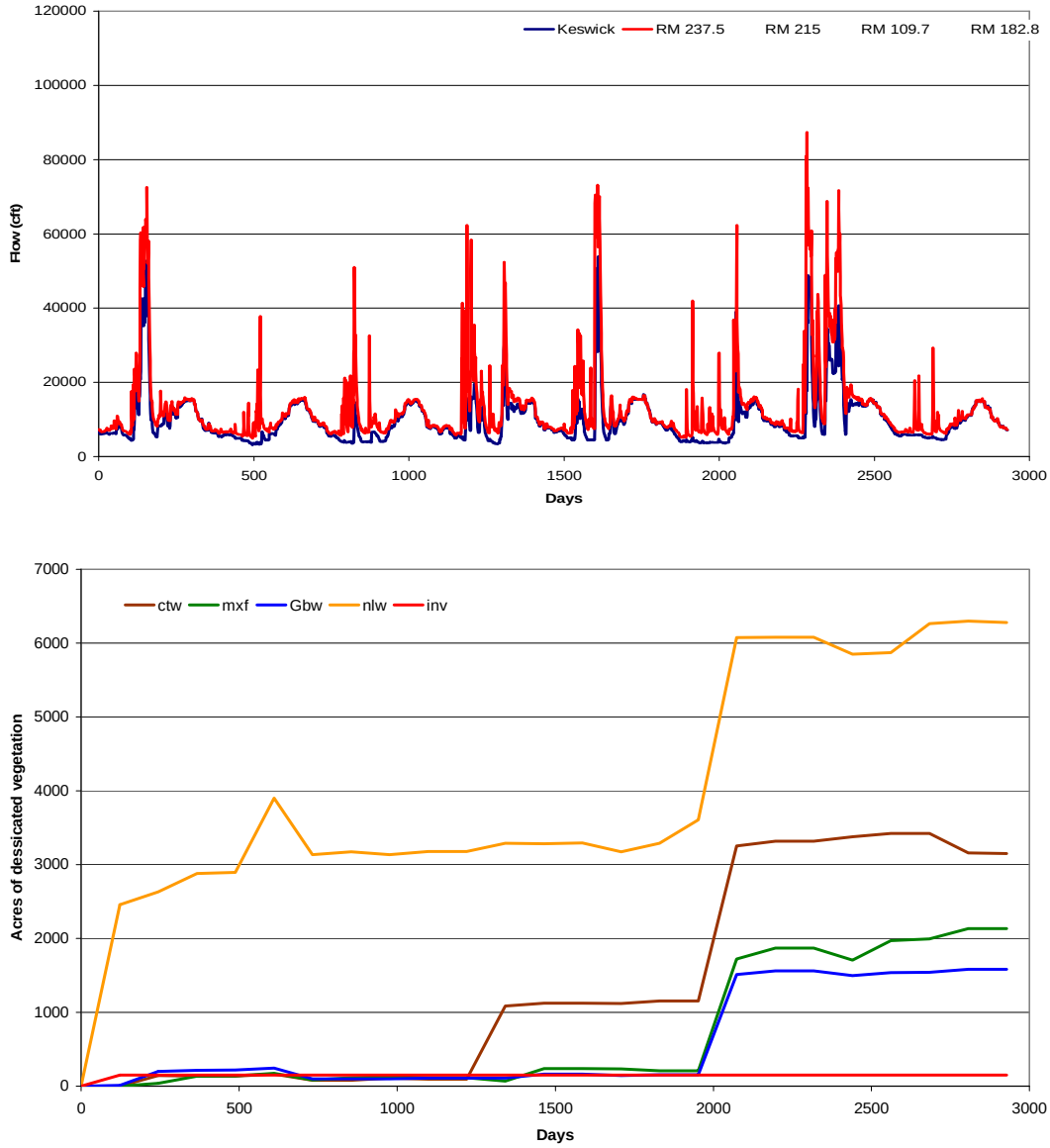

Figure 6-29. Flow regime at Keswick and at RM 237.6 shown with total acres of desiccation for each vegetation type presented over time for 8 years of simulation. The upper chart shows the hydrologic regime (gage data) and the lower chart shows the acres of desiccation.

6.8.4 Inundation

Flow regimes for the same two gages from figure 6-29 are shown a second time in figure 6-30 above a figure of inundation mortality over time. Inundation mortality is predicted to occur following every annual peak flow, but plant removal for each plant type is delayed for the period of inundation required to impact the plant. Some plants are more tolerant of submergence and can survive for a longer period. Narrow leaf willow (nlw) and riparian invasive plants (inv)

were characterized as having the highest tolerance for inundation, followed by Gooding's black willow (gbw) and cottonwood (ctw), while mixed forest (mxf) was assigned the least tolerance. Inundation tolerance for different plant types and ages were assigned based on guidance from papers including Auchincloss et al., 2010, Hosner (1958), (Neuman et al. 1996), Stromberg et al. (1993) and Yin et al. (1994).

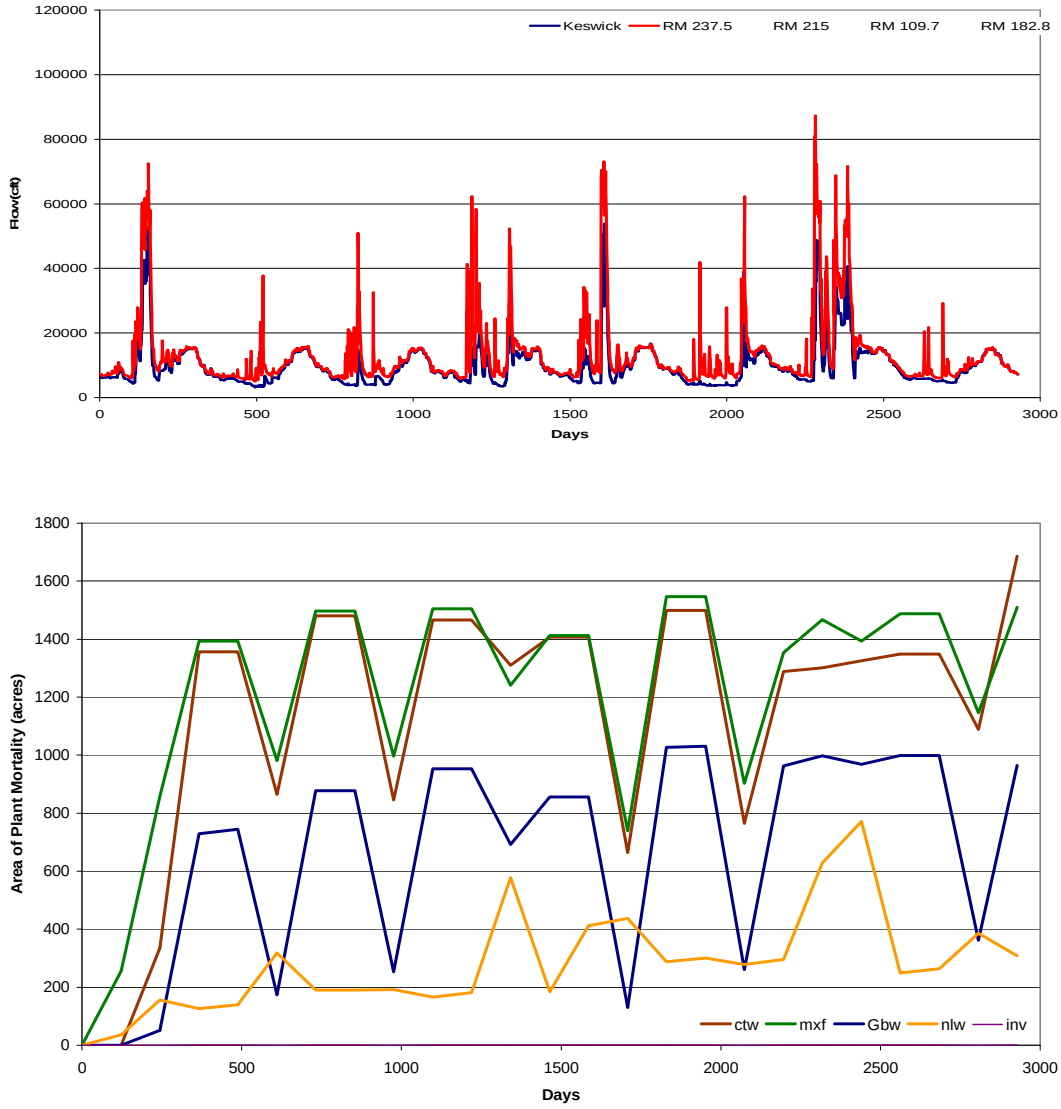

Figure 6-30. Total plant mortality from inundation with respect to time, shown with Figure 6-29 and 2 flow regimes (gage at Keswick and RM 237.5).

6.8.5 Maximum Extent of Invasive Riparian Plants

Invasive plants are the only vegetation type in the model that limit colonization to downstream propagation. Invasive vegetation was assumed to germinate primarily through waterborne propagules, released from upstream locations where older plants had already established. Acres of simulated riparian invasive plants are low in comparison to mapped acres of giant reed. Invasive coverage commonly spreads rapidly. A second simulation was analyzed to explore the maximum extent of colonization by invasive plants in the future and to assess impacts to other vegetation types. Riparian invasive plants were allowed to germinate from a presumed unlimited supply of seed or propagules, instead of restricting the supply to downstream spread during peak flow events and for specified distances downstream. Figure 6-31 shows vegetated area by vegetation type for October 2007 (8th year) when there is an unlimited availability of invasive plant propagules to establish new plants.

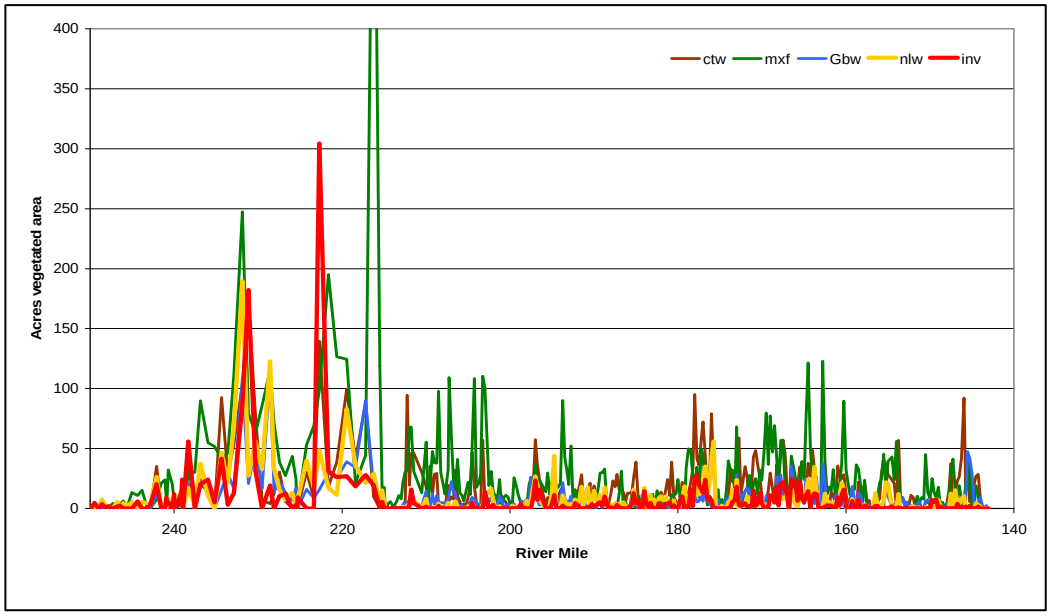

Figure 6-31. SRH-1DV simulation from October 2007 (8th year) with unlimited availability of seed and propagules where germination of invasive plants is not restricted to downstream locations. Peak not shown is over 700 acres.

Results (table 6-14) suggest that invasives can colonize an estimated 1,926 acres under the 8-year flow regime when there is an abundant supply of propagules to initiate plant establishment. Approximately 563 acres colonized by the invasive plants, were not colonized by any plants until the propagule supply for invasive plants was unlimited. Presumably, the 563 acres of newly colonized lands are too wet to support other vegetation types. The remaining 1,363 acres (1,926 – 563), colonized by invasives under a scenario of unlimited supply of propagules, are lands that previously supported other vegetation types. The invasive plants were

able to out-compete native plants at these locations. By the 8th year of the simulation, invasive plants replace cottonwood plants on 300 acres, replace mixed forest plants on 180 acres, replace Gooding's black willow on 430 acres, and replace narrow leaf willow on 450 acres.

Table 6-14 A Comparison of Vegetation Coverage Under Two Scenarios of Invasive Plant Establishment

	Cottonwood	Mixed Forest	Gooding's Black Willow	Narrow Leaf Willow	Invasive	Total
	ctw	mxf	gbw	nlw	inv	
Unlimited Propagules at all Locations						
Year 1 average	5,246	9,023	2,360	2,303	1,211	20,143
Year 8 average	5,663	8,933	2,810	2,645	1,929	21,980
Year 8/Year 1	1.08	0.99	1.19	1.15	1.59	1.09
Propagules Limited to Locations Downstream of Existing Plants						
Year 1 average	5,244	9,024	2,358	2,300	2	18,928
Year 8 average	5,961	9,113	3,242	3,098	3	21,417
Year 8/Year 1	1.14	1.01	1.37	1.35	1.81	1.13
Difference in Year 8 average values	-298	-180	-432	-453	-1,926	-563

6.9 Summary and Conclusions

A 1D flow and sediment transport model, (SRH-1D), was expanded to incorporate and assess riparian vegetation in the flood plain. SRH-1DV includes a ground water and vegetation module linking ground water fluctuations (in response to riverflow) and the growth and removal of vegetation to geomorphic processes of river hydraulics and sediment transport. Representations of vegetation germination, growth, and removal were aided by development of the RHEM desiccation model for cottonwood, laboratory studies of cottonwood desiccation by SEI (Chapter 5), and inundation studies of cottonwood by SEI.

Modeled flow was calibrated to the water surface elevation between gaging stations, and ground water was calibrated to well data. Sediment transport was then calibrated to gravel bedload measurements at the Hamilton Bridge gaging station. Following these calibrations, cottonwood germination, growth, and removal were simulated for the Sacramento River from RM 300 to RM 150, including Red Bluff to Colusa. Data from two field studies (2005 and 2006) of cottonwood growth on sand bars at three sites were used to calibrate the cottonwood model. In a second round of simulations, the Sacramento SRH-1DV model was expanded to multiple vegetation types. Cottonwood vegetation was

validated using repeat vegetation mapping from 1999 and 2007 of the Red Bluff to Colusa Reach (RM 250 to RM 143). Four additional vegetation types: mixed forest, Gooding's black willow, narrow leaf willow, and riparian invasive plants were calibrated with the 1999 and 2007 vegetation mapping. At the end of these calibrations, the SRH-1DV model with multiple vegetation types was applied to assess vegetation growth and mortality patterns in the Sacramento River flood plain between 1999 and 2007.

Through initial model runs presented in this report, SRH-1DVis proven to be an effective method of assessing the linked physical river processes and riparian vegetation growth in the Sacramento River. Development of the model increases understanding of concepts and links between vegetation growth and physical river processes. A calibration of flow, ground water, and sediment transport values, two calibration studies of model vegetation parameters, and a validation of cottonwood parameters increase confidence in model predictions. Applying the SRH-1DV model to the Sacramento River for assessment of future alternatives can aid environmental studies on effective flow management.

References

References

Ackerman, C.T. 2005. HEC-GeoRAS, an Extension for Support of HEC-RAS Using ArcGIS, User Manual, Version 4. CPD-83. U.S. Army Corps of Engineers, Hydrologic Engineering Center, HEC, Davis, California. http://www.hec.usace.army.mil. September.

Adiku, S.G.K., R.D. Braddock, and C.W. Rose. 1996. Modelling the Effect of Varying Soil Water on Root Growth Dynamics of Annual Crops. *Plant and Soil* 185:125-135.

Amlin, N.M., and S.B. Rood. 2002. Comparative Tolerances of Riparian Willows and Cottonwoods to Water Table Decline. *Wetlands* 22(2): 338-346.

Andrews, E.D. 2000. Bed Material Transport in the Virgin River, Utah. *Water Resources Research* 36:585-596.

Aquaveo LLC. 2010. XMS Wiki. http://xmswiki.com/xms/Main_Page. Accessed June 18, 2010.

Auchincloss, L.C., J.H. Richards, C. Young, and M. Tansey. 2010. Survival of Fremont Cottonwood (*Populus Fremontii)* Seedlings is Dependent on Depth, Temperature and Duration of Inundation. Draft.

Army Corps of Engineers (see USACE)

Bartholomeus, R.P., J.M. Witte, P.M. Van Bodegom, J.C. Van Dam, R. Aerts. 2008. Critical Soil Conditions for Oxygen Stress to Plant Roots: Substituting the Feddes-Function by a Process-Based Model. *Journal of Hydrology* 360(1-4):147-165.

Borman, M., and L. Larson. 2002. Cotton Establishment, Survival, and Stand Characteristics. Oregon State University Extension Service, EM 8800.

Brunner, G.W. 2002a. HEC-RAS, River Analysis System Hydraulic Reference Manual, US Army Corps of Engineers, Hydraulic Engineering Center (USACE-HEC).

Brunner, G.W. 2002b. HEC-RAS, River Analysis System User's Manual, U.S. Army Corps of Engineers, Hydraulic Engineering Center (USACE-HEC).

Buffington, J.M, and D.R. Montgomery. 1997. A Systematic Analysis of Eight Decades of Incipient Motion Studies, with Special Reference to Gravel-Bedded Rivers. *Water Resources Research* 33(8):1993-2029.

Bunte, K., S.R. Abt. 2001. Sampling Surface and Subsurface Particle-Size Distributions in Wadable Gravel and Cobble-Bed Streams for Analyses in Sediment Transport, Hydraulics and Streambed Monitoring. U.S. Department of Agriculture, Forest Service, Rocky Mountain Research Station, General Technical Report RMRS-GTR-74.

Bureau of Reclamation (see Reclamation)

California Department of Water Resources (see CDWR)

CDWR. 1980. Upper Sacramento Spawning Gravel Study. Northern District Department of Water Resources, California.

CDWR. 1981. Sacramento Valley Westside Tributary Watersheds Erosion Study, Reeds Creek Watershed. State of California. The Resources Agency, Department of Water Resources, Northern District. October.

CDWR. 1984. Middle Sacramento River Spawning Gravel Study, District Report. Northern District. August.

CDWR. 1985. Sacramento Spawning Gravel Studies. Northern District Department of Water Resources, California.

CDWR. 1991. Dataset for Sacramento River, SRCA, DWR Northern District, reaches 1-4 . Northern District Metadata. Sacramento River GIS. Contact: Alison M. Groom - alisong@water.ca.gov, 2440 Main Street, Red Bluff, California, 96080. Phone: (530) 528-7433; fax: (530) 529-7322.

CDWR. 1994. Use of Alternative Gravel Sources for Fishery Restoration and Riparian Habitat Enhancement, Shasta and Tehama Counties, California. State of California. The Resources Agency, Department of Water Resources, Northern District. August.

CDWR. 2005. Cottonwood Seedling Monitoring During 2004 and 2005 Along the Sacramento River, California. Draft Memorandum Report dated December, 30 2005. Northern District Department of Water Resources, California.

Cederborg, M. 2003. Hydrological Requirements for Seedling Establishment of Riparian Cottonwoods (*Populus Fremontii*) Along the Sacramento River, California. Unpublished Thesis, California State University, Chico, California.

Church, M., D.G. McLean, and J.F. Walcott. 1987. River Bed Gravels: Sampling and Analysis. *Sediment Transport in Gravel-Bed Rivers.* C.R. Thorne, J.C. Bathurst, and R.D. Hey (eds.). John Wiley and Sons, Chichester, p. 43-88.

Corps of Engineers (see USACE).

Crosato, A. 2007. Effects of Smoothing and Regridding in Numerical Meander Migration Models. *Water Resources Research,* Vol. 43, Issue 1, January 2007, article number W01401.

Department of Water Resources (see CDWR).

Engelund, F. 1974. Flow and Bed Topography in Channel Bends. *ASCE Journal Hydraulics Division,* 100(11):1631-1648.

ESRI. 2005. Arc Hydro Tools Overview, Version 1.1. www.esri.com. July.

Feddes, R.A., P.J. Kowalik, and H. Zaradny. 1978. Simulation of Field Water Use and Crop Yield. Halsted Press, New York. 188 pp.

Freeze, R.A., and J.A. Cherry. 1979. Groundwater. Prentice Hall.

Graham Matthews and Associates. 2003. Hydrology, Geomorphology, and Historic Channel Changes of Lower Cottonwood Creek, Shasta and Tehama Counties, California.

Han, Q. 1980. A Study on the Non-equilibrium Transportation of Suspended Load. Proceedings of the International Symposium on River Sedimentation, Beijing, China, pp. 793–802 (in Chinese).

Haschenburger, J., E. Voyde, and S. Rice. 2005. An Experimental Assessment of Bulk Sediment Sampling Criteria for Gravel-Bed Rivers. Proceedings of 6th Gravel Bed Rivers Conferences, September 5-9, 2005, Austria.

Henderson, Adam. 2006. Staff Environmental Scientist with the Department of Water Resources Northern Region Office in Red Bluff, California. California Department of Water Resources. Personal Communication).

Horton, J.L., T.E. Kolb, and S.C. Hart. 2001. Physiological Response to Groundwater Depth Varies Among Species and With River Flow Regulation. *Ecological Application* 11(14):1046-1059.

Hosner, J.F. 1958. The Effects of Complete Inundation Upon Seedlings of Six Bottomland Tree Species. *Ecology* 39:371-373.

Huang, J., and B.P. Greimann. 2007. User's Manual for GSTAR-1D 2.0 (Generalized Sediment Transport for Alluvial Rivers – One Dimensional Version 2.0). Bureau of Reclamation, Technical Service Center, April 2007.

Idaho National Engineering and Environmental Laboratory (INEEL). 2001. Central Facilities Area Sewage Treatment Plant Drainfield (CFA-08) Protective Cover Infiltration Study, Appendix D. Project file No. 021048.

Johannesson, H., and G. Parker. 1989. Linear Theory of River Meanders. *Water Resources Monograph No. 12: River Meandering.* S. Ikeda and G. Parker (eds.). American Geophysical Union, Washington, DC, pp. 181-213.

Jones, B.L., N.L. Hawley, and J.R. Crippen. 1972. Sediment Transport in the Western Tributaries of the Sacramento River, California. Geological Survey Water-Supply Paper 1798-J. Prepared in Cooperation with the California Department of Water Resources.

Julien, P.Y. 1998. Erosion and Sedimentation. Cambridge University Press, Cambridge, United Kingdom.

Kranjcec, J., J.M. Mahoney, and S.B. Rood. 1998. The Response of Three Riparian Cottonwood Species to Water Table Decline. *Forest Ecology and Management* 110:77-87.

Lai, Y.G. 2002. User's Manual for U2RANS: An Unsteady and Unstructured Reynolds Averaged Navier-Stokes Solver. IIHR Draft Document, University of Iowa.

Lai, Y.G. 2006. Watershed Erosion and Sediment Transport Simulation with an Enhanced Distributed Model. 3rd Federal Interagency Hydrological Modeling Conference, Reno, Nevada, April 2-6, 2006.

Lai, Y. 2009. Two-Dimensional Depth-Averaged Flow Modeling with an Unstructured Hybrid Mesh. *Journal of Hydraulic Engineering*, Vol. 136, No. 1, January 1, 2010.

Lai, Y.G., L.J. Weber, and V.C. Patel. 2003. A Non-hydrostatic Three-Dimensional Method for Hydraulic Flow Simulation - Part II: Application. *ASCE Journal of Hydraulic Engineering* 129(3):196-214.

Larsen, E. 2007. Predicting Modes and Magnitude of River Channel Migration and Chute Cutoff Based on Bend Geometry, Sacramento River, California, USA. Report Submitted to Denver Technical Service Center, Bureau of Reclamation.

Meyer-Peter, E., and Müller, R. 1948. "Formulas for bed-load transport." Proc., 2nd Meeting, International Association of Hydro-Environment Engineering and Research**,** Stockholm, Sweden, 39-64.

Mooney, D.M. 2006. Rapid Assessment of Sediment Impacts in Stream Networks Under Steady and Unsteady Flows. Dissertation (in draft). Colorado State University, Department of Civil Engineering, Fort Collins, Colorado.

Morgan, T. 2005. Hydrological and Physiological Factors Controlling Fremont Cottonwood Seedling Establishment Along the Sacramento River, California. Unpublished Thesis, California State University, Chico, California.

Morgan, T., and A. Henderson. 2005. Memorandum Report – Field Observations of Cottonwood Seedling Survival at River Mile 192.5 During 2002 and 2003, Sacramento River, California. California Department of Water Resources, Northern District, Red Bluff, California, 16 pp.

Mueller, E.R., J. Pitlick, and J.M. Nelson. 2005. Variation in the Reference Shield Stress for Bed Load Transport in Gravel-Bed Streams and Rivers. *Water Resources Research* 41:W04006. 10 pp.

Neitsch, S.L., J.G. Arnold, J.R. Kiniry, and J.R. Williams. 2005. Soil and Water Assessment Tool Theoretical Documentation: Version 2005. http://www.brc.tamus.edu/swat/doc.html

Nelson, C., M. Carlson, and R. Funes. 2008a. Rapid Assessment Mapping in the Sacramento River Ecological Management Zone – Colusa to Red Bluff. Sacramento River Monitoring and Assessment Program, Geographic Information Center, California State University, Chico, 22 pp.

Neuman, D.S., M. Wagner, J.H. Braatne, and J. Howe. 1996. Stress Physiology – Abiotic. *Biology of Populus and Its Implications for Management and Conservation.* R.F. Stettler, G.A. Bradshaw, P.E. Heilman, and T.M. Hinckley (eds.). NRC Research Press, Ottawa, Ontario, Canada.

Nezu, I., and W. Rodi. 1986. Open-Channel Flow Measurements with a Laser Doppler Anemometer. *Journal of Hydr. Engineering,* ASCE, 112:335-355.

Niemiec, G.R. Ahrens, S. Willits, and D.E. Hibbs. 1995. Hardwoods of the Pacific Northwest, S.S. Research Contribution 8. Oregon State University, Forest Research Laboratory

Parker G.P. 1990. Surface-Based Bedload Transport Relation for Gravel Rivers. *Journal of Hydraulic Research* 28(4):417-435.

Parker G.P., P.C. Klingemand, and D.G. McLean. 1982. Bedload and Size Distribution in Paved Gravel-Bed Streams. *Journal of the Hydraulics Division, ASCE,* Vol. 108. No HY4, April, pp. 544-571.

Reclamation. 2005. Data Collection for the Modeling of Physical River Processes and Riparian Habitat on Sacramento River, California, NODOS Project Report. Technical Service Center, Bureau of Reclamation, Denver, Colorado.

Reclamation. 2006a. Platte River Sediment Transport and Riparian Vegetation Model. Technical Service Center, Bureau of Reclamation, Denver, Colorado.

Reclamation. 2006b. A Conceptual Framework for Modeling of Physical River Processes and Riparian Habitat on Sacramento River, California. Technical Service Center, Bureau of Reclamation, Denver, Colorado.

Roberts, M.D., D.R. Peterson, D.E. Jukkola, and V.L. Snowden. 2002. A Pilot Investigation of Cottonwood Recruitment on the Sacramento River. The Nature Conservancy, Sacramento River Project. http://www.aquaveo.com/pdf/SMS_10.1.pdf, accessed June 16, 2010.

Simunek, J., M. Sejna, and M.T. van Genuchten. 1999. The Hydrus 2-D Software Package for Simulating the Two-Dimensional Movement of Water, Heat, and Multiple Solutes in Variably-Saturated Media. Version 2.0. U.S. Salinity Laboratory, Agricultural Research Service, U.S. Department of Agriculture, Riverside, California.

Spencer, D., and G. Ksander. 2001. Troublesome Water Weeds Targeted by Researchers. *Agricultural Research*, November.

Stillwater Sciences. 2006. Restoring Decruitment Processes for Riparian Cottonwoods and Willows: a Field-Calibrated Predictive Model for the Lower San Joaquin Basin. Prepared for CALFED Bay-Delta Ecosystem Restoration Program, Sacramento, California. Prepared by Stillwater Sciences and J. Stella, in conjunction with J. Battles and J. McBride.

Stromberg, J.C., D.T. Patten and B.D. Richter. 1991. Flood Flows and Dynamics of Sonoran Riparian Forests. *Rivers* 2(3):221-235.

Stromberg, J.C., B.D. Richter, D.F. Patten, and L.G. Wolden. 1993. Response of a Sonoran Riparian Forest to a 10-yr Return Flood. *Great Basin Naturalist*, 53(2):118-130.

Stromberg, J. C., R. Tiller and B. Richter. 1996. Effects of Groundwater Decline on Riparian Vegetation of Semiarid Regions: the San Pedro River, Arizona, USA. *Ecological Applications* 6:113-131.

Sun, T., P. Meakin, and T. Jøssang. 2001a. A Computer Model for Meandering Rivers with Multiple Bed Load Sediment Sizes, I. Theory. *Water Resources Research* 37(8):2227-2241.

Sun, T., P. Meakin, and T. Jøssang. 2001b. A Computer Model for Meandering Rivers with Multiple Bed Load Sediment Sizes, II. Computer Simulations. *Water Resources Research* 37(8):2243-2258.

USACE. 1945. A Laboratory Study of the Meandering of Alluvial Rivers. U.S. Waterways Experiment Station, Vicksburg, Mississippi, May 1945.

USACE. 1980. Downstream Erosion and Reservoir Sedimentation Study. Sacramento District, Sacramento, California.

USACE. 1981. Sacramento River and Tributaries Bank Protection and Erosion Control Investigation California, Study of Alternatives. Sacramento District, Sacramento, California.

USACE. 1983. Sacramento River and Tributaries Bank Protection and Erosion Control Investigation California, Sediment Transport Studies, Sacramento District, Sacramento, CA.

USACE. 2002. Sacramento and San Joaquin River Basins, California, Comprehensive Study, Technical Studies Documentation, U.S. Army Corp of Engineers, Sacramento District, December 2002.

USGS. 1972. Jones, B.L., N.L. Hawley, and J.R. Crippen. Sediment Transport in the Western Tributaries of the Sacramento River, California. Geological Survey Water-Supply Paper 1792-J. United States Government Printing Office, Washington.

USGS. 2010. USGS Water Data for the Nation. http://waterdata.usgs.gov/nwis/. Last accessed March 8, 2011.

van Genuchten, M. Th. 1980. A Closed-Form Equation for Predicting the Hydraulic Conductivity of Unsaturated Soils. *Soil Science Society of America Journal* 44:892-898.

Viers, J.H., and R.A. Hutchinson. 2008a. Rapid Assessment Mapping in the Sacramento River Ecological Management Zone – Colusa to Red Bluff, Sacramento River Monitoring and Assessment Program. Geographical Information Center, California State University, Chico, 22 pp.

Viers, J.H., and R.A. Hutchinson. 2008b. Sacramento River Vegetation Map Cross-Walk Comparison and Calibration Between Maps Created in 1999 and 2007. A Technical Report to the CAL-FED Ecosystem Restoration Program. University of California, Davis, 9 pp.

Viers, J.H., and R.A. Hutchinson. 2008c. Sacramento River Vegetation Map: Detectability of Change and Spatial Constancy 1999-2007. A Technical Report to the CALFED Ecosystem Restoration Program, Department of Environmental Science and Policy, University of California, Davis, 9 pp.

Viers, J.H., R.A. Hutchinson, and C.E. Stouthamer. 2009. Subtask 2.1.1 Sacramento River Monitoring and Assessment Project: Vegetation Map Validation and Accuracy Assessment. Technical Report to the CALFED Ecosystem Restoration Program, University of California, Davis, 17 pp.

Water Engineering and Technology, Inc. (WET). 1988. Geomorphic analysis of the Sacramento River: Draft report. DACWO5-87-C-0084. U.S. Army Corps of Engineers, 339 pp.

Wilcock, P.R., and J.C. Crowe. 2003. Surface-Based Transport Model for Mixed-Size Sediment. *Journal of Hydraulic Engineering*, American Society of Civil Engineers, 129(2):120-128.

Wood, D.M. 2003. Pattern of Woody Species Establishment on Point Bars on the Middle Sacramento River, California. The Nature Conservancy, Sacramento River Project, Chico, California, 24 pp.

WRIME, Inc. 2009. Riparian Habitat Establishment Model Parameter Development and Modeling Study. Task Order 06A3204097F in support of UISBR IDIQ Contract No. 06CS204097F. Stockholm Environment Institute and UC Davis. Prepared for the Bureau of Reclamation, Mid-Pacific Region, Sacramento.

Zhang, H., L.P. Simmonds, J.I.L. Morison, and D. Payne. 1997. Estimation of Transpiration by Single Trees: Comparison of Sap Flow Measurements with a Combination Equation. *Agricultural and Forest Meteorology* 87:155-169.

Zimmerman, Robert C. 1969. Plant Ecology of an Arid Basin Tres Alamos-Redington Area Southeastern Arizona, Geological Survey Professional Paper 485-D, U.S. Geological Survey, US. Government Printing Office, Washington D.C., 52 p.

Appendix A

Methods Used in SRH-Capacity for Computing Sediment Transport Capacity and the Sediment Budget

Contents

Page

A.1 Tributary Sediment Computations A-1

A.1.1 Bed Material..... A-3
A.1.2 Hydrology A-6
A.1.3 Hydraulics A-13
A.1.4 Sediment Transport..... A-14
A.2 Comparison of Tributary Sediment Load Computations..... A-20
A.2.1 Limitations of Tributary Sediment Computations and Areas of Improvement..... A-24
A.2.2 Conclusions from Tributary Sediment Computations A-24
A.3 Methods for Modeling Main Stem Sediment Loads..... A-26
A.3.1 Bed Material..... A-26
A.3.2 Hydrology A-30
A.3.3 Hydraulics A-31
A.3.4 Sediment Transport..... A-36

Figures

Page

A-1 Median grain diameter, D_{50}, for pebble, surface, and subsurface samples..... A-4

A-2 Median diameter, D_{84}, D_{16}, and geometric standard deviation for surface bulk samples A-5

A-3 Median diameter, D_{84}, D_{16}, and geometric standard deviation for subsurface bulk samples..... A-5

A-4 Instantaneous discharge versus mean daily value for rising limb and peak (falling limb reverse of rising limb) A-6

A-5 Observed partial duration discharge comparison to measured mean daily discharge (blue) and derived instantaneous transformation discharge (red)..... A-8

A-6 Basin tributaries and gages A-12

A-7 Sediment (surface material) yield results by grain class for each tributary (reference shear = 0.0386, hiding factor = 0.9) A-16

A-8 Comparison of sediment (surface material) yield from Parker (1990) and Wilcock and Crowe (2003)..... A-17

A-9 Constant versus variable reference shear stress (MPN)..... A-18

Figures (continued)

Page

A-10 Hiding factor sensitivity A-19
A-11 Surface material D_{16}, D_{50}, and D_{84} by dataset A-27
A-12 Subsurface material D_{16}, D_{50}, and D_{84} by dataset A-27
A-13 Power functions for surface material A-29
A-14 Power functions for subsurface material A-30
A-15 Example plot of hydraulic parameters (stream power based on friction slope) used for reach break definitions A-32
A-16 Reach identification from Keswick Dam to Hamilton City A-34
A-17 Reach identification from Hamilton City to Knights Landing A-35
A-18 Surface material transport capacity results by grain class for each main stem reach using Parker's (1990) equation with default parameters A-36
A-19 Comparison of surface material transport capacity computed with Parker's (1990) equation and Wilcock and Crowe (2003) A-37
A-20 Surface material transport capacity using slope-based reference shear stress in the Parker (1990) transport equation A-38
A-21 Hiding factor sensitivity A-39

Tables

Page

A-1 Tributaries Included in Analysis A-2
A-2 Tributaries Excluded from Analysis A-2
A-3 Association of FDC Curves With Modeled Tributaries A-11
A-4 Transport Potential Gradation, Reference Shear Stress, and Hiding Factor Scenarios A-15
A-5 MPN Reference Shear Stress for Each Tributary A-17
A-6 Comparison of Annual Yields (tons/day) to Existing Literature A-21
A-7 Tributary Bed Load Best Estimate A-25

Tables (continued)

		Page
A-8	Coefficients for Sediment Gradation Power Functions	A-29
A-9	Flow Gage Records for Historical Condition Flow Duration Curves	A-30
A-10	Sacramento River Reaches with Sediment, Tributary, and Cross Section Information	A-33

Appendix A

Methods Used in SRH-Capacity for Computing Sediment Transport Capacity and the Sediment Budget

This appendix describes the methods used for assessing bed material, hydrology, hydraulics, and sediment transport for tributaries and the main stem of the Sacramento River. Information in this appendix provides the background to Chapter 2: Sedimentation and River Hydraulics Capacity Model.

A.1 Tributary Sediment Computations

The investigation of tributary sediment loads provides information on a natural source of material to the Sacramento River downstream of Shasta Reservoir. Results support development of a sediment budget and estimates of the present and future geomorphic impacts on the Sacramento River as a result of imbalances in sediment supply and transport. Bed load, transported in the tributaries and main stem, is the fraction of sediment load most important for determining bed elevation changes in the Sacramento River; therefore, bed load rather than total sediment load (bed load and suspended load) is computed in this model. Data sources include cross section surveys, bed material sampling, U.S. Geologic Survey (USGS) Digital Elevation Models (DEMs), and USGS stream gages. Table A-1 shows the Sacramento River tributaries included in the analysis.

Table A-2 shows Sacramento River tributaries identified but not surveyed nor sampled because they were either close to, or similar to, a measured site, or they were assumed to exert only minor influences to the geomorphology of the Sacramento River. There may be a need to revise the analysis if some of these are found to contribute significant amounts of sediment.

Drainage basins were delineated using 30-meter (98.425-foot) DEM data and Arc Hydro Tools (ESRI 2005). Basin areas were computed to a cell grid resolution of approximately 0.00374 square miles (mi^2). Basin cross section surveys and sediment sampling measured 74 percent of the drainage area. Identified, but unmeasured, tributary basins account for 17 percent of the drainage area. The other 9 percent of the Lower Sacramento Basin area drains directly into the main stem of the Sacramento River. Tributaries on the main stem of the Sacramento River were identified down to a drainage area of approximately 20 mi^2.

New tributary data consisted of bed material and cross section surveys. USGS gage records provided hydrology information. The following sections describe the data processing methods.

Table A-1. Tributaries Included in Analysis

Name	River Mile (RM)	Delineated Area (mi^2)
Stony	190	780.7
Big Chico	192.8	78.2
Sandy	192.8	7.5
Deer	219.5	206
Thomes	225.3	292.9
Mill	229.9	134.3
Elder	230.4	138.9
Antelope	234.7	166.1
Red Bank	243.1	109.7
Reeds	244.8	64.8
Dibble	246.6	32.2
Blue Tent	247.7	17.7
Battle	271.4	362.4
Cottonwood	273.5	918.6
Bear	277.6	111.4
Dry	277.6	9.7
Cow	280.1	421.4
Stillwater	280.8	66.1
Clear	289.3	241

Note: RM = river mile

Table A-2. Tributaries Excluded from Analysis

Tributary	River Mile (RM)	Area (mi^2)
Mud Creek	193.0	150.7
Kusal Slough	194.6	64.3
Pine Creek	196.4	145.4
Burch Creek	209.4	146.2
Toomes Creek	223.0	73.8
McClure Creek	226.5	41.4
Coyote Creek	233.1	25.4
Dye Creek	234.1	41.3
Salt Creek	240.2	46.1
Paynes Creek	253.0	95.1
Inks Creek	264.5	29.9
Ash Creek	277.2	29.9
Anderson Creek	278.3	19.9
Churn Creek	275.9	34.7

A.1.1. Bed Material

The collection of sediment samples in the summer of 2005 identified the particle size distributions present in the bed for each tributary. The data collection is detailed in Reclamation (2005). Each site included three samples:

1. **Surface pebble count (pebble):** aerial grid with regularly spaced sampling

2. **Surface bulk sample (surface):** measurement of grains on the surface of a 1-square meter (m^2) area

3. **Subsurface bulk sample (subsurface):** measurements of grains below the 1-m^2 surface sample down to a depth of approximately twice the maximum diameter of surface material

Bed material data collected for Cottonwood Creek, Reeds Creek, Stony Creek, and Thomes Creek during the 2005 sampling trip resulted in gradations that were deemed unrepresentative of the tributary due to chosen sampling locations. A subsequent sampling trip was made in July 2008 to resample these tributaries. The results from the 2008 sampling trip yielded more representative sediment gradations, and the 2008 data supplanted the 2005 data for these four tributaries.

Pebble counts represent an aerial distribution of grains over a relatively large area, while both surface and subsurface bulk samples show a mass distribution over a narrow point.

The percentage of material passing through an opening of a given diameter is known as the percent passing. The diameter, D, of an opening for a specific percent passing amount, x, can be represented by the symbol D_x and is measured in millimeters (mm). The symbol D_{50} indicates the diameter of an opening where 50 percent of the sampled material can pass through (i.e., the median grain diameter). The D_{50} provides an estimate of the representative size of material present in the bed of the channel. Figure A-1 shows the D_{50}, median grain diameter, for each tributary and each sample method.

Surface samples show coarser material than subsurface samples. In general, surface-bulk sampling indicated larger median diameters than the pebble counts. Differences between the two sampling techniques are expected since pebble counts provide median grain sizes based on frequency and surface samples provide median grain sizes by weight. Not every site included all types of sampling. The geometric standard deviation, $\sigma g = (D_{84}/D_{16})0.5$, provides an indication of the range of material sizes present in a sample. Figure A-2 shows the median diameter and gradation range for surface samples, and figure A-3 shows the range for the subsurface.

The surface bulk sample for Elder Creek, for example, shows the highest variability of materials in the sample and one of the smallest median diameters; however, the subsurface variability of Elder Creek is close to the average for all creeks, while the median diameter remains small when compared to other creeks. The surface included a narrower range of diameters than the subsurface samples. Surface samples also contained coarser material. Few creeks contained significant amounts of sand on the surface (where $D_{10} < 4$ mm).

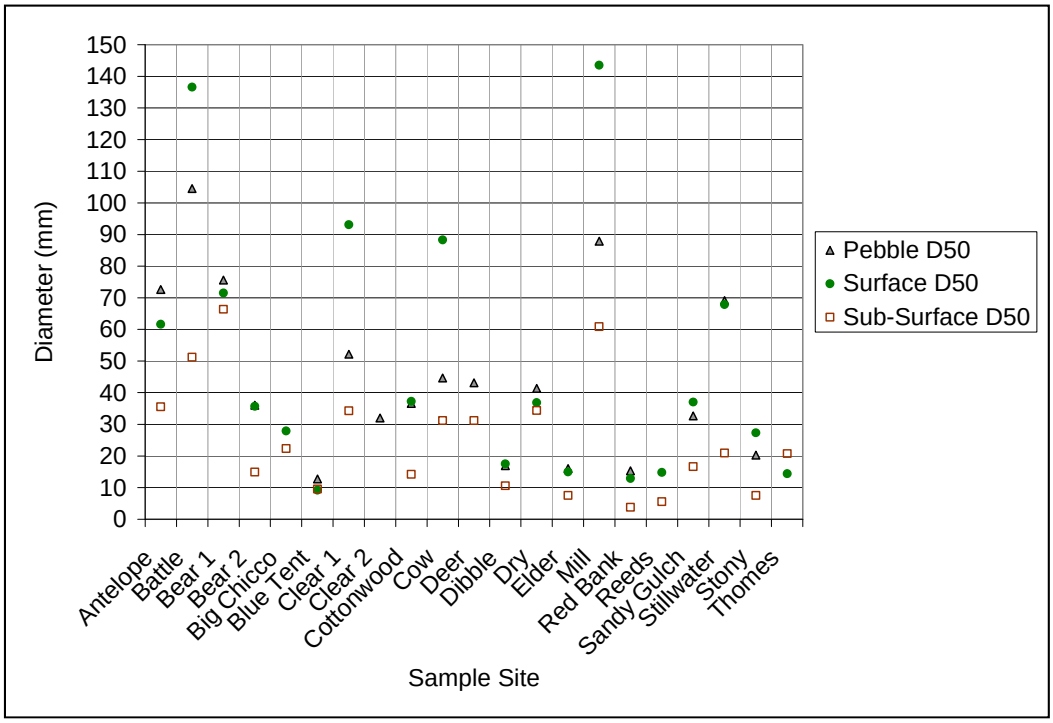

Figure A-1. Median grain diameter, D_{50}, for pebble, surface, and subsurface samples.

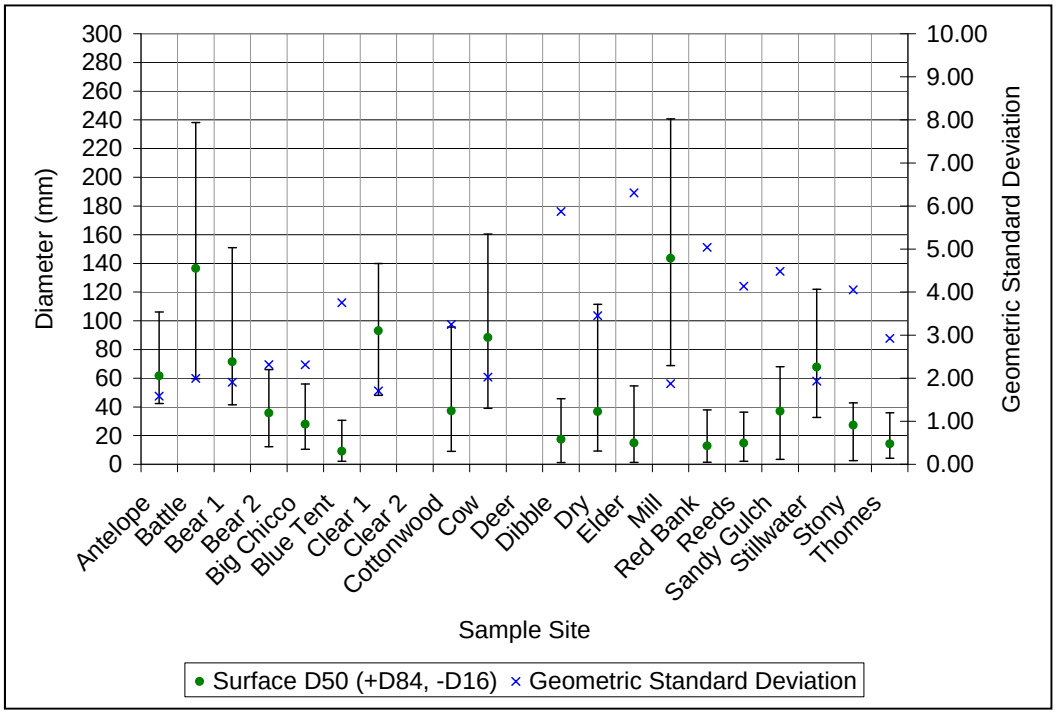

Figure A-2. Median diameter, D_{84}, D_{16}, and geometric standard deviation for surface bulk samples.

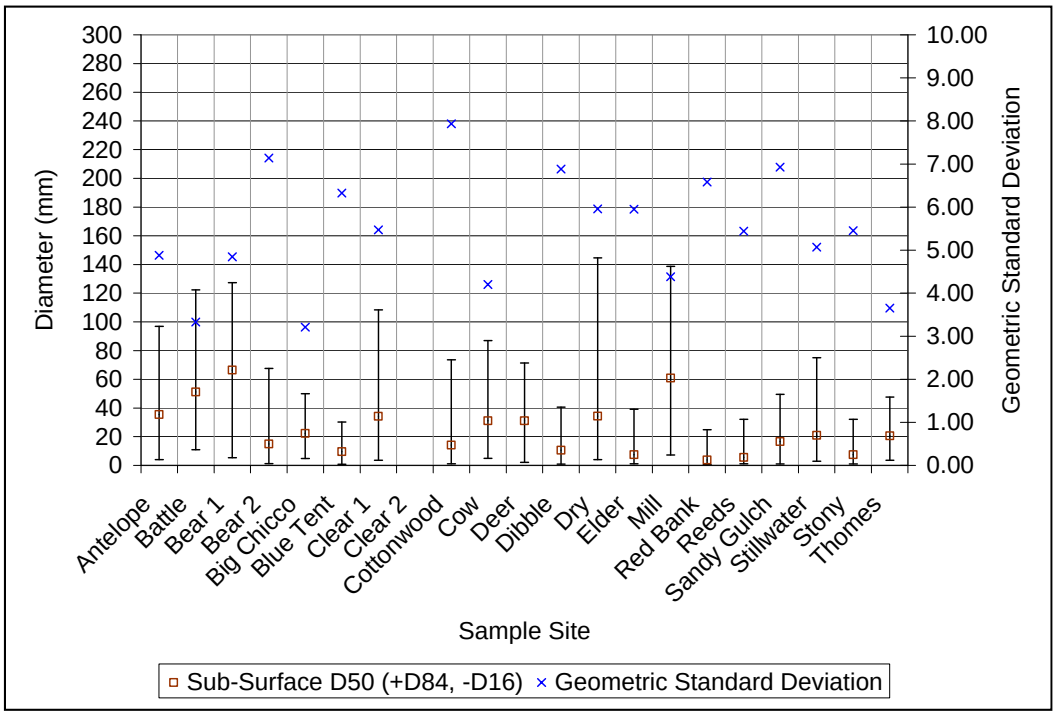

Figure A-3. Median diameter, D_{84}, D_{16}, and geometric standard deviation for subsurface bulk samples.

For sediment transport calculations, an analysis of each sample determined the amount of material present within each log base 2 (phi) size class ranging from very fine sand (0.0625-0.125 mm) to medium boulders (512-1,024 mm).

A.1.2 Hydrology

The USGS and California Department of Water Resources (CDWR) gaging stations served as the basis for creating average annual flow duration curves for the drainages of each tributary. For the ungaged sites, the model used flow duration curves from nearby basins scaled according to the square root of the ratio of drainage areas to calculate average annual flow duration curves for ungaged sites.

A.1.2.1 Mean Daily to Instantaneous Transformation

Mean daily flow and hourly records were downloaded on August 23, 2006, for the available periods of record. Using mean daily flow values to compute a sediment transport rate would underpredict total loads due to the nonlinear relationship between sediment transport and discharge. A transformation to an instantaneous time series while preserving volume provides an improved estimate. Figure A-4 shows the parameters involved.

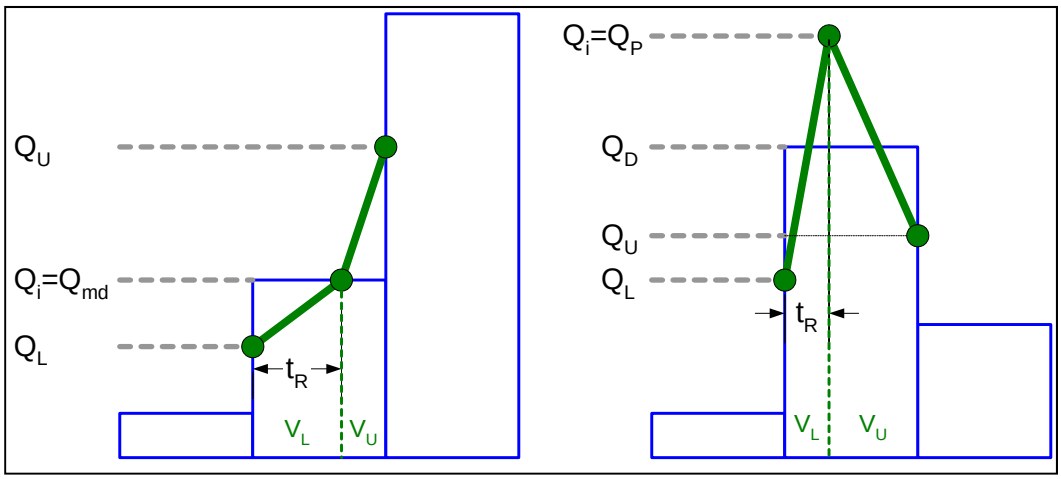

Figure A-4. Instantaneous discharge versus mean daily value for rising limb and peak (falling limb reverse of rising limb).

The instantaneous discharge at the upper (U) and lower (L) bounds of the mean daily flow record are computed by averaging with the adjacent mean daily flow records. The total daily volume equals the mean daily flow rate, Q_{md}, times the duration of 1 day. Splitting the day into two periods results in a volume of water passing during the first period, V_L, and a volume passing during the second period, V_U. A conservation of volume equation, equation A-1, provides a relationship between the time ratio (t_R), intermediate instantaneous discharge (Q_i), and the instantaneous discharges at the upper and lower boundary of the mean daily flow period (Q_L and Q_U), equation A-2.

$$V_D = V_L + V_U \tag{A-1}$$

$$Q_{md} \cdot (t_U - t_L) = \frac{1}{2}(Q_L + Q_i) \cdot (t_U - t_L) \cdot (t_R) + \frac{1}{2}(Q_U + Q_i) \cdot (t_U - t_L) \cdot (1 - t_R)$$

$$t_R = \frac{2 \cdot Q_{md} - Q_U - Q_i}{Q_L - Q_U} \tag{A-2}$$

Where:

V_D = volume of water computed from the mean daily flow
V_L = volume of water in the first time period
V_U = volume of water in the second period
Q_{md} = mean daily discharge
t_U = time at the upper boundary
t_L = time at the lower boundary
Q_L = instantaneous discharge computed at the start of the day
Q_i = intermediate instantaneous discharge
Q_U = instantaneous discharge computed at the end of the day
Q_P = peak discharge
t_R = time ratio between the time of day for flows less than the instantaneous discharge versus the total time

For rising and falling limbs, the instantaneous discharge, Q_i, equals the mean daily flow. For a peak or a trough, the intermediate discharge must be estimated. If no suitable method is available for estimating the intermediate flow, then equation A-3 solves the conservation of volume equations for discharge given a time ratio.

$$Q_i = 2 \cdot Q_{md} + t_R \cdot (Q_U - Q_L) - Q_U \tag{A-3}$$

The transformation for Sacramento River tributaries assumed that the peak occurred halfway through the day for a time ratio (t_R) of 0.5. The assumption results in an average peak flow value for unknown time ratios between the limiting cases of t_R equal to 1 or 0.

Observed annual (maximum discharge for a year) and partial duration (all flood peaks that exceed a chosen base stage or discharge, without regard for the number occurring in a year) flood series data provide a means of comparing estimated to observed peak flows. Figure A-5 shows the difference between mean daily measurements, the instantaneous transformation, and measured partial duration discharge values for all gaged basins.

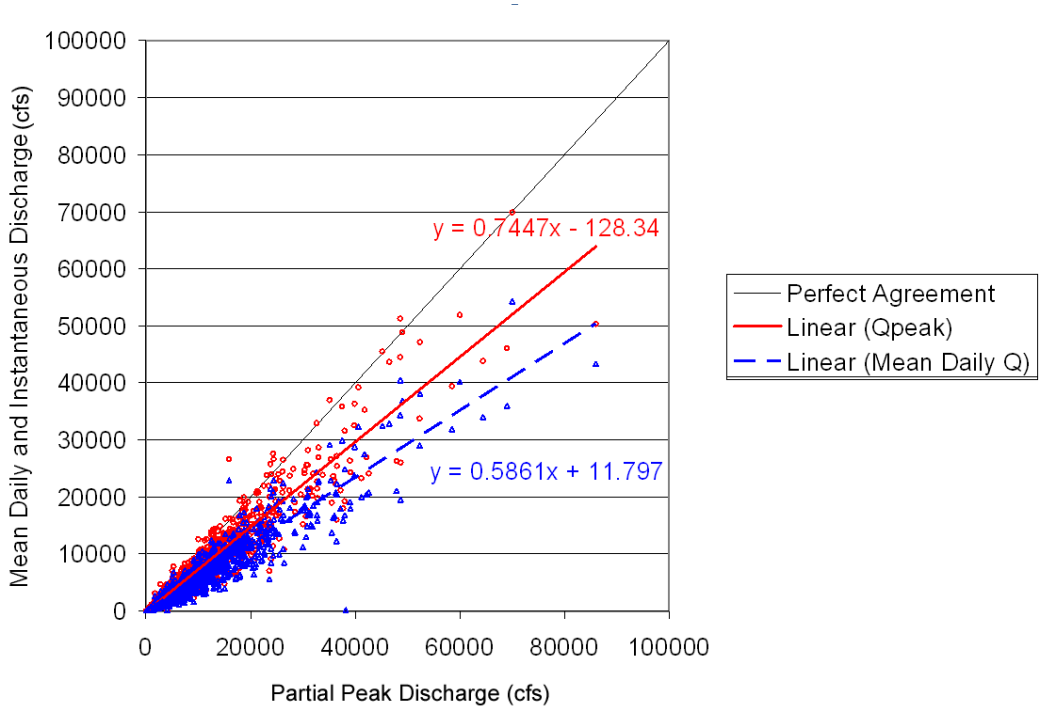

Figure A-5. Observed partial duration discharge comparison to measured mean daily discharge (blue) and derived instantaneous transformation discharge (red).

The line of perfect agreement shows where discharges are effectively captured—either by mean daily flow records or the instantaneous transformation. Neglecting the intercept, the regression lines show the amount of agreement. Mean daily records underestimate peak flows by a little less than 60 percent. The instantaneous transformation improves the ability to capture high flows to nearly 75 percent. The ability to capture high flows more accurately is important in that errors in estimating sediment loads will be reduced due to the non-linear relationship between sediment transport capacity and flow.

For two adjacent flow duration bins with the same flow rate, there is no method for conserving volume while adjusting the instantaneous point on the upper and lower bounds. Under those conditions, the instantaneous points at the upper and lower bounds equal the mean daily flow and create a discontinuity in the estimated instantaneous flow record.

A.1.2.2. Flow Duration Bins

Flow duration values were developed for each unique upper bound, lower bound, and instantaneous discharge value. The nonexceedance probability equals the amount of time equal to or below each discharge, divided by the total period of record plus 1 day. The additional day accounts for uncertainty in the empirical plotting position from using daily flow records.

The continuous empirical flow duration pattern was divided into 10 flow duration bins based on a sediment transport potential weighted volume of water. For an equivalent volume of water, lower flows transport less sediment than higher flows. A power relationship expressing sediment transport as a function of discharge can provide a rough approximation of relative transport rates. Flow duration bins were determined by first exponentially weighting each discharge and multiplying by the time to obtain a total weighted volume as shown in equation A-4.

$$\sum V_w = \sum \left(Q^b\right) \cdot t \qquad \text{A-4}$$

Where:
V_w = exponentially weighted volume
Q = discharge
b = assumed sediment rating curve exponent
t = duration of flow at discharge Q

The sum of the weighted volumes was then divided by the number of desired bins to determine the amount of weighted volume in each bin as shown in equation A-5:

$$V_{w,n} = \frac{\sum V_w}{n} \qquad \text{A-5}$$

Where:
$V_{w,n}$ = weighted volume in each bin
i = bin
n = number of bins

The sediment rating exponent varies from site to site. A conservative value of 1.5 (which underpredicts the nonlinear sediment transport behavior) was assumed for all gages for dividing the flow duration curve into bins.

The representative flow for each weighted bin was also determined according to the sediment transport weighting method. Equation A-6 computes the representative flow for each bin by dividing the exponentially weighted volume by duration of the volume to result in a flow rate. The flow rate is weighted according to the same sediment transport exponent.

$$Q_{r,i} = \left(\frac{V_{w,n}}{2 \cdot \left(t_{i+1} - t_i\right)} \right)^{1/b} \qquad \text{A-6}$$

Where:

$Q_{r,i}$ = representative flow rate for bin i
$V_{w,n}$ = weighted volume in each bin
t = nonexceedance time (plotting position)
b = assumed sediment rating curve exponent

Weighting the representative flow for each bin better captures the sediment transport potential of each bin; however, the representative flow and the duration no longer result in the same annual volume of water as the gage record. Bins conserve annual volumes of sediment, not volumes of water.

A.1.2.3 Ungaged Basins

Gage records did not always coincide with survey locations. When a gage was located on the same stream, the discharges on the flow duration curves were scaled by the drainage area ratio raised to the 0.8 power http://water.usgs.gov/software/NFF/manual/ca/index.html. When a nearby basin appeared similar in terms of basin size, mean annual precipitation, and altitude index, the gage was translated to the ungaged basin and scaled by drainage area. Table A-3 lists the gages and methods applied to each tributary.

The resulting sediment weighted flow duration curves provide input information for computing sediment loads. None of the records conserve the annual volume of water. Figure A-6 shows the location of gages and tributaries.

Table A-3. Association of FDC Curves With Modeled Tributaries

Name	Delineated Area (mi^2)	Reference Gage	Reference River	Reference Area	Area Scale Factor	Method	Comment
Antelope	166.1	11379000	Antelope	123	1.27	Scaled	
Battle	362.4	11376550	Battle	357	1.01	Scaled	
Bear	111.4	11374100	Bear	75.7	1.36	Scaled	
BigChico	78.2	11384000	Big Chico	72.4	1.06	Scaled	Automated delineation tool mistakenly selected Sandy Gultch as the primary flow path. Flow area was corrected by entering the Sandy Gultch area.
BlueTent	17.7	11378800	Red Bank	93.5	0.26	Translate and Scale	
Clear	241.0	IGO	Clear	223.5	1.06	DWR Scaled	Used DWR Hourly Data
Cottonwood	918.6	11376000	Cottonwood	927	0.99	Scaled	
Cow	421.4	11374000	Cow	425	0.99	Co-incident	
Deer	206.0	11383500	Deer	208	0.99	Scaled	
Dibble	32.2	11378800	Red Bank	93.5	0.43	Translate and Scale	
Dry	9.7	11372060	Churn	11.9	0.85	Translate and Scale	Churn Creek
Elder	138.9	11380500	Elder	136	1.02	Co-incident	
Mill	134.3	11381500	Mill	131	1.02	Co-incident	
RedBank	109.7	11378800	Red Bank	93.5	1.14	Translate and Scale	
Reeds	64.8	11378800	Red Bank	93.5	0.75	Translate and Scale	Good RedBank Reference
Sandy	7.5	11384000	Big Chico	72.4	0.16	Scaled Big Chico	Poor Area Ratio, Automated delineation tool failed to identify the Sandy Gultch Basin. Area was computed by "Big Chico" path and manually verified.
Stillwater	66.1	11374100	Bear	75.7	0.90	Bear Creek	
Stony	780.7	11388500	Stony	773	1.01	Scaled	
Thomes	292.9	11382090	Thomes	284	1.03	Scaled	

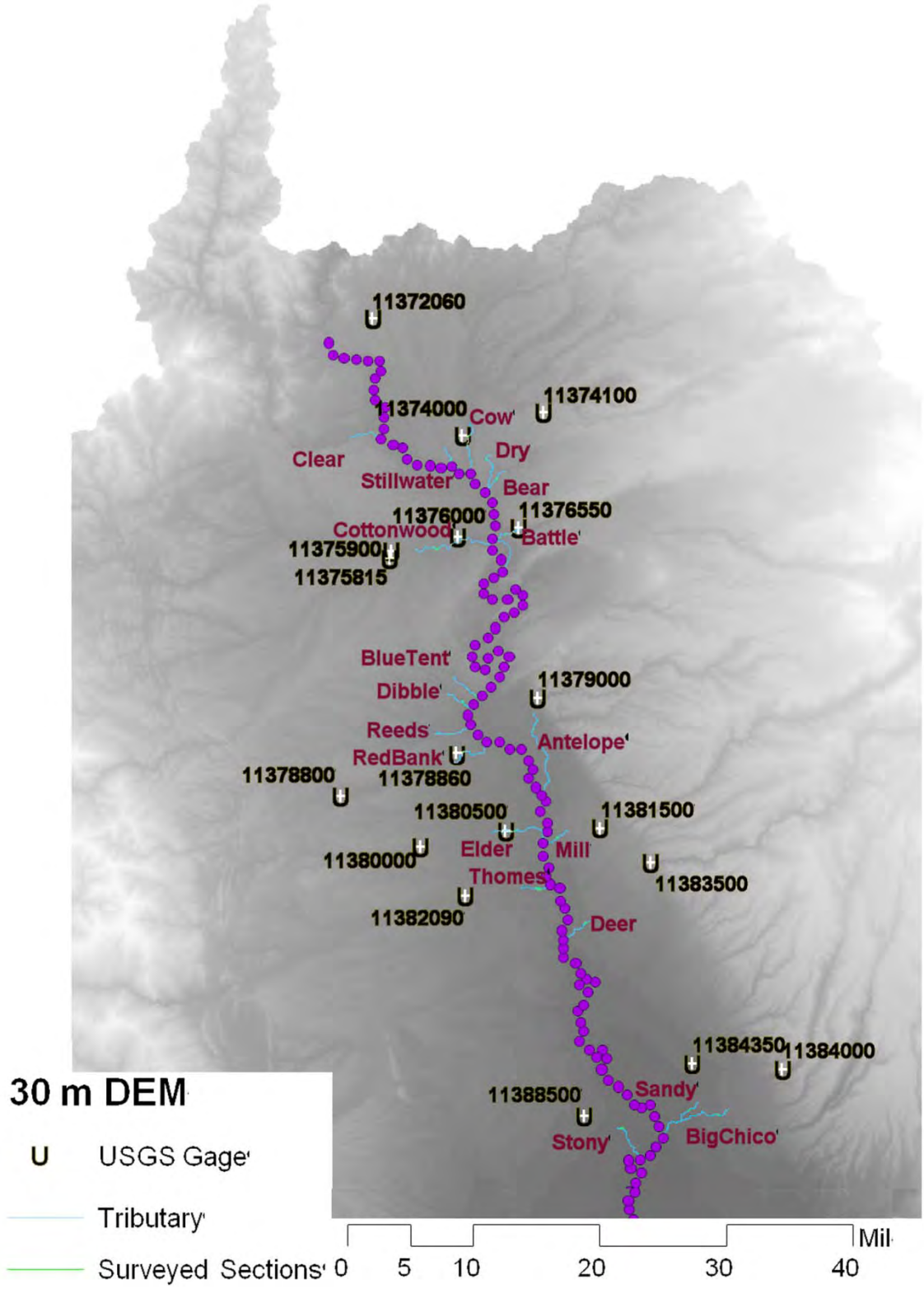

Figure A-6. Basin tributaries and gages.

A.1.3 Hydraulics

The flow hydraulics determine the force of water upon the channel boundary and, therefore, the amount of energy available for sediment transport. Hydraulic analysis used measured cross sections and the one-dimensional (1D) backwater model Hydrologic Engineering Centers River Analysis System (HEC-RAS) (Brunner 2002a and b) for the flows identified in the hydrologic analysis.

A.1.3.1 Geometry

Hydraulic computations used cross section surveys taken in June, July, and August 2005 by total station and shifted to georeferenced coordinates, North American Datum (NAD) 83 State Plane California Zone 1, feet horizontal. A local vertical datum was used. Dry and Bear Creek were georeferenced by visually using USGS quadrangle sheets. Tributary surveys accounted for 75 percent of the drainage basin upstream of Colusa and below Shasta Dam.

A thalweg profile was digitized from 2004 aerial photography at a 1:5,000 scale and oriented to point upstream. The thalweg lines were subdivided at 52.8 feet (0.01 mile) intervals and projected onto a 30-meter DEM to supply long elevation profile data. Points between grids cells were interpolated. River stations were assigned based on the 2004 thalweg lines and computed using tools within HEC-GeoRAS[1] (Ackerman 2005). Station zero begins at the bank line of the Sacramento River.

Surveyed cross sections were indexed from downstream to upstream starting with 1 for each tributary. Cross section points were planarized by fitting a regression line through the survey. Only one section required a pivot point to create a dog-leg, stony creek section 3. Surveys were visually verified for reasonability. Overbank points were marked during the survey and visually identified during post-processing using 2004 aerial photography to identify vegetation and cross section station-elevation plots.

Slopes derived from the DEM were compared with the 2004 survey to determine if significant changes occurred between the surveyed sites and the confluences with the Sacramento River. A change in slope could indicate features blocking or altering the delivery of material.

A.1.3.2 One-Dimensional Hydraulic Modeling

The backwater model used a Manning's n roughness coefficient of 0.045 for all areas, based upon the large bed material size in the tributaries. No information was available to calibrate. In addition to the survey sections, the cross section interpolation routines of HEC-RAS were used to generate sections so that the spacing between calculation steps did not exceed a distance of 100 feet. Interpolation results in smoother water surfaces and reduces the influence of cross

[1] HEC-GeoRAS is a set of procedures, tools, and utilities for processing geospatial data in ArcGIS using a graphical user interface http://www.hec.usace.army.mil/software/hec-ras/hec-georas.html.

section spacing on reach average hydraulics. The downstream boundary condition used normal depth calculated using the average slope of the channel invert through the surveyed reach.

A.1.3.3 Reach Average Hydraulics

The hydraulic characteristics of a reach were determined by averaging the hydraulic results from each surveyed and interpolated section. Results were visually checked for outliers.

A.1.4 Sediment Transport

Calculations of sediment load incorporate multiple factors to determine the amount of material moving through a system. Sediment load calculations include:

- Channel conditions: bed material, hydraulics, and hydrology
- Sediment transport potential
- Sediment transport capacity
- Sediment yield

Channel conditions described in preceding sections combine to form a scenario of the channel compositions (bed material), how water flows over the material (hydraulics), and the duration of time hydraulic forces act upon the channel boundary (hydrology). The sediment transport potential determines the ability of water to move material. The potential does not consider mitigating factors such as cohesive particles, armor control, or presence or absence of material in the beds, and only generally includes composition by using a hiding factor. The sediment transport capacity incorporates the fraction of material present in the bed available to move downstream. Finally, the sediment yield incorporates the duration of transport and any other factors to compute the total load.

For this analysis, sediment transport potential is defined by the rate of movement of bed material that assumes a bed of a single uniform gradation. However, the hiding factor is still applied from the measured gradation. The transport capacity adjusts the transport potential according to the amount of material present in each size class without considering armoring or wash material thresholds. The sediment load multiplies the transport capacity rate by the duration of the flow.

Sediment transport potential used the Parker et al. (1982) relationship. The transport formula requires a reference shear stress and hiding factor. Both parameters are site specific and require calibration to measured data to estimate. No calibration information was available. Transport calculations used two methods for determining load:

1. Assume a constant reference shear stress and hiding factor across all tributaries (default values)

2. Vary the reference shear stress according to slope

The parameters also depend upon whether the formula uses surface, subsurface, or combined gradation information. For practical purposes a surface, subsurface, or a combined gradation must be paired with a shear stress and hiding factor for each flow. Analysis using the same shear stresses and hiding factors for all tributaries included the scenarios shown in table A-4.

Table A-4. Transport Potential Gradation, Reference Shear Stress, and Hiding Factor Scenarios

Gradation	Reference Shear Stress	Hiding Factor
Surface	0.0386	0.905
Subsurface	0.0876	0.982
Combined	0.0631	0.944

The transport capacity calculations used the gradation corresponding to the surface, subsurface, or combined reference shear stress and hiding factor. Buffington and Montgomery (1997) surveyed reported reference shear stresses and found values ranging from 0.052 to 0.086. Parker et al. (1982) reported a reference shear stress of 0.0876 and a hiding factor of -0.982 for subsurface gradations. For surface gradations, Parker (1990) used a reference shear stress of 0.0386 and a hiding factor of -0.9047. The shear stress and hiding factor for the combined scenario are an average of surface and subsurface estimates and appear reasonably consistent with values reported in Buffington and Montgomery (1997).

For constant reference shear stress across all tributaries, the maximum transport capacity occurred when using the surface gradation reference shear stress and hiding factors, and the total shear stress. Applying a calculated grain shear stress as opposed to a total shear stress introduces another level of uncertainty due to the various methods used to estimate the grain shear stress.

The remainder of this analysis considers total shear stress. The transport capacity computed using the values for the subsurface and combined gradations varied in relative magnitude but, in general, resulted in approximately half to three-quarters of the transport capacity computed using the surface values. Conceptually, surface gradations would exert more control on low to moderate discharges; combined surface and subsurface transport would apply most closely to moderate discharges, and the subsurface transport would dominate during the higher flows. All of the methods appeared reasonable and yielded values within the expected variability inherent when considering the uncertainty typical of the hydraulic and sediment transport modeling. Surface material transport is of primary importance to spawning fish habitat. Figure A-7 shows the resulting surface material transport yield (reference shear of 0.0386 and hiding factor of 0.9).

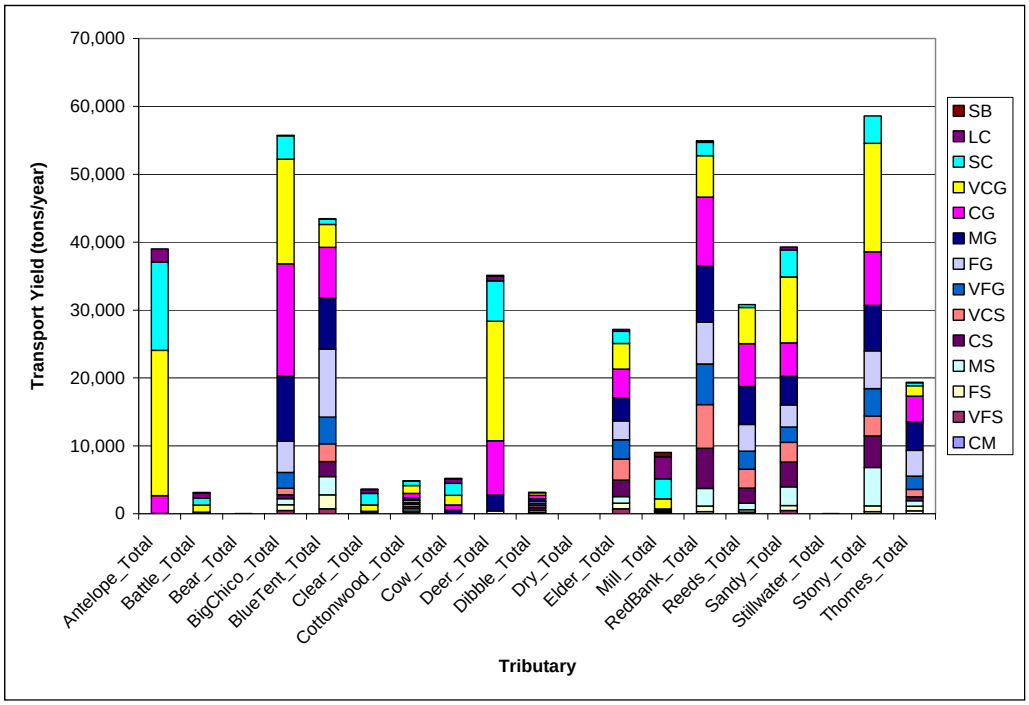

Figure A-7. Sediment (surface material) yield results by grain class for each tributary (reference shear = 0.0386, hiding factor = 0.9).[2]

Figure A-8 provides a comparison of Parker (1990) transport equation to the Wilcock and Crowe (2003) transport equation, each with the respective default reference shear stress and hiding factors.

The hydraulics for Red Bank Creek included 1D flood plain interaction artifacts, resulting in high flows with lower velocities and transport than lower discharges. The modeling limitation was neglected in order to maintain similar analysis techniques across all creeks. Deer Creek gradation estimates used pebble counts due to the absence of a surface sample. Mueller et al. (2005) studied variability in reference shear stress between different gravel-bed rivers and found the reference shear varied according to the slope described in equation A-7:

$$\tau_* = 2.18 \cdot S + 0.021 \qquad \text{A-7}$$

Where:

τ_* = reference nondimensional shear stress
S = slope of the channel

[2] For figure A-7, SB = Small Boulder, LC = Large Cobble, SC = Small Cobble, VCG = Very Course Gravel, CG = Course Gravel, MG = Medium Gravel, FG = Fine Gravel, VFG = Very Fine Gravel, VCS = Very Coarse Sand, CS = Course Sand, MS = Medium Sand, FS = Fine Sand, and VFS = Very Fine Sand
CM = Coarse Silt

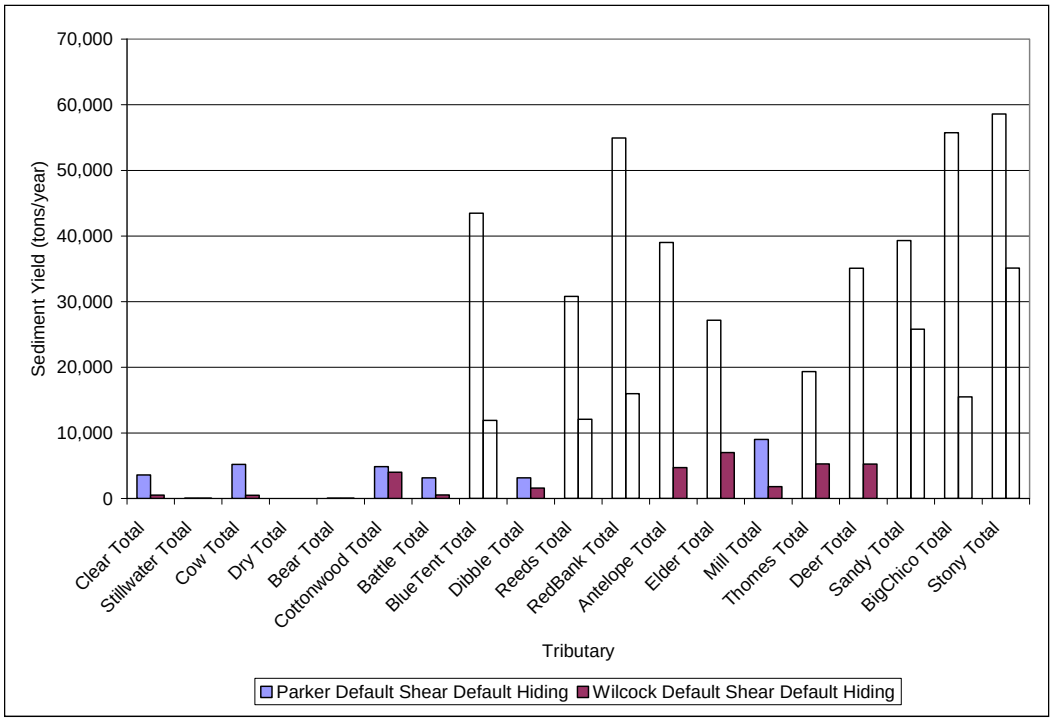

Figure A-8. Comparison of sediment (surface material) yield from Parker (1990) and Wilcock and Crowe (2003).

This analysis used the friction slope from the hydraulic calculations to predict the reference shear stress. The Mueller, Pitlick, and Nelson (2005) (MPN) relationship applies to surface based sediment transport calculations. Calculations using subsurface and combined gradations were not performed because this is outside the applicability of equation A-7. Table A-5 lists the MPN reference shear stresses based on slope by tributary.

Table A-5. MPN Reference Shear Stress for Each Tributary

Site	Friction Slope	MPN Reference Shear	Ratio (MPN/ Default)
Antelope	0.0061	0.0343	0.89
Battle	0.0042	0.0301	0.78
Bear	0.0011	0.0233	0.60
Big Chico	0.0024	0.0263	0.68
Blue Tent	0.0054	0.0328	0.85
Clear	0.0030	0.0276	0.71
Cottonwood	0.0012	0.0237	0.61
Cow	0.0024	0.0263	0.68
Deer	0.0035	0.0285	0.74
Dibble	0.0027	0.0268	0.70
Dry	0.0021	0.0255	0.66
Elder	0.0017	0.0246	0.64
Mill	0.0052	0.0322	0.84
Red Bank	0.0021	0.0256	0.66
Reeds	0.0031	0.0277	0.72

Table A-5. MPN Reference Shear Stress for Each Tributary

Site	Friction Slope	MPN Reference Shear	Ratio (MPN/ Default)
Sandy	0.0075	0.0374	0.97
Stillwater	0.0025	0.0265	0.69
Stony	0.0015	0.0242	0.63
Thomes	0.0017	0.0247	0.64

Figure A-9 compares the sediment results when the reference shear stress is varied according to MPN versus assuming a constant value across all tributaries. The results present surface transport rates.

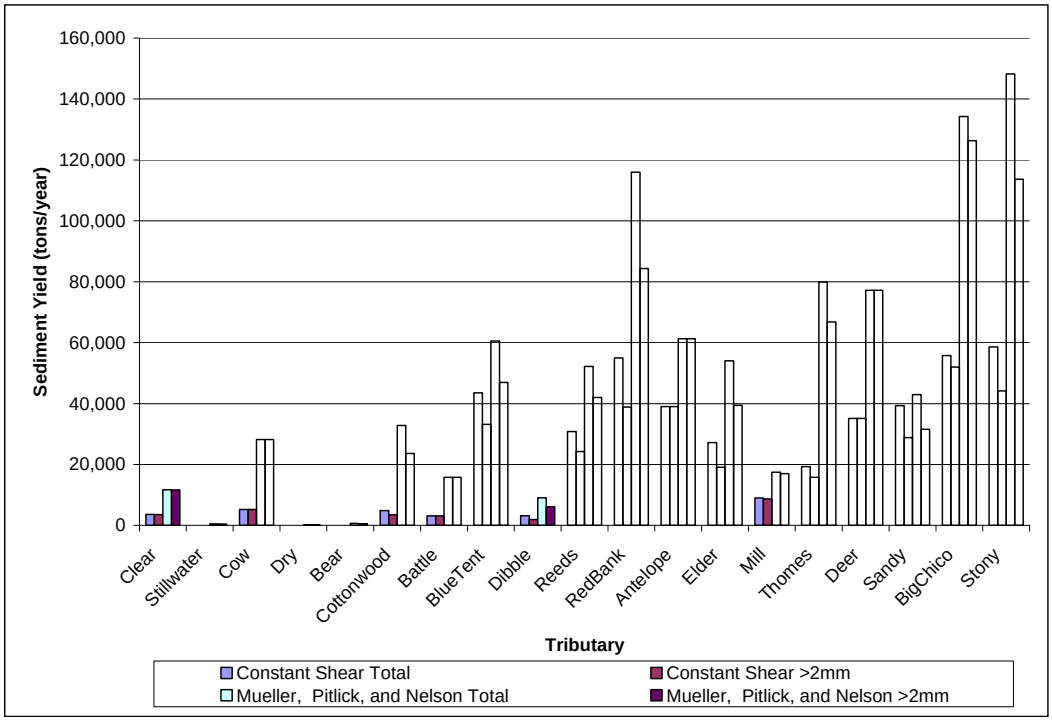

Figure A-9. Constant versus variable reference shear stress (MPN).

Slope-dependent shear stress resulted in a 118-percent increase in the total tributary yield and a 123-percent increase in tributary yield for gravel classes. There was a larger impact on gravel loads, as streams releasing small or negligible quantities began supplying increasing amounts of materials. The small fraction of sands present in these substrates causes the increase in transport potential to exert greater influence on gravel rather than finer materials (<2 mm).

The hiding factor was then reduced for all scenarios to 0.67, which is taken as a lower bound of the hiding factor as indicated by the summaries in Buffington and Montgomery (1997). The physical interpretation of a hiding factor assumes the presence of low mobility, transport capacity limited, coarse particles preventing finer particles from experiencing the full hydraulic force. The hiding factor acts as a method for controlling supply limit versus hydraulic limit on the transport of smaller particles. Higher factors, closer to one, result in less movement of small diameters. Smaller hiding factors result in greater movement in smaller classes. Figure A-10 presents the results for reducing the hiding factors for the surface material gradations.

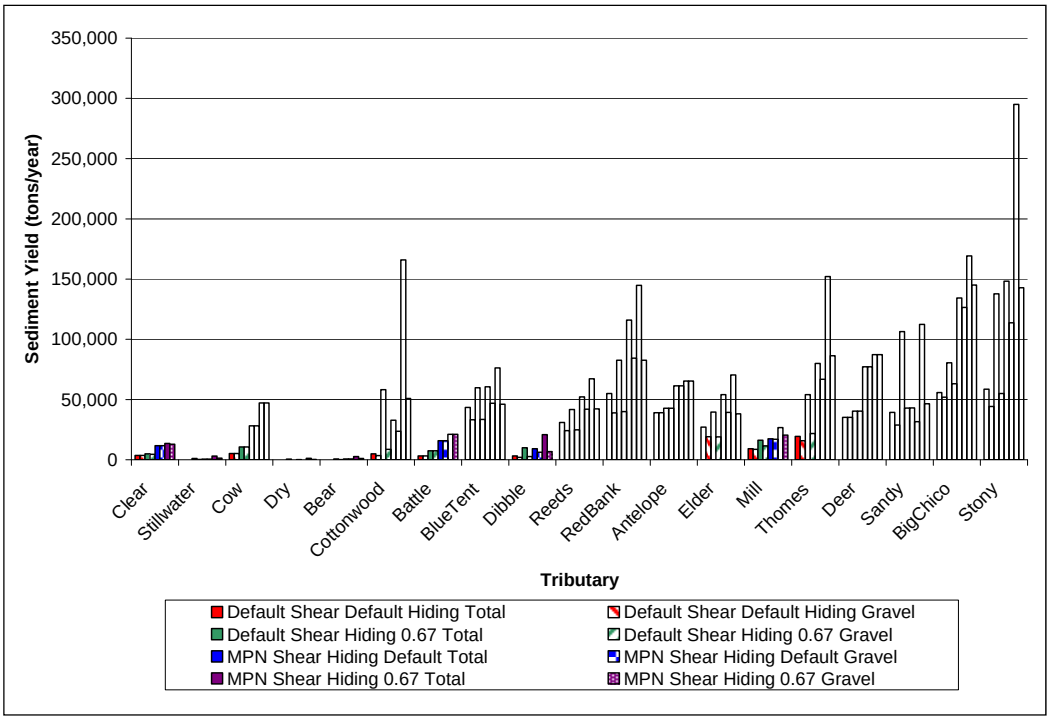

Figure A-10. Hiding factor sensitivity.

Using the default reference shear stress and reducing the hiding factor resulted in an 84 percent increase in the total load and a 20 percent increase in the gravel load. Using Mueller et al. (2005) shear stress and reducing the hiding factor resulted in a 64-percent increase in the total load and a 19-percent increase in the gravel load. The hiding factor more strongly impacts the smaller diameters by limiting the interference of large diameters on transport rates. Gravel estimates are less sensitive to the hiding factor. At higher transport rates, the hiding factor becomes less significant.

In addition, the Mueller et al. (MPN) reference shear stress was increased and decreased by 25 percent for sensitivity analysis (see Chapter 2 of main document).

A.2 Comparison of Tributary Sediment Load Computations

Table A-6 shows a comparison of sediment yields to estimated sediment loads identified in a literature review. The values reported in Table A-6 reflect the best estimate, which is an average of the following four methods:

- The MPN reference shear stress combined with the default hiding factor from Parker (1990)
- Increasing the MPN reference shear stress by 25 percent, combined with the default hiding factor from Parker (1990)
- Decreasing the MPN reference shear stress by 25 percent, combined with the default hiding factor from Parker (1990)
- Combining the 100-percent MPN reference shear stress with a hiding factor of 0.67

The average of the above four is the best estimate of the sediment load and is the most comparable to the variety of techniques used in the studies identified in the literature review. The different sources each use different techniques and methods and, in some cases, are attempting to measure different aspects of sediment transport. Methods for the different sources are described below the table.

Results from this study are compared to sediment loads from prior studies (Table A-6). The methods generally use more site-specific measurements of channel form and hydrology, and fewer assumptions of similarity between adjacent basins; however, critical shear values were not calibrated to site-specific measurements and, therefore, were subject to considerable uncertainty. Although calibration to existing data can predict more accurate transport rates, at an assessment level for the relative importance of tributaries in supplying sediment, the additional work may not be warranted. A 25-percent change in shear stress results in roughly an order of magnitude change in the estimated sediment load. Many of the comparisons to prior work fall within the order of magnitude difference.

Table A-6. Comparison of Annual Yields (tons/day) to Existing Literature

River	Bed Load	Gravel	USGS (1972)[1]	CDWR (1980)[2]	CDWR (1980)[3]	USACE (1981)[4]	CDWR (1984)[5]	USACE (1980)	CDWR (1981)
Antelope	75,467	75,467					2,500		
Battle	20,766	20,766		0	0	12,000			
Bear	1,366	870		4,400	1,100				
Big Chico	155,506	143,109							
Blue Tent	68,838	50,419					4,000		
Clear	13,568	13,351		5,500	1,100				
Cottonwood	77,423	39,659		20,000	3,000	359,000		14,640	
Cow	42,951	42,951		19,000	2,200	57,000			
Deer	90,794	90,794				92,000	3,600		
Dibble	13,093	7,108					6,000		
Dry	476	241							
Elder	60,177	40,677				32,000	34,000		
Mill	22,244	20,272				27,000	2,400		
Red Bank	129,023	88,706					19,000		
Reeds	58,279	43,847					16,000		11,000
Sandy	67,026	40,396							
Stillwater	1,485	944		7,700	1,100				
Stony	199,175	131,291	9,800						
Thomes	113,730	85,276	41,000			317,000	32,000		

[1] USGS (1972) – Table 4, Average Annual Bed load Discharge. The USGS (1972) estimate used the Meyer-Peter and Muller (MPM) equation as reported in Reclamation (1960).

[2] DWR (1980) – Table 11, Bed load Total. DWR (1980) used rough estimates for clear creek based on scaling discharge MPM in addition to the Schoklitsch equation.

[3] DWR (1980) – Table 11, Bed load > ½ Inch

[4] USACE (1981) – Table 11-42, Qs Sand and Gravel

[5] DWR (1984) as Reported in DWR (1994) Fluvial Zones bed load estimates

Elements of uncertainty also include the hydrology and the hydraulic performance. Hydrology presents an empirical flow duration method that may not encompass a full range of flow events, particularly large peaks moving large amounts of material. Shorter periods of record are less likely to capture larger events and may, therefore, bias results toward underpredicting average annual loads. An uncertainty or sensitivity evaluation of hydrology was not performed due to the complexity of evaluating a complete flow regime without empirical records. Different hydraulics can result in either an increase or decrease in sediment loads. In general, a change to friction slope exerts the largest influences. A hydraulic sensitivity study can provide an idea of the range of likely values, but the uncertainty in the exact value is unlikely to bias results towards more or less sediment. A more efficient study should wait for identification of the tributaries which have the biggest influence on the Sacramento River morphology before performing a detailed analysis.

Battle Creek: Battle Creek computed values show twice the yield of the USACE (1981) study. CDWR (1980) assumed a flat slope near the mouth of the creek, which resulted in zero delivery to the Sacramento River. The USACE (1981) estimate used a 1-year bed load record from Cow Creek in combination with the suspended load at the Battle Creek gaging station. The 2005 survey sites are located halfway between the USGS gaging station and the confluence with the Sacramento River. Slopes from the DEM show a slope near 0.0015 near the mouth of Battle Creek and a slope of 0.002 at the survey site. The visible presence of a delta on 2004 aerial photography suggests at least some delivery of material; however, there is also a large pool at the confluence that may trap a large portion of the bed load.

Bear Creek: Bear Creek calculations showed one-fourth the transport to the CDWR (1980) estimate, although CDWR (1980) used records from Cow Creek, not site-specific measurements.

Blue Tent Creek: The Blue Tent Creek estimate showed yields that were over an order of magnitude greater than CDWR (1984). CDWR (1984) calculations used a yield per square mile of drainage area method, rather than a direct calculation. Estimates from CDWR (1984) are assumed to be within the range of accuracy of general aerial techniques.

Big Chico Creek: There are no data with which to compare Big Chico Creek. A visual inspection of aerial photographs suggests that little, if any, transport material reaches the mouth of Big Chico Creek.

Clear Creek: Clear Creek estimates show three times greater yield than CDWR (1980) total loads. The methods used a reference gage approach from Cottonwood and Churn Creek, not a direct calculation.

Cottonwood Creek: The estimate for Cottonwood Creek is approximately three times that of CDWR (1980). There is a large degree of variation among various estimates on Cottonwood Creek. CDWR (1980) reviewed USACE calculations (USACE 1980) and the USGS data (source unknown), and then reduced the estimates by 60 percent to account for gravel mining. USACE (1980) used 2 years of total load measurements and an assumed fraction moving as bed load.

Cow Creek: Cow Creek estimates are from CDWR (1980) and USACE (1981). CDWR (1980) used the MPM equation and reduced the results by 50 percent to account for the presence of bedrock. USACE used a 1-year total load sample to develop a rating curve and includes suspended load in the estimate.

Deer Creek: Deer Creek results show close agreement with CDWR (1984) but not USACE (1980). A subsequent USACE report (1983) found a sand and gravel load of 8,000 tons per year.

Dibble Creek: Dibble Creek results showed twice the transport compared to CDWR (1984). CDWR (1984) methods scaled yields from Red Bank Creek based on the drainage area.

Dry Creek: No information was available to compare with Dry Creek estimates.

Elder Creek: Elder Creek estimates predicted about two times the CDWR (1984) or USACE (1981). USACE rating curve development used MPM estimation techniques and suspended load sampling.

Mill Creek: Mill Creek estimates are an order of magnitude greater than CDWR (1984) data and comparable to USACE data (1981). USACE (1981) used MPM methods and suspended load measurements.

Red Bank Creek: Red Bank Creek estimates are significantly higher than the CDWR (1984) estimates. No additional information on the 1984 estimate was identified.

Reeds Creek: Reeds Creek results showed almost three times the yield as CDWR (1984) and four times the yield as CDWR (1981). CDWR (1984) methods scaled yields from Red Bank Creek based on drainage area. The CDWR (1981) methods used sedimentation rates and surveys behind Red Bluff Diversion Dam and may underestimate load, as some sediment load may be sluiced through the diversion dam.

Sandy Creek: Sandy Creek drains into Big Chico. There is no additional information for comparison. A visual inspection of aerial photographs suggests that material may not reach the mouth of Big Chico.

Stillwater Creek: Stillwater Creek estimates show very low loads. The CDWR (1980) estimates used a flow duration curve scaled from Cow Creek and the Schoklitsch equation. The gravel fraction estimate is unsupported. There may be additional bed material sampling in Stillwater Creek to verify the measured bed material.

Stony Creek: No information was available to compare to the Stony Creek estimates. USGS empirical measurements show approximately half the estimated load. Connectivity between material from Stony and the Sacramento River may not exist.

Thomes Creek: Estimates for Thomes Creek predict transport significantly higher than those given in CDWR (1984) and lower than USACE (1981)

A.2.1 Limitations of Tributary Sediment Computations and Areas of Improvement

Computing sediment loads is subject to considerable uncertainty. A more accurate measure would calibrate to measured data; however, it is unlikely that the sufficient resources and time are available to measure sediment loads on all important tributaries. In fact, to date, no significant bed load measurements are available on any tributary in the study reach. However, limited bed load collection could be valuable in calibrating the transport formulas for at least some of the major tributaries.

Applying the estimates to future conditions requires assuming that the channel is at steady state or in dynamic equilibrium. Gravel mining, flow regulation, or other processes of geomorphic change may impact the applicability of estimates.

An attempt was made to locate the data collection sites near the confluences with the Sacramento River; however, the actual connectivity is unknown, and delivery rates would benefit from a qualitative field visit to determine if material at the sample site will reach the main stem. Sediment flows around the tributaries of Sandy Gulch, Mud Creek, and Big Chico are unknown.

Interpreting results in the context of the North of the Delta Offstream Storage (NODOS) requires applying a similar methodology to the Sacramento River. As with most sediment calculations, results are more accurate when used as a relative measure than as an absolute quantity. The conclusions in the next subsection will be compared to transport results for the Sacramento River in the following section.

A.2.2 Conclusions from Tributary Sediment Computations

Surface material transport is of primary concern for the Sacramento River. Subsurface transport rates are typically lower than surface transport rates, leading to averaged transport rates being much lower than surface transport rates. Surface

sediment transport calculations show an average annual bed load supply of 275,000 tons of sand and 936,000 tons of gravel material to the Sacramento River from tributaries. There were 745,000 tons of material supplied in the gravel size classes larger than 8-mm median axis diameter. Without the contributions from Big Chico Creek and Sandy Gulch, the sand supply drops to 236,000 tons, the gravel drops to 753,000 tons, and the gravel greater than 8 mm drops to 593,000 tons. Table A-7 shows the breakdown by tributary. The largest yields come from west side tributaries, including Cottonwood, Red Bank, Thomes, and Stony.

The estimates presented provide information for comparing tributary supply and main stem transport capacities to determine sediment surpluses or deficits and the resulting impacts on geomorphology and spawning habitat. The next steps should identify the relative influence of tributaries and select the tributaries with substantial impacts for more detailed analysis.

Table A-7. Tributary Bed Load Best Estimate (Average of Four Values; 75%, 100%, and 125% MPN Shear Coupled with Default Hiding Factor, and MPN Shear Coupled with 0.67 Hiding Factor), Compared with Default Parker Transport Yield (tons/year)

Tributary (Totals)	Bed Load Total (Sand and Gravel)	Gravel (>2 mm)	Gravel (>8 mm)	Parker Default Total (Sand and Gravel)	Parker Default Gravel (>2 mm)	Parker Default Gravel (>8 mm)
Clear	13,568	13,351	13,312	3,591	3,561	3,551
Stillwater	1,485	944	726	24	10	6
Cow	42,951	42,951	42,951	5,201	5,201	5,201
Dry	476	241	161	4	1	0
Bear	1,366	870	700	14	5	3
Cottonwood	77,423	39,659	29,802	4,873	3,490	2,937
Battle	20,766	20,766	20,766	3,138	3,138	3,138
Blue Tent	68,838	50,419	27,891	43,486	33,176	19,230
Dibble	13,093	7,108	4,905	3,153	1,935	1,358
Reeds	58,279	43,847	31,276	30,817	24,270	17,663
Red Bank	129,023	88,706	58,965	54,951	38,851	26,750
Antelope	75,467	75,467	75,467	39,016	39,016	39,016
Elder	60,177	40,677	28,320	27,163	19,084	13,483
Mill	22,244	20,272	20,103	9,018	8,700	8,649
Thomes	113,730	85,276	51,191	19,352	15,772	10,017
Deer	90,794	90,794	89,406	35,110	35,110	34,709
Sandy	67,026	40,396	30,047	39,304	28,787	23,263
Big Chico	155,506	143,109	122,144	55,752	51,980	45,089
Stonyl	199,175	131,291	97,267	58,597	44,200	34,609
Grand Total	**1,211,389**	**936,145**	**745,400**	**432,562**	**356,286**	**288,672**

A.3 Methods for Modeling Main Stem Sediment Loads

Main channel sediment loads were computed using the Sedimentation River Hydraulics Capacity Model (SRH-Capacity) for both historical conditions, as well as an analysis of alternative conditions. The investigation of main channel sediment loads provides information on the Sacramento River's ability to transport tributary material downstream of Keswick Reservoir under current conditions and under alternative conditions. Data sources include existing hydraulic models, existing bed material grain size distributions, USGS stream gages, and alternative hydrology developed by the CDWR using the CALSIM flow tool.

A.3.1 Bed Material

A review of existing sediment data for the Sacramento River was conducted. Four sources of published sediment data were found: Water Engineering & Technology, Inc. (WET 1988); USACE (1981); CDWR (1984); and CDWR (1995). Some of the data from the various reports was not considered; for example, the WET 1987 data included bank material data, as well as sediment data at the mouths of tributaries, neither of which are applicable to the SRH-Capacity model. Also, the WET (1987) data did not use the Wolman pebble count data, as this count typically did not agree well with the bulk sample data. The usable surface and subsurface bulk sample data from the various sources covered different portions of the river. Using 1991 RM as a reference (RM increase in the upstream direction), the USACE data spanned RM 226 to 189.4. WET data spanned RM 219.5 to 146.4. The 1984 CDWR data spanned RM 242.7 to 197.9, whereas the 1995 CDWR data spanned RM 298.3 to 273.1.

The WET (1987) data were presented as a D_{16}, D_{35}, D_{50}, D_{84}, and D_{95}; the CDWR (1984) data were presented as D_5, D_{16}, D_{50}, D_{84}, and D_{95}; the CDWR (1995) data were presented by size fraction from the sieve analysis; and the USACE (1981) data were presented as D_{16}, D_{35}, D_{50}, D_{84}, and D_{95}. Figure A-11 presents the D_{16}, D_{50}, and D_{84} for the surface bulk sample data as a function of RM, and figure A-12 presents the same information for the subsurface material.

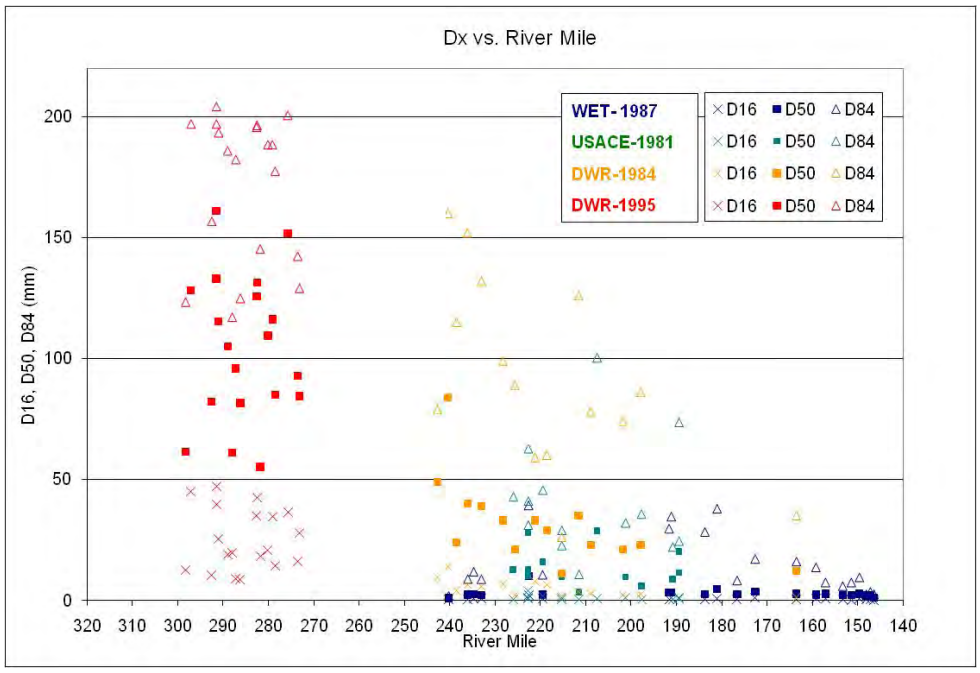

Figure A-11. Surface material D_{16}, D_{50}, and D_{84} by dataset.

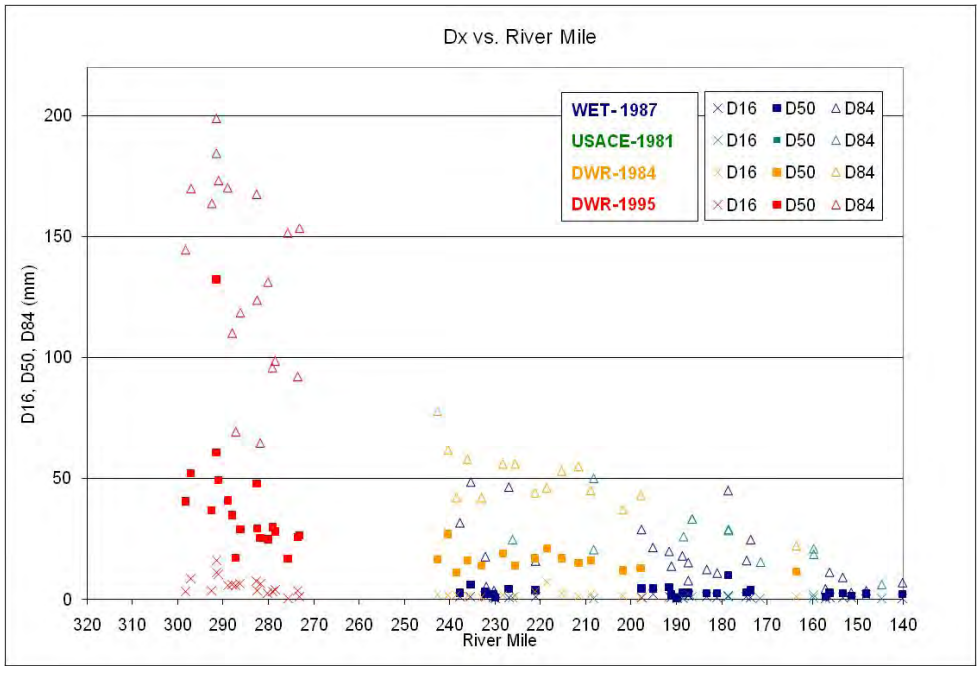

Figure A-12. Subsurface material D_{16}, D_{50}, and D_{84} by dataset.

Surface samples show coarser material than subsurface samples, and there is a general downstream fining trend; however, there is a disagreement in sediment size as a function of RM depending on the source of the data. For instance, a surface D_{50} at RM 236 is reported as 40 mm in the CDWR (1984) dataset and as 2.43 mm in the WET (1988) dataset. This type of variation exists between datasets, as well as within a given dataset. The CDWR (1994) data display a range of D_{50}s in a short distance without any sort of upstream or downstream trend. The wide range of grain size distributions between and within datasets would not produce suitable results from SRH-Capacity. It was necessary to develop a dataset consistent with the provided data but usable in SRH-Capacity.

The WET (1988) data typically reported a surface D_{50} in the fine gravel or course sand range, but a site visit to the river will not corroborate that data. Possible reasons for this discrepancy are the year the data was collected, the time of year the data was collected, the locations within the channel where the data was collected, or the methodology of collecting and sieving the data. Also, it was noted that subsurface samples were taken where surface samples were not collected. That indicated that data collection procedures were in disagreement with the methodology Reclamation followed during tributary sampling. The WET (1988) data did not seem to represent the bed material of the Sacramento River to a suitable level for SRH-Capacity modeling.

It was assumed that the two CDWR datasets would have been collected with the same methodologies. For this reason, and also due to the fact that the presentation of the USACE (1981) data was not well documented, it was decided to only consider the CDWR sediment data for the SRH-Capacity modeling and to omit the USACE (1981) data.

Power functions were developed to estimate the D_5, D_{16}, D_{50}, D_{84}, and D_{95} as a function of RM based on the CDWR (1994) and the CDWR (1984) data. The power function (equation A-8) was used to interpolate a grain size distribution for the sections of river where no sediment data exist; namely, RM 273.1 to RM 242.7. The CDWR (1984) data were presented as the D_5, D_{16}, D_{50}, D_{84}, and D_{95}, whereas the CDWR (1995) data were presented as the weights retained on each sieve as a result of the sieve analysis. A semi-logarithmic interpolation was performed on the CDWR (1995) data in order to estimate the D_5, D_{16}, D_{50}, D_{84}, and D_{95}, as shown in equation A-8.

$$d_x = a(RM - b)^c + d \qquad \text{A-8}$$

Phi-class interpolation was performed to estimate material presence in the various size classes. Table A-8 provides the coefficients for the representative power functions for the various gradation metrics as a function of RM. A plot of the data, along with the power function developed by the data, is shown in figure A-13 for the surface and in figure A-14 for the subsurface.

Table A-8. Coefficients for Sediment Gradation Power Functions

	Surface					Subsurface				
	D5	**D16**	**D50**	**D84**	**D95**	**D5**	**D16**	**D50**	**D84**	**D95**
a	2.2E-08	6.0E-05	9.0E-04	1.0E-01	2.0E-01	5.0E-09	6.0E-06	1.3E-04	1.3E-03	4.0E-03
b	163.5	163.5	163.5	163.5	163.5	163.5	163.5	163.5	163.5	163.5
c	4	2.7	2.4	1.5	1.4	4	2.8	2.5	2.4	2.2
d	0.4	1.3	12.3	35.0	53.0	0.4	1.1	11.5	22.0	39.0

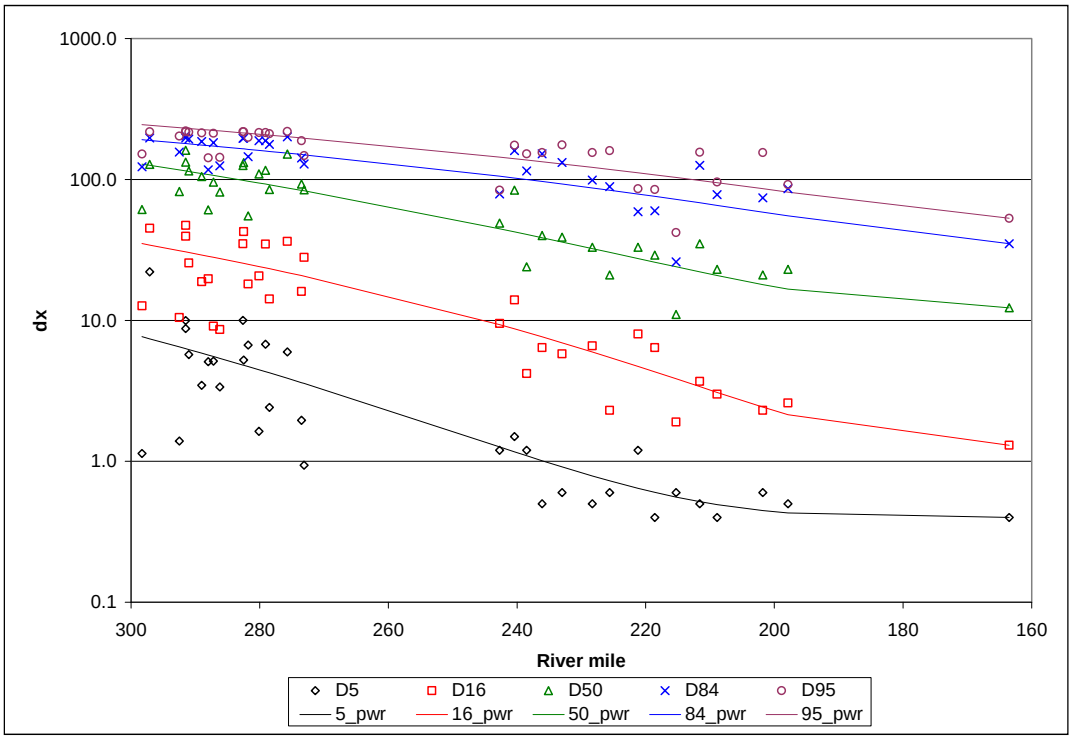

Figure A-13. Power functions for surface material.

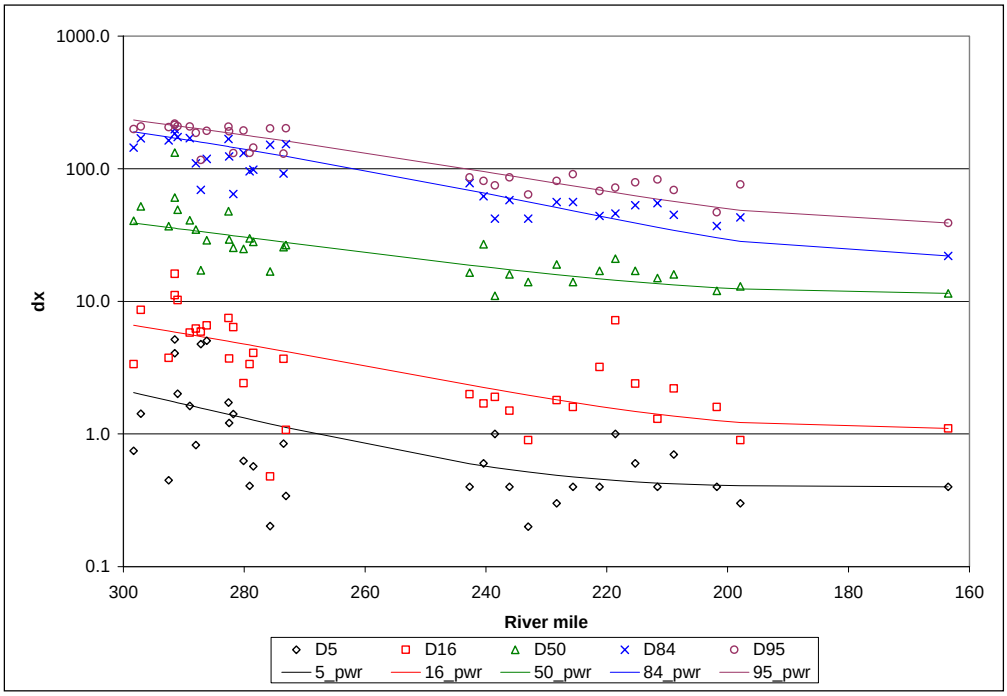

Figure A-14. Power functions for subsurface material.

A.3.2 Hydrology

The USGS and CDWR gaging stations served as the basis for creating average annual flow duration curves for the historical conditions for Sacramento River. The following gages were used to represent the hydrology of the study reach based on spatial location and flow record length: Keswick, Bend Bridge, Vina, Hamilton City, Butte, and Colusa. The gage at Shasta Dam closed in 1945, and the gage at Keswick Dam closed in 1950. If flow gage records preceded the dams, the records were abridged to exclude conditions before dam construction. Table A-9 provides the length of the gage record used and the source of the data.

Table A-9. Flow Gage Records for Historical Condition Flow Duration Curves

Gage	USGS ID	USGS Data Start Date	USGS Data End Date	DWR ID	DWR Data Start Date	DWR Data End Date
Keswick	11370500	10/01/1949	Current			
Bend Bridge	11377100	10/01/1949	Current			
Vina	11383730	10/01/1949	09/30/1978	VIN[1]	10/01/1978	Current
Hamilton City	11383800	10/01/1949	10/02/1980	HMC[2]	10/03/1980	Current
Butte City	11389000	10/01/1949	06/30/1995			
Colusa	11389500	10/01/1949	Current			

[1] Vina Woodson Bridge (VIN)
[2] Hamilton City (HMC)

A.3.2.1 Mean Daily to Instantaneous Transformation

Mean daily flow was not transformed to instantaneous flow for the Sacramento River as it had been for the tributaries. Larger rivers show a more gradual, longer-lasting flood hydrograph than smaller tributaries, and it is assumed that an instantaneous transform as described for the tributaries would yield little to no change in flow discharges.

A.3.2.2 Flow Duration Bins

Flow duration bins were developed for the main stem sediment budgets in the same manner as the tributary sedimentary budgets (see Section A.1.2.2 Flow Duration Bins).

A.3.3 Hydraulics

The flow hydraulics determines the force of water upon the channel boundary and, therefore, the amount of energy available for sediment transport. Hydraulic analysis used existing cross sections from a USACE and a CDWR study. The 1D backwater model HEC-RAS (Brunner 2002a and b) was used for the flows identified in the hydrologic analysis.

A.3.3.1 Geometry

Hydraulic computations used cross section data from USACE 2002. RM references refer to 1991 RMs. The USACE study extends approximately from RM 219 (south of Vina, California) to RM 80 (southeast of Knights Landing, California). The CDWR study extends approximately from RM 296 (Keswick Dam, California) to RM 217.5. There is approximately 1.5 miles of overlap between the two studies. The geometry from the two studies was shifted to georeferenced coordinates, NAD83 UTM Zone 10N, feet horizontal, and then integrated. The vertical datum is NAVD88.

A.3.3.2 One-Dimensional Hydraulic Modeling

The backwater model used a variable Manning's n roughness coefficient resulting from model calibration completed by USACE and CDWR. Additional model calibration after integrating the two datasets was not performed. The average slope of the channel invert down by Knights Landing was used to develop a downstream boundary condition.

A.3.3.3 Reach Average Hydraulics

The hydraulic characteristics of a reach were determined by averaging the hydraulic results from each cross section. Interpolated cross sections generated by HEC-RAS were not used when averaging hydraulics. Hydraulic parameters at cross sections near bridges and other inline structures were not used while averaging hydraulics, although they were used to define reaches. Results were visually checked for outliers. Reach breaks were identified using the hydraulic parameters of velocity, flow depth, top width, flow, hydraulic radius, hydraulic depth, and wetted perimeter. Only in-channel parameters were used as flood plain

hydraulics; overbank areas do not contribute significantly to downstream transport of channel sediment. Twenty-three distinct reaches were identified between RM 296 and RM 80 (Keswick Dam to Knights Landing). Table A-10 shows a list of the reaches (upstream to downstream) and their corresponding upstream/downstream HEC-RAS cross sections. Figure A-15 is an example of reach break definitions based on stream power (using friction slope). The example is a plot of the product of in-channel flow and friction slope as a function of HEC-RAS cross sections by RM for a specific total flow rate. Figures A-16 and A-17 visually present the reaches.

Reach break identification depends on the hydrology applied to a given reach. Hydrology was not interpolated for each reach. Reach breaks were identified from the hydraulics developed using historical hydrology.

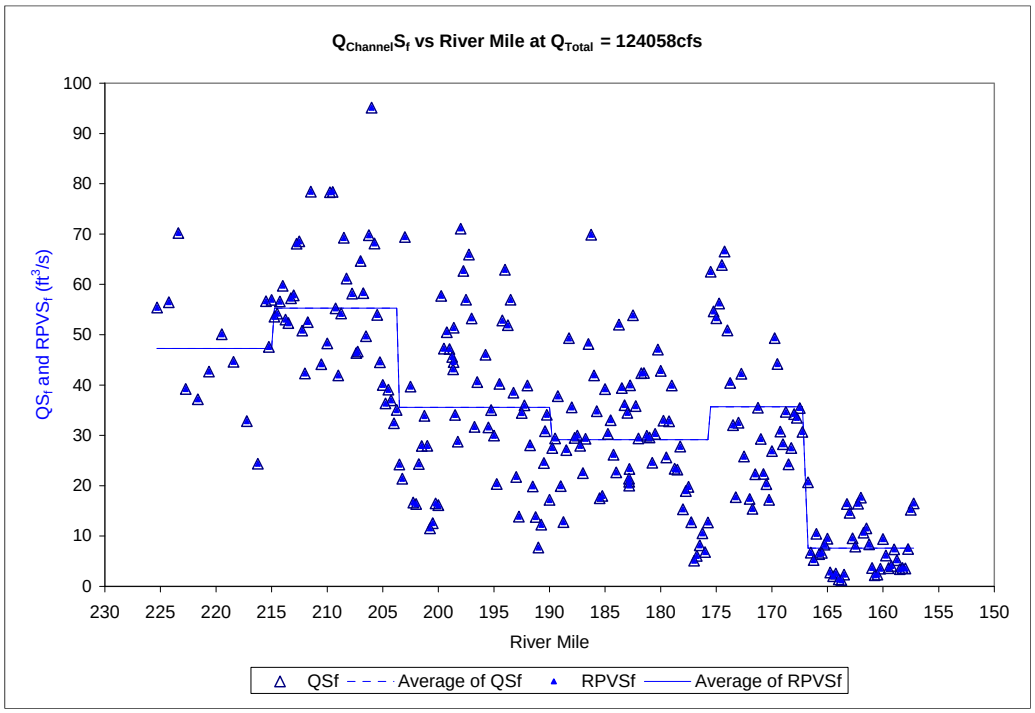

Figure A-15. Example plot of hydraulic parameters (stream power based on friction slope) used for reach break definitions.

Table A-10. Sacramento River Reaches with Sediment, Tributary, and Cross Section Information

Reach	Sediment Samples	Sample Source	Tributary 1	Tributary 2	Tributary 3	Tributary 4	Upstream HEC-RAS Cross Section	Downstream HEC-RAS Cross Section
23	0	N/A	None				295.92	292.427
22	2	CDWR-95	None				292.3	290.06
21	4	CDWR-95	None				289.32	283.79
20	7	CDWR-95	Clear	Stillwater			283.33	274.95
19	6	CDWR-95	Cow	Dry	Bear		274.42	268.6
18	1	CWR-95	Cottonwood	Battle			267.52	252.34
17	0	N/A	Blue Tent	Dibble	Reeds	Red Bank	252.233	238.33
16	5	CWR-84	Antelope				237.54	225.362
15	4	CWR-84	Elder	Mill	Thomes		225.29	215
14	3	CWR-84	Deer				214.835	203.75
13	2	CWR-84	Sandy	Big Chico			203.5	190
12	0	N/A	Stony				189.75	175.75
11	0	N/A	None				175.5	166.76
10	1	CDWR-84	None				166.75	157.25
9	0	N/A	None				156.94	145.75
8	0	N/A	None				145.5	144
7	0	N/A	None				143.75	131.25
6	0	N/A	None				131	126
5	0	N/A	None				125.75	119.25
4	0	N/A	None				119.2	107.75
3	0	N/A	None				107.5	90.3
2	0	N/A	None				90.25	84.75
1	0	N/A	None				84.5	80.38

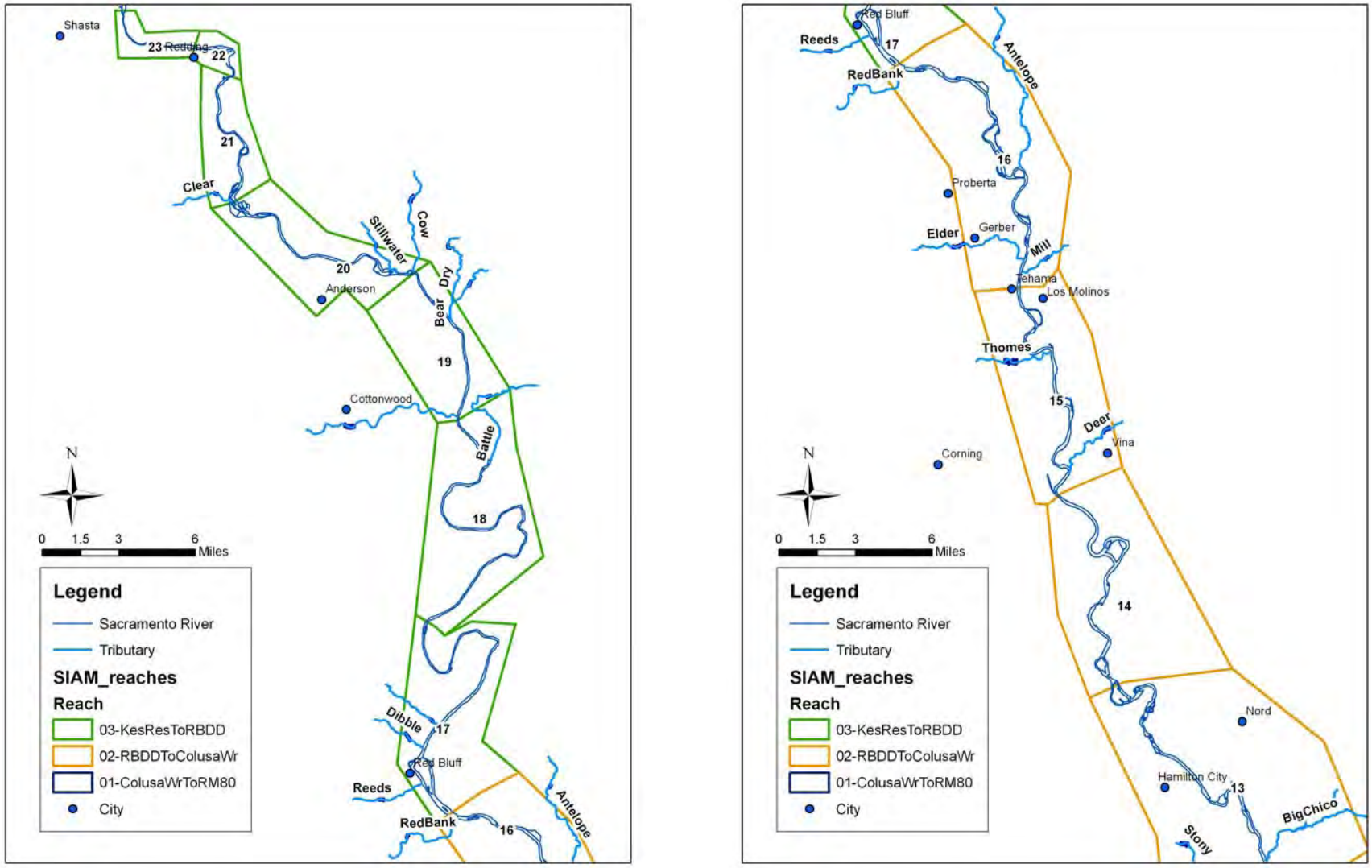

Figure A-16. Reach identification from Keswick Dam to Hamilton City.

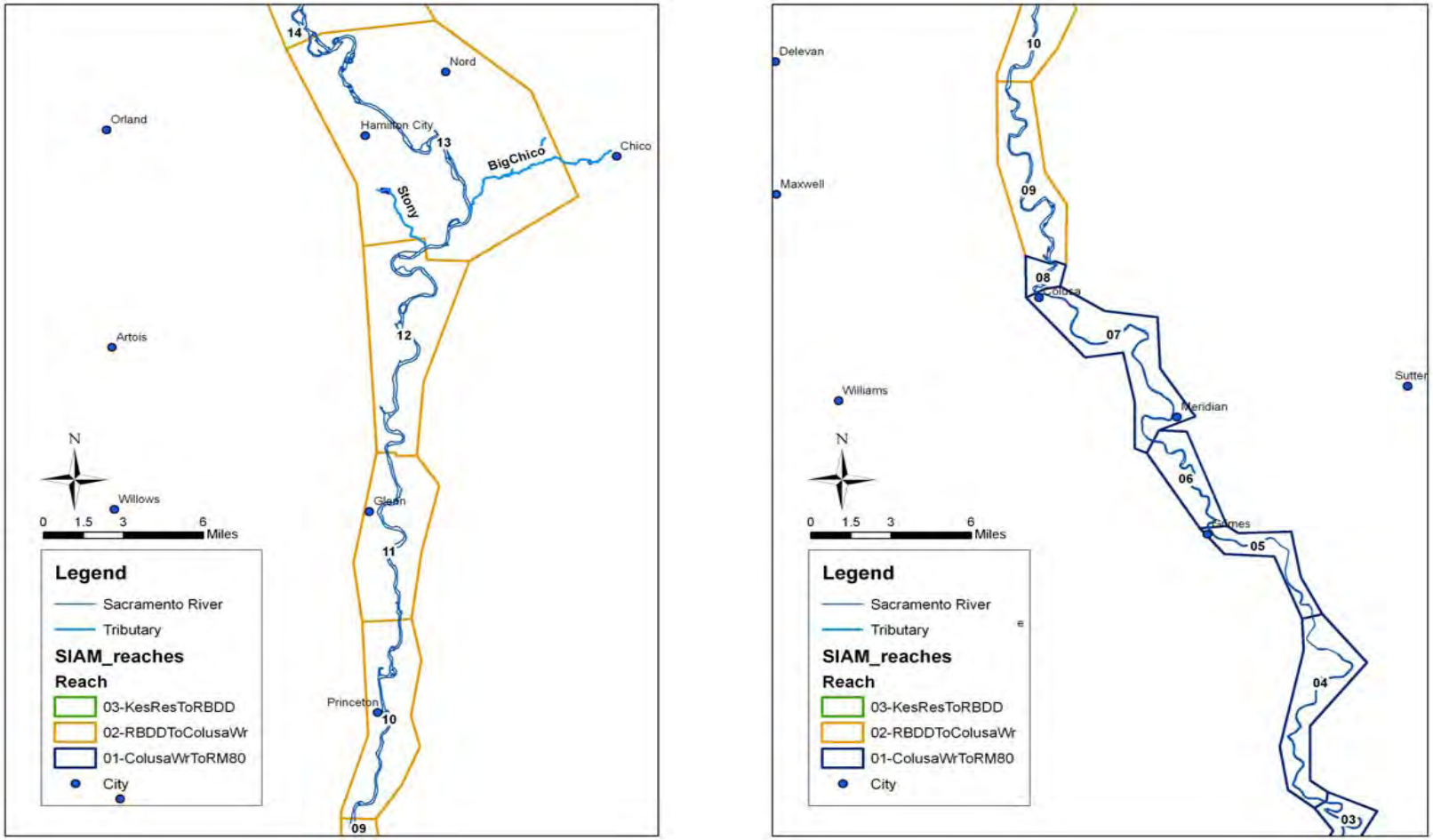

Figure A-17. Reach identification from Hamilton City to Knights Landing.[3]

[3] Note that reach identification is from ArcGIS and Sediment Impact Analysis Methods (SIAM).

Sediment data collection and tributary modeling was not performed downstream of Reach 10 (figure A-17). The lower reaches were identified for future study purposes, but only Reaches 23 to 10 are discussed in subsequent sections and in Chapter 2.

A.3.4 Sediment Transport

Using methods described in A.1.4 Sediment Transport for Tributaries, the reference shear stress values and hiding factors from Table A-4 were used for computing the mainstem river surface material transport capacity for historical hydrology (reference shear 0.0386 and hiding factor 0.905) (figure A-18).

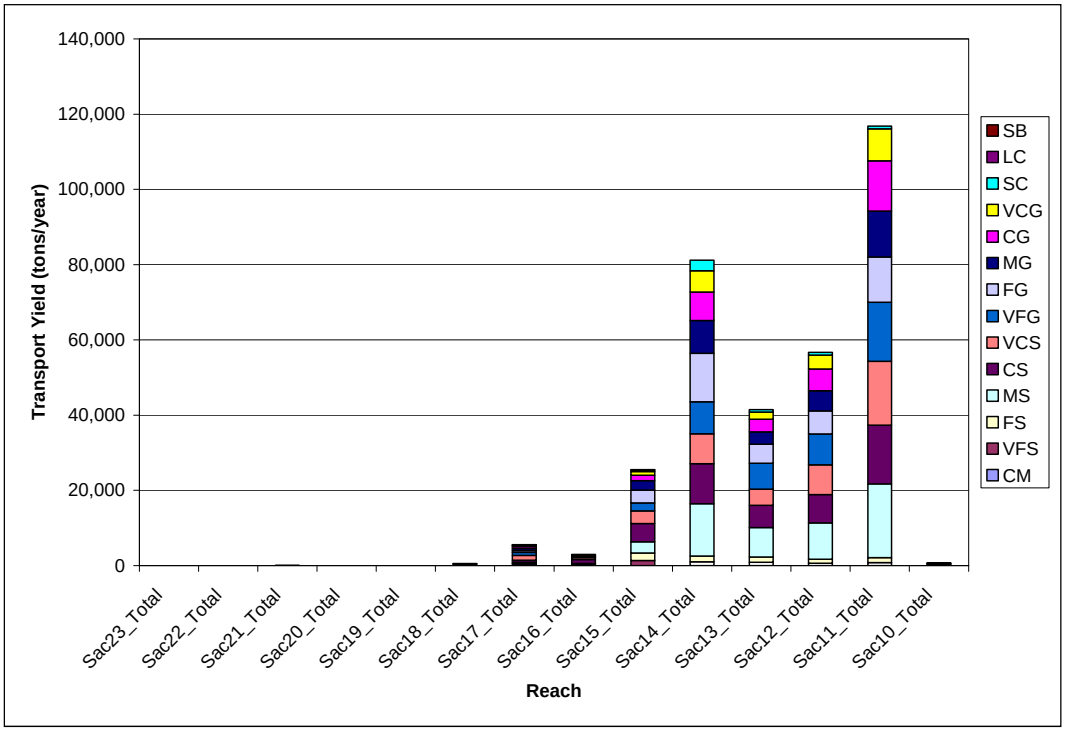

Figure A-18. Surface material transport capacity results by grain class for each main stem reach using Parker's (1990) equation with default parameters.

Transport computed with Parker's (1990) equation was compared with transport computed from Wilcock and Crowe's (2003) equation (figure A-19), each with the respective default transport reference shear stress and hiding factors. The comparison in figure A-19 is for the entire bed gradation.

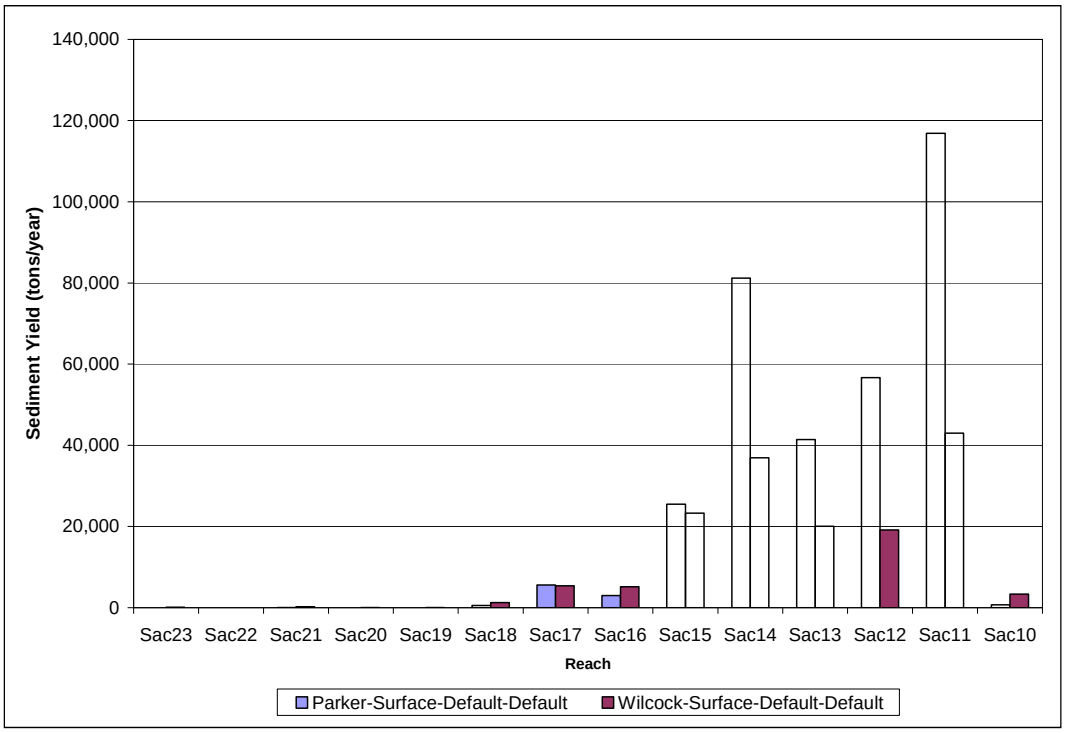

Figure A-19. Comparison of surface material transport capacity computed with Parker's (1990) equation and Wilcock and Crowe (2003).

Predictions of reference shear stress were made using equation A-7 from Mueller, Pitlick, and Nelson (2005) (MPN) which relates reference shear stress to slope, and the friction slope from the hydraulic calculations. The MPN relationship applies to surface-based sediment transport calculations using the Parker (1990) equation. Mueller, Pitlick, and Nelson (2005) considered 45 gravel-bed streams and used a single representative slope for each stream to estimate reference shear stress. The study did not attempt to vary reference shear with varying sub-reach slope changes. With no justification for using individual reach slopes, a single, average friction slope of 4.3×10^{-4} foot per foot (ft/ft) was calculated from the 215-mile longitudinal profile available for the Sacramento River. The friction slope value averages over a range of flow profiles for the entire modeled section of the Sacramento River, with a range from 2.13×10^{-5} ft/ft to 1.39×10^{-3} ft/ft. Figure A-20 shows the surface material results of estimating the shear stress with a slope of 4.3×10^{-4} ft/ft (reference shear .022).

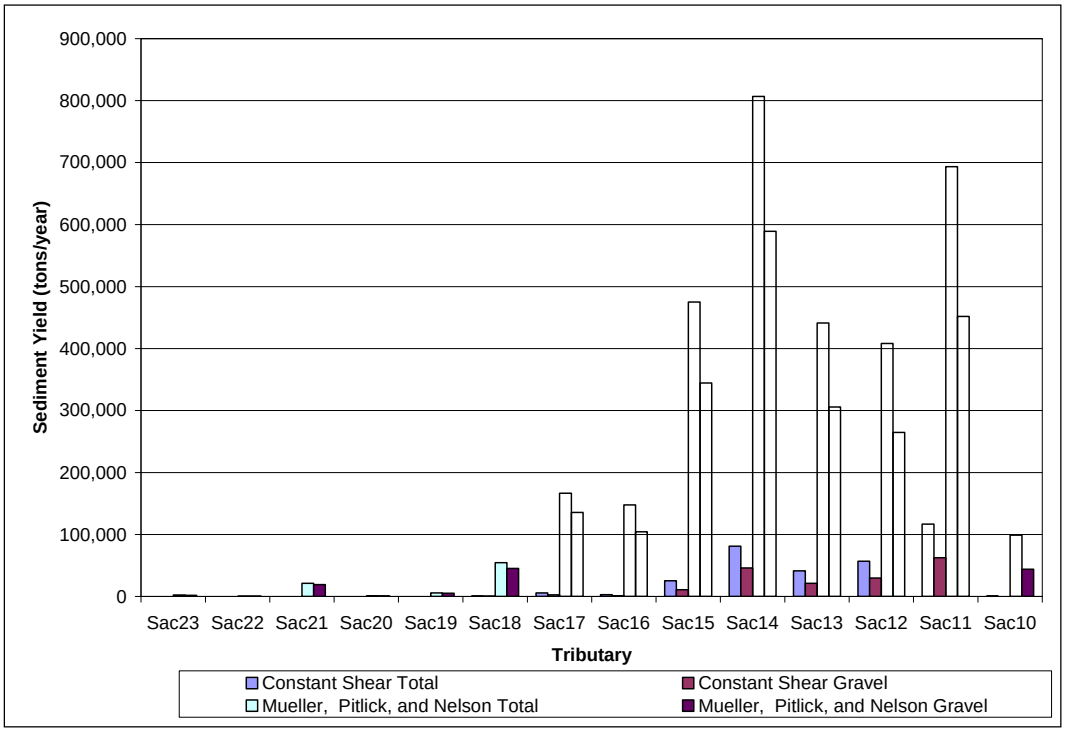

Figure A-20. Surface material transport capacity using slope-based reference shear stress in the Parker (1990) transport equation.

Slope-dependent shear stress resulted in a dramatic increase in transport capacity for both total and material greater than 2 mm. The general trends from reach to reach generally hold true with an increase in quantity.

Similar to the tributary assessment, the hiding factor for the mainstem was reduced for all scenarios to 0.67. As described in Section A.1.4, Sediment Transport, a hiding factor assumes the presence of low mobility, transport capacity limited, coarse particles that shelter finer particles from the full force of flows. Smaller hiding factors result in greater movement in smaller classes. Figure A-21 presents the transport capacities with a reduced hiding factor. Using the default reference shear stress and reducing the hiding factor resulted in a significant increase of both the total transport capacity and the transport for material greater than 2 mm. The hiding factor more strongly impacts the smaller diameters by limiting the interference of large diameters on transport rates. Gravel estimates are less sensitive to the hiding factor. At higher transport rates, the hiding factor becomes less significant. Transport capacities for the Sacramento River are more sensitive to reference shear than to the hiding factor. Transport capacities calculated using the respective default reference shear stresses for Parker (1990) and for Wilcock and Crowe (2003) are lower than expected and appear to be too low compared with other estimates.

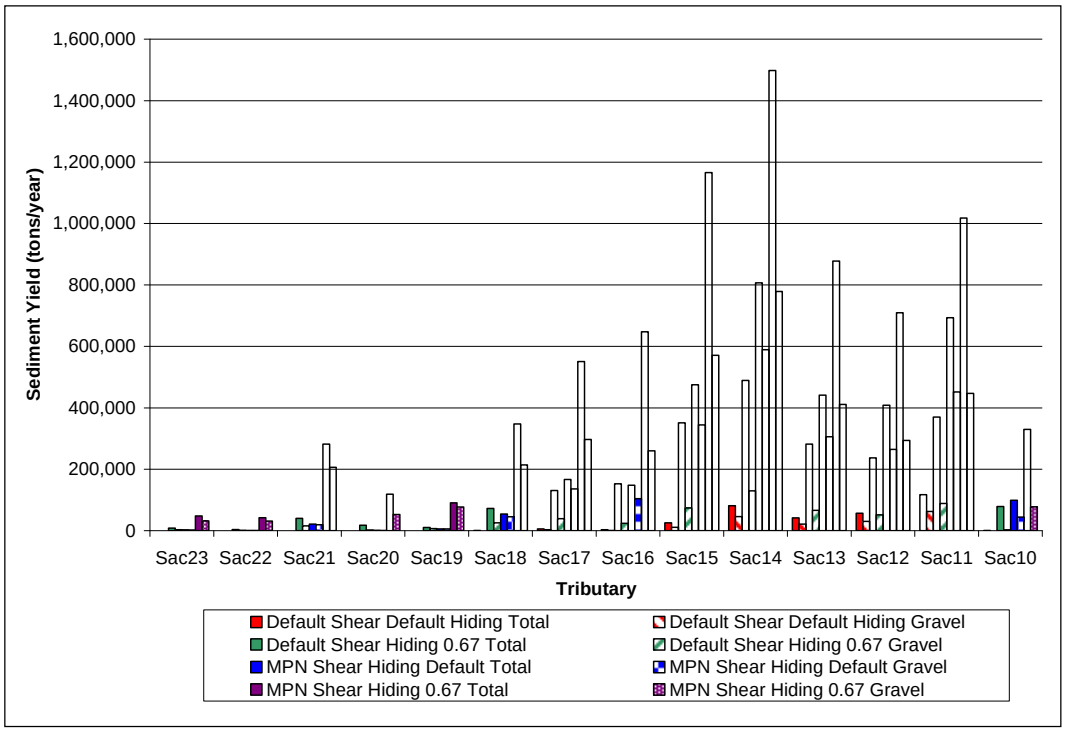

Figure A-21. Hiding factor sensitivity.

There is significant uncertainty associated with predicting bed load in natural streams; therefore, this analysis is more valuable when comparing the relative amounts of sediment being transported between tributaries and reaches.

Summary and conclusions for the tributary sediment yield modeling and the mainstem sediment transport capacity modeling, including a mass balance integrating these two pieces can be found in Chapter 2 of the main document.

Appendix B

Description of Vegetation Input Files for SRH-1DV

Appendix B

Description of Vegetation Input Files for SRH-1DV

Appendix B describes the computer field codes needed for the vegetation input files for SRH-1DV. The records and fields for general parameters and initial vegetation conditions of the model are outlined table B.1 Table B.2 documents the information used for General Input Records in the model simulations.

Table B.1. Description of General Vegetation Input Records and Vegetation Initial Condition Records for SRH-1DV

Record	Fields		Field Descriptions
VNM	NVEG		Number of vegetation types
	NSOIL		Number of soil types
VPM	VDT		Vegetation time step
	VDTPLT		Vegetation output time step
VTM	SYR		Start year
	SMN		Start month
	SDY		Start day
	SHR		Start hour
VIN	GIS_NAME		Name of ARC-GIS shapefile that will be read to determine initial vegetation coverage
VIT	VEG_ID		Name of field in shapefile that will be read to identify the vegetation type
VIV	FIELD_NAME		Vegetation code correspond to names in shapefile GIS_NAME field name VEG_ID
	1 to NVEG	AGE_INIT	Initial age of vegetation
		DENS_INIT	Initial aerial density of vegetation, if less than one then a fraction of points are assigned to that vegetation type

Table B.2. General Vegetation Parameters Used in Simulations

Record	2005 simulation and 2006simulation	1999 to 2007 simulation
VNM	2 veg types, 2 soil types 2 veg types, 2 soil types	8 veg types, 2 soil types
VPM	6 hours, 1 day 6 hours, 1 day	1 day, 121.75 days (3 days per year)
VTM	5/1/2005, 0 hrs 10/1/2005, 0 hrs	10/1/1999, 0 hrs
VIN	updateLUwVeg.shp updateLUwVeg.shp	StatePlaneCAII_updateLUwVeg.shp
VIT	COVERCODE COVERCODE	COVERCODE

Table B.3. Description of Vegetation Input Parameters for SRH-1DV Repeated for Each Vegetation Type. (Length in feet, time counted in days, calendar day by Julian date)

Record	Fields		Field Descriptions
VVN	VNAME		Name of vegetation type, used for output descriptions
GERMINATION			
MMT	MTYPE		Simulation method for germination: 1 = Seed dispersal by air, 2 = Seed dispersal by water
If MTYPE = 1			
MDY	MSTART		Start day for germination (Julian date)
	MEND		End day for germination (Julian date)
MPR	MDAYS		Days from time seeds fall on ground until growth starts during germination period.
	MMAX		Maximum number of days between germination and time when water table was within MHEIGHT of ground surface
	MHEIGHT		Height above ground water table considered moist enough for germination
	MBELOW		Depth below ground water table germination can still occur
If MTYPE = 2			
MPW	MDEPTH		Critical depth above which seed is released
	MDIST		Distance which seed may travel
	MTIME		Maximum time which seed remains viable
Lateral Root Spread for both MTYPE = 1 or 2			
MLT	1 to N	MLT AGE	Age specified for lateral root spread rates
		MLT_RATE (1 to 12)	Root growth rate each month
MEL	Maximum height of plant establishment above low water		
GROWTH			
GMT	GTYPE		Simulation method for growth (1 is only option)
GST	1 to N	GST AGE	Age at which stalk growth rates are given
		GST RATE (1 to 12)	Stalk growth rate at each month
GSM	GST_MAX		Maximum height of stalk
GCP	1 to N	GCP _AGE	Age at which canopy spread rates are given
		GCP _RATE (1 to 12)	Canopy spread rates at each month
GCM	GST_MAX		Maximum width of canopy
GRT	1 to N	GRT_AGE	Age at which root growth rates are given
		GRT_RATE (1 to 12)	Root growth rate at given month

Table B.3. Description of Vegetation Input Parameters for SRH-1DV Repeated for Each Vegetation Type. (Length in feet, time counted in days, calendar day by Julian date)

Record	Fields		Field Descriptions
GRS	GRT		Depth below ground water table at which growth of root stops
	GRT_DEPTH		Maximum depth of root growth
ROUGHNESS			
RMT	RTYPE		Simulation method of vegetation roughness computation (0 if input roughness is not altered, 1 if based on plant age)
RAM	1 to N	RAM_AGE	Average age of plants in cell
		RAM_ ROUGHNESS	Roughness value for average age of plants
MORTALITIES			
Competition			
CMT	CTYPE		Type of competition simulation performed (0 if none, 1 if age comparison)
If CTYPE = 1			
CID	CDEATH_ID		Identification number of competition death
CMP	1 to NVEG	CAGE	Age of species which could be killed
		KILL_AGE 1 to NVEG	Age of other species which could outcompete the species at given age
Shading			
CSH	SHADE_AGE		Age at which species become shade tolerant
Scour			
SMT	STYPE		Type of scour simulation performed (0 if none, 1 if critical velocity method)
If STYPE = 1			
SID	SDEATH_ID		Identification number of scour death
SVC	SAGE		Age at which critical velocity is given
	SVEL_CRIT		Critical velocity above which plant is killed due to scour
Burial			
BMT	BTYPE		Type of burying simulation performed (0 if none, 1 if local depth above top of plant is used as criteria)
If BTYPE = 1			
BID	BDEATH_ID		Identification number of burying death
BDP	BDEPTH		Depth of burial above top of plant required to kill plant.
Drowning			
DMT	DTYPE		Type of drowning simulation performed (0 if none, 1 if depth below water surface method)
If DTYPE = 1			

Table B.3. Description of Vegetation Input Parameters for SRH-1DV Repeated for Each Vegetation Type. (Length in feet, time counted in days, calendar day by Julian date)

Record	Fields		Field Descriptions
DID	DDEATH_ID		Identification number of drowning death
DTM	DAGE		Age at which time and depth of drowning is given
	DTIME		Number of days the root crown must be below DDEPTH for drowning
	DDEPTH		Depth below water surface the root crown must be for drowning to take place
Desiccation			
YMT	YTYPE		Type of desiccation simulation performed (0 if none, 1 if number of days above capillary fringe method, 2 is water stress method)
If YTYPE = 1 or 2			
YID	YDEATH_ID		Identification number of desiccation death
If YTYPE = 1			
YTM	YAGE		Age at which time and height above capillary fringe is given
	YTIME		Number of days the root elevation must be YHEIGHT above the capillary fringe
	YHEIGHT		Height above capillary fringe the roots must be for death by desiccation
If YTYPE = 2			
YWT	1 to N	YWT_RATE	Rate of water table decline
		DESC_RATE (1 to NSOIL)	A desiccation rate is entered for each soil type (NSOIL).
If YTYPE = 1 or 2			
YMN	YMN (1 to 12)		Indicates if desiccation can or cannot occur in a given month (1 or 0, respectively)
Ice Scour			
IMT	ITYPE		Type of ice scour simulation performed (0 if none, only current option
Senescence			
AMT	ATYPE		Type of age death simulation performed (0 if none, only current option)
If ATYPE = 1			
AID	ADEATH ID		Identification number of age death
ATM	AMAX		Age at which death occurs
END			

Abbreviations and Acronyms

1D	one-dimensional
2D	two-dimensional
3D	three-dimensional
ADP	Acoustic Doppler Profiler
ARS	Agricultural Research Service
CDWR	California Department of Water Resources
CFD	computational fluid dynamics
CIMIS	California Irrigation Management Information System
CNPS	California Native Plants Society
DEM	Digital Elevation Models
EMZ	Ecological Management Zone
ET	evapotranspiration
ETo	reference evapotranspiration
GCID	Glen-Colusa Irrigation District
GIC	Geographical Information Center
GIS	geographic information system
hCritA	minimum allowable pressure head at the soil surface
HMC	Hamilton City
HUC-ID	Hydrological Unit Classification identification
MPN	Mueller, Pitlick, and Nelson
NAD	North American Datum
NAVD	North American Vertical Datum
NODOS	North of the Delta Offstream Storage
ORD	Ord Ferry
PVC	polyvinyl chloride
Reclamation	Bureau of Reclamation
RM	river mile
RMRatio	root-mass-ratio
RTK-GPS	real time kinematic global positioning system
SEI	Stockholm Environment Institute
SMS	surface-water modeling system
SRH	Sedimentation and River Hydraulics
TIN	triangular irregular network
TSC	Technical Service Center
USACE	U.S. Army Corps of Engineers
USDA	U.S. Department of Agriculture
USGS	U.S. Geological Survey
UTM	Universal Transverse Mercator
VIN	Vina Woodson Bridge
WET	Water Engineering & Technology, Inc

Measurements

cfs	cubic feet per second
cm	centimeters
cm^2	square centimeters
cm^3	cubic centimeters
cm/d	centimeters per day
cm/h	centimeters per hour
ft/d	feet per day
ft/ft	feet per foot
ft/s	feet per second
g/cm^3	grams per cubic centimeter
$g\ m^{-3}$	grams per cubic meter
$g\ m^{-2}s^{-1}$	grams per square meter per second
$J\ g^{-1}$	joules per gram
$J\ kg^{-1}\ {}^oK^{-1}$	joules per kilogram per degree Kelvin
$kg\ m^{-2}$	kilograms per square meter
$kg\ m^{-3}$	kilograms per cubic meter
$kg\ MJ^{-1}$	kilograms per mega-joule
$kg\ MJ^{-1}\ kPa^{-1}$	kilograms per mega-joule per kilopascal
kPa	kilopascals
$kPa\ {}^oC^{-1}$	kilopascals per degree centigrade
h	hours
m	meters
m^2	square meters
$m\ m^{-2}$	meters per square meter
$m\ kg^{-1}$	meters per kilogram
mg	milligrams
mi^2	square miles
$MJ\ m^{-2}\ s^{-1}$	mega-joules per square meter per second
mm	millimeters
m/s	meters per second
m^3/s	cubic meters per second
m/m	meters per meter
ton/d	tons per day
s^{-1}	per second
$s\ m^{-1}$	seconds per meter
$W\ m^{-2}$	watts per meter squared

Computer Program and Model Names

CIMIS	California Irrigation Management Information System
HEC-RAS	Hydrologic Engineering Centers River Analysis System
RHEM	Riparian Habitat Establishment Model
RTK-GPS	real-time-kinematic global positioning system
SMS	Surface-Water Modeling System
SRH-1D	Sedimentation and River Hydraulics One-Dimensional Sediment Transport Dynamics Model
SRH-1DV	Sedimentation and River Hydraulics One-Dimensional Sediment Transport and Vegetation Dynamics Model
SRH-2D	Sedimentation and River Hydraulics Two-Dimensional Model
SRH-Capacity	Sedimentation and River Hydraulics Capacity Model
SRH-Meander	Sedimentation and River Hydraulics Meander Model
SRH-W	Sedimentation and River Hydraulics Watershed Model
U^2RANS	Unsteady and Unstructured Reynolds Averaged Navier-Stokes Solver
USRDOM	Upper Sacramento River Daily Operations model